C-MYC DEPENDENT GENOMIC INSTABILITY OF THE *RIBONUCLEOTIDE REDUCTASE R2* GENE

BY

Theodore I. Kuschak, B.Sc. (Hons.), M.Sc.

A Thesis
Submitted to the Faculty of Graduate Studies
In Partial Fulfillment of the Requirements
For the Degree
Doctor of Philosophy

University of Manitoba
July, 2000

THE UNIVERSITY OF MANITOBA

FACULTY OF GRADUATE STUDIES

*****

COPYRIGHT PERMISSION PAGE

c-Myc Dependent Genomic Instability of the *Ribonucleotide Reductase R2* Gene

BY

Theodore I. Kuschak

A Thesis/Practicum submitted to the Faculty of Graduate Studies of The University of Manitoba in partial fulfillment of the requirements of the degree of

Doctor of Philosophy

Doctor of Philosophy
(Department of Microbiology)

University of Manitoba
Winnipeg, Manitoba, CANADA

Title: c-Myc-Dependent Genomic Instability of the *Ribonucleotide Reductase R2* Gene

Author: Theodore Ivan Kuschak, B.Sc. (Hons.) University of Manitoba
M.Sc. University of Manitoba

Supervisors:
Sabine Mai, Ph.D.
Jim A. Wright, Ph.D.

Number of Pages: xxiv, 400

ABSTRACT

c-Myc deregulation has been shown to generate locus-specific chromosomal and extrachromosomal gene amplification, as well as karyotypic instability. My studies focused on c-Myc-dependent amplification of a new c-Myc amplification target, the *ribonucleotide reductase R2* gene. Using a mouse Pre-B cell line we showed chromosomal and extrachromosomal amplification and rearrangement of the *R2* gene locus within 72 hours of transient and inducible c-Myc deregulation. We further showed that the initiation of c-Myc-dependent *R2* instability occurs as early as 24 hours of transient c-Myc deregulation.

Previous studies have demonstrated gene amplification using cell cycle inhibiting drugs, resulting in locus-specific gene amplification within 5-22 replication cycles. My study is novel in that it uses an inducible system to study initiation of c-Myc-dependent *R2* amplification. The results of this work suggest that the c-Myc-dependent initiation of amplification of *R2* is replication-driven. This does not exclude subsequent gene amplification through other mechanisms.

To study c-Myc-dependent extrachromosomal gene amplification, we developed two methods for the analysis of extrachromosomal DNA amplicons. These methods include fluorescent *in situ* hybridization to characterize the genes found in the total population of purified extrachromosomal DNA and the specific isolation of histone-bound extrachromosomal DNA, which is associated with active genes.

AIMS OF THIS THESIS

The aim of this study was to examine c-Myc-dependent genomic amplification of the *ribonucleotide reductase R2* gene. This thesis work had the following aims:

1. To determine the effect of transient and constitutive c-Myc overexpression on the genomic (in)stability of the *ribonucleotide reductase R2* gene and to establish whether any observed c-Myc-dependent perturbations in *R2* genomic stability resulted in altered *R2* mRNA and protein expression in cultured Pre-B cells.

2. To determine whether the four non-canonical E-box motifs found flanking the Exon VIII region of the *ribonucleotide reductase R2* gene bind c-Myc/Max heterodimers, and whether these E-box-containing DNA sequence motifs play a role in c-Myc-dependent *R2* gene amplification in cultured Pre-B cells.

3. After inducible c-Myc deregulation, we observed extrachromosomal and chromosomal gene amplification of the *ribonucleotide reductase R2* gene locus (See results of Aim 1). To further characterize the c-Myc-dependent extrachromosomal amplification of the *R2* gene (and of other genes), we have developed two experimental approaches. First, we used fluorescent *in situ* hybridization (FISH) to probe for the presence of the *R2* and other genes in a total isolation population of purified extrachromosomal DNA. Second, we developed a method to specifically isolate extrachromosomal DNA that is bound by histone proteins, which are associated with potentially active genes.

DEDICATION

This work is dedicated to the most important things in my life: To my father Fred, my mother Louise Elizabeth, my beloved wife Brenda, and to The Eternal and Almighty Lord who made each of them.

ACKNOWLEDGEMENTS

I thank Dr. Jim A. Wright for accepting me as a graduate student in his lab and for his financial support throughout the course of my Ph.D. studies.

I thank Dr. Sabine Mai for accepting the role as my *de facto* supervisor. It has been an extraordinary honour (and a lot of fun) to study under a mentor such as Sabine. Danke, Frau Doktor!

Thanks to Dr. J. Frederic Mushinski (NCI/NIH, Bethesda, MD) for his invaluable contributions to my work and for a place to go after I "get outa Dodge". Thanks also to Dr. Francis Wiener (Karolinska Institute, Sweden) for some very interesting and extremely amusing discussions about life, about science, and about how dogma affects both. Oh, and "Spasiba" for the "anti-cramp medicine" and the recipe apple strudel! I feel much better. Thanks to my committee members in the Department of Microbiology, Dr. Isamu Suzuki, and Dr. Peter Loewen for their support and for constructive criticism of my work. It was truly a pleasure to have met Dr. Jeremy Squire (Ontario Cancer Institute) in an informal setting and certainly an honour to have him as my external examiner. I am grateful to Michael Mowat, Ph.D. for his good advice, especially at those really important times, like my candidacy. Thanks to Ms. Sharon Berg (Department of Microbiology) for getting all of the messages through and to Ms. Rosemarie Contreras, Mrs. Anita Saxena, and Mrs. Tuntun Sarkar (Manitoba Institute of Cell Biology) for helping me to get all of those really important FedEx letters off. Thanks to our administrative assistant, Nikki Ryan, without whom the entire place would quickly grind to a halt. You all know its true!

I thank my good friends, Dr. Travis Takeuchi and his wife, Dr. Elizabeth Hrycak, and Dr. Donald Dubik and his wife Dr. Deborah Tsuyuki for their friendship and support.

Thanks to Lou Guffei (the microscope guy) and to Terry for looking after my furry Eμ-myc friends. Thanks also to Elizabeth Henson, Shibani Bal, Cheryl Taylor, Amanda Guffei, Dr. Denis Bosc, Marlon Hagerty, Rahul Sarkar, and James Paul, for their camaraderie (and tolerance of my *grumpy-bear* days). Thanks to Jeanne Fourie, Tracy Brown, Reena Ray, Mariko Moniwa, Cheryl Peltier, Ileana Strelkov, Katherine Dunn, Gracjan Bozek, Bisera Vukovic, and Laurie Lange for the funny day-to-day stuff. You all represent the face of *good humour incarnate* for those who toil on *The Dark Side*. Finally, to my lab buddy, co-conspirator, co-under-my-breath grumbler, and *R2* veteran Gregory M. Smith, I extend very special thanks for helping me to survive *The Womb Whence Entropy Come*.

As I have in the past, I must again thank my mother Louise for instilling in me her love of reading and literature, and my father Fred for instilling in me my respect for education. I am ever grateful for wonderful parents. I thank my aunt, Anne for her constant encouragement and moral support.

I am grateful to my parents-in-law, Duck and Shea Chan, as well as my sisters-in-law Pensy and Madge, my brother-in-law and Jeff and his wife Karen. I am truly a part of a wonderful family!

Finally, I thank my beloved wife, Brenda Chan Kuschak for her moral and financial support, and constant encouragement. Thanks for your love, patience, and for being my very best friend through the easy and the difficult times. I will always love you!

I am grateful to *CancerCare Manitoba*, for financial awards of the *David and Mona Copp* (1998-1999) and the *George. H. Sellers Graduate Studentships* (1999-2000).

July 2000.

TABLE OF CONTENTS

LIST OF ABBREVIATIONS

Chemical Compounds

BIO	biotin
BrdU	bromodeoxyuridine
DABCO	diazabicyclo[2.2.2]-octane
DAPI	4',6' diamidino-2-phenylindole
DIG	digoxigenin
DTT	dithiothreitol
HEPES	N-2-Hydroxyethylpiperizine-N'-2-Ethane sulphonic acid
NH_4COOCH_3	ammonium acetate
NH_4Cl	ammonium chloride
$NaHCO_3$	sodium bicarbonate
Na_2CO_3	disodium carbonate
Na_2HPO_4	disodium phosphate
NaH_2PO_4	monosodium phosphate
KH_2CO_3	monopotassium carbonate
KH_2PO_4	dipotassium phosphate
K_2HPO4	dipotassuim phosphate
MOPS	3-[N-Morpholino]propanesulphonic acid
NA_2EDTA	ethylaminediaminetetraacetic acid, disodium salt
Triton X-100	t-Octylphenoxypolyethoxyethanol
Trizma/Tris	Tris[hydroxymethyl]aminomethane
Tween-20	polyoxyethylenesorbitan

Prepared Solutions, Reagents, or Supplements

FBS	Fetal Bovine Serum
FSP	Formamide SSC Phosphate Buffer
HSB	High Salt Buffer
GTE	Glucose Trizma EDTA Buffer
IL-6	Interleukin 6
PBS	Phosphate Buffered Saline
SDS	Sodium Dodecyl Sulphate
SCP	Sodium Citrate Phosphate Buffer
SSC	Standard Sodium Citrate Buffer
STE	Sodium chloride Trizma EDTA Buffer
TE	Trizma EDTA Buffer
TBE	Trizma Borate EDTA Buffer

Conjugated Fluorochromes

TXRD	Texas Red
FITC	Fluorescein isothiocyanate

Drugs

4-HT:	4-hydroxytamoxifen
Amp	ampicillin
HU	hydroxyurea

Genes

ARF	gene encoding ARF
CAD	gene encoding carbamoyl-phosphate synthetase-aspartate transcarbamoyl-dihydroorotase
c-myc	gene encoding *c-myc*
cdc25a	gene encoding cdc25a
cylcin A	gene encoding cyclin A
cyclin D2	gene encoding cyclin D2
cyclin E	gene encoding cyclin E
N-myc	gene encoding N-myc
DHFR	gene encoding dihydrofolate reductase
ECA39	gene encoding ECA39
eIF2α	gene encoding elongation factor 2α
eIFE	gene encoding elongation factor E
Gadd 45	gene encoding Gadd45
GAPDH	gene encoding glyceraldehyde-3-phosphate dehydrogenase
GSHPX	gene encoding glutathione peroxidase
IGF2	gene encoding insulin growth factor 2
LDH-A	gene encoding lactose dehydrogenase A
MrDb	gene encoding MrDb
ODC	gene encoding ornithine decarboxylase
p27	gene encoding p27
p53	gene encoding p53

R1	gene encoding ribonucleotide reductase R1
R2	gene encoding ribonucleotide reductase R2
RCC1	gene encoding RCC1
RCL	gene encoding RCL
TERT	gene encoding TERT
TK	gene encoding thymidine kinase

Measurements

Distance

cM	centiMorgans

Mass

kg	kilogram	(10^3 grams)
g	gram	(10^0 grams)
mg	milligram	(10^{-3} grams)
µg	microgram	(10^{-6} grams)
ng	nanogram	(10^{-9} grams)
kDa	kilodalton(s)	

Volume

L	litre	
mL	millilitre	(10^{-3} litres)
µL	microlitre	(10^{-6}litres)

Concentration

mol	Avagadro's Number	(6.022×10^{23})
M	molar	($molesLitre^{-1}$)
mM	millimolar	(10^{-3} molar)
nM	nanomolar	(10^{-6} molar)
IU	international unit(s)	
O.D.	optical density	

Miscellaneous

2D	two-dimensional
bp	base pair(s)
cDNA	DNA complementary to RNA
dd	distilled and deionized
EEs	Extrachromosomal Elements
IgG	immunoglobulin G
LTR	long terminal repeat
MMTV	Mouse Mammary Tumor Virus (promotor)

Protocols and Equipment

EM	Electron Microscope
DCA	Dispersed Cell Assay
FISH	Fluorescent *In Situ* Hybridization
FISH-EEs	Fluorescent *In Situ* Hybridization on Extrachromosomal Elements

LIST OF FIGURES

Section 3.2

APPENDICES

Appendix A

Appendix B

LIST OF TABLES

CHAPTER 1

INTRODUCTION

Chapter 1. INTRODUCTION

1.1. The Focus of this Study

The focus of this thesis work is the c-Myc-dependent amplification of the *ribonucleotide reductase R2* gene in cultured mouse lymphoid B cells. My hypothesis is that because the mouse *R2* gene contains E-box motifs that are putative Myc/Max binding sites, it is a target of c-Myc dependent gene amplification. In this thesis work I have examined the role of c-Myc deregulation in the genomic (in)stability of the *ribonucleotide reductase R2* gene. I have also analyzed the mechanism by which c-Myc interacts and initiates the amplification of the *R2* gene.

This thesis work advances the way we are able to study genomic instability, but more importantly it adds to the list of detrimental effects mediated by c-Myc deregulation. Since one of the phenomena often encountered in the study of genomic instability is the generation of extrachromosomal DNA molecules, also known as double minutes (DMs) or extrachromosomal elements (EEs), it was to our advantage to develop a better method of detecting and probing them. During the course of this thesis work, a variation of the current fluorescent *in situ* hybridization (FISH) method was developed. FISH-EEs (fluorescent *in situ* hybridization of extrachromosomal elements) was developed as a method to aid in the detection of genes on extrachromosomal DNA molecules. In addition, we have developed a way to specifically enrich for histone-bound EEs that carry genes.

The main emphasis of this thesis work was initiated to examine the c-Myc dependent genomic (in)stability of the *ribonucleotide reductase R2* gene locus. In this study we began with three questions:

(i) Does deregulation of the protooncogene c-Myc in cultured B lymphocytes play a role in genomic (in)stability of the *ribonucleotide reductase R2* gene locus? If so, what are the effects on *R2* expression following its amplification?

(ii) Does the c-Myc protein interact physically in any way with the *R2* gene locus? If so, does c-Myc interaction with the *R2* gene play a role in its amplification?

(iii) Finally, what is the mechanism of the c-Myc dependant amplification of the *R2* gene locus? Is the amplification of *R2* a replication-driven or a segregation-driven phenomenon?

In brief, the results of the experiments conducted answered the questions posed above. These results are summarized as follows:

I have demonstrated that the transient and constitutive deregulation of c-Myc results in the chromosomal and extrachromosomal amplification as well as rearrangement of the mouse *ribonucleotide reductase R2* gene locus. Unexpectedly, we found that amplification of the *R2* gene locus does not result in a corresponding over-expression of the *R2* mRNA and protein products. c-Myc target genes such as *dihydrofolate reductase* (Mai, 1994) and *Cyclin D2* (Mai *et al.*, 1999) are over-expressed following their amplification. In contrast, my work shows for the first time that c-Myc-dependent amplification is not necessarily followed by over-expression of the amplified gene product. To this end, this work also defined different classes of c-Myc amplification target genes: Those that are over-expressed following amplification of a gene locus, and those that are not.

Next, my thesis work answered a number of questions about the role of c-Myc in the amplification of the *ribonucleotide reductase R2* gene locus and about the mechanism

of the amplification process. I demonstrated that the c-Myc protein does interact with each of a cluster of four non-canonical E-box motifs that are found flanking the Exon VIII region of the *R2* gene *in vitro*. This interaction was shown to be specific, since anti-Myc antibodies, but not control antibodies were able to disrupt the interaction and complex formation in *in vitro* analyses. I confirmed through a series of 2-dimensional gel electrophoresis and Southern analyses that the amplification of the *R2* gene was a c-Myc dependent phenomenon that occurred specifically through a replication-driven mechanism. These results are reminiscent of the *onionskin* re-replication model initially proposed by Varshavsky (1981) and later by Mariani and Shimke (1984), as well as others. Moreover, each of the four E-box motifs identified in the region flanking Exon VIII of the *R2* gene is part of an initiation zone for the initiation of *R2* gene replication. Finally, my work demonstrated that transient c-Myc over-expression resulted in a higher metaphase index, but more importantly that c-Myc deregulation resulted in enhanced bromodeoxyuridine incorporation in band A of mouse chromosome 12 where the *R2* gene resides.

The most important contribution of this thesis study to the rapidly expanding field of c-Myc is novel information showing that when deregulated, c-Myc is capable of a replication-driven amplification mechanism. Although, replication-driven gene amplification was described nearly two decades earlier by Varshavsky (1981) and Mariani and Schimke (1984), their descriptions involved drug-dependent amplification of the *dihydrofolate reductase* gene locus. This study demonstrates for the first time the capacity of c-Myc protein to amplify the *ribonucleotide reductase R2* gene in a

replication-driven mechanism, and as such this study adds to the understanding of c-Myc-dependent gene amplification and genomic instability.

1.2 Tumor Initiation and Progression

Ordered and regulated cellular proliferation is the rule in healthy cells, whereas, uncontrolled cellular proliferation is the hallmark of cancer. The changes that occur in cells, turning them from normal to cancerous are not singular, nor do they necessarily follow the same path in each case. The current model of cancer development is a multi-step theory, where most tumors are believed to arise following a series of alterations that alter the regulation of a cell. The theory of multi-step carcinogenesis originated with Foulds (1958). Farber and Cameron (1980) proposed that the alterations can be simplified and broken down into three phases namely, initiation, promotion, and progression of cancer. These alterations can be either lethal or they can be advantageous for cell growth. The alterations that confer a survival advantage are selected for and will eventually allow for the selection of predominant population(s) with altered growth characteristics.

The classic model that describes the genetic basis for colorectal neoplasia was published by Fearon and Vogelstein (1990). Although it describes the genetic basis leading to colorectal carcinogenesis, it is applicable to tumorigenesis and tumor progression in general. In summary their model stated that:

(i) Colorectal tumors appear to arise following the mutational activation of oncogenes in conjunction with the mutational inactivation of tumor suppressor genes, where the latter predominate.

(ii) Mutations in at least four or five genes are required for the formation of a malignant tumor, although fewer changes are sufficient for the development of a benign tumor.

(iii) The genetic consequences are due more to the total number of the mutations than to the order in which they accumulate.

(iv) In some cases mutations in tumor suppressor genes appear to exert phenotypic effects, even though they are present in the heterozygous state, suggesting that these genes may not be recessive at the cellular level.

Overall, this model depicts a picture that shows a set of conditions that are required and must be met for the "successful" development of a cancer cell.

The model described above requires that specific changes occur at the genetic level that will provide the cell with an advantage to an abundance of selective pressures. This Darwinian natural selection of cancer cells allows these cells to free themselves from the confines of controlled growth. Weinberg (1989) suggested that the Darwinian selection of cancer cells, which is the outcome of a multistep cancer development process, is a reasonable model. Each step in the progress toward a cancer cell represents a physiological barrier that must be crossed in order for the cell to progress toward the endpoint of malignancy. Bishop (1995) summarized this eloquently by suggesting that each tumor is the outcome of an individual experiment in cellular evolution, driven by genomic instability and guided by rigid selection for advantageous cellular properties.

1.3. B Lymphocytes and Their Development

Since this thesis focuses on mouse B lymphocytes in the context of genomic instability, it is prudent to begin with some discussion of B cell development. The

development of B lymphocytes *in vitro* and *in vivo* has been studied very thoroughly. In fact, more than a dozen stages of B cell development can be distinguished in the mouse and a similar number of stages is becoming discernable in human B cell development studies. Moreover, the complex issues of proliferation, differentiation, and programmed cell death can now be investigated at more than one stage of the B cell development process. Human and murine tumors arising from various stages of B cell development add to the understanding of the specific developmental stages of B cells that are susceptible to transformation. The c-Myc oncoprotein is clearly implicated in the normal control of B cell development and in the events that lead to neoplasia.

The development of the B lymphocyte will be discussed briefly in this section with emphasis on the potential roles of the developmental and maturation processes upon the initiation of the preneoplastic and neoplastic conditions in the B cell and the role that the protooncogene c-Myc plays in these processes. This discussion is by no means exhaustive, but it serves to illustrate the potential for deregulation of the *c-myc* gene locus and potentially other genes downstream of *c-myc*.

1.3.1. B Lymphocyte Development

The normal development of B lymphocytes requires that these cells proliferate and undergo differentiation at appropriate times in order to fill all of the compartments of the primary and secondary lymphoid organs. In addition, the development system is charged with the task of selecting for antigen-receptor expressing cells, in order that all "anti-self" as well as other receptor-negative cells that arise from non-productive V(D)J rearrangements during development in the primary lymphoid organs do not appear in the secondary peripheral regions of the system.

It was demonstrated that B cells are generated in waves. In the mouse, a first wave is initiated in the embryonic blood and placenta, followed by a second wave originating in the fetal liver (Melchers, 1979; Rolink *et al.*, 1993). Throughout life, these cells continue to be generated in the bone marrow. The rate at which these cells are generated daily is approximately 5×10^{10} in humans and 5×10^{7} in the mouse. Only 2 to 5% of the cells generated each day will reach maturity as surface-immunoglobulin positive (sIg^+) cells that will be found in the peripheral blood. The remaining 95 to 98% are unsuitable for further development and die at the site of their generation. The key to the survival or death of these cells lies in the selection of functional sIg-bearing cells. This process begins with the rearrangement of the immunoglobulin gene loci. These rearrangements are either successful or they fail. If rearrangements fail to generate a functional cell, the cell dies. If the rearrangement is successful, a signal is given, often as a receptor or a successfully assembled molecule, which prompts the next step of the development process. The phases in B cell cytoplasmic and surface marker development and presentation are illustrated in Figure 1.3.1.1. The successes and failures of heavy and light chain rearrangement are illustrated in Figure 1.3.1.2.

The oversimplified chronology and molecular signaling involved in B cell development are as outlined below. The pluripotent stem cell, which is the ancestor of all of the different lineages of blood cells, gives rise to progenitor cells. These progenitor cells are developmentally committed to generate cells of the B lineage. Many early cells develop and function in close contact with an environment of stromal cells. Stromal cells are important since they provide the developing lymphoid cell with cell contacts and cytokines that regulate the proliferation and differentiation of the B cell lineage (Era *et*

al., 1994; Kincade *et al.*, 1994). Interleukins such as IL-3 and IL-7 with a role in B cell development have been identified in the mouse, and c-kit and flk-2 are membrane-bound tyrosine kinases found on B lineage precursors, which interact with corresponding membrane-bound ligands found on stromal cells (Era *et al.*, 1994; Ogawa *et al.*, 1991; Rolink *et al.*, 1991a, Rolink *et al.*, 1991b; Winkler *et al.*, 1994).

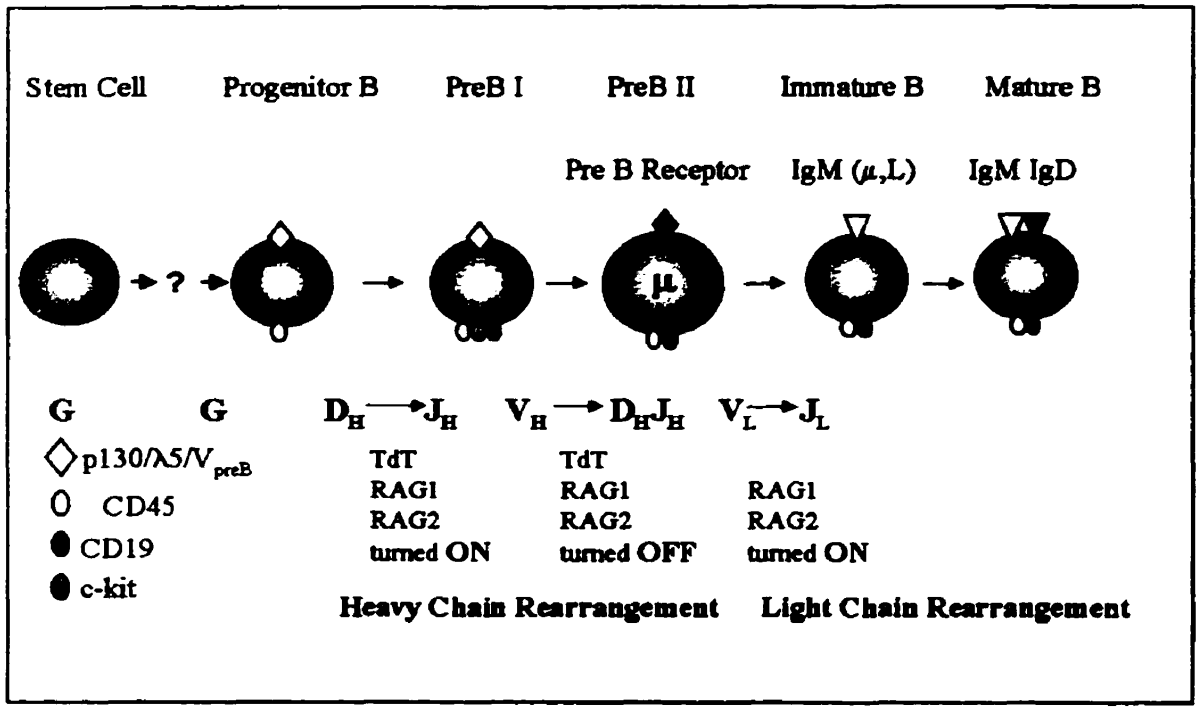

Figure 1.3.1.1. B Lymphocyte Development

Modified from Siwarski *et al.* (1997) in ***c-Myc in B-Cell Neoplasia*** (Potter and Melchers, Eds.) in *Mechanisms of B Cell Neoplasia* 1997, Roche. (Not shown is the plasma cell, a non-proliferating, end-differentiated B cell that form mature B cells.)

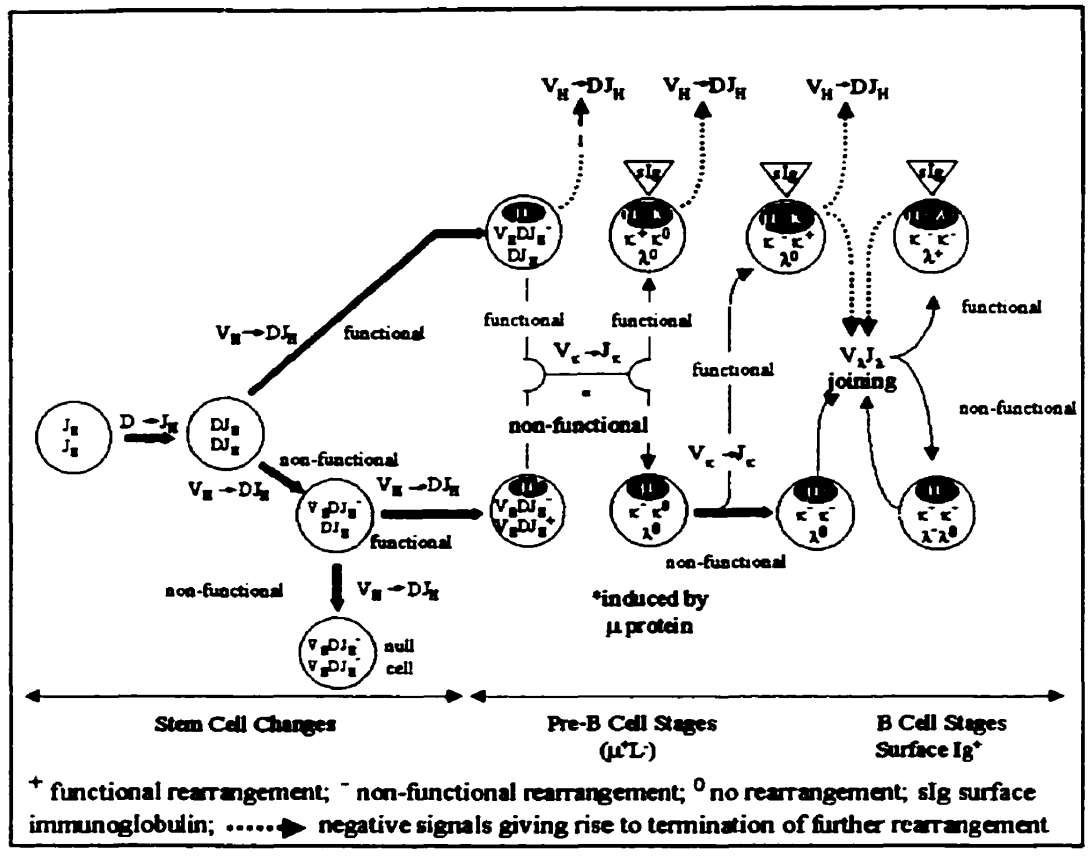

Figure 1.3.1.2. Heavy and Light Chain Rearrangement and Allelic Exclusion: The Generation of Functional and Non-Functional Heavy and Light Chains. Modified from: Klein, J. in *Immunology*, 1991. Blackwell Scientific Publications. p.108.

Transcription of the non-rearranged, germline μ heavy (H) chain gene locus and the V_{preB} and λ_5 genes encoding the surrogate light (SL) chain (Melchers *et al.*, 1993), as well as the activation of the rearrangement machinery genes such as *terminal deoxyribonucleotidyl transferase* (*TdT*), and the rearrangement-active genes *RAG1* and *RAG2* (Mombaerts *et al.*, 1992; Oettinger, *et al.*, 1990; Schatz *et al.*, 1989; Shinkai, *et al.*, 1992), are the earliest evidence for the commitment of a cell to the B lineage of development (see Figure 1.3.1.1.). These events occur at the time when the cells are

$B220^+$ ($CD45^+$ in humans), but not yet $CD19^+$ (Hardy *et al.*, 1994; Rolink *et al.*, 1996). At this stage of the cells' maturation process, the first Ig rearrangements (D_H segments to J_H) are already detectable. The role of TdT is N sequence insertion at the joints of the rearrangements. TdT is active during rearrangements that occur in the bone marrow, but does not function in the liver. For this reason, the heavy chains of the antibodies that are derived from the bone marrow are N region-diverse, while those generated in the liver are not. This rearrangement continues while the cells are in the subsequent distinguishable B cell population. In this stage, known as the PreBI stage, cells are $B220^+$ ($CD45^+$), $CD19^+$ and also express c-kit ($CD\text{-}117^+$) and SL chains on their surface. Moreover, at this stage, practically all H chain alleles D_HJ_H are rearranged (Melchers, 1995).

At this point, a second round of chain rearrangement occurs on one of the heavy chains, where V_H joins the D_HJ_H sequence. Whenever this rearrangement takes place successfully, and the rearrangement is in frame, a μH chain can be made. This μH chain then combines with the SL chain forming a PreB receptor. This sequence of events has a number of consequences and leads to the generation of a new cell population. In a suitable environment such as in the bone marrow or in another B lymphocyte generating organ, cells expressing surface PreB receptors are induced to cycle and for this reason they are quite large during this phase, during which they are called PreBII cells. Cells that have not generated productive rearrangements and cannot form a PreB receptor do not proliferate and will die. Conversely, cells expressing PreB receptors following productive μ heavy chain rearrangement outgrow their compartment. These cells no longer express c-kit and have completely down-regulated their rearrangement machinery. This includes TdT, RAG1, and RAG2. They now express CD25 (the α-chain of the IL-2 receptor)

(Grawunder *et al.*, 1995). The down-regulation of the rearrangement machinery is likely to play a pivotal role in the prevention of potentially successful V_H to D_HJ_H rearrangement within the other, as yet non-rearranged heavy chain locus. This is likely the mechanism by which allelic exclusion is ensured, so that one B cell is able to generate only one heavy chain.

Following the generation of a successfully VDJ-rearranged heavy chain, the expression of V_H may still undergo gene replacements or conversions, known as editing. This editing process in V_H expression is likely to occur in the transition between PreBI and PreBII during the B cells' development, when the VDJ rearrangement is completed and before the rearrangement machinery is down regulated. These large PreBII cells then undergo three to five cycles of replication and lose their PreB receptor expression. The loss of PreB receptor is followed by a reactivation of the *RAG1* and *RAG2* genes and by the transcription of the non-rearranged λ and κ light chain loci. These cells fall into a resting state where they become small and are referred to as small PreBII cells.

During the second phase of rearrangement, *RAG1* and *RAG2* rearrangement-active genes are activated, but *TdT* is not. Consequently, all cells contain rearranged V_LJ_L-rearranged L gene chain loci, but no N insertions are made. At this point, half of the cells have successfully rearranged their light chains and express these chains in the cytoplasm, but not yet on the surface. The other half consists of cells which have either non-rearranged or out-of-frame loci. It is important to note that the expression of RAG1 and RAG2 enables shuffling of light chain rearrangements which result in correct and productive light chains, or continued reshuffling which might allow for the alteration of a non-productive light chain to a productive chain. This process, receptor L chain editing,

might also rearrange a productive L chain, giving rise to an auto-antigen-reacting Ig receptor. Secondary L chain rearrangements may allow for the expression of two L chains whenever the rearrangement process allows both chains to be used. It has been shown that only 1 to 3% of all mature peripheral B cells express two light chains. Also, less than 1% of all peripheral B cells have been shown to express two heavy chains. Together, this implies that for the most part, one B cell produces only one antibody by virtue of allelic exclusions. This is the basis for clonal evolution within the immune system, where a single antigen is selected from all of the lymphocytes that were generated, the single cell that has given rise to the "correct" receptor.

1.3.2. Positive and Negative Selection of B Lymphocyte Clones

As described in the previous section, the survival or death of a given B cell clone depends on the functional rearrangement of the germline immunoglobulin loci (see Figure 1.3.1.2.). In the proper *in vivo* developmental environment of the bone marrow, the expression of an autoreactive immunoglobulin receptor on an immature B cell results in the arrest of differentiation and death of that cell (Chen *et al.*, 1995a, 1995b; Goodnow *et al.*, 1995; Nemasee, 1991; Prak and Weigert, 1995). They can attempt to rearrange their receptor specificity through secondary L-chain rearrangements (Young *et al.*, 1994). Through this method of differentiation arrest, the emerging B cell repertoire is purged of those cells which are autoreactive to antigens present in the marrow. A small percentage (2 to 3%) of the $sIgM^+$ immature B cells that do not recognize autoantigens are selected to become mature, resting antigen-sensitive sIgM/sIgD-double-expressing B lymphocytes which are allowed to migrate to the peripheral system and eventually become longer-lived cells.

1.3.3. c-Myc Expression During Normal B Lymphocyte Development

It has been clearly demonstrated in mouse models, that *myc* genes play a critical role in embryonic development. The *myc* family consists of *c-myc*, *N-myc*, *L-myc*, *S-myc*, *B-myc*. The best characterized of these is *c-myc*. The most closely related members of the *myc* family of proteins are L-Myc, N-Myc, and c-Myc. They share significant functional and structural homology. S-Myc shares only about 60% sequence homology and may play a role in transcriptional regulation of genes whose expression induce apoptosis *in vitro* and *in vivo* (Asai *et al.*, 1994). B-myc shares homology with exon 2 of *c-myc* and is expressed in multiple tissue types, although its expression is highest in the brain, both at the embryonic and adult stages (Ingvarsson *et al.*, 1988). It has been shown to inhibit neoplastic transformation and transcriptional activation by c-Myc (Resar *et al.*, 1993).

L-myc, *N-myc*, and *c-myc* play crucial roles in mammalian development. Mice that are nullizygous for *c-myc* die *in utero* between 9.5 and 10 days (Davis *et al.*, 1993). Before death, the embryos are smaller and a number of the organs show defects in their development. The authors (Davies *et al.*, 1993), cite pathologic abnormalities in the heart, pericardium, neural tube and delay or failure in turning of the embryo. Mice that are nullizygous for *N-Myc* die *in utero* between 10.5 and 12.5 days of their gestation (Charron *et al.*, 1992). Histological analysis of mutant embryos reveals lack of organ and tissue development; in particular, these embryos reveal a lack in development of the cranial and spinal ganglia, mesonephros, lung, and gut (Stanton *et al.*, 1992; Sawai *et al.*, 1993). These abnormalities occur in spite of a compensatory up-regulation of *c-myc* expression in the neuroepithelium (Stanton *et al.*, 1992). Unexpectedly, it was demonstrated that although these embryos die prematurely, they survive to

developmental stages that are well beyond the onset of normal *c-myc* and *N-myc* expression. The survival of the mutant embryos is attributed to some redundancy in the functional properties of the *myc* family proteins in early, but not in later developmental stages of embryogenesis. This redundancy allows them to survive through the early stages of embryogenesis in spite of their mutations (Charron *et al.*, 1992; Stanton *et al.*, 1992; Sawai *et al.*, 1993).

Interestingly, cell lines derived from c-Myc null embryos are able to proliferate *in vitro*, though it is not understood why this happens (Davis *et al.*, 1993). The notion that L-Myc or N-Myc are able to substitute for the absent c-Myc in these cells does not apply in these cells since experiments also indicate that they have no detectable N-Myc or L-Myc expression (Mateyak *et al.*, 1997). Cultured c-Myc-knockout cell lines continue to grow, but have a prolonged G_1 and G_2 phase, though S phase is unaffected (Mateyak *et al.*, 1997). It was demonstrated that *c-myc-/-* cells have a 12-fold lower activity of cyclin D1/Cdk4 and Cdk6 complexes as well as a reduction in activity of cyclin E/Cdk2 and cyclin A/Cdk2 complexes. These cells also showed elevated expression of $p27^{Kip1}$ and decreased expression of Cdk7 (Mateyak *et al.*, 1999).

It is possible that L-Myc or N-Myc may be able to substitute for c-Myc in other cell lines, however. For example, Coppola and Cole (1996) demonstrated that *c-myc* expression blocks dimethylsulphoxide- (DMSO) inducible cellular differentiation of the Murine Erythroleukemia (MEL) F4-12B2 cell line. Later, Dmitrovsky *et al.* (1986) demonstrated the same block of DMSO-inducible differentiation by c-Myc over-expression in Friend-virus-derived MEL cell lines. Birrer *et al.* (1989) showed that L-Myc was able to substitute for c-Myc in blocking DMSO-inducible differentiation in the

Friend virus-derived Murine Erythroleukemia cell line, C19. Also, Birrer *et al.* (1988) showed that L-Myc cooperated with *ras* to transform primary rat embryo fibroblasts. Bush *et al.* (1998) report that c-Myc null cells show no deregulation of any putative transcriptional c-Myc target genes except for *CAD* and *GADD45*, and suggest that these two deregulated genes may contribute to the slow growth phenotype of c-Myc null cells.

In an *in vivo* study, mice were generated where their endogenous *c-myc* coding sequences were replaced by *N-myc* coding sequences (Malynn *et al.*, 2000). These mice were able to survive into adulthood and reproduce. Moreover, when N-myc was expressed from the c-Myc locus, it was regulated in the same way as, and is functionally complimentary to c-Myc in the context of a number of cellular growth and differentiation processes.

Deregulation of the *c-myc* gene as a result of genetic alterations often results in consequences downstream. This type of deregulation is a prerequisite for certain B cell neoplasms. The molecular basis for transformation and neoplasia following deregulation of *c-myc* are still not well understood. The basis for Myc-mediated transformations are slowly being unraveled by studies that reveal Myc target genes and events which are able to link deregulated expression of c-Myc with the transformed phenotype.

Differentiation of B cells involves c-Myc and N-Myc. In general, the *myc* family of genes displays distinct tissue- and stage-specific expression (Zimmerman *et al.*, 1986). N-myc expression in mammals is primarily restricted to the developing embryo, more specifically during the onset of organogenesis (Stanton and Parada, 1992). N-Myc is expressed in a stage-specific manner in differentiating mouse B lymphoid cells. More importantly, c-Myc and N-Myc are differentially expressed during the progression of the

B lymphoid lineage. In B cells, N-Myc and c-Myc are expressed at the PreB cell stage of differentiation and the expression of both is dramatically induced by interleukin-7 (IL-7) (Morrow *et al.*, 1992; Malynn *et al.*, 1995) secreted by the stromal cells. The presence of N-Myc during only the early stages of B cells differentiation suggests a specific function for N-Myc in the early stages of this developmental process. Although there is a significant degree of homology between L-Myc, N-Myc, and c-Myc, there is little overlap in their expression patterns (DePinho *et al.*, 1991). Despite their high sequence homology and minor functional overlap, L-Myc, N-Myc and c-Myc are able to transform cells through common genetic pathways (Mukherjee *et al.*, 1992), though their individual potential to transform cells differs (Hatton *et al.*, 1996 and references therein).

Up-regulation of the *c-myc* gene is seen only twice in the development of B lymphocytes from progenator cells in the bone marrow to Ig-secreting plasma cells in the peripheral blood. c-Myc levels are first increased to high levels in pro-, preBI, and large PreBII cells. During this stage c-Myc is maintained at high levels during the continued proliferation of B cells through several cell cycles. c-Myc protein levels are increased the second time when resting, mature, antigen-sensitive $sIgM^+/sIgD^+$ B cells are stimulated by antigen or polyclonal activation. At this stage, the up-regulation of *c-myc* precedes the entry of G_0-resting cells into the cell cycle (Francis *et al.*, 1997). During the latter up-regulation, the up-regulation of c-Myc is not maintained, but falls to low and even undetectable levels in mature B cells. At the first stage of development, proliferating B cells maintain their level of differentiation so long as they are in contact with stimulating environment of stromal cells and the cytokine IL-7. At the second stage of *c-myc* up-

regulation, these cells mature to memory cells and Ig-secreting plasma cells (see Figure 1.3.1.1 and accompanying figure legend).

The first down-regulation of *c-myc* occurs during cell cycling where large, mature PreBII cells become small, resting PreBII cells and $sIgM^+$ immature B cells (Winkler *et al.*, 1994) and coincides with the rearrangements of V_L to J_L segments of the *Ig L* chain gene loci. The expression of TdT is already down-regulated at this stage and may not be affected by the reduced expression of c-Myc, while the *rearrangement active genes* (*RAG1* and *RAG2*) may be influenced by the alteration in c-Myc expression at this developmental stage. Similarly, Taylor *et al.* (1997), showed that the expression of surrogate L chain is down-regulated at this transition and loss of expression of c-Myc expression.

The reduction of c-Myc levels appears to play an important role in the differentiation of B cells. The PreBII cell compartment is expanded and continuously proliferating in the bone marrow of mice where c-Myc expression is driven by heavy chain enhancer EμH as a transgene that is expressed early in PreB cell development when the μH chain is first expressed (Adams *et al.*, 1985). This suggests that the deficiency in the down-regulation of c-Myc expression at the transition from large PreBII to immature B cells is able to disrupt this transition.

Resting, mature B cells can be stimulated from inactivity to proliferation though Helper-T cell-independent and dependent pathways (Melchers, 1997). In resting, mature B cells, where the cells are activated from the G_0 state into the G_1 stage of the cell cycle, the up- and down-regulation of c-Myc occurs synchronously. c-Myc is up-regulated within the first hours and down-regulated after 5 to 10 hours of stimulation in *all* cells

(Kelly *et al.*, 1984). These stimulated cells enter the first cell cycle asynchronously in spite of synchronous c-Myc activation. In this way a constant part of all of the cells enter the G-phase and the first mitosis from 12 to 24 hours following stimulation, continuing several cycles of 18 hours at low or undetectable c-Myc expression levels. The complex role of c-Myc in the entry of B lymphocytes into cell cycle, and the progression of these cells in their balance of proliferation, differentiation, and programmed cell death through succeeding cell cycles is being elucidated.

1.3.4. The Role of c-Myc in Lymphomagenesis

The process of lymphomagenesis requires the accumulation of several genetic lesions (Magrath, 1992), that are able to provide the lymphoma cell with a selective survival advantage over the normal lymphocytes that are co-localized in the same secondary lymphoid tissue. The translocation of the *c-myc* locus into the immunoglobulin heavy chain enhancer region is a common occurrence observed in many B lymphoid neoplasias (Ohno *et al.*, 1979; Klein and Klein, 1985; Cory, 1986) and results in the constitutive deregulation of the c-Myc protein where affected clones exhibit altered growth characteristics.

Deregulation of c-Myc causes changes in proliferation and differentiation in cells however, singular DNA lesions appear as initiating and necessary factors, but are not in transforming events. Transgenic mice expressing a deregulated *c-myc* gene exclusively in the B lymphocytes are reported to exhibit polyclonal expansion of the preB cell compartment, but without a dramatic increase in the total B cell population (Langdon *et al.*, 1986). The appearance of B cell lymphomas does not occur until 3 to 4 months, despite early *c-myc* deregulation. These PreB cells do exhibit altered growth

characteristics during the initial 3 to 4 months however, the majority of the cells are short-lived. This is likely due to c-Myc-dependent apoptosis of the B cells. It is also likely that the deregulation of c-Myc results over time, in the genomic instability and deregulation of a number of Myc target genes. Over time, the accumulation of genomic lesions in a given cell can result in the triggering of an apoptotic pathway and cell death.

The translocation of *bcl-2* is also common to B cells neoplasias (Tsujimoto *et al.*, 1985) and is a significant event since its translocation plays a fundamental role in the tumorigenic process. Mice expressing a deregulated *bcl-2* gene carry an increased number of small, resting B cells in their secondary lymphoid organs due to a Bcl-2-dependent blockage of normal B cell turnover mediated by programmed cell death mechanisms (Cory, 1986; McDonnel, 1989). *bcl-2* translocation is not in itself transforming, since mice with *bcl-2* translocations do not exhibit tumors until 15 months of age. It is noteworthy though, that 50 % of these mice also carry *c-myc* translocations (McDonnell and Korsmeyer, 1991). The findings in mice are validated by human studies that revealed the translocation of both *bcl-2* and *c-myc* in human B cell neoplasias (Gauwerky *et al.*, 1988). In summary, these data are supportive of a "multi-hit" mechanism for cellular transformation, since mice over-expressing either c-Myc or Bcl-2 alone do not develop neoplasia for extended periods of time, even though DNA lesions and over-expression of both proteins is detectable quite early.

It is not yet understood why the translocation of *c-myc* and *bcl-2* into the heavy chain locus of the immunoglobulin gene appear to be the most commonly translocated genes during the course of B cell development and proliferation. It is possible that there are numerous translocation targets. Translocation of *c-myc* and/or *bcl-2* into other targets

may be lethal or simply not offer a growth advantage, so these cells are selected against. Translocations into the immunoglobulin loci may offer a growth advantage and facilitate tumorigenesis. It is likely that these translocations are occurring during the V(D)J rearrangement of the immunoglobulin loci. It is thought that during this process, some preB cells undergo illegitimate translocations, resulting in rearrangements within *c-myc* or *bcl-2* and in the over-expression of either c-Myc and/or Bcl-2. While it is agreed that these changes are not sufficient to transform the cells, these cells are considered to be in a preneoplastic state. It is possible that a combination of carcinogens and antigenic stimulation of cells already in a preneoplastic state may confer a growth advantage over other unaltered cells. This growth advantage coupled with additional lesions in Myc target genes may facilitate the transformation process and progression to a neoplastic state. In essence, *c-myc* deregulation alone is insufficient for the development of a tumor. Müller *et al.* (1996) demonstrated that the molecular machinery for interchromosomal rearrangements is found in the cells of all strains of mice, however, some mice are resistant to the subsequent development of plasmacytomas. Moreover, it is possible for normal mice to generate a large number of lymphocytes that carry a recombined *c-myc*, yet they do not develop plasmacytomas (Müller *et al.*, 1997). These data suggests that the recombination that leads to *myc* deregulation is not the only requirement for tumorigenesis or tumor progression. Other genetic perturbations must occur that will give rise to a clone with a selective growth advantage. In some strains, the cells are susceptible to those changes and develop a high incidence of tumors. Cells from other stains are resistant and do not develop tumors as frequently in spite of the recombination of *c-myc* with an immunoglobulin locus.

1.4 c-Myc

1.4.1 c-Myc Deregulation

c-Myc is of considerable interest, since the frequency of genetic alterations of the *c-myc* gene resulting in altered expression of the protein in could directly be involved in the estimated 70,000 cancer deaths in the United States each year (for review see Dang and Lee, 1995). These deaths represent roughly one seventh of the total of the annual cancer-related mortality in that country. Literature searches conducted for topics concerning c-Myc reveal span several decades of work. More than 10,000 citations are made to-date, yet there is still much that remains unclear about the c-Myc gene and its protein product.

In human cancers, the c-Myc protein can be deregulated through translocation (as described earlier) by gene amplification, or by point mutation, The *c-myc* gene can be translocated into the immunoglobulin loci (see Section 1.3.), giving rise to lymphoid malignancies (Cole, 1986; Marcu *et al.*, 1992). Its expression can also be deregulated through amplification of the *c-myc* gene, a phenomenon found in lung (Little *et al.*, 1983), breast (Mariani-Constantini *et al.*, 1988; Munzel *et al.*, 1991), and colon carcinomas (Augenlicht, 1997). In addition to *c-myc* activation through deregulated expression, point mutations in the coding sequence have been found in the translocated *c-myc* alleles of Burkitt lymphoma patients. These mutations are clustered around two major phosphorylation sites in the transactivation domain of c-Myc (Bhatia *et al.*, 1993, 1994; Clark *et al.*, 1994; Yano *et al.*, 1993). One of these sites is subject to O-linked glycosylation (Chou *et al.*, 1995a, 1995b; Gu *et al.*, 1994; Hoang *et al.*, 1995; Lüscher and Eisenman, 1992; Lüscher *et al.*, 1989; Lutterbach and Hann, 1994). Though there is

no concrete evidence, it is thought that these mutations abrogate negative regulation of the protein (Smith-Sorensen *et al.*, 1996). Alternatively, these mutations may prolong the half-life of the mutant protein, since the affected regions are implicated in the proteosome-mediated degradation of c-Myc (Flinn *et al.*, 1998).

1.4.2. A Brief History of c-Myc Oncoprotein

The history of *c-myc* is one that started in the early part of the twentieth century (For review see, Potter and Marcu, 1997 in *c-Myc in B Cell Neoplasia*). It begins ca. 1908 with Wilhelm Ellerman and Olaf Bang, who demonstrated that erythroleukemias in chickens could be transmitted with cell free lysates. The first avian tumor containing what was later identified as the *v-myc* gene was the Murray-Begg endothelioma, known as MH-2 (Begg, A.M., 1927; Graf, T. and Beug, H., 1978). In the end, the virus isolated from MH-2 was found to contain *v-myc* and *v-raf-1* (Sutrave *et al.*, 1984). In the mid 1960's, the prototypic *v-myc*-producing MC29, a virus strain was isolated in Bulgaria and thought to be a myelocytoma (Bister *et al.*, 1979; Mladenov *et al.*, 1967; Vogt, 1979). Two additional myelocytomatosis viruses were isolated, the CMII virus in 1964 and the OK10 virus in 1977. The four viruses MH-2, MC29, CMII, and OK10, were grouped on the basis of their ability to transform monocytes (Graf, T. and Beug, H., 1978). RNA fingerprinting studies of the MH-2, MC29, CMII, and OK10 transforming viruses revealed that they all contained a common element, the *v-myc* oncogene, associated with transformation (Bister *et al.*, 1979; Duesberg, and Vogt, 1979). Myc was not found in any other transforming viruses, including the Rous Sarcoma Virus.

Manolov and Manolova (1972) were the first to show evidence of chromosomal translocations on human chromosome 14 and described them as marker bands for

Burkitt's lymphoma. Hayward *et al.* (1981) were the first to demonstrate that Avian Leukemia Virus (ALV) induced lymphomas in the chicken and that ALV was consistently associated with retroviral insertion into the 5' region of *c-myc*. They made first associations of the *c-myc* gene with B cell neoplasia. These lymphomas were shown to form in the Bursa of Fabricius and to be of B cell origin. The association of the cell type was based first on histological evidence of the preneoplastic lesions in the bursa (Cooper *et al.*, 1968). The first paper by Hayward *et al.* (1981) was followed by the identification of the *c-myc* protooncogene as the consistent target of the retroviral insertion (Neel *et al.*, 1981). With the discovery of the retroviral promoter insertion came the understanding of a new form of oncogenic mutagenesis and this generated a novel direction in cancer research (Payne *et al.* 1981).

An equally exciting discovery was made regarding B cell neoplasia, but in a non-virus-associated system. An increasing volume of evidence revealed that the t(8;14) chromosomal translocation was a consistent feature of sporadic and endemic Burkitt lymphomas in humans (Zech *et al.*, 1976). In humans *c-myc* is located on chromosome 8q24.12-13 and the Immunoglobulin Heavy chain locus (*IgH*) is located on chromosome 14q32.33 (NIBC Genbank, http://www.ncbi.nlm.nih.gov/Omim/Homology/). Recently, Gerbitz *et al.* (1999) demonstrated deregulation of *c-myc* that resulted from t(8;22) translocation in Burkitt lymphoma as well. Ohno *et al.* (1979) analyzed a series of early transfer generation paraffin oil induced peritoneal plasmacytomas in mice, and found that they all had either t(12;15) or t(6;15). Based on the locations of the *immunoglobulin* (*Ig*) *heavy chain* on chromosome 12, the *kappa light chain* on chromosome 6, and *c-myc* on chromosomes 15, it suggested the possibility that one of the translocation partners was an

immunoglobulin (Ohno, *et al.*, 1979). A number of laboratories described *Ig* switch regions that were found to contain non-*Ig* DNA sequences. Several important studies demonstrated that the non-*Ig* DNA was *c-myc*. Dalla-Favera *et al.* (1982) showed that the non-Ig DNA on chromosome 8 at the t(8;14) breakpoint was human *c-myc* gene locus. At the same time, Shen-Ong *et al.* (1982) studying the structure of the *c-myc* gene locus in mouse plasmacytoma, demonstrated that it was rearranged and recombined with the *Ig* heavy chain switch region on chromosome 12 in the t(12;15). Then Harris *et al.* (1982) showed DNA sequences in plasmacytoma cells that are not found in normal B lymphocytes. These aberrant sequences did not originate from the heavy chain region, C_H, and were referred to as non-immunoglobulin-associated rearranging DNA (NIARDs), were found to involve the switch regions of the C_α gene and chromosome 15. Harris *et al.* (1982) proposed the idea of reciprocal translocation, rcpT(12;15) model to explain their data.

Based on the studies of cellular localization of the *v-myc* gene (Hann *et al.*, 1983), it was established that the c-Myc protein was found primarily in the nucleus. Land *et al.* (1983) had shown in their cellular transformation studies that oncogenes could be separated into two complementary groups, one located in the cytoplasm and the other in the nucleus. The prototypic nuclear oncogene was *myc* and in the cytoplasmic group was *H-ras*. Alone neither of these genes was able to transform rat embryo fibroblasts, but together they did succeed in immortalizing them.

It was suspected for quite some time that Myc was a sequence specific DNA binding protein (Donner *et al.*, 1982; Persson and Leder, 1984), though its ability to bind DNA sequences specifically was also heavily debated (Kato *et al.*, 1992). After structural

comparison with other E-Box proteins, Myc was assigned as one of the founding members of the dimerizing helix-loop helix family of transcription factor proteins (Murre *et al.*, 1989). It was not until Blackwell *et al.* (1990) demonstrated sequence specificity on synthetically synthesized oligonucleotides that a specific DNA binding activity was assigned to Myc. They showed that the CACGTG sequence was the canonical six base pair core for the Myc protein-binding motif. Blackwood and Eisenman (1991) revealed very soon after, that at physiological concentrations, Myc was only able to bind DNA *in vivo* as a heterodimeric complex consisting of Myc and Max, another helix-loop-helix transcription factor.

Further experiments involving the *c-myc* oncogene were also conducted in animal models. *c-myc* transgenic mice were developed in 1984 using a normal mouse *v-myc* gene and driven by mouse mammary tumor virus (MMTV) promotors (Stewart *et al.*, 1984). These mice developed a high incidence of mammary adenocarcinomas as well as other tumors (Pattengale *et al.*, 1986; Leder *et al.*, 1986). A different type of *c-myc* transgenic mouse was developed in 1985 (Adams *et al.*, 1985). It was constructed using the *c-myc* gene driven by immunoglobulin enhancers that ensured the constitutive expression of the c-Myc protein in B lineage cells. These mice developed a high incidence of PreB and B cell lymphomas. It was shown that these mice developed a polyclonal expansion of the early B cell population and clonal B cell tumors that developed after several months. It is thought that these begin with the deregulated *c-myc* gene and are followed by additional stochastic oncogenic changes in the cells of this expanded population of early B cells. These changes accumulate, and in accordance with the multi-step model for tumorigenesis and tumor progression, a number of genetic lesions are accrued that allow

for the cell to escape growth control and can initiate the formation a tumor. More changes may occur which can allow for the development of a metastatic phenotype within these PreB and B cell compartment.

1.4.3. The Role of c-Myc in the Cell

c-Myc is a multifunctional oncoprotein (Lüscher and Eisenmann, 1990; for review see Marcu *et al.*, 1992). It is known to play pivotal roles in the cell cycle and in cell cycle progression (Heikkila *et al.*, 1987; Kam *et al.*, 1989), replication (Classon *et al.*, 1987; Classon *et al.*, 1990; Classon *et al.*, 1993), and development (Paria *et al.*, 1992; Lemaitre *et al.*, 1996). Furthermore, it is involved in transformation (Eilers *et al.*, 1989; Thompson *et al.*, 1989; Chisholm *et al.*, 1992), neoplasia and tumor progression (Cole, 1986; Spencer and Groudine, 1990), and apoptosis (Evan *et al.*, 1992; Shi *et al.*, 1992; for review, see Packham and Cleveland, 1995; Donzelli *et al.*, 1999). During normal cellular proliferation, c-Myc protein expression is tightly regulated (Cole, 1986; Heikkila *et al.*, 1987; Kam *et al.*, 1989; Hanson *et al.*, 1994). c-Myc has been reported to be involved in the transcriptional regulation of specific cyclins, such as *cyclins E, A*, and *D1* (Jansen-Dürr *et al.*, 1993; Daksis *et al.*, 1994; Philipp *et al.*, 1994), cyclin dependent kinases (cdks) (Steiner *et al.*, 1995), and the phosphatase *cdc25a* (Galaktionov *et al.*, 1996). c-Myc activation has recently been shown to play a role in cell cycle progression and proliferation through the sequestration of $p27^{Kip1}$ and $p21^{Cip1}$ (Bouchard *et al.*, 1999; Perez-Roger *et al.*, 1999). In addition, c-Myc promotes DNA replication (Classon *et al.*, 1987; Classon *et al.*, 1990; Classon *et al.*, 1993). Lewis *et al.* (1997) describe the characterization of *rcl*, a growth related gene that is stimulated by expression of c-Myc. Later studies showed that *rcl* is involved in cell cycle regulation and/or apoptosis control (Fang *et al.*, 1999). Recently, Kyo *et al.* (2000)

demonstrated c-Myc and SP1cooperate to the activate transcription of the human telomerase catalytic subunit (hTERT) and may play a role in attainment of cellular immortality.

An increased half-life of c-Myc is associated with immortalization and transformation (Eilers *et al.*, 1989; Thompson *et al.*, 1989; Chisholm *et al.*, 1992). It has also been shown that elevated c-Myc levels disrupt proliferation control. A recent paper by Li and Dang (1999) suggest that deregulated c-Myc expression plays a role in genomic instability through c-Myc-dependent induction of DNA re-replication by activating CDK2 in G_1-state cells that are usually low in CDK2 at that the G_1 stage of the cell cycle. Iratini and Eisenman, (1999) recently described findings showing that constitutive expression of *c-myc* in Eμ-myc mice results in increased cell size and an elevated rate of protein synthesis in pretransformed B lymphocytes at all stages of B cell development. They hypothesize that these c-Myc dependent alterations may predispose cells to cancer by enhancing cell growth rates to levels required for unrestrained cell division.

The deregulation of c-Myc is emerging as an important component in promoting or enhancing genomic instability. In was shown that c-Myc promotes gene amplification of the *dihydrofolate reductase* (*DHFR*) (Denis *et al.*, 1991; Mai, 1994a; Mai *et al.*, 1996a) and *cyclin D2* (Mai *et al.*, 1999) genes. Mai *et al.* (1996b), were the first to describe c-Myc-induced karyotypic instability in Rat1A cells that over-express c-Myc.

The deregulation of c-Myc (but not L-Myc) expression, coupled with the loss of p53 cooperates to promote genomic instability. However, *c-myc* deregulation can bypass wildtype p53 function (Mai *et al.*, 1996b) The restoration of p53 function in these c-Myc over-expressors results in apoptosis, suggesting the restoration of the ability to induce the killing of cells that are genetically damaged and beyond repair (Yin *et al.*, 1990). Chernova

et al. (1998) describe coamplification of *carbamoyl-phosphate synthetase-aspartate transcarbamyol-dihydroorotase* (*CAD*) and *N-myc* in "non-permissive" REF/52 cells exposed first to non-selective concentrations of *N*-(phosphonacytyl)-L-aspartate (PALA) followed by high selective concentrations of PALA. The study demonstrates two distinct events where initial low levels of PALA result in DNA damage resulting in the coamplification of both *N-myc* and *CAD*. Subsequent increases in N-Myc protein due to the amplification of *N-myc* allow for the cell to bypass p53-mediate arrest and apoptosis following DNA damage. At the same time, the coamplification of *CAD* facilitates CAD protein over-expression and allows for the cell to survive high, selective doses of PALA.

In *in vivo* studies, Fukasawa *et al.* (1997) showed that in p53-nullizygous ($p53^{-/-}$) mice, multiple centromeres and abnormally formed mitotic spindles were found in an increased number of cells from several organs. c-Myc levels were also elevated in an increased population of these mouse cells. Moreover, these cells showed amplification and over-expression of two c-Myc target genes, *DHFR* and *CAD*, as had been shown earlier in *in vitro* studies of c-Myc deregulated cells. Recently, Felsher and Bishop, (1999) described genomic instability and tumorigenicity in the same cells following transient c-Myc deregulation.

It has been shown that c-Myc/Max heterodimers in cellular extracts bind to two adjacent E-box motifs 5' of the gene encoding *DHFR* (Mai and Jalava, 1994; Wells *et al.*, 1996). Binding was correlated with cellular proliferation and DNA synthesis. Inducible over-expression of c-Myc was followed by increased binding of c-Myc/Max heterodimers to the *DHFR* 5'-flanking E-box motifs and *DHFR* gene amplification (Mai, 1994a; Mai *et al.*, 1996a). The amplification of the *DHFR* gene leads to the enhanced

expression of the DHFR protein (Lücke-Huhle *et al.*, 1997). c-Myc was also shown to bind to four E-box motifs located in the 5' flanking region of both murine and human *cyclin D2* genes (Mai, 1994b).

1.4.4. c-Myc Targets and Neoplastic Transformation

A gene whose expression is altered by direct interaction with a particular protein is considered to be a target of that protein. By virtue of this definition, a direct Myc target gene can be defined as a gene whose expression has been altered by direct interaction of the c-Myc protein with the gene-regulatory *cis*-acting elements, or with transactivating factors that bind these *cis*-elements. A transcriptional c-Myc target is a gene that is directly up- or down-regulated by c-Myc expression. There are a number of regulatable systems that are able to directly test the effect of c-Myc on a target gene. One system consists of a pJ5 plasmid harboring a dexamethasone-inducible mouse mammary tumor virus long terminal repeat- (MMTV-LTR) driven *c-myc* DNA (exons II and III) (Mai, 1994a). Addition of 1 μM dexamethasone to the culture medium of cells containing this expression vector induces the increased transcription and translation of c-Myc. A different system, the Myc-Estrogen Receptor (Myc-ER) was initially developed by Eilers and Bishop (1989) to be activated by estrogen. A later version, the Myc-ER™ (Littlewood *et al.*, 1995) was designed to be refractory to estrogen, but activated by the antiestrogen, 4-hydroxytamoxifen. Both Myc-ER versions are able to test the effect of controlled c-Myc deregulation on the expression of a target gene. In either version of this system, the Myc-ER or Myc-ER™ constructs are tethered to chaperone proteins on the carboxyl terminus of the fusion protein in the absence of the estrogen or 4-hydroxytamoxifen, respectively. The addition of the estrogenic ligands results in the

displacement of the chaperone proteins and allows c-Myc to heterodimerize with its functional partner, Max. Once dimerized, the heterodimers are able to translocate to the nucleus and activate target genes. Figure 1.4.4.1. illustrates the multiple links between c-Myc and its putative target genes as well as the cellular functions in which c-Myc plays a role. One can envision that activation of a target gene by c-Myc occurs within several hours of the up-regulation of c-Myc. The immediate expression from a target gene following deregulation of c-Myc is understandable.

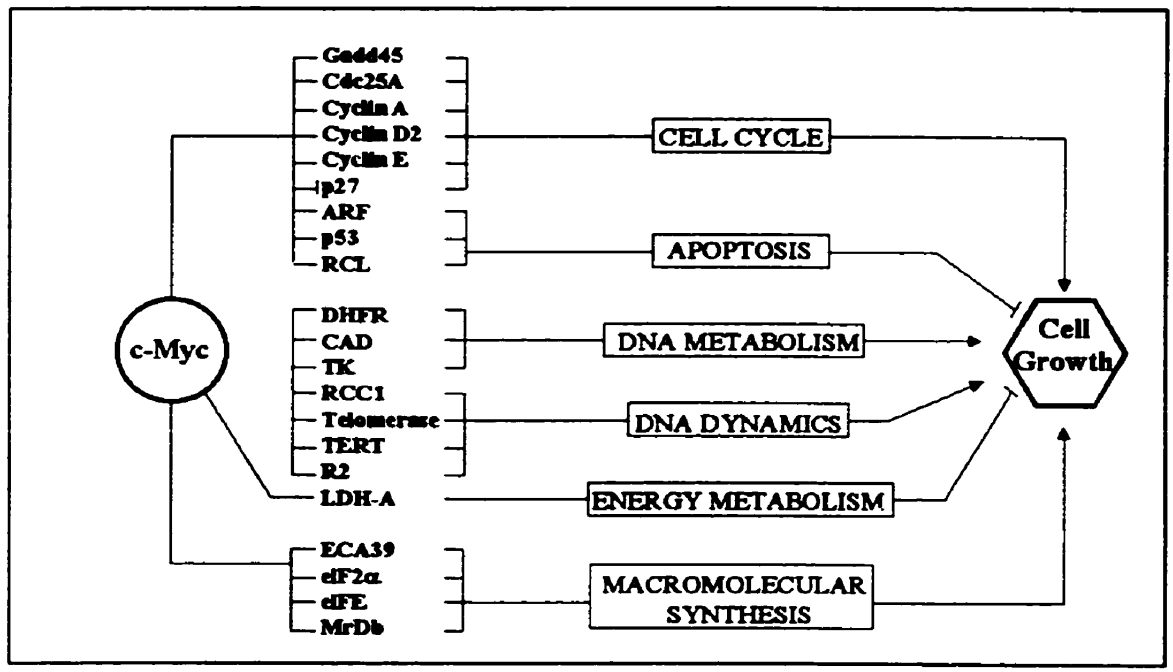

Figure 1.4.4.1. Links Between c-Myc and Putative Target Genes.

Note the complexity of c-Myc interactions with its numerous targets, according to their functions. Various functions cooperate to promote cell growth. (Modified from Dang, 1999; Wu *et al.*, 1999; Fang *et al.*, 1999). (Note: This diagram does not reflect controversies over authentication of various target genes).

Myc-dependent genomic or karyotypic instability is not visible as the immediate result (*i.e.* with a few hours) of c-Myc deregulation. It is noteworthy that c-Myc dependent locus-specific instability is visible within 24 hours (this thesis), while karyotypic instability becomes apparent following roughly three passages.

For the purpose of this study we focus on c-Myc targets defined as those whose gene copy number or general genomic stability and/or subsequent expression are altered deregulated following c-Myc deregulation. The genes that can thus far be classed as amplification targets of c-Myc include only *DHFR* (Mai, 1994a; 1996; Mai and Jalava, 1994) and *Cyclin D2* (Mai *et al.*, 1999). These genes both carry Myc/Max-binding E-box sequence motifs in their 5'-flanking regions and are amplified and over-expressed following transient c-Myc deregulation. The effect of c-Myc on gene copy number is observed by fluorescent *in situ* hybridization (FISH) and dispersed cell assays (DCAs) following several cycles of replication and illegitimate re-replication of the genome, usually only within 72 hours of deregulation. This work allowed us to define the initiation of c-Myc-dependent genomic instability of the *ribonucleotide reductase R2* gene within 72 hours. Two-dimensional gel electrophoresis and Southern analyses and bromodeoxyuridine (BrdU) incorporation assays were able to demonstrate illegitimate re-replication leading to chromosomal amplification of the *R2* gene within 24 hours of *c-myc* deregulation.

Indirect targets of c-Myc are those whose expression requires the new synthesis of proteins following activation of Myc and whose expression is directly related to c-Myc mediated phenotype such as cellular proliferation, transformation, or apoptosis. Examples of this include the c-Myc dependent genomic and/or karyotypic instability that

leads to a p53-mediated programmed cell death in the absence of appropriate growth factors.

It is not difficult to envision the broad spectrum of effects that might be elicited on several levels of cellular function by the deregulation of the *c-myc* gene. c-Myc deregulation, be it due to *c-myc* locus translocation, gene amplification, *c-myc* mutation, or lack of negative control of the protein, is detrimental to the cell.

1.4.5. Regulation of *c-myc* Transcription and the c-Myc Protein

The function of c-Myc is regulated in at least six ways, based on the present information: (i) transcription, (ii) mRNA stability, (iii) post-translational modification of the Myc proteins, (iv) Myc protein stability, (v) c-Myc binding to other proteins and (vi) rate of Myc/Max complex formation. These are described in more detail below. (For review see Potter and Marcu, 1997)

1.4.5.1. Transcription of the *c-myc* Gene

As many as 20 transcription factors have been documented to recognize control elements positioned within the promoter regions of the human and mouse *c-myc* genes. Some of these include TBP, YY1, TF-II and are described in more detail below. *c-myc* was the first cellular gene that was shown to be regulated by transcriptional elongation (Bently and Groudine, 1986; Eick and Bornkamm, 1986; Nepveu and Marcu, 1986), representing stalled RNA polymerase II initiation complexes which are proximally paused on the major *c-myc* P2 translation start site (Strobl and Eick, 1992; Krumm *et al.*, 1992, 1995; Wolf *et al.*, 1995). Proximal pausing is regulated by positive and negative inducers of transcription. For example, *c-myc* in humans and mice is positively regulated by direct interaction with FBP, Sp1, YY-1, and NFκB and negatively regulated by

interaction with CTCF and ZF5 (For review see Potter and Marcu, 1997 and references therein). This allows for more flexible regulation of *c-myc* transcription.

There is reason to believe that distant dominant control elements also play a role in the regulation of *c-myc* transcription. Transcriptional initiation is governed by a number of *cis*-acting elements that have been identified within the 5'-flanking region. These promoter-proximal control elements have been shown to correct initiation and expression of *c-myc* in transfection assays (Nishikura, 1986; Hay *et al.*, 1987; Lipp *et al.*, 1987) however, they are not sufficient for *c-myc* expression after stable transfection (Polack *et al.*, 1991) or in transgenic mice (Lavenu *et al.*, 1994). Reconstructed *c-myc* genes that carry all three exons and varying amounts of the 3'- and 5'- sequences are regulated differently in both cell culture (Mautner *et al.*, 1996) and in *c-myc* transgenic mouse models (Lavenu *et al.*, 1994). Maunter *et al.* (1995) identified two enhancer elements downstream of the human *c-myc* gene. Lavenu *et al.* (1994) suggested that additional regulatory elements found upstream as far as 3500 bp from the P1 promoter and downstream as far as 1500 bp from the polyadenylation sites are required for the proper initiation of transcription.

The *c-myc* gene is also subject to transcriptional autosuppression mediated *in vivo*, directly or indirectly by Myc/Max heterodimer binding. This function overlaps structurally with Myc domains that are required for cellular transformation (Penn *et al.*, 1990). The members of the Myc family of proteins are also known to reciprocally repress one another, which is strongly suggestive of a conserved control mechanism (DePinho *et al.*, 1991). Such a mechanism may allow for a threshold level where the over-expression of Myc is concerned and may be critical for the control of normal physiological growth.

It was demonstrated that many transformed cell lines have lost autocontrol of their endogenous Myc, while other immortal cell lines maintain their Myc autoregulation loop and retain contact inhibition during their growth (Penn *et al.*, 1990; Facchini, *et al.*, 1997).

1.4.5.2. *c-myc* mRNA Stability

The second mechanism controlling c-Myc expression is the stability of its messenger RNA. This question has been studied quite intensively following the initial report by Dani *et al.* (1984) that *c-myc* mRNA normally exhibited a very short half-life. Yeilding *et al.* (1996) have shown that the (in)stability of the *c-myc* transcript is regulated in two areas, one in the 3'-untranslated region (3'-UTR), and the other in exon 3. *c-myc* mRNA half-life is extended from its normal 30 minutes to several hours by mutations in either region (Yeilding *et al.*, 1996.)

1.4.5.3. Post Translational Modification of the c-Myc Protein

The third mechanism regulating *c-myc* expression in cells is post-translational modification of the c-Myc protein. Modifications include phosphorylation (Lüscher *et al.*, 1989, 1992; Bousset *et al.*, 1994) and transport of the c-Myc protein from the cytoplasm to the nucleus, though modifications such as phosphorylation and are not considered a major regulatory mechanism.

1.4.5.4. Binding of c-Myc to Other Proteins and Transcription Factors

The c-Myc protein interacts with a number of proteins as is shown by Figure. 1.4.5.4.1. Many of the interactions with the c-Myc protein occur on domains other than the helix-loop-helix/leucine zipper domain, which are bound by Max. These proteins include TFII-I, YY1 (transcription regulators), myoD, Retinoblastoma, cyclin D1 (also

known as Bcl-1), Blimp-1, (for B lymphocyte-induced maturation protein), an inducer of terminal differentiation in B lymphocytes) (Lin *et al.*, 1997), and Miz-1 (Myc-interacting zinc-finger protein) (Schneider *et al.*, 1997), whose function is not yet understood. c-Myc also binds to a growing list of other transcription factors. In addition to TF-II-I and YY1 (mentioned above) it binds TFII-F and TBP (TATA Binding Protein). A number of these bind Myc, resulting in repression of *c-myc* transcription (Roy *et al.*, 1993; Lee *et al.*, 1996; Li *et al.*, 1994) or repression of differentiation (La Rocca *et al.*, 1994). The c-Myc protein has been shown to repress transcription through motifs located in the 143 amino acid amino terminal transactivating domain, especially in the highly conserved myc BOX I (Sakamuro *et al.*, 1996) and myc BOX II (Li *et al.*, 1994) regions. Mai and Mårtensson (1995) showed that c-Myc/Max heterodimers interact with the transcription initiator sequences of *TdT* and *λ5* resulting in repression of their transcriptional activities.

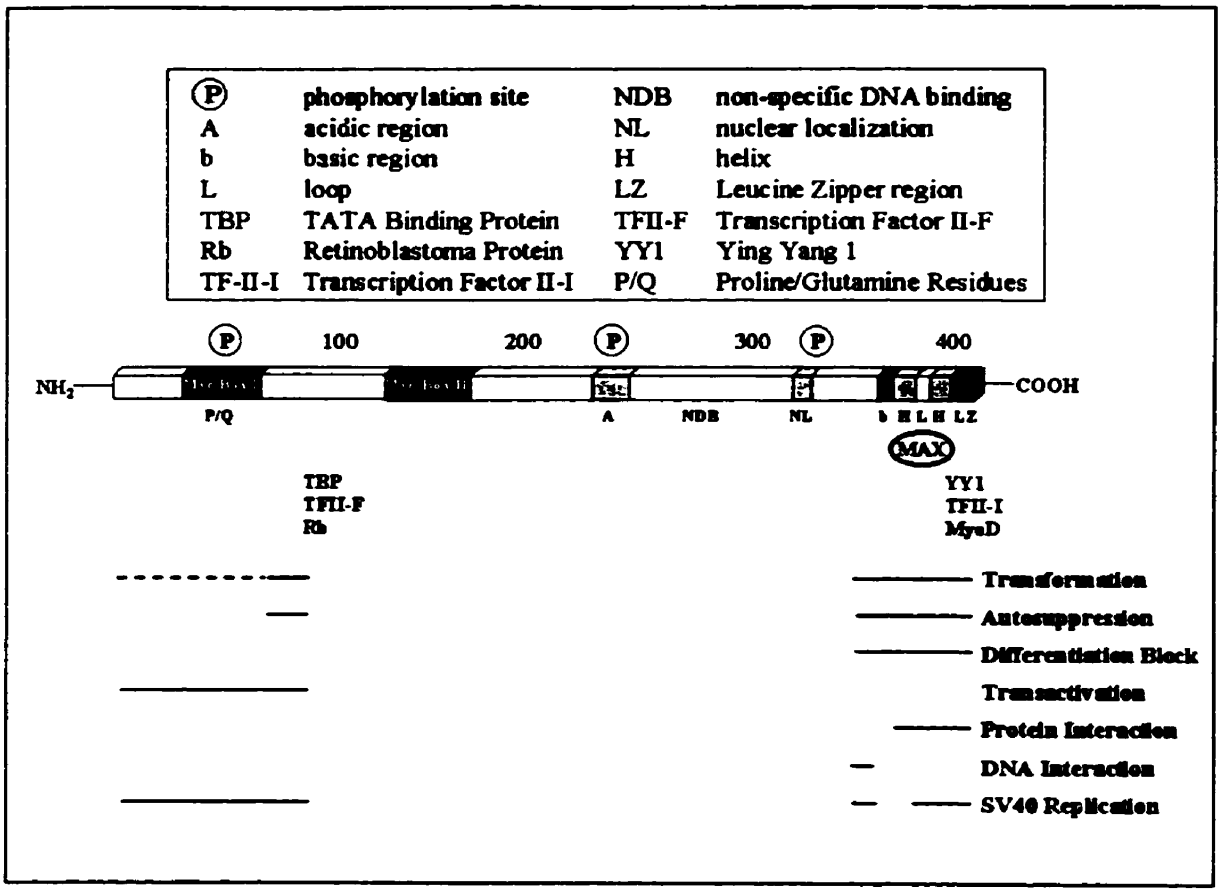

Figure. 1.4.5.4.1. The c-Myc Protein and its Binding Domains.

Modified from Potter and Marcu (1997) in **c-Myc in B Cell Neoplasia.** *Curr. Top. Microbiol. Immunol.* **224:** 1-17. Potter and Melchers (Eds.) and Classon *et al.* (1993).

1.4.5.5. c-Myc Protein Stability

One of the most important factors regulating c-Myc function is the stability of the protein product. An essential feature of c-Myc function is its scarcity in the cell. Studies of cycling fibroblasts by Waters *et al.* (1991) gave estimates of only 3000 to 6000 Myc protein molecules per cell. Hann and Eisenman (1984) describe a Myc half-life of only 20 to 30 minutes.

1.4.5.6. Heterodimerization of c-Myc with Max

Heterodimerization of Max with the c-Myc protein is an important regulatory feature. The Myc/Max heterodimer is known to play a significant role in a number of cellular functions (see section 1.4.3.) such as cellular proliferation, differentiation, apoptosis, and transformation. The E-box motif which is bound by Myc/Max is found on a number of genes such as outlined in (Mai *et al.*, 1999; Kuschak *et al.*, 1999a) and perhaps *LDH-A* (Lee and Dang, 1997). The formation of heterodimers with Max governs the binding to and regulation of a number of genes and their expression.

It was shown by Eisenman *et al.* (1991), that Myc/Max heterodimers recognize the CACGTG sequence with high affinity. Non-canonical E-box motifs are also bound by Myc/Max heterodimers (Sommer *et al.*, 1999). Max/Max homodimers are also able to bind, but with a lesser affinity. Studies involving the activation of a reporter gene linked to a four-fold repeat of CACGTG sequence showed that transfection of exogenous Myc resulted in the activation of the reporter gene, exogenous Max resulted in repression of tanscription (Kretzner *et al.*, 1992). It was concluded that even though Myc is unable to function without Max and only functions through Max, excessive levels of the Max protein lead to the formation of Max/Max homodimers. These are associated with repression of transcription. Ayer *et al.* (1993) showed that Max associates with a protein called Mad (for Max Associated Dimer), and Zervos *et al.* (1993) showed Max interaction with yet another protein, Mxi. Mad has a basic region that is similar to that found in Myc, but its helix-loop-helix and leucine zipper region are quite different. For this reason, Mad is not considered a part of the Myc or Max families. Both Mad and Mxi are similar, showing roughly 50% amino acid sequence homology in the HLH-zip and C-

terminal tail. Experiments measuring interaction of Myc/Max with the CACGTG sequence showed that this heterodimer interacts with high specificity, while Mad, like Myc, does not form homodimers or bind DNA on its own.

Clearly, the network of proteins that interact with the c-Myc protein is complicated. For example, the function of c-Myc is regulated by interactions with Max, as has been mentioned above. Max interaction is in turn regulated by a "secondary" network of proteins from the Mad family of proteins. These include Mnt (Hurlin *et al.*, 1997), Mad1, Mad2 (Mxi-1), Mad3, and Mad4 (Hurlin *et al.*, 1994). Regulation of mad interactions are in turn governed by another complex of proteins such as the N-COR and SMRT/mSin3 proteins which interact with histone deacetylase (HDAC) protein to suppress transcription (Ayer *et al.*, 1995; Laherty *et al.*, 1997; Heinzel *et al.*, 1997; Wong and Privalsky, 1998). The interaction Mad protein with Max is further governed by Mlx (Billin *et al.*, 1999). As can be envisioned, the regulatory umbrella of proteins that play a role in c-Myc function is large and it is still expanding.

1.5 Ribonucleotide Reductase

1.5.1. The Ribonucleotide Reductase Enzyme

Ribonucleotide diphosphate reductase (EC1.17.4.1) is a unique and highly regulated enzyme. From biological, structural, and regulatory perspectives, it is one of the most complex enzymes in the cell (Wright, 1989 and references therein). It catalyzes the first unique steps leading to DNA synthesis (Thelander and Reichard, 1979; Reichard 1988). It is present in all dividing cells and provides the cell with a balanced supply of the four deoxyribonucleotides required for DNA synthesis (Thelander and Reichard, 1979).

Ribonucleotide reductase is solely responsible for the conversion of ribonucleosides to deoxyribonucleosides (Wright, 1989).

Enzyme activity is correlated strongly with the rate of DNA synthesis and shows maximum activity in the S phase of the cell cycle. It resembles other enzymes such as thymidine kinase (Littlefield, 1996), thymidine synthetase (Conrad, 1971), and DNA polymerase (Fry and Loeb, 1986) in this respect, since these enzymes are also most active during DNA synthesis.

1.5.2. Structure of the Ribonucleotide Reductase Enzyme

The mammalian ribonucleotide reductase protein is composed of two non-identical subunits, proteins R1 and R2 (Figure 1.5.2.1). Both subunits have been purified to homogeneity and the corresponding cDNAs have been cloned from mouse cells and sequenced (Caras *et al.*, 1985: Thelander and Berg, 1986). The R1 protein has a molecular weight of 2 x 84 kDa and contains binding sites for nucleoside triphosphate allosteric regulators and ribonucleotide disphosphate substrates (Thelander *et al.*, 1980). Immunocytochemical studies have demonstrated that R1 protein is only present in actively dividing cell lines and it is absent in terminally differentiated cells that no longer synthesize DNA (Engström and Rozell, 1988). The R2 protein has a molecular weight of 2 x 45 kDa and contains a stoichiometric amount of iron in a unique non-heme iron centre that generates and stabilizes a tyrosyl free radical essential for activity (Thelander *et al.*, 1985). Engström and Rozell (1988), demonstrate exclusive cytoplasmic localization of the R2 subunit.

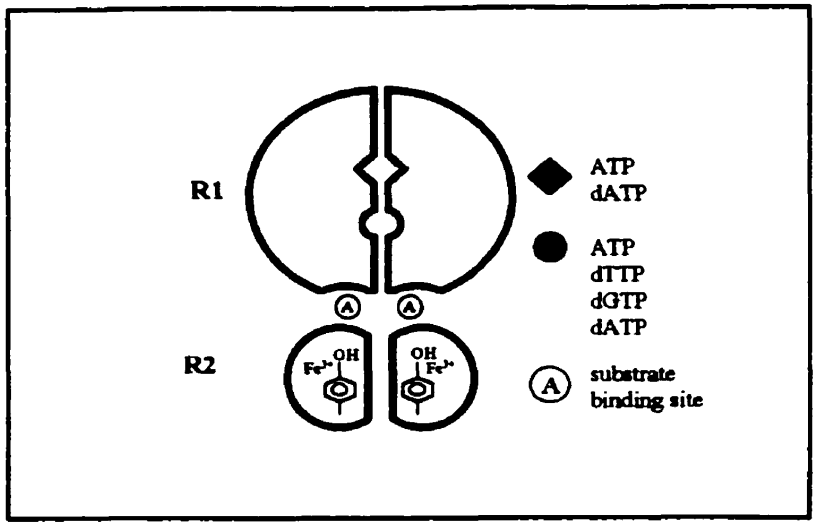

Fig.1.5.2.1 A model for Ribonucleotide Diphosphate Reductase Structure

(Modified from Wright, 1989.)

The R1 protein has a half-life of roughly 20 hours in proliferating cells. Measurements in cell extracts as well as whole cells show that the levels of R1 are nearly constant throughout the cell cycle (Engström *et al.*, 1985: Mann *et al.*, 1988). In contrast, the R2 protein, has a half-life of only 3 hours under the same conditions. Electron paramagnetic resonance measurements of the levels of active R2 in the cell during the cell cycle have shown that it is expressed only in the S phase of the cell cycle (Eriksson *et al.*, 1984; Engström *et al.*, 1985). Holoenzyme activity is controlled during cell cycle by R2 levels in the cell, which are in turn regulated by *de novo* synthesis and breakdown of this subunit (Eriksson *et al.*, 1984). It has been demonstrated that both subunits of the ribonucleotide reductase enzyme are localized in the cytoplasm of the cell (Engström *et al.*, 1984; Engström and Rozell, 1988).

1.5.3 Reactions and Regulation of the Ribonucleotide Reductase Enzyme

DNA synthesis requires an uninterrupted and balanced supply of the four deoxyribonucleoside triphosphates that originate directly from the reduction of the 2'-carbon atom located on the ribose moiety of ribonucleosides. The oxidation-reduction reaction whereby ribonucleosides are reduced to deoxyribonucleosides is shown in Figure 1.5.3.1. Two small proteins, thioredoxin, through the thioredoxin reductase system and glutaredoxin, via glutathione and glutathione reductase, are able to function as hydrogen carriers in these reactions.

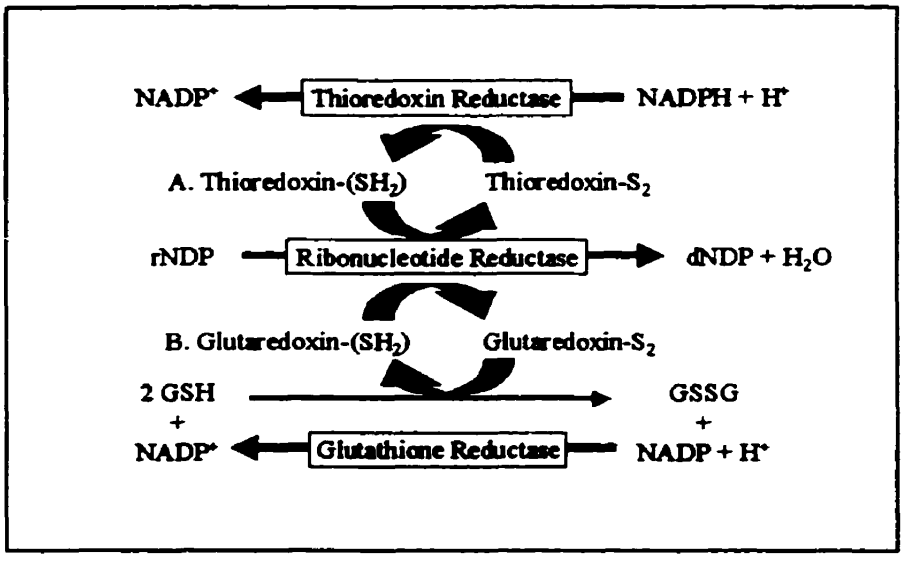

Figure 1.5.3.1 The Reduction of Ribonucleosides to Deoxyribonucleosides (Modified from Wright, 1989).

In mammalian cells the reduction of ribonucleosides to deoxyribonucleosides occurs at the diphosphate level in the presence of ribonucleotide reductase. There is but one exception, dTTP, which arises from the reduction of either UDP or CDP, by the

introduction of a methyl group at the monophosphate level. Enzyme substrate specificity and activity are regulated in a complex manner by nucleoside triphosphate effectors (Figure 1.5.3.2). A brief and simplified outline of ribonucleotide reductase regulation is described as follows: The reductions of CDP to dCDP and UDP to dUDP occur in the presence of an ATP-activated ribonucleotide reductase enzyme. Reduction of GDP to dGDP requires dTTP to be present, while the reduction of ADP to dADP requires dGTP. The reduction of all four ribonucleotide substrates is inhibited in the presence of dATP. Based on these allosteric properties of ribonucleotide reductase, deoxyribonucleotide diphosphate formation begins with the reduction of CDP and UDP to dCDP and dUDP, through an ATP activated reaction. This reaction proceeds to reduction of GDP by a dTTP-regulated activity. ADP reduction is the final step, activated by dGTP. Accumulation of dATP, as is the case during slowing down or complete absence of DNA synthesis, results in the turning off of the enzyme, since dATP is a potent inhibitor of all ribonucleotide reductase reductions. Moreover, dTTP is a good inhibitor of pyrimidine reduction and dGTP functions as a negative feedback inhibitor of GDP reduction as well as inhibiting the reduction of pyrimidines.

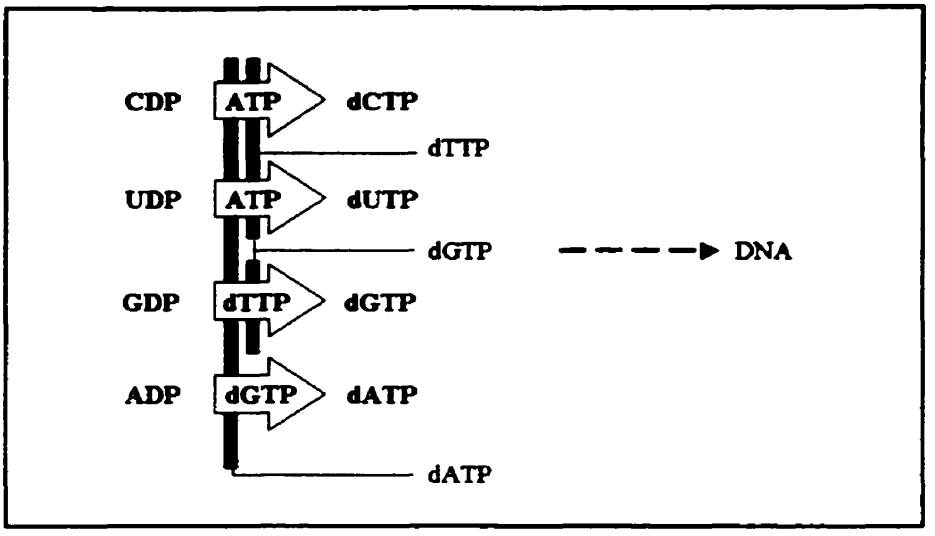

Figure 1.5.3.2 The Allosteric Regulation of Ribonucleotide Diphosphate Reductase. (Modified from Wright, 1989. The thick black bars indicate inhibitory effects; nucleotides shown in the arrows act as positive effectors).

1.5.4. Characterization of Mammalian *Ribonucleotide Reductase* Genes

The genes encoding the R1 and R2 proteins are located on different chromosomes in both human and murine cells. The *R1* gene is found on chromosome 11 in humans and on chromosome 7 in mice (Brissenden *et al.*, 1988). In humans, the active *R2* gene is located on chromosome 2 and in mouse it is found on chromosome 12. In addition to the active *R2* gene, three *R2* pseudogenes are found in both mouse and human genomes (Yang-Feng *et al.*, 1987; Brissenden *et al.*, 1988). The balance of this section will focus on the *R2* gene and protein.

Recently, Tanaka *et al.* (2000) reported the discovery of *p53R2*, a ribonucleotide reductase-related gene in human cells that functions as a p53-dependent cell cycle

checkpoint for DNA damage. The *p53R2* gene shares 80% homology with human *R2*. The up-regulation of p53 (following UV irradiation or treatment with the antineoplastic agent adriamycin) is followed by the subsequent elevation of p53R2, and a corresponding reduction in R2 levels. Little is known about this gene or its product at this time, though it is suggested that is likely to play a role in cell survival and tumor suppression after DNA damage.

Digestion of mouse genomic DNA with *Hin*dIII gives rise to four different sites for *R2*-related sequences and to three fragments of 21, 13, 4.2 kb (Yang-Feng *et al.*, 1987). *R2* related sequences are present on the mouse chromosomes 4, 7, 12, and 13 Mouse cells overproducing the R2 protein show at least 5-fold amplification of the chromosome 12-specific 13 kb *Hin*dIII fragment of the *R2* gene, which is the active *R2* gene (Thelander and Thelander, 1989).

Use of this 13 kb DNA fragment from the parental mouse cell has led to the cloning and characterization of the functional mouse *R2* gene (Thelander and Thelander, 1989). The 5770 bp transcribed *R2* sequence contains ten exons separated by nine introns that vary in length from 95-917 bp. Following the general rules (Mount, 1982), all introns begin with the sequence GT and end with AG. The active tyrosyl free radical is encoded in exon 5. A TATAAA homology region can be found at position -29 to -24, and a CCAAT sequence at -79 to -75. Two putative Sp1 sites in different orientations are located upstream of the transcription start site. The 501 bp 5'- flanking region of the gene is G+C rich containing 65% G+C.

1.5.5. Studies on Perturbation of Ribonucleotide Reductase Function

As described previously, ribonucleotide diphosphate reductase plays a pivotal role in the provision of a balanced supply of precursors that are used for DNA synthesis and repair. The enzyme catalyzes the reduction of ribonucleosides to deoxyribonucleosides. As such, it is of central importance in cell proliferation. Furthermore, changes in regulation of ribonucleotide reductase have been observed in a number of malignancies and higher levels of this enzyme have been found in cultured malignant cells than in nonmalignant cells (Weber, 1983, Wright *et al.*, 1989). Furthermore, positive correlation has been established between increased ribonucleotide reductase activity and increased tumor growth rate in mice (Weber, 1983). Studies in human tissues have further demonstrated that *R2* mRNA and protein levels are higher in malignant than in non-malignant cells (Saeki *et al.*, 1995; Jensen *et al.*, 1994). For these reasons ribonucleotide reductase has been the target for development of anti-neoplastic drugs (Wright, 1989; Wright *et al.*, 1989; Wright *et al.*, 1990) and the subject of many regulatory studies.

Much effort has been focused on unraveling the complex functions and regulation of the ribonucleotide reductase enzyme. A number of the studies involved treatment of cultured mouse cells with a number of different DNA synthesis-inhibiting drugs and tumor promotors. This was done with the hope of understanding how ribonucleotide reductase is affected by those agents and to elucidate the effects of alterations in one or both of the ribonucleotide reductase subunits on these cells and perhaps their tumorigenic and metastatic potential. In the middle to late 1980's, a number of studies showed that there was a significant increase in the levels of *R2* mRNA in cells that are drug resistant and over-express the R2 protein. In contrast, only the most highly resistant cells over-

express the R1 component (McClarty *et al.*, 1987a; Choy *et al.*, 1988; Cocking *et al.*, 1987; Wright *et al.*, 1987a). From a regulatory perspective, it is interesting to note that while R1 has a single mRNA transcript, mammalian cells contain two distinct *R2* mRNA species (Wright *et al.*, 1987a), further emphasizing the differences which exist between R1 and R2 regulation. Increases in the levels of R2 protein have been frequently associated with amplification of the *R2* gene, while *R1* amplification appears to be a more uncommon phenomenon found in hydroxyurea-resistant cells (McClarty *et al.*, 1987b). In fact, increases in R1 protein expression can occur without *R1* gene amplification (McClarty *et al.*, 1987b; Choy *et al.*, 1988). Hydroxyurea is a potent R2 inhibiting drug (Wright, 1989). Hydroxyurea (Äkerblom *et al.*, 1981) and other DNA synthesis-inhibiting drugs (for review see Wright, 1989), target the non-heme iron tyrosyl free radical. Both human and rodent cells have been selected for hydroxyurea resistance and have been shown to overproduce the R2 protein as a consequence of *R2* gene amplification (Thelander and Berg, 1986). Other studies have reported that increases in R2 expression levels following hydroxyurea treatment are due to increases in R1 and *R2* mRNA stability (Amara *et al.*, 1995a). R2 protein overproduction has also been shown to occur in mouse fibroblasts as a consequence of treatment with phorbol esters such as the potent tumor promotor 12-*O*-tetradecanoyl-13-acetate (TPA). It has been reported that treatment of cells with TPA increases the level of R2 protein (Choy *et al.*, 1989) and that this increase also occurs through an alteration in the post-transcriptional stability of *R2* mRNA (Amara *et al.*, 1994). Interestingly enough, similar studies of the R1 protein component indicate that its levels are also elevated (Choy *et al.*, 1989), through an increase in *R1* mRNA stability following TPA treatment (Chen *et al.*, 1993). Treatment

of cells with transforming growth factor-β1 (TGF-β1) has also been reported to affect the expression of the R2 protein. Studies by Amara *et al.* (1995b) concluded that the treatment of BALB/c 3T3 cells with TGF-β1, which results in the induction of expression from the *R2* gene (Hurta *et al.*, 1991, Wright *et al.*, 1993), is due to post-translational stabilization of its mRNA message.

Thus, studies by Amara *et al.* (1994, 1995a, b) described the alterations in R1 and R2 expression that resulted from alterations in *R1* or *R2* mRNA stability. These perturbations in mRNA stability were mediated by a mechanism involving specific binding proteins that interact with protein-binding regulatory regions located in the 3'-untranslated regions (3'-UTR), of the *R1* and *R2* mRNAs. These interactions were reported to alter the *R1* and *R2* mRNA half-lives. This body of data gave rise to another group of studies. A series of experiments were conducted using gene transfections into cultured mouse cells in order to study the effects of a number of transfected genes or combinations of co-transfected genes on ribonucleotide reductase, and how alterations in the enzyme or its components were involved in malignancy. Fan *et al.* (1996a) performed experiments where only the 3'-UTRs of the *R1* or *R2* mRNAs were transfected into BALB/c *nu/nu* mouse fibroblasts. The authors reported that these transfections result in significant suppressive effects on the tumorigenic and metastatic properties of the cells.

Subsequent studies by Fan *et al.* (1996b) using a retroviral expression vector for the *R2* component were used to investigate the *in vitro* and *in vivo* malignancy properties of the cells infected with this *R2*-carrying vector in four lines of H-*ras*-transformed mouse 10T½ fibroblasts. The cells showed increased colony transformation in soft agar after infection with an *R2*-carrying virus vector. *In vivo* experiments were also conducted.

Expression of c-Myc-epitope-tagged *R2* in benign BALB/c 3T3 and NIH 3T3 mouse fibroblasts exhibited reduced subcutaneous tumor latency and increased tumor growth rates in syngeneic mice and elevated metastatic potential in lung metastasis assays. This study led to the conclusion that the R2 protein can participate in other critical functions of the cell.

Ribonucleotide reductase was also shown to interact with members of the Mitogen Activated Protein (MAP) Kinase Pathway (Fan *et al.* 1996b). MAP Kinases are important intermediates in signal transduction pathways that are initiated by a variety of cell surface receptor molecules (for review see Davis, 1993). The MAP Kinase (MAPK) pathway is important since it functions as a link in the transduction pathway between the cytoplasm and the nucleus. MAPKs are Threonine/Tyrosine Kinases. MAP Kinase isoforms function to regulate a number of proteins, among them other protein kinases, nuclear proteins such as c-Myc, c-Jun, c-Fos and others, as well as cell surface molecules such as EGF-R and $cPLA_2$. The R2 protein cooperates with *ras* in mechanism of malignant progression, mostly thorough a Ras pathway involving the Raf-1 protein and mitogen-activating protein kinase-2 activity, suggestive of a mechanism for the reported Ras/R2 synergism. This idea is supported by data describing activation of Rac-1, which operates in parallel with Raf-1 in Ras activated pathways, and also cooperates with R2 in cellular transformation. This led the authors to conclude that in addition to R2 functioning as a critical component of ribonucleoside reduction, it can also participate in other important cellular functions. Moreover, the authors suggest that deregulated R2 is a "novel tumor progresser determinant" that cooperates in oncogene-mediated mechanisms that are able to control malignant potential (Fan *et al.*, 1996b).

In gene transfer studies of the R1 component, Fan *et al.* (1997) demonstrate a decreased anchorage dependence and malignant potential in cultured 10T½ cells that over-express the R1 component. Ectopic expression of R1 in highly metastatic and tumorigenic cells was shown to have significant effects in *in vivo* experiments as well. Studies with the RMP-6 cell line, a mouse 10T½ fibroblast line co-transformed with *myc*, *ras*, and mutant *p53*, led to lung metastases following tail vein injection in mice. Transfection of the RMP-6 cells with the *R1* gene resulted in a >85% reduction in the tumorigenicity and metastatic potential when mice were injected in the tail vein with these RPM-6 cells. From these data the authors concluded that the R1 and R2 components of ribonucleotide reductase are both unique malignancy determinants that play opposing roles in the regulation of the whole enzyme and that there is a novel control which governs a balance in the levels of R1 and R2 expression. Furthermore, the authors suggest that alterations in this delicate balance, either by over-expression of R2 or reduced expression of R1, can significantly modify cellular transformation, tumorigenicity, and metastatic potential.

1.6. DNA Replication

1.6.1. Basic Concepts in DNA Replication

Genomic DNA replication is a critical process shaped by strong evolutionary pressure. Rapid replication affords a viral or cellular genome an immediate advantage over its competitors, provided that a high degree of accuracy is not sacrificed (Spradling, 1999). A central issue in the understanding of cellular proliferation is the understanding of the processes that govern and facilitate the replication of cellular DNA (for review see

DePamphilis, 1997). Moreover, unraveling the functions and regulation of DNA replication initiation sites and the proteins involved in the regulation and function of these replication sites is central to understanding of replicative process. The replicative process is complex and therefore, understanding how these multiple sites of replication initiation ensure controlled and faithful replication of the entire genome within the duration of the S phase is central to understanding replication.

Escherichia coli DNA replicate their DNA bidirectionally initiating the process from a single origin on their circular chromosome. The replication is then inactivated by methylation of the DNA. Amaldi *et al.* (1973) demonstrated in bacteria and yeast, that origins are defined sequence elements and that loci serving as initiation sites during one cell cycle were often reutilized in the next cell cycle. In Yeast, these sequences are known as Autonomously Replicating Sequences (ARSs) and are essential for replication in yeast. The are comprised of base pair sequences that are either an exact match of very close to the core consensus sequence 5'-($^{A}/_{T}$)TTTAT($^{A}/_{G}$)TTT($^{A}/_{T}$)-'3 (Diffley and Stillman, 1990). In *S. cerevisiae*, control over these initiation events occurs at the Origin Recognition Complex (ORC) that consists of a complex of six binding proteins. This complex is essential to the initiation process (Bell and Stillman, 1992; Bell *et al.*, 1993; Foss *et al.*, 1993; Micklem *et al.*, 1993; Loo *et al.*, 1995).

The faithful duplication of the mammalian genome is physically and temporally ordered (Michaelson *et al.*, 1997). Replication of the significantly larger mammalian genome is initiated from multiple origins and at fixed intervals of time throughout the S phase of the cell cycle (Michaelson *et al.*, 1997).

1.6.1.1. Early DNA Replication Studies

Some of the important early findings concerning DNA replication were made as a result of the *Fiber Audiographic Technique* developed by Huberman and Riggs in 1968. Using this technique, Huberman and Riggs and others demonstrated a number of features of the replication process (Reviewed in Hamlin, 1992). Replication forks travel at approximately 2 kb (Carroll *et al.*, 1991) to 3 kb (Huberman and Riggs, 1968) per minute and there are multiple growing points along each chromosome. It was also demonstrated in most (but not all) cases, that replication forks travel bidirectionally from the origins of replication. Initiation sites are spaced approximately 100 kb apart, ranging from 10 to 330 kb apart, and there are roughly 20,000 to 50,000 replication origins in the mammalian genome. Clusters of 5 to 10 of these origins fire simultaneously, suggesting that they are coordinately activated. Later, Hand (1975), described coordinated bidirectional fork in mouse L cells. By inhibition of protein synthesis, Hand showed that he could provoke an increase in the firing of unidirectional origins. These results suggested that the coordinated movement from bidirectional origins occurs only when there are enough proteins (*i.e. trans*-activating factors) to ensure that both template strands initiate replication synchronously.

1.6.1.2. Initiation of DNA Replication

The study of DNA of replication is actually the study of initiation zones and origins of replication. Initiation zones are central to DNA replication. Understanding the function and regulation of origins is central to understanding the overall process of DNA replication. Origins dictate where and when replication occurs and they prescribe which

origins of replication fire and when they fire. This is a pivotal feature of the replication process.

The process of DNA replication is highly complex. A somatic cell containing roughly 6 x 10^9 bp of DNA must initiate DNA replication at 5,000 to 50,000 different sites and completed within the duration of a typical S phase, or within roughly 8 hours. In the cells of organisms that are able to replicate their genomes very rapidly, the number of initiation sites may be as much as 50-fold higher. This is true in the early embryos of frogs, flies, and sea urchins, which can replicate their genomes in 10 to 40 minutes. Early *Drosophila melanogaster* embryo cells have about 100 times more DNA than *E.coli* and replicate their genome in 3 to 4 minutes. This is because replication originates synchronously from many origins that are spaced roughly 8 kb apart (Blumenthal *et al.*, 1973). The process of DNA replication is non-stochastic. If the process of DNA replication relied on a strictly stochastic process of initiation, as much as 10 to 15% of the genome would fail to be replicated during the course of each cell division (Coverley and Laskey, 1994).

Not all genomes have the same requirements for initiating replication. The replication of chromosomes is restricted to a single phase of the cell cycle (S phase) and initiation at each of several thousand replication initiation origins is also restricted to once per S phase (Blumenthal *et al.*, 1974). It is possible for multiple initiation events to occur in the cell during the processes of gene amplification (discussed below) as is found in tumors and transformed cell lines, but rarely in normal animal cells during the course of development (Tlsty, 1990). Every genome analyzed thus far was found to contain at least one replication origin per chromosome (Kornberg and Baker, 1992), and the

genomes of eukaryotes contain about one origin of replication for every 10 to 330 kb (Hand, 1978).

A number of factors govern the initiation of DNA replication. Initiation depends on sequence context, however it also depends on tissue and cell specific factors. When replication does occur, the origins are activated in a temporal order that is determined by their context in, and their proximity to other sequences (Simon and Cedar, 1996; Friedman *et al.*, 1996). The role a gene plays in a given cell also plays a role in the timing of its replication within the S phase. For example, Goldman *et al.* (1984) report that "housekeeping" genes replicate during the first half of the S phase during the cell cycle and tissue specific genes are replicated early in those cells in which the genes are potentially expressed. Moreover, changes in the timing of replication of a given tissue-specific gene are reflective of a commitment of that gene to transcriptional competence or to quiescence during ontogeny. For instance, the β-globin gene locus is early replicating in murine erythroleukemia (MEL) cell, while it is late replicating in other types of cells such as lymphocytes (Epner *et al.*, 1988; Hatton *et al.*, 1988). Recent work by Ermakova *et al.* (1999) describes a single replication event in the non-B cell MEL line that is achieved by a single replication fork during the replication of the *IgH* locus. This replication event proceeds chronologically 3' to 5' from early (Michaelson *et al.*, 1997) to late (Brown *et al.*, 1987) replicating S phase domains. In contrast, in both mature B and Pre-B cells, sequences immediately 3' of the *IgH* locus, the entire *IgH* coding region as well as all of the expressed V_H regions are all replicated in early S phase (Brown *et al.*, 1987; Michaelson *et al.*, 1997). This ability of specific sequences to direct the initiation

of replication is critical since it provides a means through which to prevent interference between replication and transcription.

The replication of DNA has been shown to be asynchronous and genetically imprinted. Genomic imprinting is an inherited epigenetic phenomenon that results in parental-origin-specific gene expression in somatic cells. Kitsberg *et al.* (1993) described maternal and paternal imprinting of endogenous genes in the mouse. It has been demonstrated also, that the loss or relaxation of this feature has been associated with several adult and pediatric neoplasms. For example, the loss of imprinting at the *IGF2* and *H19* genes has been associated with head and neck tumors (El-Naggar *et al.*, 1998) and with Beckwith-Wiedemann syndrome (Squire *et al.*, 2000).

The initiation of DNA replication involves three sequential steps (reviewed in DePamphilis, 1997). (i) One or more proteins bind to a specific, *cis*-acting sequence often referred to as the genetic origin or replicator. The protein(s) that bind(s) here is/are referred to as origin recognition proteins. (ii) DNA unwinding begins at sites where DNA is most easily unwound, and this is where DNA replication actually begins. These sequences are also known as DNA Unwinding Elements or DUEs. DUEs can be found throughout the genome as frequently as 1 per 3,000 bp, but they do not function as origins on their own. They function in the company of the sequences that are able to bind the origin recognition proteins. (iii) DNA replication is initiated on one or both templates. The first Okazaki fragment initiated on each template strand is continuously extended by DNA Polymerase δ and its accessory proteins to become the long, leading nascent (leading) DNA strands on the forward arm of each of the replication forks. This results in bidirectional DNA replication.

1.6.1.3. Structural Features and Licensing of DNA Replication

Beyond the actual initiation of DNA replication itself, resides an array of regulatory mechanisms. Much of the control exerted over the initiation of DNA replication is maintained by actual structural or topographic features found on the DNA itself. The simple double helical structure proposed by Watson and Crick in 1953 has now emerged as a structure that includes more than the canonical β-form DNA. It is now known to contain a variety of structures. Alternate structures within DNA can influence the interaction of the DNA with proteins, the consequence of which is the stimulation or repression of processes that are governed by these binding proteins. These processes include transcription, DNA repair, recombination and replication.

One of the common structural features collectively important in the initiation of DNA replication is Inverted Repeats. Inverted Repeats (IRs) are found mostly in the DNA replication control regions and replications origins of prokaryotic and eukaryotic DNA. They are functionally important for initiation of DNA replication in plasmids, bacteria, eukaryotic viruses and mammalian cells. IRs can form cruciform structures that may play a role in mammalian DNA replication. Cruciform extrusions have been shown to effectively relax DNA structure (White and Bauer, 1987). These structures may indirectly influence the onset of replication by their effects on the levels of superhelicity of the DNA and binding of specific protein factors. Supercoiling is known to affect the binding of specific protein factors for transcription, recombination, and replication (Cozzarelli and Wang, 1990). Cruciforms may influence chromatin architecture and nucleosome binding, which in turn interfere with binding of initiation factors to promotors (Workman *et al.*, 1991) and origins of replication (Cheng and Kelly, 1989;

Simpson, 1990). Histones and/or nucleosomes bind poorly to IRs (Weintraub, 1983) and stem-loop (Nickol and Martin, 1983) or cruciform structures (Nobile *et al.*, 1986; Battistoni *et al.*, 1988; Kotani and Kmiec, 1994; van Holde and Zlatanova, 1994).

Replication can be initiated at any site that is easily unwound. The reopening of the chromatin over a broad DNA region may induce strong torsional stress in this area due to unrestrained supercoiling. This might in turn lead to the melting of several areas of low helical stability, provoking the initiation of Origins of Bidirectional Replication (OBRs). Some complex origins may show initiation of replication over several kilobases in addition to initiation at a predominant site of initiation. Extrusion of cruciforms in the regions of these origins of replication may be a method by which the torsional stress of opening of chromatin is relieved. The cruciform may absorb the stress and suppress the opening of "false" DNA sites and restrict or favor the opening and firing of the "correct" OBRs. Cruciforms may also play a role in transcription and replication by themselves being components of a nucleosome-protein complex.

There are also a number of more complex regulatory components and molecular interactions that govern the initiation of DNA replication. The replication of DNA is a fundamental step in the cell cycle, and as such, it must be coordinated with cytokinesis in order to ensure the correct ploidy in both daughter cells (for review see Kearsy and Labib, 1998). Initiation of DNA replication must be restricted to once per cell cycle, in order to prevent the illegitimate re-replication of parts of the genome. It appears as though the function of the ORC is to permit the loading of other replication factors onto the origin DNA. In *S. cerevisiae,* Cdc6 plays a key role in triggering the initiation process, and has been shown to be specifically associated with DNA origins at the G_1

phase of the cell cycle. Cdc6 appears to be a central player in the limiting of DNA replication to once per cell cycle (Tanaka *et al.*, 1997). Another family of replication proteins consists of the six minichromosome maintenance proteins (MCMs). In *S. cerevisiae*, replication-regulating proteins equivalent to the MCMs are encoded by the *ORC1-6* genes (Chevalier and Blow, 1996). MCMs 2-7 are a related family of DNA replication regulating proteins that function in the initiation step of DNA replication. They are bound to the chromatin around the origins of replication during G_1, but are subsequently displaced during the S phase of the cell cycle and remain unbound until the end of the mitotic process. This periodic association with the origins is thought to ensure that the replication origins are only able to fire once during the S phase. MCM10 (Merchant *et al.*, 1997) is essential for the continuation of initiation by interacting with MCMs 2-7 and releasing origin-bound factors (Homesley *et al.*, 2000). The binding of MCM proteins to chromatin requires other initiation proteins such as Cdc6 and the overall regulation of origin firing seems to be orchestrated by the protein kinases Cdk2/cdc2 and Cdc7-Dbf4. Cdc7 and Dbf4 form a protein complex that is required for the initiation process. The kinase activity of Cdc7 is periodic in the cell cycle, peaking at the $G_1 \rightarrow S$ phase transition (Chevalier and Blow, 1996). The reinitiation of replication appears to be blocked by a *cis*-regulatory mechanism, whereby the elongation of the replication forks away from the origins is thought to disrupt the MCM protein complex that is essential for the initiation process.

The involvement of MCM proteins in replication is complex. They were first implicated as possible regulators of the replicative process by the observation that the *S. Cerevisiae* Cdc46 (MCM5) protein accumulates in the nucleus during G_1, but disappears

rapidly from the nucleus upon the onset of the S phase (Hennesy *et al*, 1990). Similar observations were made by Yan *et al.* (1993) regarding MCM2, MCM3, and Cdc47 (MCM7) (Dalton *et al*, 1995), leading to the speculation about a possible 'licensing factor' that governs the initiation of DNA replication. The notion of such a licensing factor had emerged from studies of *Xenopus* egg extracts demonstrating that permiabilization of the nuclear envelope is required in order for the G_2 phase chromatin to regain competence for another round of replication (Blow and Laskey, 1988). It was thought that a pre-replicative step (*i.e.* licensing) makes the chromatin competent for the initiation of DNA replication. This would involve the binding of licensing factors to the chromatin at the end of mitosis, thus allowing a single initiation event at the replication origins in the subsequent interphase, after which the licensing factor is inactivated. It was proposed that the licensing factor is unable to traverse the nuclear membrane, so that the licensing of DNA for replication can occur only after the nuclear membrane is broken down during mitosis. In this way, replication is restricted to a single round per cell cycle. Subsequent studies of MCMs in eukaryotic cells showed that they do not follow the behavior initially predicted for them. It was demonstrated that these proteins remain in the nucleus during interphase and are probably able to cross the nuclear membrane during interphase. Despite their not following predicted behavior, MCMs do show a cell cycle change in chromatin binding, which likely reflects their involvement in a licensing-type regulation of DNA replication.

A specific area of study focusing on mitotic Cdks and their role in prevention of re-replication in *S. cereviciae* is of importance in understanding genomic instability and specifically gene amplification. (Gene amplification is discussed in Section 1.6.2.) In the

yeast *S. Pombe*, mutations in *cdc2* or deletion of *cdc13* (a major cyclin partner of Cdc2 for entry into mitosis), lead to re-replication of DNA without an intervening mitosis (Brock *et al.*, 1991; Hayles *et al.*, 1994). When Rum1, an inhibitor of Cdc2 is over-expressed, the cells are unable to enter M phase and undergo multiple rounds of DNA replication (Moreno and Nurse, 1994). Another study showed that the over-expression of Rum1 results in the accumulation of Cdc18, rescuing the cells from *cdc18* mutant lethality (Jallepalli and Kelly, 1996). It was also demonstrated that the over-expression of cdc18 itself causes re-replication of DNA, possibly by leading to unscheduled assembly of competent re-replication complexes (Nishitani and Nurse, 1995; Muzi-Falconi *et al.*, 1996). Nishitani *et al.* (2000) have shown recently that in the fission yeast, Cdt1 is a requirement for replication licensing. Cdt1 cooperates with Cdc18 to promote DNA replication. Both Cdt1 and Cdc18 are required for loading of MCM protein Cdc21 onto chromatin at the end of mitosis, which is also necessary for the initiation of DNA replication. XCDT1, a relative of Cdt1 in the fission yeast, is required for the assembly of pre-replicative complexes in *Xenopus laevis* (Maiorano *et al.*, 2000). It is required for the loading of MCM2-7 replication licensing proteins onto pre-replicative chromatin and as such is an essential component in the system that regulates origin firing during S phase.

Clearly, the initiation of DNA replication is highly regulated and disruption of this system is precipitous to illegitimate DNA replication and amplification in the *S. Pombe* genome. It is not unlikely that illegitimate re-replication in higher organisms occurs in a similar fashion.

1.6.2. Genomic Instability

Genomic instability is a broad term encompassing a number of genetic lesions that often confer a growth advantage to the cells acquiring them. On a global scale, genomic instability can be manifested as duplication or deletions of whole chromosomes. On a smaller scale, genomic instability can take the form of changes at the level of single genes. These changes include rearrangements, translocations, amplifications, deletions, inversions, and point mutations. Specific chromosomal alterations provide molecular signatures for certain cancers (Wahl, 1989).

DNA lesions that are able to generate genomic instability can occur for a number of reasons. For example, DNA damage can occur as a result of exposure to ultraviolet or γ-irradiation, transient hypoxia, or to drugs such as alkylating agents, cross-linking agents, and intercalating agents. DNA damage can also occur following the over-expression of oncoproteins such as c-Myc, where target genes may be amplified and over-expressed following its deregulation. Alternatively, previously acquired lesions in the genome may be passed to the daughter cells due to the disruption of the normal functioning of tumor suppressor gene products such as p53 or the pRb Retinoblastoma protein. When the function of gene products such as pr3 or pRb is lost, errors in the genome are not repaired or the cell is not killed off before replication occurs.

Genomic instability is considered to be a major driving force of multistep carcinogenesis. It can affect the genome in a number of ways and is able to alter the function of different classes of genes. In recent years, it has been shown that genomic instability plays a crucial role in the initiation and progression of a variety of different cancers and that most cancers may be genetically unstable. Four classes of genes are

presently identified that are able to contribute to tumor progression by constitutive activation, mutation, or deletion. In order of discovery, these are oncogenes, tumor suppressor genes, DNA repair genes, and genes that influence programmed cell death by apoptosis. There are four major classes of genomic instability. These are (i) subtle changes in gene sequence, such as mutations, (ii) alterations in chromosome number, (iii) chromosomal translocations, and (iv) gene amplifications (for review see Lengauer *et al.*, 1998). Subtle sequence changes involve deletions, insertions, or base-substitutions of a few nucleotides. Alteration in chromosome number is an alteration that involves the gain or loss of entire chromosomes. These types of changes are found in nearly all of the major types of tumors. Chromosome translocations involve the juxtaposition of different chromosomes or of non-contiguous segments of a single chromosome. Translocations lead to the fusion of two different genes, conferring tumorigenic properties by virtue of the fused transcript. Gene amplifications are at the molecular level, multiple copies of a gene. These appear as homogeneously staining regions (HSRs) or extrachromosomal elements (EEs). These amplified gene sequences or amplicons, often contain growth-promoting gene(s) and are roughly 0.5 to 10 megabases in size. For example, there is a Chinese Hamster Ovary fibroblast cell line (CHO400) that harbours 1000 copies of the *DHFR* gene (Anachkova and Hamlin, 1989). All of the types of lesions described above occur commonly in specific types of tumors and are almost never seen in normal cells (Tlsty, 1990; Wright 1990; Prody, 1989). The focus of this study is gene amplification.

1.6.2.1 Gene Amplification

Gene amplification is one of the most common phenomena found in biology and it has been shown to occur in virtually all types of organisms (Schimke, 1984b; Stark and

Wahl 1985: Anderson and Roth, 1977). Single genes are sufficient for the slow accumulation of large amounts of RNAs and proteins. In contrast however, when expression must be more rapid, multiple copies of genes are found in normal cells (Stark and Wahl, 1984). For example, in *Drosophila*, eggshell development occurs over a very limited time frame. The genes encoding proteins involved in eggshell formation are found in two clusters and are expressed early (stages 12 and 14) in the ovarian follicle cell. One is one the X chromosome and the other on chromosome III. These single copy chorion genes in the X and chromosome III clusters are amplified as much as 15- and 60-fold, respectively. This occurs in order to achieve the high rates of protein synthesis required in order to accumulate a sufficient amount of chorion proteins during the limited time available for the formation of the eggshell. This allows for faster gene expression than can be produced from a single gene copy. By contrast, no such amplification occurs in the chorion genes of the silk moths during oogenesis since multiple copies of this gene are found in the germ line of these moths (Jones and Kafatos, 1980). Multiple genes are usually carried in the germ line DNA in most organisms, but in a few cases specific genes or even sets of genes are amplified in certain cell types. Amplification can be transient or it can be permanent, as is the case in terminally differentiated cells. The loss of p53 in mice results in genomic instability, characteristically associated with gene amplification and alterations in chromosome ploidy (Fukasawa *et al.*, 1997). The mice had cells in various organs at 2-6 weeks that showed aneuploidy, frequent gene amplification and apoptosis. This study also demonstrated that cells derived from p53 nullizygous mice showed amplification and over-expression of *c-myc*, *DHFR*, and *CAD*.

Gene amplification is regarded as one feature of genomic instability, though it is also known to occur as a part of normal development in insects, amphibia, and lower organisms as mentioned above (Santelli *et al.*, 1991; Delikadis and Kafatos, 1989; Stark and Wahl, 1984). Quantitative measurements indicate that the rate of amplification is higher in cancer cells than in normal cells (Tlsty *et al.*, 1989). Other studies indicate that gene amplification has not been observed in normal diploid mammalian cells (Lücke-Huhle, 1989; Wright *et al.*, 1990; Tlsty, 1990). Prody *et al.* (1989) describe amplification of the *CHE* gene coding for butyrylcholinesterase (BtChoEase) in a farmer exposed to high levels of organophosphate insecticides, to which all members of his family have long been exposed. While he carries a 100-fold of the *CHE* gene, there is no evidence of a cancerous or precancerous phenotype.

There are however, non-developmental or "illegitimate" amplifications. The probability of an illegitimate round or replication occurring is very low, though it is not zero. It has been estimated to be as low as 10^{-6} (Beverley *et al.*, 1984). The idea that illegitimate replication and amplification functions as a mechanism by which malignant phenotypes are generated was initially formally proposed by Varshavsky (1981) who suggested that these events occur as a result of "replicon misfiring" triggered by a "firone". He suggested then, that these misfirings of the origins might generate extrachromosomal copies of cellular genes that result in the duplication or amplification of cellular genes. Mariani and Schimke (1984) suggested that the initial amplification event results following re-replication of a variable, but large portion of the genome. This re-replication event is followed by a selection process that might include recombination events, or loss of non-selected DNA, and results in what eventually appears as a

differential gene amplification. Hill and Schimke (1985) went on to prove that treatment of cells with hydroxyurea results in the generation of a broad spectrum of chromosomal aberrations shown to consist of increased frequency of sister chromatid exchange, polyploidization, breakage-fusion-breakage chromosomes, extrachromosomal DNA, and gapped fragmented chromosomes. The amplification events are selected for and sometimes prove advantageous, since amplification is a means by which a cell can overcome growth control, be it in a cellular environment, or following chemotherapy (Schimke *et al.*, 1984a), and gain an advantage over other cells. The molecular consequences and biological implications of overreplication and DNA recombination in higher eukaryotes are described by Schimke *et al.* (1986). In short, these aberrations are thought to play a role in the generation and progression of cancer and it is thought that they have consequences in its treatment (see below). Furthermore, chromosomal aberrations play a role in the aging of the cell and therefore, the organism as a whole. Finally, chromosomal aberrations play a role in rapid speciation evolution.

The clinical relevance of gene amplification is discussed by Schimke (1986). Chemotherapeutic intervention as a method to kill cancer cells has its own negative consequences. It was shown that even transient growth arrest (as short as 6 hours) mediated by antitumor agent results in nonspecific gene amplification of a large portion of the cells (Mariani and Schimke, 1984). This amplification involves the re-replication of early replicating genes that have already fired and begun to replicate (Varshavsky, 1981). The re-replication of the early genes is likely followed by selection for cells that carry resistance to the chemotherapeutic agent in use. These include classic examples such as the amplification of the early replicating gene *DHFR* that occurs following

treatment with methotrexate (MTX), a drug that targets and inhibits the function of the DHFR protein as a folate analog, and prevents the synthesis of thymidylate synthesis (Nogrady, 1988). Other competitive enzyme inhibitors such as hydroxyurea, aphidocolin, carcinogens such as N-acetoxy N-acetylaminofluorine, as well as ultraviolet radiation are also able to amplify *DHFR* (Schimke, 1986 and references therein).

Amplification of oncogenes is reported to occur in a subset of late-stage cancers of a number of organisms. Amplification of genes involved in metabolic processes or in the metabolizing or deactivation of antineoplastic agents exemplifies the advantage of a gene amplification process which is able to confer drug resistance during the course of a chemotherapeutic regimen (Brodeur and Hogarty, 1998).

Gene amplification is a significant factor in human cancers since it has been clearly associated with tumor progression (Brodeur and Hogarty 1998). The amplification of genes that occurs in these cancers can also play an important role as a prognostic indicator. This is demonstrated by *myc*, *myb*, and *Ha-ras* proto-oncogenes (Yokota *et al.*, 1986) as well as by others.

1.6.2.2. Gene Amplification in Cultured Cells

Gene amplification has been frequently described in cultured cells and in tumors that have been treated with drugs (Stark 1993; Schimke *et al.*, 1978). The amplification of genes has also been demonstrated following constitutive growth factor expression in cultured cells (Huang and Wright, 1994; Huang, *et al.*, 1994, Huang *et al.*, 1995), or after DNA damage (Tlsty *et al.*, 1989; Lücke-Huhle *et al.*, 1989, 1990; Yalkinoglu *et al.*, 1990; Lavi 1981). Over-expression of the oncogene *c-myc* is also known to be associated

with gene amplification (Mai *et al.*, 1996, 1999; Mai, 1994a, Denis *et al.*, 1991). Johnston *et al.* (1983) have even reported spontaneous gene amplification of the *DHFR* gene locus.

One of the main approaches used to learn about gene amplification is the study of early events that occur in the process. Although not all gene amplification events result in the creation of a tumor cell, these early events in the gene amplification process can be critical steps in tumorigenesis and their study may give clues to the path(s) that cells take in their evolution from normal cells to tumors. For example, Rath *et al.* (1984) showed that a high degree of *DHFR* gene amplification could be achieved by extremely low methotrexate step-selection protocols. A study by Guilotto *et al.* (1987) demonstrated that dual selection with *N*-(phosphonacytyl)-L-aspartate (PALA) for *CAD*, and with MTX to select for *DHFR* amplification, resulted in selection frequencies 200 times greater than were predicted from individual drug selection frequencies. Similar results were obtained by Rice *et al*, (1987) during co-selection for adriamycin (doxorubicin) and methotrexate resistant cells. Guilotto *et al.* (1987) also demonstrated that dually selected clones were also likely to have a higher frequency for the amplification of a third gene. These results raised the question of a possible "amplification-prone" phenotype, which in turn lead to a deeper question: Has the "amplification-prone" phenotype been selected for by prolonged drug selection process, or do cells subjected to drug selection have an amplification phenotype during a prolonged growth recovery? This has not yet been resolved. Of interest is the fact that amplificator phenotypes have been generated by exposure of cells to X-rays (Lücke-Huhle and Herrlich, 1987) and carcinogens (Kleinberger, 1988), where gene amplification results in the non-treated partner of a somatic cell fusion product. In contrast however, Tlsty *et al.* (1992) who investigated the genetic control of gene

amplification in hybrids of tumorigenic cells and normal diploid cells showed that the ability to amplify an endogenous gene was a recessive genetic trait, and control of gene amplification potential segregated independently of tumorigenicity and immortality.

1.6.2.3. Gene Amplification Mechanisms

More recent studies in mammalian gene amplification have given rise to a number of ideas and potential mechanisms which may begin to explain some of the phenomena observed in mammalian tumors and in cultured cells (for review see Stark *et al.*, 1989). A basic premise is that it is likely that several mechanisms could function in different situations. It is also possible that a single basic mechanism might give rise to a variety of initial clones, which might in turn give rise to different final clones, depending on the stability of the different amplified structures generated in the primary event. It is reasonable to assume that like lower animals that use different mechanisms, mammalian cells are also capable of alternative mechanisms for the generation of amplified genes. It seems likely that mechanistically different primary amplification events occur at different loci within the same cells, at the same loci in different cells, or during different steps of the amplification process. A single mechanism may dominate eventually.

Gene amplification has been shown to occur in stages or phases. Chromosomal amplification steps that occur in the early stages of amplification process are rarely amplified any further. It appears that there is preferential, subsequent re-amplification of a sub-region of the early-amplified area of the chromosome. This is coupled with a loss of some of the co-amplified DNA sequences. Thus the overall increase in gene copy number is small in the initial stages of the process, but can be substantial as the subsequent amplification process continues (Saito *et al.*, 1989).

Some of the most commonly proposed ideas regarding gene amplification, namely replication-driven and segregation-driven amplification mechanisms (reviewed by Stark *et al.*, 1989) are described below. The replication-driven models are described first. The *onionskin* model was experimentally validated in studies of developmentally controlled amplification of chorion genes in *Drosophila* follicular cells (reviewed by Kafatos *et al.*, 1985). Schimke *et al.* (1986) suggest that the onionskin amplification model is flexible enough to account for nearly all of the molecular products observed, including the generation of extrachromosomal DNA. Passinanti *et al.* (1987) described the *extrachromosomal double rolling circle model*, which was initially proposed in order to explain the amplification of the 2 μm yeast plasmid. The chromosomal spiral model was developed by Hyrien *et al.* (1988), in order to explain the inverted properties of an inverted joint in the AMP deaminase system. In this system an inverted duplication can be generated if the replication switches strands and proceeds around the fork as it progresses through the region enriched in palandromic sequences, as proposed initially by Nalbantoglu and Meuth, (1986). This model accounts quite well for cases where the amplified array is located at the original chromosomal locus of the selected gene and is organized as a tandem array of inverted units.

The *sister chromatid exchange model*, which is a segregation-driven mechanism, was suggested following the analysis of the CAD gene amplification in Syrian hamster cells. In this study, Giulotto, *et al.* (1986) demonstrated that many first-step mutants, with only three to six extra copies of the CAD gene, were found to have amplified as much as 10,000 kb of DNA along with each copy of the gene. The largesse of the amplicon could be predicted by the *onionskin* model, but only if unscheduled replication were to occur

over a region that contained about 100 origins. Alternatively, the model could work if very large episomes of extrachromosomal DNA were involved. The study revealed that only three novel joints were found in a set of 33 independent mutants, and each joint was present in a single copy. The *double rolling circle*, *the spiral*, and the *episome models* (above) predict that novel joints will be created and amplified as much as the gene in a single step. Since no amplified joints have been found, these models may not apply in this case. Unequal chromatid exchange has already been shown by Endow and Atwood, (1988) to cause the amplification of rRNA in *Drosophia*, and may explain intrachromosomal amplification of very large regions of DNA. This model explicitly predicts the presence of single-copy joints in mutants that were recovered after only two or three successive recombination events. In its most basic form, the model is able to predict head-to-tail joining of amplified domains. Thus, one can expect an unusually long chromosome in which each extra copy of the selected gene is separated from the rest by a long expanse of coamplified DNA. The other homologue should be normal, containing only a single copy of the single gene. Therefore, to generate more that one extra copy of the amplified gene per cell, more than a single unequal sister chromatid exchange would need to occur in different cell generations. The first event, generating an extra copy of the gene may allow the cell to survive the selection process, giving rise to a slow-growing colony. A second event occurring in one cell of this colony might give this cell a greater growth advantage. Both events are considered to be part of the operationally defined first step of selection.

Another segregation-driven mechanism, the *deletion-plus-episome model*, requires that episomes contain functional replicating origins. There are two different

mechanisms that are able to generate circular molecules that contain origins: re-replication (Schimke *et al.*, 1986) and recombination across a replication loop (Passananti *et al.*, 1987; Carroll *et al.*, 1988; Wahl, 1989). The first step of recombination is deletion accompanying episome formation, though the evidence for such a deletion step is difficult to obtain. In most cultured and tumor cell, the chromosomes are often hyperdiploid and thus, deletion in one chromosome can be concealed by the presence of additional copies of the locus in the homologous chromosomes. Carroll *et al.* (1988) showed that by using cells containing transfected genes initially present in only one chromosome and in cells with only a single copy of the *DHFR* gene, it was possible to assess whether these deletions occurred. When episome-containing cells from transfected cell lines were passaged without drug selection, clones were detected that were completely devoid of the transfected DNA sequences. Karyotypic and molecular analyses of these cells failed to show chromosome loss thus, deletion coincident with the formation of episomes is favoured. Therefore, amplification of both transfected and endogenous genes can be mediated by deletion.

It has been proposed that deletions equivalent in size to the episomes detected thus far may arise by recombination across the bases of the looped replication domains that are believed to exist in mammalian cells (Vogelstein *et al.*, 1980). Moreover, circular molecules that contain origins of replication may well be one product of this kind of recombination. The generation of episomes that are associated with the formation of inverted novel joints have also been found (Ruiz and Wahl, 1988). Since episomes are acentromeric, amplification can arise simply from unequal segregation during mitosis. Only one or two recombination events are required for coordinate deletion and episome

formation, accounting for extrachromosomal amplification. This model may also be relevant to chromosomal amplification. Double minutes can be derived from episomes and reintegration of DNA sequences that were initially extrachromosomal could lead to the formation of an extended chromosomal region (ECR) as has been demonstrated by Carroll *et al.* (1988).

1.6.2.4. The Initiation and Chronology of Gene Amplification

It is assumed that normal cells rarely amplify their DNA. It has been estimated to occur at a frequency of 10^{-6} (Beverley *et al.*, 1984). It follows therefore, that cells that are able to amplify their DNA at a higher frequency must somehow be stimulated, possibly by some "firone", as described by Varshavksy (1981). As described briefly above, it has been shown that amplification can be induced by a number of agents or treatments that are able to interfere with DNA synthesis or to damage the DNA. Examples of these are hydroxyurea, aphidicolin, carcinogens, hypoxia, ultraviolet and ionizing radiation (for reviews see Stark and Wahl, 1984, Schimke, 1988, Stark, 1993). It is likely that such stresses are able to initiate the induction of gene expression (Kleinberger *et al.*, 1988), and that some of these induced gene expression products are able to act in a dominant manner to stimulate gene amplification (Lücke-Huhle, 1988). Of interest is the fact that protein synthesis is necessary in order for amplification to be induced (Sherwood *et al.*, 1988). Though, later experiments do not readily support this idea (Painter *et al.*, 1987), Schimke *et al.* (1984a, 1986, 1988) suggest that cells may respond to relief from inhibition of DNA synthesis by reinitiating synthesis in a single cell. Varshavsky (1981) describes an early or "illegitimate" firing of origins that can occur in the G_1 phase of the cell cycle after growth arrest. The "illegitimate" firing is then followed by "legitimate"

replication along the same area of the genome during the normal S phase, giving rise to a second replication of the same locus, once "illegitimately", and a second time "legitimately". It is possible that the assays conducted lacked the necessary sensitivity and that a small fraction of cells do restart in S phase in response to the stress. Schimke *et al.* (1988) later proposed that the relationship between S and M phases may be perturbed in the stressed cells so that mitosis occurs in what may be refereed to as a second S phase.

The molecular chronology of gene amplification is of interest, since it is helpful in understanding the mechanism(s) of gene amplification (for review see Wahl, 1989; Stark, 1993). Double minute (DM) and expanded or homogeneous staining regions (HSRs) are the predominant sites of gene amplification in mammalian cells. DMs are paired, acentric extrachromosomal chromatin bodies which are known to replicate autonomously. Segregation of DMs is a random event and consequently in the absence of selective pressure, they are lost from the cell population over time. Conversely, HSRs are found on chromosomes and are thus linked to a centromere. Their segregation assures distribution of the amplified gene(s) to the daughter cells during mitosis. For this reason, HSRs are not lost during the course of cell divisions even in the absence of selective pressures. However, small HSRs may be lost in the absence of further selection pressure. (Mai *et al.*, 1996b)

Several interesting questions were posed regarding the two species of amplified DNA. For example, is either one of these species the predominant carrier of amplified genes *in vivo*? Are these two species of amplified genes produced by a single mechanism, or are they the products of two mutually exclusive pathways? Is it possible that one of these structures is the precursor of the other? (For instance, do DMs integrate to generate

HSRs, or are DMs a breakdown product of HSRs? On the other hand, might they exist in equilibrium, where HSRs and DMs can coexist in the same cell or population of cells?). It was once thought that in a given cell, it is customary to observe either DMs or HSRs, but never both containing the same amplified sequences. This belief was considered to be indicative of a selective outgrowth of cells containing only a single form of an amplified gene. Currently it is known that both HSR and DM DNA can coexist in the same cell. There are a number of possible explanations for this phenomenon. First, DM formation may be more highly selected for *in vivo* than is HSR formation, since cells containing DMs may have a growth advantage *in vivo* and predominate even though DM and HSR forms of amplified DNA may both be carried in the cells of a population. Second, it might be that formation of DMs represents an earlier event in gene amplification than HSR formation, and may occasionally integrate into the chromosomes to form HSRs, as suggested previously by others (Biedler, 1982; Lin *et al.*, 1985; Trent *et al.*, 1986). The third suggested possibility is that the initial step in amplification is the generation of HSRs, which continually break down, giving rise to DMs (see Wahl, 1989 for references).

A multi-step model for the chronology of gene amplification (Wahl, 1989), suggested the progression from episomes to selection of amplified sequences, to integration of episomal or DM sequences, then to a change in cytogenetic manifestation of amplified DNA from DMs to HSRs. Wahl (1989) stated that it was not clear why episomes enlarge to form DMs. However, he suggested that it is reasonable to assume that the enlargement of episomes to DM size confers a growth advantage, enabling a greater probability of transmission of the amplified DNA to daughter cells during mitosis.

1.6.2.5. Properties of Amplified Genes

A large body of information describing gene amplification following drug selection has been assembled through the study of cultured cells. The studies have been instrumental in elucidating properties and characteristics of amplified genes and have also provoked some thoughts about possible mechanisms.

Amplified genes have been studied in cultured cells as a means of investigating drug resistance. While not related directly to oncogene-mediated amplification, results of these studies suggest that all of these genes seem to share at least three characteristic properties (for review see Schimke, 1988). First, gene amplification often occurs in a step-wise fashion during the course of drug treatment, resulting in high degrees of amplification. Second, some clones are able to survive toxic concentrations of drug, although only a few actually become resistant to the selective conditions. These resistant clones are capable of forming resistant colonies. The genes which are able confer drug resistance are found to be amplified and reside on one or two chromosomes in cytologically enlarged regions known as Homogenous Staining Regions (HSRs) or Abnormal Banding Regions (ABRs). Third, amplified DNA structures can change. Cells that are maintained under constant drug selection conditions often change the structure of their amplified DNA. These changes, which are often a consequence of altered amplified gene stability, can give rise to extrachromosomal DNA circles. Some amplified DNA becomes integrated into the chromosomal component of the genome, whereas the less stable phenotype carries much of its amplified DNA in the form of extrachromosomal DNA (Gaubatz, 1990; Varshavsky, 1981). Extrachromosomal DNA such as is found in the form of double minutes, is less common in normal cells, but is often found in

malignant tumors (Varshavsky, 1981 and references therein). These double minutes can be created during *in vitro* culture conditions by incubation with drugs (Kaufman *et al.*, 1979) or *in vivo* as a result of chemotherapy (Bertino *et al.*, 1963). Double minutes are often found in certain drug-resistant cells and disappear gradually upon introduction into *in vitro* culture conditions, but reappear following implantation of the cells into a susceptible animal (Varshavsky, 1981 and references therein). The structural features and putative role(s) of extrachromosomal DNA in gene amplification and genomic instability in general, will be discussed in more detail in section 1.6.2.7.

1.6.2.6. The Structures of Amplified Genes

The study of the mammalian gene amplification mechanism begins with the analysis of amplified gene structure. Understanding the structure of amplified genes may allow for the elucidation of the mechanism of their amplification.

Early experiments performed to study the structure of amplified genes involved chromosome walking and restriction fragment analyses. These studies revealed that amplified DNA is essentially a linear representation of the normal DNA sequence (Federspiel *et al.*, 1984; Giulotto *et al.*, 1986, Van der Bliek *et al.*, 1986). The length of these amplified sequences can be highly variable. For instance, in Chinese hamster ovary cells that carry as many as 1000 *DHFR* genes, it was estimated that the approximate length of amplified sequences was 250 kilobase pairs in three different methotrexate-resistant variants, each variant having been obtained from different laboratories (Looney and Hamlin, 1987). Orientation of amplified sequences was shown to vary. Studies of *DHFR* in Chinese hamster ovary cells (Looney and Hamlin, 1987), *CAD* in Syrian hamster cells, *c-myc* in human tumor cell line (Ford and Fried, 1986), and a *DHFR*

plasmid construct transfected into Chinese hamster ovary cells (Wahl, 1989), each revealed some DNA sequences with head-to-head type amplification. These head-to-head structures were found in both HSRs and in minute chromosome forms of amplification, though not in all studies. This variation indicates that different structures of amplification can be generated by a variety of mechanisms and that details may vary between different amplification events, be it in different cell isolates, or sequentially within the same cells.

One important consequence of *DHFR* gene amplification in cultured cells is the rearrangement of the *DHFR* gene locus. Federspiel *et al.* (1984) used a chromosome walking technique and described numerous rearrangements of the *DHFR* gene locus that result from amplification of that gene. They found that amplification-specific DNA rearrangements or junctions are unique to each cell line. Moreover, within a given cell line, multiple amplification-specific DNA sequence rearrangements. They demonstrated that the degree of amplification of the sequences flanking the *DHFR* gene shows quantitative variation both among and within a given number of cell lines. Finally, their work showed that both the arrangement of the amplified sequences as well as the magnitude of the gene amplification may vary with prolonged culture, even under selective maintenance conditions. They conclude their study by stating that there is no evidence for a static repetitive unit of amplification, rather there is a dynamic and complex arrangement of these amplified sequences that is always changing.

1.6.2.7. Extrachromosomal DNA

The eukaryotic genome was once regarded as an unchanging set of genes where every cell in a metazoan organism possessed the same DNA sequences, in the same amounts, all of which resided in all of the same places. The eukaryotic genome was

regarded as static and unable to respond to changes in its environment. Where changes did occur in the genome, it was believed that they did so on the slow evolutionary time scale. From a large number of studies on a considerable range of topics, came the conclusion that the genomes of higher organisms were indeed much more flexible than previously imagined. Studies in DNA mutation and repair, replication, amplification, and other phenomena in higher organisms, changed these views. Not only were there differences among DNA sequences, they differed also in their structures and compartmentalization. For example, DNA in the nuclear compartment was found in arrayed in long linear duplexes, in addition to other smaller covalently closed circular DNA sequences, known as extrachromosomal DNA (Hotta and Bassel, 1965; Radloff *et al*, 1967) (for review, see Gaubatz, 1990).

Extrachromosomal DNA appears to be ubiquitous since all primary and immortalized as well as transformed eukaryotic cells that have been studied have been shown to carry them (Gaubatz, 1990). These include mouse embryo (Yamagishi *et al.*, 1983a), mouse tissues (Tsuda *et al.*, 1983; Flores *et al.*, 1988; Gaubatz and Flores, 1990), mouse thymocytes (Yamagishi *et al.*, 1983a), mouse lymphocytes (Tsuda *et. al.*, 1983), human tissues (Calabretta *et al.*, 1982), cultured human fibroblasts (Smith and Vinograd, 1972; Riabowol *et al.*, 1985). These extrachromosomal DNA molecules have also been found in cultured mammalian cell lines including those originating in mouse (Smith and Vinograd, 1972; Kunisada *et al.*, 1983; Sunnerhagen *et al.*, 1986) and man (Radloff *et al.*, 1967; Smith and Vinograd, 1972).

Extrachromosomal DNA is found in tumor cells. Extrachromosomal DNA has been shown to contribute to the phenotype of the cells that carry them. Functionally, EEs

are amplicons that express the mRNA of the amplified gene(s) on the amplicon and in this way they are able to affect the phenotype of the cell. For example, VanDevanter *et al.* (1990) showed that of six of eight neuroblastoma tumors (three primary tumors as well as three metastatic lesions), amplification of the protooncogene *NYCN* was carried on extrachromosomal DNA. The extrachromosomal DNA circles were different sizes among different patients. Unfortunately, there was no evaluation of the functional capacity of these amplicons to express *MYCN* mRNA or protein. More recently, the question of extrachromosomal DNA function was assessed. It was recently shown in a translocation-negative DCPC mouse plasmacytoma, that extrachromosomal DNA amplicons carry gene sequences that correspond to *c-myc/IgH*-translocated DNA found in translocation-positive plasmacytomas. Moreover, these amplicons transcribe mRNA and contribute to the tumorigenic potential of the cell, as does the corresponding translocation in mouse plasmacytoma (Wiener *et al.*, 1999).

The physical characteristics of extrachromosomal DNA (extrachromosomal elements, EEs) are variable and depend on the cell or tissue of origin. Furthermore, the generation of EEs is determined by growth conditions and physiological parameters. Within a single cell type, the sizes of these circular molecules can range from smaller than 500 bp to as large as 85,000 or more bp (Yamagishi *et al.*, 1983a). Much data has been assembled regarding characteristics and sizes of EEs from cultured mammalian cells (for review see Gaubatz *et al.*, 1990). From these data two general conclusions have been drawn: First, all cells have a heterogenous population of circles and the size distribution is usually greater in cells *in vivo* and in primary cells (Yamagishi *et al.*, 1982; Yamagishi *et al.*, 1983b; Kunisada, *et al.*, 1983; Riabowol *et al.*, 1985). Second, a number of

sequence families have been identified in extrachromosomal DNA as well as variations in the number of EEs per cell. The number can range from as few as 100 EEs per cell in human fibroblasts (Kunisada *et al.*, 1985) to as many as several thousand per cell in cultured monkey kidney cells. For instance DeLap *et al.* (1978) showed that confluent monolayers of the BSC-1 line of African green monkey kidney cells contained about 1000 EE molecules per cell and that most of these were smaller than 1 kb in size. The sizes ranged from 0.05 to 1.7 μm. Furthermore, these EEs could be resolved by gel electrophoresis into abundant size classes of 0.3, 0.8, 1.2, and 1.5 kb, indicating periodicity of 300-500 bp in circle formation, roughly the length of DNA found coiled around and between two or three nucleosomes. Most interesting is the fact that further analysis of cloned EEs showed that all of the characterized extrachromosomal DNA sequences were homologous to chromosomal, but not mitochondrial BSC-1 DNA (Bertelsen *et al.*, 1982; Krolewski and Rush, 1984; Krolewski *et al.*, 1984). In agreement with these studies, analyses of cloned HeLa cell EEs by Kunisada and Yamagishi (1984) showed that all clones that were investigated shared homologies with chromosomal DNA sequences. These studies as well as others (Smith and Vinograd, 1972; Stanfield and Helsinki, 1984; Jones and Potter, 1985a) lead to the proposal that all mammalian EEs are derived from pre-existing chromosomal DNA (For review see Gaubatz, 1990). The homology of extrachromosomal sequences with chromosomal DNA is an important feature since extrachromosomal DNA carries many sequences that are thought to contribute to the gene amplification process. The homology to chromosomal sequences may be explained by a study by Carroll *et al.* (1988) who demonstrated that extrachromosomal DNA molecules could be generated through deletion of corresponding

chromosomal sequences. Initially, episomes are roughly 250 kb in size and they gradually enlarge until they are the size of double minutes. More over, once generated, they are able to integrate into chromosomes. A recent study by Singer *et al.* (2000) demonstrated that in methotrexate-resistant cells, HSRs and *DHFR* sequence-bearing DMs are both initiated through chromosome breaks. Of further interest in this study is the finding that in all but one of the cell lines tested, the cells suffered a partial or complete loss of the parental DHFR-bearing chromosomes.

Extrachromosomal DNA molecules are autonomously replicating DNA circles. It has been shown that altering gene position within the genome can dramatically alter replication timing. In that sense, the generation of extrachromosomal DNA molecules during gene amplification is considered an extreme case of gene repositioning. Carroll *et al.* (1991) demonstrated that once generated, extrachromosomal DNA may be able to replicate and it is of interest to note that the mechanisms which are responsible for ensuring that DNA replicates only once per cycle are functional in maintaining the same control over extrachromosomal DNA and its replication. Whether this phenomenon is true for all cells has not been shown.

The replication of genes on extrachromosomal DNA differs from replication on chromosomally positioned genes. For example, while genes such as chromosomally positioned *DHFR* from a variety of mouse, human, and hamster cells lines appears to replicate during a discreet time interval within the first half of S phase (D'Andrea *et al.*, 1983; Hatton *et al.*, 1988; Kellems *et al.*, 1982), extrachromosomally positioned *DHFR* in the mouse 3T6R50 cell line replicate throughout the S phase (Tlsty and Adams., 1990). Later work by Carroll *et al.* (1991) described the replication of extrachromosomal

amplicons that harbour either *CAD* or the *adenosine deaminase* (*ADA*) gene in mouse cells. The study shows that within experimental error, the *CAD*- and *ADA*-bearing extrachromosomal amplicons replicated within a narrow window of the S phase that corresponded to the time of the replication of the corresponding chromosomally positioned genes. This suggests that the replication timing of extrachromosomal DNA can be preserved in some experimental systems, possibly by *cis*-acting timing control elements located on the amplicons, even though the genes in question are no longer physically associated with their parent chromosome.

In interesting contribution regarding the temporal location of double minutes in the nuclei synchronized Colo320DM at different times in the cell cycle was made by Itoh and Shimizu (1998). The DMs in cells were shown to be preferentially located at the nuclear periphery during the G_1 phase of the cell cycle until the onset of G_1/S boundary, where upon, the DMs relocated promptly to the interior of the nucleus once DNA replication started. Moreover, simultaneous detection of DMs at the sites of DNA replication indicated that the inward relocation of the DMs was initiated immediately prior to DNA replication.

The DNA replication process is a dynamic process that occurs in microscopically visible complexes at discrete replication foci found in the nucleus. The replication foci are comprised of DNA and replication machinery. Studies by Leonhardt *et al.* (2000) indicate that replication occurs at sites that are stably anchored in the nucleus and that these sites assemble and disassemble in a gradual and coordinated, though asynchronous pattern throughout the S phase of the cell cycle.

REFERENCES

Adams, J.M., Harris, A.W., Pinkert, C.A, Corcoran, L.M., Alexander, W.S., Palmiter, R.D., and Brinster, R.L. (1985). *Nature* 318: 533-538.

Äkerblom, L., Ehrinberg, A., Gräslund, A., Lankinen, H., Reichard, P., and Thelander, L. (1981). *Proc. Natl. Acad. Sci. USA* 78: 2159-2163.

Amara, F.M., Chen, F.M., Wright, J.A. (1994). *J. Biol. Chem.* 269:6709-6715.

Amara, F.M., Hurta, R.A.R., Huang, A., and Wright, J.A. (1995a). *Cancer Res.* 55: 4503-4506.

Amara, F.M., Chen, F.M., Wright, J.A. (1995b). *Nucl. Acids Res.* 23:1461-1467.

Anachkova, B. and Hamlin, J.L. (1989). *Mol. Cell. Biol.* 9: 532-540.

Artishevsky, A., Wooden, S., Sharma, A., Resendez, E. Jr., and Lee, A.S. (1987). *Nature* 328: 823-827.

Asai, A., Miyagi, Y., Sugiyama, A., Nagashima, H., Obinata, M., Mishima, K., and Kuchino, Y. (1994). *Oncogene* 9: 2345-2352.

Augenlicht, L.H., Wadler, S., Corner, G., Richards, C., Ryan, L., Multani, A.S., Pathak, S., Benson, A., Haller, D., and Heerdt, B.G. (1997). *Cancer Res.* 57: 1769-1775.

Ayer, D.E., Kretzner, L., and Eisenman, R.N. (1993). *Cell* 72: 211-222.

Ayer, D.E., Lawrence, Q.A., and Eisenman, R.N. (1993). *Cell* 80: 767-776.

Battistoni, A., Leoni, L., Sampaolese, B., Savino, M. (1988). *Biochim. Biophys. Acta* 950: 161-171.

Begg, A.M. (1927). *Lancet* 912-915.

Bently, D.L. and Groudine, M. (1986). *Nature* 321: 702-706.

Benvinisty, N., Leder, A., Kuo, A., and Leder, P. (1992). *Genes Dev.* 6: 2513-2523.

Bertelsen, A.H., Zafri Humayun, M., Karfopoulos, S.G., and Rush M.G. (1982). *Biochemistry* 21: 2076-2085.

Bertino, J.R., Donohue, D.M., Simmons, B., Gabrio, W., Silber, R., and Huennekens, F.M. (1963). *J. Clin. Invest.* 42: 466-474.

Beverley, S.M., Coderre, J.A., Santi, D.V., Schimke, R.T. (1984). *Cell* 38: 431-439.

Bhatia, K., Huppi, K., Spangler, G., Siwarski, R. Iyer, R., and Magrath, I. (1993). *Nat. Genet.* 5: 56-61.

Bhatia, K., Spangler, G., Gaidano, G., Hamdy, N., Dalla-Favera, R., and Magrath, I. (1994). *Blood* 84: 883-888.

Biedler, J.L. (1982). In: R.T. Schimke, Gene Amplification, pp. 39-45. Cold Spring Harbor, NY: Cold Spring Harbor Laboratory.

Billin, A.N., Eilers, A.L., Queva, C., Ayer, D.E. (1999). *J. Biol. Chem.* 274: 36344-36350.

Birrer, M.J., Raveh, L., Dosaka, H., and Segal, S. (1989). *Mol. Cell. Biol.* 9: 2734-2737.

Birrer, M.J., Segal, S. DeGreve, J.S., Kaye, F., Sausville, E.A., and Minna, J.D. (1988). *Mol. Cell. Biol.* 8: 2668-2673.

Bishop, J.M. (1985). *Genes Dev.* 9: 1309-1315.

Bister, K., and Duesberg, P.H. (1979). *Cold Spring Harbor Symp.Quant. Biol.* 44: 801-822.

Blackwell, T.K., Kretzner, L., Blackwood, E.M., Eisenman, R.N., and Weitraub, H. (1990). *Science* 250: 1149-1151.

Blackwood, E.M. and Eisenman, R.N. (1991) *Science* 251: 1211-1217.

Blumenthal, A.B., Kriegstein, H.J., and Hogness, D.S. (1974). *Cold Spring Harbor Symp. Quant. Biol.* 38: 205-223.

Bourchard, C., Thieke, K., Maier, A., Saffrich, R., Hanley-Hyde, J., Ansorge, W., Reed, S., Sicinski, P., Bartek, J., and Eilers, M. (1999). *The EMBO J.* 18: 5321-5333.

Bousset, K., Oelgeschlager, M.H., Henriksson, M., Schreek, S., Burkhardt, H., Litchfield, D.W., Lüscher-Firzlaff, J.M., and Lüscher, B. (1994). *Cell. Mol. Biol. Res.* 40: 501-511.

Brissenden, J.E., Caras, I., Thelander, L., and Francke U. (1988). *Exp. Cell Res.* 174: 302-308.

Brodeur, G.M. and Hogarty, M.D. (1998). in *The Genetic Basis of Human Cancer* 1st Ed. (eds. Kinzler, K., Brodeur, W., and Vogelstein, B.) 161-179 (McGraw-Hill New York.).

Broek, D., Bartlett, R., Crawford, K., and Nurse, P. (1991). *Nature* 349: 388-393.

Brown, E.H., Iqbal, Stuart, S., Hatton, K.S., Valinsky, J., amd Schildkraut, C.L. (1987). *Mol. Cell. Biol.* 7: 450-457.

Bush, A., Mateyak, M., Dugan, K., Obaya, A., Adachi, S., Sedivy, J., and Cole, M. (1998). *Genes Dev.* 12: 3797-3802.

Calabretta B., Robberson, D.L., Barrera-Saldana, H.A., Lambrou, T.P., and Saunders, G.F. (1982). *Nature* 269: 219-225.

Caras, I.W., Levinson B.B., Fabry M., Williams S.R., and Martin D.W. Jr. (1985). *J. Biol Chem.* 260: 7015-7022.

Carroll, S.M., DeRose, M.L., Gaudray, R., Moore, C.M., Needham-Vandevanter, D.R., Von Hoff, D.D., and Wahl, G.R. (1988). *Mol. Cell. Biol.* 7: 1740-1750.

Carroll, S.M., Trotter, J., and Wahl, G.M. (1991). *Mol. Cell. Biol.* 11: 4779-4785.

Charron, J., Malynn, B.A., Fisher, P., Stewart, V., Jeanotte, L., Goff, S.P., Robertson, E.J., and Alt, F.W. (1992). *Genes Dev.* 6: 2248-2257.

Chen F.Y., Amara F.M., and Wright J.A. (1993) *The EMBO J.* 12: 3977-3986.

Chen, C., Nagy, Z., Prak, E.L., and Weigert, M. (1995b). *Immunity* 3: 747-755.

Chen, C., Nagy, Z., Radic, M.Z., Hardy, R.R., Huszar, D., Camper, S.A., and Weigert, M. (1995a). *Nature* 373: 252-255.

Cheng, L. and Kelly, T.J., (1989). *Cell* 59: 41-51.

Chernova, O.B., Chernov., M.V., Ishizaka, Y., Agarwal, M.L., Stark, G.R. (1998). *Mol. Cell. Biol.* 18: 536-545.

Chevalier, S. and Blow, J.J. (1996). *Curr.Opin. Cell. Biol.* 8: 815-821.

Chisholm, O., Stapleton, P., and Symonds, G. (1992). *Oncogene* 7: 1827-1836.

Chou, T.Y., Dang, C.V., and Hart, G.W. (1995a). *Proc. Natl. Acad. Sci. USA* 92: 4417-4421.

Chou, T.Y., Hart, G.W., and Dang, C.V. (1995b). *J. Biol.Chem.* 270: 18961-18965.

Choy, B.K., McClarty G.A., and Wright J.A., (1989). *Biochem. Biophys. Res. Commun.* 162: 1417-1424.

Choy, B.K., McClarty G.A., Chan A.K., Thelander L., and Wright J.A. (1988). *Cancer Res.* 48: 2029-2035.

Christoph, F., Schmidt, B., Scmitz-Drager, B.J., and Shultz, W.A. (1999). *Int. J. Cancer* 84: 169-173.

Clark, H.M., Yano, T., Otsuki, T., Jaffe, E.S., Shibata, D., and Raffeld, M. (1994). *Cancer Res.* 54: 3383-3386.

Classon, M., Henrikson, M., Klein, G., and Hammaskjold M-L. (1987). *Nature* 330: 272-274.

Classon, M., Henrikson, M., Klein, G., and Sümegi, J. (1990). *Oncogene* 5: 1371-1376.

Classon, M., Wennborg, A., Henrikson, M., and Klein, G. (1993). *Gene* 133: 153-161.

Cocking, J.M., Tonin P.M., Stokoe N.M., Wensing E J., Lewis W.H., and Srinivasan P.R. (1987). *Somat. Cell Mol. Genet.* 13: 221-223.

Cole, M.D. (1986). *Annu. Rev. Genet.* 20: 361-384.

Conrad, A.H. (1971). *J. Biol. Chem.* 246: 1318-1323.

Cooper, M.D., Payne, L.N., Dent, P.B., Burmester, B.R., and Good, R.A. (1968). *J. Natl. Cancer. Inst.* 41: 373-378.

Copolla, J. A. and Cole M.D. (1986). *Nature* 320: 760-763

Cory, S. (1986). *Adv. Cancer Res.* 47: 189-234.

Coverley, D. and Laskey, R.A. (1994). *Annu. Rev. Biochem.* 63: 745-776.

D'Andrea, A.D., Tantravahi, U., Lelande, M., Perle, M.A., and Latt, S.A. (1983). *Nucl. Acids. Res.* 11: 4753-4774.

Daksis, J.I., Lu, R.Y., Facchini, L.M., Marhin, W.W., and Penn, L.J.Z. (1994). *Oncogene* 9: 3635-3645.

Dalla-Favera, R., Bregni, M., Erikson, J., Patterson, D., Gallo, R.C., and Croce, C.M. (1982) *Proc. Natl. Acad. Sci. USA* 79: 7824-7827.

Dang, C.V. and Lee, L.A. (1995). c-Myc Function in Neoplasia. R.G Landes and Springer-Verlag, Austin Texas.

Dani, C., Blanchard, J.M., Piechaczyk, M., El Sabouty, S., Marty, L., and Jeanteur, P. (1984). *Proc. Natl. Acad. Sci. USA* 81: 7046-7050.

Davis, A.C., Wims, M., Spotts, G.D., Hann, S.R., Bradley, A. (1993). *Genes Dev.* 7: 671-682.

Davis, R.J. (1993). *J. Biol. Chem.* 268: 14553-14556.

DeLap, R.J., Rush, M.G., Zouzias, D., and Khan S. (1978). *Plasmid* 1: 508-521.

Delikadis, C. and Kafatos, F.C. (1989). *The EMBO J.* 8: 891-901.

Denis, N., Kitzis, A., Kruh, J., Dautry F., and Crocos, D. (1991) *Oncogene* 6: 1453-1457.

DePamphilis, M.L. (1997). *Methods: A Companion to Methods in Enzymology*, 13: 211-219.

DePinho, R.A., Schreiber-Agus, N., and Alt, W. (1991). *Adv. Cancer Res.* 57: 1-46.

Diffley, J.F.X. (1996). *Genes Dev.* 10: 2819-2830.

Diffley, J.F.X. and Stillman, B. (1990). *Trends Genet.* 6: 426-432.

Dmitrovsky, E., Kuehl, W.M., Hollis, G.F., Kirsch, I.R., Bender, T.P., and Segal, S. (1986). *Nature* 322: 748-750.

Donner, P., Greiser-Wilke, X., and Moelling, K. (1982). *Nature* 296: 262-265.

Donzelli, M., Bernardi, R., Negri, C., Prosperi, E., Padovan, L., Lavialle. C., Brison, O., and Scovassi, A.I. (1999). *Oncogene* 18: 439-448.

Duesberg, P.H. and Vogt, P.T. (1979). *Proc. Natl. Acad. Sci. USA* 76: 1633-1637.

Eick, D. and Bornkamm, G.W. (1986). *Nucl. Acids. Res.* 14: 8331-8346.

Eilers, M., Picard, D., Yamamoto, K.R., and Bishop, J.M. (1989). *Nature* 340: 66-68.

El-Naggar., A.K., Lai, S., Tucker, S.A., Clayman,G.L., Goepfert, H., Hong, W. K., and Huff, V. (1998). *Oncogene* 18: 7063-7069.

Endow, S.A. and Atwood, K.C. (1988). *Trends Genet.* 4: 348-351.

Engström Y. and Rozell B (1988). *The EMBO J.* 7: 1615-1620.

Engström Y., Eriksson S., Jildevik I., Skog S., Thelander L., and Tribukait B. (1985) *J. Biol. Chem.* 260: 9114-9116.

Engström Y., Rozell B., Hansson H-A, Stemme S., amd Thelander L. (1984). *The EMBO J.* 3: 863-867.

Epner, E., Forrester, W.C., and Groudine, M. (1988). *Proc. Natl. Acad. Sci. USA* 85: 8081-8085.

Era, T., Nishikawa, S., Sudo, T., Fu-Ho, W., Ogawa, M., Kunisada, T., Hayashi, S-I., and Nishikawa, S-I. (1994). In *Immunol. Rev.*, G. Möller (ed.) Munksgaard (Copenhagen), pp. 35-51.

Eriksson S., Gräslund A., Skog S., Thelander L., and Tribukait B. (1984). *J. Biol Chem.* 259: 11695-11700.

Ermakova, O.V., Nguyen, L.H., Little, R.D., Chevillard, C., Riblet, R., Ashouian, N., Birshtein, B.K., and Schildkraut. (1999). *Mol. Cell* 3: 321-330.

Evan, G.I., Lewis, G.K., Ramsay, G., and Bishop, J.M. (1985). *Mol. Cell. Biol.* 5: 3610-3616.

Evan, G.J., Wyllie, A.H., Gilbert, C.S., Littlewood,T.D., Land, H., Brooks, M., Waters, C.M., Penn, L.Z., and Hancock, D.C. (1992). *Cell* 69: 119-128.

Facchini, L.M., Chen, S., Marhin, W.W., Lear, J.N., and Penn, L.Z. (1997). *Mol. Cell. Biol.* 17: 100-114.

Fan H., Huang A., Villegas C., and Wright J.A. (1997) *Proc. Natl. Acad. Sci. USA* 94: 13181-13186.

Fan H., Villegas C., and Wright J.A. (1996b) *Proc. Natl. Acad. Sci. USA* 93: 14036-14040.

Fan H., Villegas C., Huang A., and Wright J.A. (1996a). *Cancer Res.* 56: 4366-4369.

Fang, C.M., Shi, C., and Xu, Y.U. (1999). *Cell Res.* 9: 305-314.

Farber E. and Cameron R. (1980). *Adv. Cancer Res.* 31: 125-226.

Federspeil, N.A., Beverley, S.M., Schilling, J.W., and Schimke, R.T. (1984). *J. Biol. Chem.* 259: 9127-9140.

Fearon, E.R. and Vogelstein, B. (1990). *Cell* 61: 759-767.

Felsher, D.W. and Bishop, J.M. (1999). *Proc. Natl. Acad. Sci. USA* 96: 3940-3944.

Feo, S., Liegro, C.D., Jones, T., Read, M., and Fried, M. (1994). *Oncogene* 9: 955-961.

Flemington E., Bradshaw H.D. Jr., Traina-Dorge V., Slagel V., and Deininger P.L. (1987) *Gene* 52: 267-277.

Flinn, E.M., Busch, C.M.C., and Wright, A.P.H. (1998). *Mol. Cell. Biol.* 18: 5961-5969.

Flores, S.C., Sunnerhagen, P., Moore, T.K., and Gaubatz, J.W. (1988). *Nucl. Acids Res.* 16: 257-260.

Ford, M. and Fried, M. (1986). *Cell* 45: 425-430.

Foulds, L. (1958). *J. Chronic Dis.* 8: 2-37.

Francis, D.A., Sen, R., and Rothstein, T.L. (1997). C-Myc in B Cell Neoplasia *Curr. Top. Microbiol. Immunol.* 224: 85-90. Potter and Melchers (Eds.)

Friedman, K.L., Diller, J.D., Ferguson, B.M., Nyland, S.V., Brewer, B.J., and Fangman, W.L. (1996). *Genes Dev.* 10: 1595-1607.

Fry M. and Loeb L.A. (1986). *In Animal Cell DNA Polymerases* CRC Press. Boca Raton FL. pp. 13-60.

Fukasawa, K., Wiener, F., Vande Woude, G.F., and Mai, S. *Oncogene* 15: 125-1302.

Galaktionov, K., Chen, X., and Beach, D. (1996). *Nature* 382: 511-517.

Galaktionov, K., Lee, A.K., Eckstein, J., Draetta, G., Meckler, J., Loda, M., and Beach, D. (1995). *Science* 269: 1575-1577.

Gaubatz, J.W. (1990). *Mutation Research* 237: 271-292.

Gaubatz, J.W. and Flores, S.C. (1990). *Mutation Research* 237: 29-36.

Gerbitz, A., Mautner, J., Geltinger, C., Hörtnagel, K., Christoph, B., Asenbauer, H., Klobeck, G., Polack, A., and Bornkamm, G.W. (1999). *Oncogene* 18: 1745-1753.

Giulotto, E., Knights, C., and Stark, G.R. (1987). *Cell.* 48: 837-845.

Giulotto, E., Saito, I., and Stark, G.R. (1986). *The EMBO J.* 5: 2115-2121.

Goldman, M.A., Holmquist, G.P., Gray, M.C., Caston, L.A., and Nag, A. (1984). *Science* 224: 686-692.

Graf, T. and Beug, H. (1978). *Biochim. Biophys. Acta* 516: 269-299.

Gräslund A., Ehrenberg A., and Thelander M. (1982) *J. Biol. Chem.* 257: 5711-5715.

Grawunder, U., Leu, T.M.J., Schatz, D.G., Werner, A., Rolink, A.G., Melchers, F., and Winkler, T.H. (1995). *Immunity* 3: 601-608.

Griffin-Shea, R., Thireos, G., and Kafatos, F.C. (1982). *Dev. Biol.* 91: 325-336.

Gu, W., Bhatia, K., Magrath, I.T., Dang, C.V., and Dalla-Favera. (1994). *Science* 264: 251-254.

Hahn, P.J. (1993). Molecular biology of double-minute chromosomes. *Bio Essays* 15: 477-484.

Hand, R. (1978). *Cell* 15: 317-325.

Hann, S.R., Abrams, H.D., Rohrschneider, L.R., Eisenman, R.N. (1983). *Cell* 34: 789-98

Hann, S.R. and Eisenman, R.N. (1984). *Mol. Cell. Biol.* 4: 2486-2497.

Hanson, K.D., Shichiri, M., Follansbee, M.R., and Sedevy, J.M. (1994). *Mol. Cell. Biol.* 14: 5748-5755.

Hardy, R.R., Carmack, C.E., Li, Y.S., and Hayakawa, K., (1994). In *Immunol. Rev.*, G. Möller (ed.) Munksgaard (Copenhagen), pp. 91-118.

Harris, L.J., D'Eustachio, P., Ruddle, F.H., Marcu, K.B. (1982). *Proc. Natl. Acad. Sci. USA* 79: 6622-6626.

Hatton, K.A., Dhar, V., Brown, E.H., Iqbal, M.A., Stuart, S., Didamo, V.T., and Schildkraut, C.L. (1988). *Mol. Cell. Biol.* 8: 2149-2158.

Hatton, K.A., Mahon, K., Chin, L., Chiu, F-C., Lee, H-W., Peng, D., Morgenbesser, S.D., Horner, J., and DePinho, R.A. (1996). *Mol. Cell. Biol.* 16: 1794-1804.

Hawley , R.S. and Tardoff, K.D. (1985). *Genetics* 109: 691-700.

Hay, N., Bishop, M., and Levens D. (1987). *Genes Dev.* 1: 659-671.

Hayles, J., Fissher, D. Woollard, A., and Nurse, P. (1994). *Cell* 78: 813-822.

Hayward, W.S., Neel, B.G., and Astrin, S. (1981). *Nature* 290: 475-480.

Heikkila, R., Schwab, G., Wickstrom, E., Loke, S.L., Pluznik, D,H., Watt, R., and Neckers, L.M. (1987). *Nature* 328: 445-449.

Heinzel, T., Lavinsky, R.M., Mullen, T.M., Soderstrom, M., Laherty, C.D., Torchia, J., Yang, W.M., Brard, G., Ngo, S.D., Davie, J.R., Seto, E., Eisenman, R.N., Rose, D.W., Glass, C.K., Rosenfeld, M.G. (1997). *Nature* 387: 43-48.

Henriksson, M. and Lüscher, B. (1996). *Adv. Cancer Res.* 68: 109-182.

Hill, A.B. and Schimke, R.T. (1985). *Cancer Res.* 45: 5050-5057.

Hoang, A.T., Lutterbach, B., Lewis, B.C., Yano, T., Chou, T.-Y., Barret, J.F., Raffeld, M., Hann, S.R., and Dang, C.V. (1995). *Mol. Cell. Biol.* 15: 4031-4042.

Homesley, L., Lei, M., Sawyer, S., Christensen, T., Tye, B.K. (2000). *Genes Dev.* 14: 913-926.

Hotta, Y. and Bassel, A. (1965). *Proc. Natl. Acad. Sci. USA* 53: 356-362.

Huang, A. and Wright, J.A. (1994). *Oncogene* 9: 491-499.

Huang, A. Jin, H., and Wright, J.A. (1994). *Exp. Cell Res.* 213: 335-339.

Huang, A. Jin, H., and Wright, J.A. (1995). *Cancer Res.* 55: 1758-1762.

Hurlin, P.J., Ayer, D.E., Grandori, C., and Eisenman, R.N. (1994). *Cold Spring Harbor Symp. Quant. Biol.* 59: 109-116.

Hurlin, P.J., Queva, C., Eisenman, R.N. (1997). *Curr. Top. Microbiol. Immunol.* 224: 115-121.

Hurta R.A.R., Samuel S.K., Greenberg A.H., and Wright J.A. (1991). *J. Biol. Chem.* 266: 24097-24100.

Hyrien, O., Debatisse, M., Buttin, G., and Robert de Saint Vincent, B. (1987). *The EMBO J.* 7: 407-417.

Ingvarsson, S., Asker, C., Axelson, H., Klein, G., and Sümegi, J. (1988). *Mol. Cell. Biol.* 8: 3168-3174.

Iritani, B.M. and Eisenman, R.N. (1999). *Proc. Natl. Acad. Sci. USA* 96: 13180-13185.

Itoh, N. and Shimizu, N. (1998). *J. Cell Sci.* 111: 3275-3285.

Jaffe, B.M., Eisen, H.N., Simms, E.S., and Potter, M. (1969). *J. Immunol.* 103: 872-878.

Jallepalli, P.V. and Kelly, J.T. (1996). *Genes Dev.* 10: 541-552.

Jansen-Dürr, P., Meichle, A., Steiner, P., Pagano, M., Finke, K., Botz, J., Wessbecher, J., Draeta, G., and Eilers M. (1993). *Proc. Natl. Acad. Sci. USA* 90: 3685-3689.

Jensen R.A., Page D.L., and Holt J.T. (1994). *Proc. Natl. Acad. Sci. USA* 91: 9257-9261.

Johnston, R.N., Beverly, S.M., and Schimke R.T. (1983). *Proc. Natl. Acad. Sci. USA* 80: 3711-3715.

Jones, C.W. and Kafatos, F.C. (1980). *Cell* 22: 855-867.

Jones, R.S. and Potter, S.S. (1985a). *Proc. Natl. Acad. Sci. USA* 82: 1989-1993.

Kafatos, F.C., Orr, W., and Delidakis, C. (1985). *Trends Genet.* 1: 301-306.

Kam, J., Watson, W., Lowe, A.D., Green, S.M., and Vedeckis, W. (1989). *Oncogene* 4: 773- 787.

Kato, G.J., Wechsler, D.S., and Dang, C.V. (1992). Cancer Treat. Res. 63: 313-325.

Kaufman, R.J., Brown, P.C., and Schimke, R.T., (1979). *Proc. Natl. Acad. Sci. USA* 76: 5669-5673.

Kellems, R.E., Harper, M.E., and Smith, L.M. (1982). *J. Cell Biol.* 92: 531-539.

Kelly, K., Cochran, B., Stiles, C., and Leder, P. (1984). *Curr. Top. Microbiol. Immunol.* 113: 117-126.

Kincade, P.W., Medina, K.L., and Smithson, G. (1994). In *Immunol. Rev.* G. Möller (ed.) Munksgaard (Copenhagen), pp. 119-134.

Kitsberg, D., Selig, S., Brandeis, M., Simon, I., Keshet, I., Driscoll, D.J., Nicholls, R.D., Cedar, H. (1993). *Nature* 364: 459-63.

Klein G. and Klein, E. (1985). *Immunol. Today* 6: 208-215.

Kleinberger, T., Flint, Y.B., Blank, M., Etkin, S., and Lavi, S. (1988). *Mol. Cell. Biol.* 8: 1366-1370.

Kornberg, A. and Baker, T.A. (1992). *DNA Replication*, 2nd ed., Freeman, New York.

Kotani, H. and Kmiec, E.B. (1994). *Mol. Gen. Genet.* 243: 681-690.

Kretzner, L., Blackwood, E.M., and Eisenman, R.N. (1992). *Nature* 359: 426-429.

Krolewski, J.J. and Rush, M.G. (1984). *J. Mol. Biol.* 174: 31-40.

Krolewski, J.J., Schindler, C.W., and Rush, M.G. (1984). *J. Mol. Biol.* 174: 41-54.

Krumm, A., Hickey, L.B., and Groudine, M. (1995). *Genes Dev.* 9: 559-572.

Krumm, A., Meulia, T., Brunvand, M., and Groudine, M. (1992). *Genes Dev.* 6: 2201-2213.

Kunisada, T., Yamagishi, H., and Sekiguchi, T. (1983). *Plasmid* 10: 242-250.

Kunisada, T., Yamagishi, J. (1984). *Gene* 31: 213-223.

Kunisada, T., Yamagishi, J., Ogita, A., Kirakawa, T., and Mitsui. (1985). *Mech. Aging Dev.* 29: 89-99.

Kyo, S., Takakura, M., Taira, K., Itoh, H., Yutsodo, M., Ariga, H., and Inue, M. (2000). *Nucleic. Acids Res.* 28: 669-677.

La Rocca, S.A., Crouch, D.H., and Gillespie, D.A. (1994). *Oncogene* 9: 3499-3508.

Land, H., Parada, L.F., and Weinberg, R.A. (1983). *Nature* 304: 596-602.

Langdon, W.Y., Harris, A.W., Cory, S., and Adams, J.M. (1986). *Cell* 47: 11-18.

Lavenu, A., Pournin, S., Babinet, C., Morello, D. (1994). *Oncogene* 9: 527-536.

Lavi, S. (1981). *Proc. Natl. Acad. Sci. USA* 78:6144-6148.

Leder, A., Pattengal, P.K., Kuo, A., Stewart, T.A., and Leder, P. (1986). *Cell* 45: 485-495.

Lee, L.A. and Dang, C.V. (1997). in C-Myc in B Cell Neoplasia *Curr. Top. Microbiol. Immunol.* 224: 131-135. Potter and Melchers (Eds.)

Lee, L.A., Dolde, C., Barrett, J., Wu, C.S., and Dang, C.V. (1996). *J. Clin. Invest.* 97: 1687-1695.

Lemaitre, J-M., Buckle, R.S., and Mechali,. M. (1996). *Adv. Cancer Res.* 70: 96-144.

Lengauer C., Kinzler, K.W., and Vogelstein, B. (1998) *Nature* 396: 643-649.

Leonhardt, H., Rahn, H-P., Weinzierl, P., Sporbert, A., Cremer, T., Zink, D., and Cardoso, M.C. (2000). *J. Cell Biol.* 149: 271-279.

Lewis, B.C., Shim, H., Li, Q., Wu, C.S., Lee, L.A., Maity, A., and Dang, C.V. (1997). *Mol. Cell. Biol.* 17: 4967-4978.

Li L.H., Nerlov, C., Prendergast, G., MacGregor D., Ziff, E.B. (1994). *The EMBO. J.* 13: 4070-4079.

Li, Q. and Dang, C.V. (1999). *Mol. Cell Biol.* 19: 5339-5351.

Lin, C.C., Alitalo, K., Schwab, M., George, D., Varmus, H.E., and Bishop, J.M. (1985). *Chromosoma (Berl.).* 92: 11-15.

Lin, Y., Wong, K-K, Calame, K. (1997). *Science* 276: 596-599.

Little, C.D., Nau, M.M., Carney, D.N., Gazdar, A.F., and Minna, J.D. (1983). *Nature* 306: 194-196.

Lipp, M., Schilling, R., Wiest, S., Laux, G., and Bornkamm, G.W. (1987). *Mol. Cell. Biol.* 7: 1393-1400.

Littlefield, J.W. (1996) *Biochim. Biophys. Acta.* 114: 398-403.

Littlewood, T.D., Hancock, D.C., Danielian, R.S., Parker, M.G., and Evan, G.I. (1995). *Nucl. Acids Res.* 23: 1686-1690.

Looney, J.E. and Hamlin, J.L. (1987). *Mol. Cell. Biol.* 7: 569-577.

Lücke-Huhle, C. (1989). *Mol. Toxicol.* 2: 237-253.

Lücke-Huhle, C. (1994). *Int. J. Radiat. Biol.* 65: 665-673.

Lücke-Huhle, C. and Herrlich, P. (1987). *Int. J. Cancer* 39: 94-98.

Lücke-Huhle, C. and Herrlich, P. (1991). *Int. J. Cancer* 47: 461-465.

Lücke-Huhle, C., Mai, S., and Moll, J., 1997. c-Myc overexpression facilitates radiation-induced DHFR gene amplification. *Int. J. Radiat. Biol.* 71: 167-175.

Lücke-Huhle, C., Pech, M., and Herrlich, P. (1990). *Int. J. Radiat. Biol.* 58: 577-588.

Lüscher, B. and Eisenman. R.T. (1990). *Genes Dev.* 4: 2025-2035.

Lüscher, B. and Eisenman. R.T. (1992). *J. Cell. Biol.*118: 775-784.

Lüscher, B.Kuenzel, E.A., Krebs, E.G., and Eisenman. R.T. (1989). *The EMBO J.* 8: 1111-1119.

Lutterbach, B. and Hann, S.R. (1994). *Mol. Cell. Biol.* 14: 5510-5522.

Mai, S. (1994a). *Gene* 148: 253-260.

Mai, S. (1994b) Cyclin D2, a target for c-Myc-mediated gene amplification in *Basel Institute for Immunology Annual Report for 1994.* p.53.

Mai, S. and Jalava, A. (1994). *Nucleic Acids Res.* 22: 2264-2273.

Mai, S., Hanley-Hyde, J., and Fluri, M. (1996) *Oncogene* 12: 277-288.

Mai, S., Hanley-Hyde, J., Rainey, G.J., Kuschak, T.I., Fluri, M., Taylor, C., Littlewood, T.D., Mischak, H., Stevens L.M., Henderson, D.W., and Mushinski, J.F. *Neoplasia*, 1: 241-252.

Mai, S., Lücke-Huhle, C., Kaina, B., Rahmsdorf, H.J., Stein, B., Ponta, H., and Herrlich, P. (1990). In: Ionizing Radiation Damage of DNA. Molecular Aspects. Wiley-Liss., New York, NY. 319-331.

Mai, S. and Mårtensson, I-L. (1995). *Nucl. Acids. Res.* 23: 1-9.

Maiorano, D., Moreau, J., and Méchali, M. (2000). *Nature* 404: 622-625.

Malynn, B.A., Demengeot, J., Stewart, V., Charron, J., and Alt, F.W. (1995). *Int. Immunol. 7*: 1637-1647.

Malynn, B.A., de Alboran, I.M., O'Hagan, R.C., Bronson, R., Davidson, L., DePinho, R.A., and Alt, F.W. (2000). *Genes Dev.* 1390-1399.

Mann G.J., Musgrove E.A., Fox R.M., and Thelander L. (1988). *Cancer Res.* 48: 5151-5156.

Manolov, G. and Manolova, Y. (1972). *Nature*, 237: 33-34.

Marcu, K.B., Bossone, S.A., and Patel, A.J. (1992). *Ann. Rev. Biochem.* 61: 809-860.

Mariani, B.D. and Schimke, R.T. (1984). *J. Biol. Chem.* 259: 1901-1910.

Mariani-Constatini, R., Escot, C., Theillet, C., Gentile, A., Merlo, G., Lidereau, and Callahan, R. (1988). *Cancer Res.* 48: 199-205.

Mateyak, M.K., Obaya, A.J., Adachi, S., and Sedivy, J.M. (1997). *Cell Growth Differ.* 8: 1039-1048.

Mateyak, M.K., Obaya, A.J., and Sedevy, J.M. (1999). *Mol. Cell. Biol.* 19: 4672-4683.

Mautner, J., Behrends, U., Hortnagel, K., Briemeir, M., Hammerschmidt, W., Strobl, L., Bornkamm, G.W., and Polack, A. (1996). *Oncogene* 12: 1299-1307.

Mautner, J., Joos, S., Werner, T., Eick, D., Bornkamm, G.W., and Polack, A. (1995). *Nucleic Acids Res.* 23: 72-80.

McClarty G.A., Chan A.K.M., Choy B.K., and Wright J.A. (1987a). *Biochem. Biophys. Res. Commun.* 145: 1276-1282.

McClarty G.A., Chan A.K.M., Engström Y., Wright J.A., and Thelander L. (1987b). *Biochemistry* 26: 8004-811.

McDonnell, T.J. and Korsmeyer, S.J. (1991). *Nature* 349: 254-256.

McDonnell, T.J., Diane, N., Platt, F.M., Nunez, G., Jaeger, U., McKearn, J.P., and Korsmeyer, S.J. (1989). *Cell* 57: 79-88.

Melchers, F. (1979). In Melchers (1997) in C-Myc in B Cell Neoplasia *Curr. Top. Microbiol. Immunol.* 224: 19-30. Potter and Melchers (Eds.)

Melchers, F. (1995). In *Immunoglobulin Genes* (Honjo and Alt, eds.) Academic Press (London).

Melchers, F. (1997). In C-Myc in B Cell Neoplasia *Curr. Top. Microbiol. Immunol.* 224: 19-30. Potter and Melchers (Eds.)

Melchers, F., Karasuyama, H., Haasner, D., Bauer, S., Kudo, A., Sakaguchi, N., Jameson, B., Rolink, A. (1993). *Immunol. Today* 14: 60-68.

Merchant, A.M., Kawasaki, Y., Chen,Y., Lei, M., Tye, B.K. (1997). *Mol. Cell. Biol.* 17: 3261-3271.

Michaelson, J.S., Ermakova, O., Birshtein, B.K., Ashouian, N., Chevillard, C., Riblet, R., and Schildkraut, C.L. (1997). *Mol. Cell. Biol.* 17: 6167-6174.

Mladenov, Z., Heine, U., Beard, D., and Beard, J.W. (1967). *J. Natl. Cancer Inst.* 38: 251-285.

Mombaerts, P., Iacomini, J., Johnson, R.S., Herrup, K., Tonegawa, S., and Papaioannou, V.E. (1992). *Cell* 68: 869-877.

Moreno, S. and Murse, P. (1994). *Nature* 367: 236-240.

Morrow, M.A., Lee, G., Gillis, L.G., Yancopoulos, G.D., and Alt, F.W., (1992). *Genes Dev.* 6: 61-70.

Mount, S.M. (1982). *Nucleic Acids Res.* 10: 459-472.

Müller, J., Jones, G.M., Janz, S., and Potter, M. (1997). *Blood* 89: 291-296.

Müller, J., Jones, G.M., Potter, M., and Janz, S. (1996). *Cancer Res.* 56: 419-423.

Munzel, P., Marx, D., Kochel, H., Shauer, A., and Bock, K.W. (1991). *J. Cancer. Res. Clin. Oncol.* 117: 603-607.

Mukherjee, B., Morgenbesser, S.D., and DePinho, R.A. (1992). *Genes Dev.* 6: 1480-1492.

Murre, C., McCaw, P.S., and Baltimore, (1989). *Cell* 56: 777-783.

Muzi-Falconi, M., Brown, G.W., and Kelly, G.T. (1996). *Proc. Natl. Acad. Sci. USA* 93: 1566-1570.

NIBC Genbank, http://www.ncbi.nlm.nih.gov/Omim/Homology/. Cited May, 2000.

Nalbantoglu, J. and Meuth, M. (1986). *Nucl. Acids Res.* 14: 8361-8371.

Namazee, D., Russell, D., Arnold, B., Haemmerling, G., Allison, J., Miller, J.F., Morahan, G., and Buerki, K. (1991). *Immunol. Rev.* 122: 117-132.

Nashitani, H. and Nurse, P. (1995). *Cell* 83: 397-405.

Nass, S.J. and Dickson, R.B. (1998). *Cancer Res.* 4: 1813-1822.

Neel, B.G., Hayward, W.S., Robinson, H.L., Fang, J., and Astrin, S. (1981). *Cell* 23: 323-334.

Nepveu, A. and Marcu, K.B. (1986). *The EMBO J.* 11: 3307-3314.

Nishikura, N. (1986). *Mol. Cell Biol.* 6: 4093-4098.

Nickol, J., Martin, R.G. (1983). *Proc. Natl. Acad. Sci. USA* 80: 4669-4673.

Nishitani, H., Lygerou, Z., Nishimoto, T., and Nurse, P. (2000). *Nature* 404: 625-628.

Nobile, C., Nickol, J., Martin, R.G. (1986) *Mol. Cell. Biol.* 6: 2916-2922.

Nogrady, T. *Medicinal Chemistry A Biochemical Approach, Second Edition.* (1988) Oxford University Press, New York, Oxford. pp.390-391.

Oettinger, M.A., Schatz, D.G., Gorka, C., and Baltimore, D. (1990). *Science* 248: 1517-1523.

Ogawa, M., Matzusaki, Y., Nishikawa, S., Hayashi, S.I., Kunisada, T., Sudo, T., Kina, T., Nakauchi, H., Nishikawa, S.I. (1991). *J. Exp. Med.* 174: 63-70.

Ohno, S., Babonits, M., Weiner, F., Spira, J., Klein, G., and Potter, M. (1979). *Cell* 18: 1009-1007.

Packham, G. and Cleveland, J.L. (1995). *Biochim. Biophys. Acta.* 1242: 11-28.

Painter, R.B., Young, B.R., and Kapp, L.N. (1987). *Cancer Res.* 47: 5595-5599.

Paria, B.C., Dey, S.K., and Andrews, G.K. (1992). *Proc. Natl. Acad. Sci. USA* 89: 10051-10055.

Passananti, C., Davies, B., Ford, M., and Fried, M. (1987). *The EMBO J.* 6: 1697-1703.

Pattengale, P., Leder, A., Kuo, A., Stewart, T., and Leder, P. (1986). *Curr. Top. Microbiol. Immunol.* 132: 9-16.

Payne, G.S., Bishop, J.M, and Varmus, H.E. (1981). *Nature* 295: 209-214.

Pegram, M.D., Lipton, A., Hayes, D.F., Weber, B.L., Baselga, J.M., Tripathy, D., Baly, D., Baughman, S.A., Twaddell, T., Glaspy, J.A., Slamon, D.J. (1998). *J. Clin. Oncol.* 16:2659-2671.

Penn, L.J.Z., Brooks, M.W., Laufer, E.M., Littlewood, T.D., Morgenstem, J.P., Evan, G.I., Lee, W.M.F., and Land, H. (1990). *Mol. Cell. Biol.* 10: 961-966.

Perez-Roger, I., Kim, S-H., Griffiths, B., Sewing, A., and Land, H. (1999). *The EMBO J.* 18: 5310-5320.

Persson, H. and Leder, P. (1984) *Science* 225: 718-721.

Philipp, A., Schneider, A., Vastrik, I., Finke, K., Xiong, Y., Beach, D., Alitalo, K., and Eilers M. (1994). *Mol. Cell. Biol.* 14: 4023-4032.

Polack, A., Strobl, L., Feederle, R., Schweizer, M., Koch, E., Eick, D., Wiegand, H., and Bornkamm, G.W. (1991). *Oncogene* 6: 2033-2040.

Potter, M. and Marcu, K.B. (1997) in C-Myc in B Cell Neoplasia *Curr. Top. Microbiol. Immunol.* 224: 1-17. Potter and Melchers (Eds.)

Prak, E.L. and Weigert, M. (1995). *Curr. Opin. Immunol.* 4: 171-176.

Prody, C.A., Dreyfus, P., Zamir, S.M., Zakut, H., and Soreq, H. (1989) *Proc. Natl. Acad. Sci. USA* 86: 690-694.

Radloff, R., Bauer, W., and Vinograd, J. (1967). *Proc. Natl. Acad. Sci. USA* 57: 1514-1522.

Rath, H., Tlsty, T.D., and Schimke, R.T. (1984). *Cancer Res.* 44: 3303-3306.

Reichard P. (1988). *Annu. Rev. Biochem.*, 57: 349-374.

Resar, L.M., Dolde, C., Barrett, J.F., and Dang C.V. (1993). *Mol. Cell. Biol.* 13: 1130-1136.

Riabowol, K., Smookler Ries R.J., and Goldstein, S. (1985). *Nucl. Acids Res.* 13: 5563-5584.

Rice, G.C., Ling, V., and Schimke, R.T. (1987). *Proc. Natl. Acad. Sci. USA* 84: 9261-9264.

Rolink, A., Haasner, D., Nishikawa, S.I., and Melchers, F. (1993). *Blood* 81: 2290-2300.

Rolink, A., Kudo, A., Karasuyama, H., Kikuchi, Y., and Melchers, F. (1991a). *The EMBO J.* 10: 327-336.

Rolink, A., Streb, M., Nishikawa,. S.I., and Melchers, F. (1991b). *Eur. J. Immunol.* 21: 2609-2612.

Rolink, A., ten Boekel, E., Melchers, F., Fearon, D.T., Krop, I., Andersson, J. (1996). *J. Exp. Med.* 183: 187-194.

Roy, A.L., Curruthers, C., Gutjahr, T., and Roeder, R.G. (1993). *Nature* 365: 359-361.

Ruiz, J.C. and Wahl, G.M. (1988). *Mol. Cell. Biol.* 8: 4302-4313.

Saeki T., Takahashi T., Okabe M., Furuya A., Hanai, N., Yamagami K., Mundai K., Moriwaki S., Diohara H., Takashima S., and Solomon D.S. (1995) *Int. J. Oncol.* 6: 523-533.

Saito, I., Groves, R., Giulotto, E., Rolfe, M., Stark, G.R. (1989). *Mol. Cell. Biol.* 9:2445-2452.

Sakamuro, D., Elliott, K.J., Wechsler-Reya, R., and Predergast, G.C. (1996). *Nature Genet.* 14: 69-77.

Santelli, R.V., Machado-Santelli, G.M., Pueyo, M.T., Navarro-Cattapan, L.D., and Lara, F.J.S. (1991) *Mech. Dev.* 36: 59-66.

Sawai, S.A., Shimono, K., Yakamatsu, Y., Palmes, C., ans Kondoh, H. (1993). *Development*: 117: 1445-1455.

Schatz, D.G., Oettinger, M.A., and Balitmore, D. (1989). *Cell* 59: 1035-1048.

Schimke, R.T., (1984a). *Cancer Res.* 44: 1735-1742.

Schimke, R.T., (1984b). *Cell* 37: 705-713.

Schimke, R.T., (1986). *Cancer* 10: 1912-1917.

Schimke, R.T., (1988). *J. Biol. Chem.* 263: 5989-5992.

Schimke, R.T., Kaufman, R.J., Alt, F.W., and Kellems, R.F. (1978) *Science* 202: 1051-1055.

Schimke, R.T., Sherwood, S.W., Hill, A.B., and Johnston, R.N. (1986). *Proc. Natl. Acad. Sci. USA* 83: 2157-2161.

Schneider, A., Peukert, K., Eilers, M., and Hänel, F. (1997). c-Myc in B Cell Neoplasia *Curr. Top. Microbiol. Immunol.* 224: 137-146. Potter and Melchers (Eds.).

Seeger, R.C., Brodeur, G.M., Sather, H., Dalton, A., Siegel, S.E., Wong, K.Y., Hammond, D. N. (1985). *Engl. J. Med.* 313:1111-1116.

Seiser C., Knötler M., Rudelstorter I., Haas R., and Winterberger E. (1989). *Nucleic Acids Res.* 17: 185-196.

Shen-Ong, G.L., Keath, E.J., Piccoli, S.P., and Cole, M.D. (1982). *Cell* 31: 443-452.

Sherwood, S.W., Schumacher, R.I., and Schimke, R.T. (1988). *Mol. Cell. Biol* 8: 2822-2827.

Shim, H., Lewis, B.C., Dolde, C., Li, Q., Wu, C.-S., Chun, Y.S., and Dang, C.V. (1997) in C-Myc in B Cell Neoplasia *Curr. Top. Microbiol. Immunol.* 224: 181-190. Potter and Melchers (Eds.)

Shinkai, Y., Rathbun, G., Lam, K.P., Oltz, E.M., Stewart, V., Mendelsohn, M., Charron, J., Datta, M., Young, F., Stall, A.M., and Alt, F.W. (1992). *Cell* 68: 855-867.

Simon, I. and Cedar, H. (1996). In *DNA Replication in Eukaryotic Cells* (DePamphilis, M.L. Ed.) pp. 387-408. Cold Spring Harbor Laboratory Press, Plainview, N.Y.

Simpson, R.T. (1990). *Nature* 343: 387-389.

Singer, M.J., Menser, L.D., Friedman, C.L., Trask, B.J., Hamlin, J.L. (2000). Early edition online publication: *Proc. Natl. Acad. Sci. USA*, 10.1073/pnas.130194897.

Smith, C.A. and Vinograd, J. (1972). *J. Mol. Biol.* 69: 163-178.

Smith-Sorensen, B., Hijmans, E.M., Beijersbergen, R.L., and Bernards, R. (1996). *J. Biol. Chem.* 271-5513-5518.

Sommer, A., Bousset, K., Kremmer, E., Austen, M., and Lüscher, B. (1998). *J. Biol. Chem.* 273: 6632-3342.

Spencer, C.A. and Groudine, M. (1990). Adv. *Cancer Res.* 56B 1-48.

Spradling, A.C. (1981). *Cell* 27: 193-201.

Spradling, A.C. (1999). *Genes Dev.* 13: 2619-2623.

Spradling, A.C. and Mahowald, A.P. (1980). *Proc. Natl. Acad. Sci. USA* 77: 1096-1100.

Squire, J.A., Li, M., Perlikowski, S., Fei, Y.L., Bayani, J., Zhang, Z.M., Weksberg, R. 2000). *Genomics* 65: 234-242.

Stanfield, S.W. and Helsinki, D.R. (284). *Mol. Cell. Biol.* 4: 173-180.

Stanton, B.R. and Parada, L.F. (1992). *Brain Pathol.* 2: 71-83.

Stanton, B.R., Perkins, A., Tessarollo, L., Sassoon, D., and Parada, L.F. (1992). *Genes Dev.* 6: 2235-2247.

Stark, G.R. (1993). *Adv. Cancer Res.* 61: 87-113.

Stark, G.R. and Wahl, G.M. (1984). *Ann Rev. Biochem.* 53: 447-491.

Stark, G.R., Debatisse, E.G., and Wahl, G M. (1989). *Cell* 57: 901-908.

Steiner, P., Philipp, A., Lukas, J., Godden-Kent, D., Pagano, M., Mittnacht, S., Bartek, J., and Eilers, M. (1995). *The EMBO J.* 14: 4814-4826.

Stewart, T.A., Pattengale, P.K., and Leder, P. (1984). *Cell* 38: 627-637.

Strobl, L.J. and Eick (1992). *The EMBO J.* 11: 3307-3314.

Sunnerhagen, P., Sjoberg, R.M., Karlssen, L., Lundh, A.L., and Bjusell, G. (1986). *Nucleic Acids Res.* 14: 7823-7838.

Sutrave, P., Bonner, T.I., Rapp, U.R., Jansen, H.W., Patschinsky, T., and Bister, K. (1984). *Nature* 309: 85-88.

Tanaka, H., Arakawa, H., Yamaguchi, T., Shiriashi, K., Fukuda, S., Matsui, K., Takei, Y., and Nakamura, Y. (2000). *Nature* 404: 42-49.

Taylor, C., Jalava, A., and Mai, S. (1997). In C-Myc in B Cell Neoplasia *Curr. Top. Microbiol. Immunol.* 224: 201-207. Potter and Melchers (Eds.)

Thelander L. and Berg P. (1986). *Mol. Cell. Biol.* 6: 3433-3442.

Thelander L. and Reichard P. (1979). *Annu. Rev. Biochem.*, 48: 133-158.

Thelander L., Eriksson S., and Åkerman M. (1980). *J. Biol. Chem.* 255: 7426-7432.

Thelander M. and Thelander L. (1989). *The EMBO J.* 8: 2475-2479.

Thelander M., Gräslund A., and Thelander L. (1985). *J. Biol. Chem.* 260: 2737-2741.

Tlsty, T.D. (1990). *Exp. Cell Res.* 188: 164-168.

Tlsty, T.D. (1990). *Proc. Natl. Acad. Sci. USA* 87: 3132-3136.

Tlsty, T.D., Brown, P.E., and Schimke, R.T. (1984). *Mol. Cell Biol.* 4: 1050-1056.

Tlsty, T.D., Margolis, B.H., and Lum, K. (1989). *Proc. Natl. Acad. Sci. USA* 86: 9441-9445.

Tlsty, T.D., White, A., and Sanchez, J. (1992). *Science* 255:1425-1427.

Trent, J., Meltzer, P., Rosenblum, M., Harsh, G., Kinzler, K., Marshal, R., Feinberg, A., and Vogelstein, B. (1986). *Proc. Natl. Acad. Sci. USA* 83: 470-473.

Tsuda, T., Yamagishi, H., Ohnishi, N., Yamada, H., Izumi, H., and Mori, K.J. (1983). *Plasmid* 10: 235-241.

Tsujimoto, Y., Cossman, J., Jafee, E., and Croce, C.M. (1985). *Science*, 228: 1140-1143.

Van der Bliek, A.M., Van der Velde-Koerts, T., Ling V., and Borst, P. (1986). *Mol. Cell. Biol.* 6: 1671-1678.

Van Holde K, Zlatanova, J. (1994). *Bioessays* 16: 59-68.

VanDevanter, D.R., Piaskowski, V.D., Casper, J.T., Douglass, E.C., and Von Hoff, D.D. (1990). *J. Natl. Cancer. Inst.* 82: 1815-1821.

Varshavsky, A. (1981). *Proc. Natl. Acad. Sci. USA* 78: 3673-3677.

Vogelstein, B., Pardoll, D.M., and Coffee, D.S. (1980). *Cell* 22: 79-85.

Wahl, G.M. (1989). *Perspect.Cancer. Res.* 49: 1333-1340.

Waters, C.M., Littlewood, T.D., Hancock, D.C., Moore, J.P., and Evan, G.I. (1991). *Oncogene* 6: 797-805.

Weber G. (1983). *Cancer Res.* 43: 3466-3492.

Weintraub, H. (1983). *Cell* 32:1191-1203.

Wells, J., Held, P., Illeye, S., and Heintz, N.H. (1996). *Mol. Cell. Biol.* 16: 634-647.

Wiener, F., Kuschak T.I., Ohnu, S., and Mai, S. (1999). *Proc. Natl. Acad. Sci. USA* 96:13967-13972.

Winkler, T.H., Melchers, F., and Rolink, A.G. (1994). *Blood* 85: 2045-2051.

Wolf, D.A., Strobl, L.J., Pullner, A., and Eick, D. (1995). *Nucl. Acids. Res.* 23: 3373-3379.

Wong, C.W., and Privalsky, M.L. (1998). *Mol .Cell. Biol.* 18: 5500-5510.

Workman, J.L., Taylor, I.C., Kingston, R.E. (1991). *Cell* 64: 533-544.

Wright, J.A. (1989). *Encycl. Pharmacol. Therapeut.* 128: 89-111.

Wright ,J.A., Alam, T.G., McClarty, G.A., Tagger ,A.Y., and Thelander, L. (1987a). *Somat. Cell Mol. Genet.* 13: 155-165.

Wright, J.A., Chan, A.K., Choy, B.K., Hurta, R.A.R., McClarty, G.A., and Tagger A.Y. (1990). *Biochem. Cell. Biol.* 68: 1364-1371.

Wright, J.A., McClarty, G.A., Lewis, W.H., and Srinivasan P.R. (1989). In: R.S. Gupta (ed.), *Drug Resistance in Mammalian Cells*. pp. 15-27. Boca Raton, FL: CRC Press, Inc.

Wright, J.A., Turley, E.A., and Greenberg ,A.H. (1993). *Crit. Rev. Oncogenesis* 4: 47-492.

Wright, J.A., Smith H.A., and Watt, F.M., Hancock, M.C., Hudson, D.L., and Stark,G.R. (1993). *Proc. Natl. Acad. Sci. USA* 87: 1791-1795.

Wu, K.J., Grandori, C., Amacker, M., Simon-Vermot, N., Polack, A., Lingner, J., and Dalla-Favera, R. (1999). *Nat. Genet.* 21: 220-224.

Yakota, J., Tsunetsugu-Yakota, Y., Battifora, H., Le Fevre, C., and Cline, M.J. (1986). Science 231: 261-265.

Yalkinoglu, A.Ö., Zentgraf, H., amd Hübscher, U. (1990). *J. Virol.* 65: 3175-3184.

Yamagishi, H., Kunisada, T., Iwakura, Y., Nishimune, Y., Ogiso, Y., and Matsushiro, A. (1983b). *Dev. Growth Dev.* 25: 563-569.

Yamagishi, H., Tsuda, T.,Fujimoto, S., Toda, M., Kato, K., Maekawa, Y., Umeno, M., and Anai, M. (1983a). *Gene.* 26: 317-321.

Yang-Feng, L.T., Barton, D.E., Thelander, L., Lewis, W.H., Srinivasan, P.R., and Francke, U. (1987). *Genomics* 1: 77-86.

Yano, T., Sander, C., Clark, H., Dolezal, M., Jaffe, E., and Raffeld, M. (1993). *Oncogene* 8: 2741-2748.

Yeilding, N.M., Rehman, M.T., and Lee, W.M.F. (1996). *Mol. Cell. Biol.* 16: 3511-3522.

Yin, X.Y., Grove, L., Datta, N.S., Long M.W., and Prochownik, E.V., 1999. *Oncogene* 18: 1177-1184.

Yokota, Y., Tsunetsugu-Yokota, Y., Battifora, C.L., and Cline M.J. (1986) *Science* 231: 261-265.

Young, F., Ardman, B., Shinkai, Y., Lansford, R., Blackwell, T.K., Mendelsohn, M., Rolink, A., Melchers, F., Alt, F.W. (1994). *Genes Dev.* 8: 1043-1057.

Zech, L., Haglund, U, Nilsson, K., and Klein, G. (1976). *Int. J. Cancer* 17: 47-56.

Zervos, A.S., Gyuris, J., and Brent, R. (1993). *Cell* 72: 223-232.

Zimmerman, K.A., Yancopalous, G.D., Collum, R.G., Smith, R.K., Kohl, N.E., Denis, K.A., Nau, M.M., Witte, O.N., Toran-Allerand, D., Gee, C.E., Minna, J.D., and Alt, F.W. (1986). *Nature* 319: 780-783.

CHAPTER 2

METHODS AND MATERIALS

Chapter 2. METHODS AND MATERIALS

This chapter is divided into four sections. These sections are: (2.1) Bacterial Protocols; (2.2) Mammalian Cell Culture Protocols; (2.3) Molecular Protocols; and (2.4) Supplies, which lists all of the chemicals, reagents, and disposable supplies used in this thesis work.

2.1 Bacterial Protocols

Bacteria were used to amplify plasmids from which cDNAs were prepared for Northern, Southern (1- and 2-dimensional), FISH, and FISH-EEs procedures. The cDNAs prepared include murine *c-myc* exon II (kindly provided by Dr. Konrad Huppi, NIH), *glutathione peroxidase* (*GSHPX*) (Chambers *et al.*, 1986), *glyceraldehyde-3-phosphate dehydrogenase* (*GAPDH*) (kindly provided by Dr. Aiping Young), and *ribonucleotide reductase R2* (*R2*) (Thelander and Berg, 1986). All cDNAs were cloned into plasmids expressing β-lactamase enzyme and conferring resistance to ampicillin. Plasmid DNA carrying most of the cDNA sequences for this thesis work were prepared and amplified following transfection into either HB101 *E.coli* bacteria provided in the Invitrogen T/A cloning kit. IGF2 (Kitsberg *et al.*, 1993) was isolated from DH5α. The isolation of cDNA fragments from the isolated plasmids is described in Section 2.3.16.

DH5α *E.coli* bacteria carrying pGEX Myc (Clone 92) and pGEX Max (Clone 124) (Blackwood and Eisenman, 1991) isopropyl-β-thiogalactoside- (IPTG) inducible expression vectors were also grown to generate c-Myc- and Max-GST fusion proteins respectively, for use in gel shift experiments. The bacterial transformation, growth and

induction of the bacterial culture and GST fusion protein extraction procedures are described in Section 2.1.5.

2.1.1 Large Scale Alkaline Procedure for Plasmid DNA Isolation from E. coli.

(Sambrook *et al.*, 1989; Modified by Kunz, B.A., Ramachandran, K., and Armstrong, J., 1994.)

The plasmid-bearing *E.coli* were grown in 20 mL LB+Amp overnight in a 37°C shaking incubator. Two 500 mL volumes of LB in two 2 L flasks were inoculated next day with 2 mL of the overnight culture. Bacterial cultures were incubated at 37°C for 16 to 18 hours in a shaking incubator. Following overnight growth, the 500 mL cultures were centrifuged at 3,500 rpm/ 15 minutes/ 4°C in two 500 mL centrifuge bottles. The supernatant was discarded and the bacterial pellets were resuspended in 18 mL of Solution I (50 mM glucose 25, mM Tris, pH 8.0, 10 mM Na_2EDTA, pH 8.0). 2 mL of lysozyme (10 $mgmL^{-1}$) dissolved in 10 mM Tris-Cl (pH 8.0) was added to the resuspended bacteria. The suspension was mixed thoroughly and incubated on ice for 10 minutes. Following this incubation, 40 mL freshly prepared Solution II (200 mM NaOH, 1% (w/v) SDS) was added, mixed by inverting several times, and incubated on ice for 10 minutes. 20 mL ice-cold filter-sterile Solution III (23 mL glacial acetic acid, 57 mL dd H_2O, 120 mL 5 M potassium acetate) was added. The suspension was inverted and shaken several times to produce flocculant white precipitate and then incubated on ice for 10 minutes. Following incubation the suspension was centrifuged at 4,000 rpm for 25 minutes at 4°C. The centrifuge rotor was allowed to stop without using the electric break in order to minimize disruption of the delicate pellet. The supernatant was carefully

transferred and filtered through 5 layers of sterile cheesecloth and into fresh 250 mL centrifuge bottles. Isopropanol (0.6 volumes) was added to each volume of filtered supernatant and the mixture was incubated at room temperature for 10 minutes. Following the incubation, the solution was centrifuged at 5,000 rpm for 15 minutes at room temperature. The supernatant and isopropanol were decanted and aspirated off as much as possible. 50 mL 70% ethanol (at room temperature) was added to the DNA pellet and swirled gently to wash the pellet. The ethanol was carefully decanted off as much as possible and the remainder of the ethanol was evaporated off by air drying at room temperature. The nucleic acid pellet was dissolved in 3 mL TE buffer (10 mM Tris, 1 mM EDTA, pH 8.0). 500 µL of the DNA solution was delivered to six 1.5 mL microfuge tubes. 500 µL of -20°C 5 M LiCl were added to each microfuge tube in order to precipitate high molecular weight RNA. The suspension was mixed well and centrifuged at 10,000 rpm for 10 minutes at 4°C. Following centrifugation, the supernatant was transferred to fresh microfuge tubes and equal an volume of isopropanol was added to each sample, mixed well and allowed to stand at room temperature for 5 minutes. The suspension was centrifuged at 10,000 rpm for 10 minutes at room temperature after which the supernatant was carefully decanted away. The pellet was washed with 70% ethanol at room temperature and the excess ethanol was aspirated off. The pellet was allowed to air dry. All pellets were dissolved in a total of 500 µL of TE buffer (pH 8.0), pooled into one microfuge tube and digested for 30 minutes at 37°C with 4 µL (10 $mgmL^{-1}$) RNAse. 500 µL 1.6 M NaCl containing 13% polyethylene glycol (PEG 8000) was added to the solution, mixed well and centrifuged at 12,000 rpm for 5 minutes at 4°C. The supernatant was again aspirated off and the DNA pellet was

dissolved in 570 µL TE buffer (pH 8.0). The DNA solution was extracted once with 570 µL phenol, once with 530 µL 1:1 phenol/chloroform, and once with 490 µL chloroform. After chloroform extraction, 225 µL of the aqueous layer were transferred to each of two new microfuge tubes. 56 µL 10 M ammonium acetate were added to each tube and mixed well. 2 volumes (562 µL) of 100% ethanol at room temperature was added to the extracted DNA solution and allowed to stand for 10 minutes at room temperature. The suspension was centrifuged for 5 minutes at 4°C and 12,000 rpm. After centrifugation, the supernatant was aspirated off and 500 µL of 70% ethanol (-20°C) were added to each of the tubes. The tubes were inverted several times and then centrifuged at 12,000 rpm for 2 minutes at 4°C. Each of the pellets was resuspended in 250 µL 1x TE buffer and combined.

Solutions:

LB (Luria Broth) (Sambrook *et al.* 1989).

Bacto tryptone (10 g), Bacto yeast extract (10 g), and sodium chloride (5 g) were dissolved in 900 mL dd H_2O. The solution was titrated to pH 7.5 and volume was adjusted to 1 L with distilled and deionized (dd) H_2O. The medium was autoclaved. Ampicillin (100 μgmL^{-1}) was added (when required) after autoclaving and cooling of the medium to 45°C. The medium was designated LB+Amp (Sambrook *et al.*, 1989).

Preparation of LB Agar Plates

Agar dishes were prepared by addition of 1.5 g Bacto agar per litre of LB prepared as described above. The medium was autoclaved as described, and allowed to cool to 50°C. When the medium had cooled to 50°C, ampicillin (100 μgmL^{-1}) was added if required and plates were poured (Sambrook *et al.*, 1989).

2.1.2 Rapid Alkaline Procedure for Plasmid DNA Isolation from E. coli

(Modified from Morelle, 1989 by Kunz, B.A., Ramachandran, K., and Armstrong, J., 1994.)

Bacteria were grown overnight in 5 mL LB+Amp medium in a 37°C shaking incubator. The cells were pelleted by centrifugation at 3,000 rpm for 10 minutes at room temperature. The pelleted cells were resuspended in 1 mL of GTE (50 mM glucose, 25 mM Tris, pH 8.0, 10 mM Na_2EDTA, pH 8.0) buffer and transferred into a 1.5 mL microfuge tube. The bacterial cells were again pelleted by centrifugation, as described above, and resuspended in 190 µL GTE buffer. The cell suspension was mixed gently and then transferred to ice. 400 µL of freshly prepared lysis solution (200 mM NaOH/1.0% SDS) was delivered dropwise to the suspension and incubated on ice for 10 minutes. After the incubation, 300 µL of neutralizing solution were added drop-wise to the lysed bacteria and incubated on ice for 10 minutes. Following this incubation, the precipitate was pelleted by centrifugation for 30 minutes at 13,000 rpm and at 4°C for 30 minutes. The supernatant was decanted into a fresh microfuge tube. The centrifugation was repeated twice more, but the time of centrifugation was reduced to 20 minutes. Following the third centrifugation and decanting of the supernatant, 500 µL isopropanol were added and the contents were mixed by inversion. The solution was incubated at room temperature for 10 minutes. The nucleic acid was isolated by 2 minutes of centrifugation at 13,000 rpm and at room temperature. The nucleic acid pellet was then washed with 70% ice-cold ethanol and allowed to air dry briefly. The pellet was dissolved in 50 µL TE buffer, treated with 2 µL RNAse A (10 $mgmL^{-1}$) for 30 minutes at 37°C, and stored 4°C.

Solutions:

LB (Luria Broth)

See 2.1.1 LB (Luria Broth) (Sambrook *et al.* 1989).

6.17 M Ammonium Acetate

Ammonium acetate (142.7 g) was dissolved in 30 mL dd H_2O and 60 mL glacial acetic acid. The solution was heated to dissolve the ammonium acetate. The volume was adjusted to 300 mL with glacial acetic acid.

2.1.3 Preparation of Competent Bacteria

DH5α *E.coli* bacteria were inoculated into LB as an overnight culture. Next morning, one mL of this culture was inoculated into 50 mL of LB and incubated until an optical density (OD) of $OD_{650nm} = 0.75$ or $OD_{540nm} = 0.5$-0.6 was attained. At this density, bacteria were incubated on ice for 25 minutes. The bacteria were centrifuged at 4°C and at 4,000 rpm for 5 minutes. The supernatant was decanted off and the bacteria were resuspend in 12.5 mL 50 mM $CaCl_2$ and incubated in this solution for one hour at 2-4°C. The bacteria were centrifuged at 4°C at and 4,000 rpm for 5 minutes. The pellet was resuspend in 600 µL of 50 mM $CaCl_2$, 1.4 mL 87% glycerol, and 3 mL dd H_2O. The competent bacteria were aliquoted into 125 µL volumes and stored at -75°C.

2.1.4 Transformation of Competent Bacteria

2.1.4.1 Transformation of Competent Bacteria Without Use of a Kit.

DNA (0.5-1.0 µg) was dissolved in 10 µL TE buffer and then mixed with 40 µL TE buffer on ice. 20µL 10x TCM Buffer (100 mM Tris, pH 8.0, 1mM Na_2EDTA, 100

mM $CaCl_2$, 100 mM $MgCl_2$, pH = 7.5) was added to the DNA solution. Competent bacteria were thawed on ice and 125 µL was delivered to the DNA solution. The bacteria and DNA were incubated on ice for 20 minutes. After the incubation, the bacteria were heat-shocked at 41°C for 2 minutes and then allowed to cool to room temperature for 10 minutes. LB (800 µL, without ampicillin) was added and the suspension was allowed to incubate for 60 minutes (or longer to maximum of 4 hours) at room temperature. The bacteria were plated onto selective plates (prepared with 100 μgmL^{-1} ampicillin) and selected as described above.

2.1.4.2 Transformation of Competent Bacteria Using an Invitrogen Kit

Bacterial transformation procedures were performed using an Invitrogen TA Cloning® Kit (Version 2.0). The kit included Invitrogen TA Cloning® OneShot™ competent HB101 bacterial cells and all required solutions and medium. Transformation was performed according to supplier's instruction. Briefly: Vials of SOC medium and 0.5 M β-mercaptoethanol (vial TA11) were thawed to room temperature. Invitrogen TA Cloning® OneShot™ competent HB101 bacterial cells were thawed on ice. One vial of cells was thawed for each transformation. 2 µL of 0.5 M β-mercaptoethanol was added to each vial of competent cells and mixed by gentle tapping. 1.0 µL of plasmid was added to the cells and mixed by gentle tapping and incubated on ice for 30 minutes. The mixture was then incubated for precisely 30 seconds in a 42°C water bath and then placed on ice for 2 minutes. 450 µL of prewarmed SOC medium was added to the competent transformed cells. The bacterial suspension was mixed by tapping or inverting the microfuge tube. The cells were plated out onto two LB+Amp agar dishes and allowed to grow overnight at 37°C. One dish was plated with 100 µL of the transformed bacteria and

another was plated with 25 µL of bacteria. The plates were allowed to grow overnight and single colonies were amplified on LB+Amp agar plates.

Solutions:

SOC medium, 0.5 M β-mercaptoethanol, 50 µL OneShot™ competent HB101 bacterial cells, 1.0 µL of plasmid of choice (1.0 $\mu g \mu L^{-1}$).

SOC medium consists of 2% (w/v) Bacto tryptone, 5% (w/v) Bacto yeast extract, 8.5 mM NaCl, 20 mM glucose, 2.5 mM KCl, 10 mM $MgCl_2$.

2.1.5 Freezing of Bacterial Stocks

Bacterial colonies were picked and streaked out on a LB+Amp dish. After overnight growth at 37°C, the bacteria were collected and dispersed in a sterile solution of 50% glycerol*. These suspensions were frozen at -75°C.

*The 50 % glycerol solution was prepared by mixing pure glycerol with dd H_2O in 1:1 proportions. The 50% glycerol was delivered to 1.5 mL screw-capped microfuge tubes, sealed with screw caps and autoclaved. These can be stored indefinitely.

2.1.6 Generation of c-Myc- and Max- GST Fusion Proteins from Bacteria

GST-Myc and GST-Max fusion proteins were kindly provided by Dr. Beth Blackwood (Blackwood and Eisenman, 1991). The constructs were transformed into DH5α bacteria and were selected with ampicillin (100 $\mu g mL^{-1}$).

Protocols:

2.1.6.1 Inoculation of Bacteria

A 500 mL LB containing 100 $\mu g mL^{-1}$ ampicillin was inoculated with bacterial stock culture of choice (pGEX Myc C92 or pGEX Max C 124), and grown overnight in a

shaker at 37°C. Next morning, 450 mL of LB+Amp culture medium was inoculated with the 50 mL of overnight bacterial culture and allowed to grow in a shaker at 37°C to an O.D. = 0.6 (at λ= 600 $_{nm}$). 1.0 M ITPG was delivered to the bacterial culture, giving a final ITPG concentration of 1 mM.

2.1.6.2 Isolation of Fusion Proteins

The 500 mL of bacterial culture was sampled first prior to addition of ITPG to serve as a source of control protein. For this sample, 100 mL of the culture were removed and processed as described below. The remaining 400 mL were allowed to incubate at 37°C and 100 mL volumes were removed at the time of ITPG addition and at each 1 hour interval following the addition of ITPG. The samples removed at 0, 1, 2, 3, and 4 hours after the addition of provided bacteria that were incubated in the presence of ITPG for different lengths of time. This allowed for the titration of the best induction point and for the selection of the best protein isolate. The details are as follows:

Prior to the addition of ITPG, 100 mL of bacteria (to be used as a source of control *E. coli*) was removed from the 500 mL of growing bacterial culture of which 10 µL counted on a hemocytometer. An appropriate volume containing 10^7 bacteria was removed form the 100 mL of bacteria and delivered to a 1.5 mL microfuge tube and pelleted. The supernatant was pipetted away and 20 µL of 2x protein sample buffer (1 mL 0.5 M Tris pH 6.8, 2 mL 10% SDS, 6.2 mg Dithiothreitol (DTT), 500 µL 98% glycerol, 175 µL 10% (w/v) Bromophenol Blue [final concentration of 0.5%]) was added and the pellet was resuspended and denatured. This suspension was stored at -20°C until needed. The rest of the 100 mL was pelleted, and resuspended in 50 µL of Band Shift Buffer (10 mM N-2-Hydroxyethylpiperizine-N'-2-Ethane sulphonic acid (HEPES) pH 7.9,

60 mM KCl, 1mM Na_2EDTA, 4% (w/v) Ficoll, 1mM DTT, 1mM AEBSF). The remaining 400 mL of the bacterial culture was allowed to grow for one hour. The removal of 100 mL of bacteria, the counting and pelleting of 10^6 bacteria and their resuspension on protein sample buffer was repeated every hour, as was the pelleting and resuspension in Band Shift Buffer of the remainder of the 100 mL of the hourly sample.

2.1.6.3 Determining Optimal Generation of Fusion Proteins

The samples of 10^7 bacteria in sample buffer samples were removed from storage at -20°C and boiled for 15 minutes. The bacterial samples and a molecular weight marker were loaded onto a 10% SDS-PAGE gel and run at 80 V in SDS-PAGE electrophoresis running buffer (100 mM Trizma base, 100 mM glycine, 2% SDS.). The gel was stopped once the 220 kDa molecular weight marker had run into resolving gel. The gel was stained for at least 2 hours in Commassie Brilliant Blue staining solution (35% ethanol, 10% acetic acid, 0.25% (w/v) Bromophenol Brilliant Blue R) for a minimum of 1 hour and then destained with destaining solution (35% ethanol, 10% acetic acid). The gel was then soaked for one hour in 20% methanol, 10% glycerol and then dried at 80°C under vacuum. A successful induction of GST fusion protein synthesis was indicated by the appearance of a pronounced band only following ITPG induction. The bands of interest were 36 and 40 kDa, indicating the ITPG-induced expression of the GST-Myc and GST-Max fusion proteins, respectively. The band of interest is most abundant in the optimally induced time point. This fraction, which represented the best time-point of the ITPG induction, was used for further experimentation. The protein was isolated from the pelleted, 100 mL sample(s) wherein the optimal induction had been reached. The bacteria were lysed and the protein isolated by three cycles of freeze/thaw in ethanol/dry ice and a

37°C bath, respectively. After each cycle of freezing and thawing, the suspension was vigorously vortexed for 5 minutes before refreezing in the dry ice/ethanol.

Solutions:

LB (Luria Broth) (Sambrook *et al.*, 1989) (See 2.1.1)

Isopropyl β-D Thiogalactopyranoside (IPTG)

A 5 g vial of IPTG (F.W. 238.5 $gmol^{-1}$) was dissolved in 20.9 mL dd H_2O to give a final concentration of 1.0 M. The 1 M ITPG was filter-sterilized through a 0.2 µm syringe filter, aliquoted into 1 mL volumes and stored at –20°C.

1.0 M Dithiothreitol (DTT) Stock Solution

15.42 mg DTT (F.W. = 154.2 $gmol^{-1}$) was dissolved into 100 µL of sterile dd H_2O and stored at -20°C.

AEBSF Stock Solution (Pefabloc®SC)

23.95 mg of AEBSF (F.W. = 239.5 $gmol^{-1}$) was dissolved into 1 mL of sterile dd H_2O and stored in 100 µL aliquots at -20°C.

2.2 Mammalian Cell Culture

2.2.1 Cell Culture Media

2.2.1.1 Preparation of B Cell Medium for B Cultured Lymphoid Cells

The medium for B cell culture was comprised of 500 mL RPMI 1640 + L-glutamine, 50 mL Fetal Bovine Serum, 5 mL MEM sodium pyruvate (100x), 5 mL L-glutamine (200 mM), 5 mL penicillin (5,000 units mL^{-1})/ Streptomycin (5,000 μgmL^{-1}), and 500 µL β-mercaptoethanol (5.5 x 10^{-2} M). Medium to be used for growing MOPC460D was also supplimented with Interleukin-6 (IL-6). All culture ingredients except for IL-6, were purchased from Canadian Life Technologies. IL-6 was generated from IL-6-secreting hybridoma cells.

2.2.1.2. Growth Arrest and Synchronization Media

Selectamine™ RPMI 1640 medium (Canadian Life Technologies) was prepared according to the manufacturer's instructions. For the purposes of these experiments, isoleucine was withheld during the preparation in order to prepare a medium that would facilitate arrest of the cells at the G_1 phase of the cell cycle. All ingredients except for isoleucine were added and the volume was adjusted to 1 L with sterile dd H_2O. Measurement of the medium showed that it was at approximately pH 7.5 to 8.0 and did not require adjustment.

Release of cells from G_1 arrest and synchronization at the G_1/S boarder was induced by transfer of these cells into whole culture medium containing 400 µM of the plant amino acid L-mimosine (Dijkewel *et al.*, 1991).

Preparation of L-Mimosine

The F.W. of L-Mimosine is 198.2 $gmol^{-1}$. A 1 g vial containing 5.045 mmoles of mimosine was deilvered into 400 mL PBS. The suspension was acidified with concentrated HCl to aid in dissolving the mimosine. Once dissolved, the solution was titrated to pH 7.4. The volume of the mimosine solution was adjusted to 504.5 mL with dd H_2O. The final concentration of the mimosine was 10 mM. The solution was filter sterilized and stored at 4°C. The 10 mM L-Mimosine solution was stable for several months at 4°C in our hands.

2.2.2 B Cell Growth Conditions

All cells were grown in darkness at 37°C, in a humidified cell culture incubator containing an atmosphere of 5% (v/v) CO_2.

2.2.2.1 Normal Growth Conditions

WEHI231 and MOPC460D cells were seeded at a density of $5x10^5$ $cellsmL^{-1}$ in B cell medium, prepared as described in 2.2.1. The latter were supplemented with IL-6. ABM Pre-B cells were seeded at a density of 10^5 $cellsmL^{-1}$ in B cell medium. Pre-B cells that were to be treated with 4-hydroxytamoxifen in order to activate Myc-ER™ were treated with the drug 24 hours after seeding, unless otherwise described. A number of 4-hydroxytamoxifen preparations (*i.e.* 100 % E, 1:1 E:Z, minimum 70% Z, or minimum 98% Z isomer) were used, depending on availability and efficacy, which was tested before use. The dosage of every freshly prepared vial of 4-HT was titrated to determine the optimal dosage for the activation of the Myc-ER™ construct. The cells were activated with 0.5 to 1.0 µL of the 10 $mgmL^{-1}$ 4-hydroxytamoxifen (4-HT) preparation per 10 mL

of culture medium. Control cells received the corresponding volume of 100% ethanol per 10 mL of culture medium (See Section 2.3.17. for preparation and titration of 4-hydroxytamoxifen).

2.2.2.2 Growth Arrest and Synchronization of Pre-B Cells

Growth arrest of the Pre-B cells at the G_1 stage of the cell cycle was accomplished by transferring of the cells from normal whole cell medium (See 2.2.1.1) to a medium lacking isoleucine (Cooper and Wharton, 1985)* (See 2.2.1.2.). The cells were incubated in a humidified incubator at 37°C in 5% CO_2 (v/v) for 45 hours. The cells were further synchronized close to the G_1/S boarder by transfer of the cells into normal whole cell medium containing 400 μM mimosine (See 2.2.1.2.) for 12 hours. Following this procedure, cells were transferred to normal medium and used for experiments as described below.

*Cooper J.L. and Wharteon, W. (1985). *J. Cell. Physiol.* 124:433-438.

2.2.3 Freezing of Cultured Mammalian Cells

Cultured cells were pelleted, washed twice in sterile ice-cold PBS, and resuspended in fetal calf serum at a concentration of roughly 10^7 cellsmL^{-1}. Volumes of 900 μL were delivered to labeled cryovials. 100 μL of cell culture grade dimethylsulphoxide (DMSO) was delivered to each of the cryovials of cells in serum. The vials were capped and inverted to mix the suspension, and frozen at -80°C for a minimum of 12 hours and a maximum of 24 hours after which they were transferred to liquid nitrogen storage.

2.3 Molecular Protocols

2.3.1 Detection of Bromodeoxyuridine (BrdU) Incorporation

BrdU incorporation is used as a measure of DNA replication and repair.

Modified from: Leonhardt, H., Page, A.W., Weier, H.U., Bestor, T.H. (1992). *Cell* **71**: 865-873.

- All solutions were prepared in PBS with 1.5 mM $MgCl_2$ and 1 mM $CaCl_2$. This solution will be referred to as $PBS^{\dagger}$.
- All solutions were prepared and used at room temperature.
- Formaldehyde was deionized before use.

Solution:

Phosphate Buffered Saline (PBS):

A 10x stock was prepared by dissolving 80 g of sodium chloride, 2 g of potassium chloride, 14.4 g of sodium phospate (dibasic) and 2.4 g of potassium phosphate (monobasic) in 800 mL of dd H_2O. The solution was titrated to pH 7.4 and volume was topped up to 1 L. The solution was then sterilized by autoclaving.

2.3.1.1 Immunohistochemical Staining for BrdU Incorporation

Cells were fixed on slides in 3.7% formaldehyde for 10 minutes, rinsed twice in $PBS^{\dagger}$ and then permeabilized with 0.2% Triton X-100 in dd H_2O for 12 minutes. The slides were washed twice more in $PBS^{\dagger}$. The fixed cells were incubated in 2% formaldehyde in $PBS^{\dagger}$ for 10 minutes at room temperature and then incubated in $PBS^{\dagger}$ + 50 mM glycine for 10 minutes. The slides were then incubated in a solution of freshly prepared 4N HCl + 0.1% Triton X-100 in dd H_2O for 10 minutes. The slides were washed in $PBS^{\dagger}$ + 50 mM glycine and then blocked in 5% lamb serum diluted in $PBS^{\dagger}$ for

5 minutes. The primary anti-BrdU (Becton Dickenson) antibody was diluted 1:5 in 5% blocking buffer (5% (v/v) fetal lamb serum in PBS†) and 25 µL was delivered to each of the slides and incubated for 45 minutes under coverslips. The slides were washed three times in PBS† and then again blocked in 5% lamb serum for 5 minutes. The secondary antibody, a Texas Red-conjugated anti-mouse IgG antibody was diluted 1:400 in 5% lamb serum and 25 µL was added to each of the slides and incubated under coverslips and in darkness for 30 minutes. After this incubation, the slides were washed three times in PBS†. The slides were then counterstained with 25 µL of 4'6' diamidino-2-phenylindole (DAPI) (1 μgmL^{-1} in PBS, no $MgCl_2$, no $CaCl_2$) and incubated in darkness for 5 minutes and then mounted in antibleach (Mai *et al.*, 1994, see Section 2.3.14), covered with a coverslip, and analyzed immediately after staining was completed.

2.3.1.2 Preparation of 50 mM Bromodeoxyuridine in PBS

BrdU was dissolved at 15.33 $mgmL^{-1}$ in sterile PBS and aliquoted into 100 µL volumes and stored at -75°C.

2.3.1.3 Incubation of Cultured Cells with Bromodeoxyuridine Solution

Cultured cells were incubated in the presence of 10 µM BrdU for 10 minutes prior to preparation of cytospins. 1 µL of 50 mM BrdU stock solution was delivered per mL of culture.

2.3.1.4 Preparation of Bromodeoxyuridine-Labeled Metaphase Chromosomes

Cells were synchronized as described in Section 2.2.2.2 and activated as described in Section 2.3.18. The cells were pulsed with 10 µM BrdU for 30 minutes after which they were washed and delivered into normal medium. After an additional 24 hour

incubation under normal cell culture conditions, cells were harvested and metaphase chromosomes were prepared as described in Section 2.3.15.3.

2.3.2 Isolation of Genomic DNA from Cultured Cells

2.3.2.1 Isolation of Genomic DNA without the use of an isolation kit.

Protocol:

B cells were lysed in a polypropylene conical tube by resuspending 10^7 cells in 200 µL of PBS. 5 mL DNA lysis buffer (10 mM Tris HCl, pH 8.0, 150 mM NaCl, 10 mM Na_2EDTA, 0.2% SDS) was then added to the cell suspension and mixed. Proteinase K (100 μgmL^{-1}) was added to the lysed cell suspension and then mixed and incubated overnight at 37°C. The nucleic acids were extracted with an equal volume of phenol:chloroform (1:1v/v). The nucleic acids were extracted again with an equal volume of chloroform and then precipitated overnight in 300 mM ammonium acetate (pH 4.8) and 2.5 volumes 95% ethanol (-20°C). The suspension was centrifuged at 10,000 rpm, at 4°C for 30 minutes, and the supernatant decanted off. The nucleic acid pellet was washed with 70% ethanol and allowed to air dry for 5 minutes. The pellet was dissolved in 1x TE buffer. The absorbance (λ = 260 nm) of the DNA in TE buffer was measured and the concentration was calculated using the following formula.

NOTE: **[DNA]** $(\mu gmL^{-1}) = (50\ \mu gmL^{-1})(vol._i/vol._f)(Abs_{260nm})$

2.3.2.2 Isolation of Genomic DNA from Cultured Cells Using a Kit

[Protocol #3 of *Invitrogen* Easy-DNA™ Kit]

2.3.2.2.1 ***DNA Isolation and Precipitation***

Cultured B cells numbering from 10^3 to 10^7 were resuspended in 200 µL of PBS and lysed with 350 µL Solution A* (* means that the solution was supplied by Invitrogen). This mixture was vortexed until evenly dispersed and then incubated at 65°C for 10 minutes. 150 µL of Solution B* was added to the suspension and vortexed vigorously until the suspension moved freely in the tube and the sample was uniformly viscous. 500 µL chloroform was added to the suspension and then vortexed until viscosity decreased and the mixture was homogenous. The mixture was centrifuged at 13,000 rpm at 4°C for 20 minutes and the upper aqueous phase was removed and delivered into a fresh microfuge tube. 1 mL of -20°C 100% ethanol was added to the nucleic acid solution and vortexed to mix. The mixture was incubated on ice for 30 minutes and then centrifuged at 13,000 rpm at 4°C for 20 minutes. The ethanol was removed from the pellet using a Pasteur pipette. 500 µL of - 20°C 80% ethanol was added to the tubes and the tubes were slowly inverted several times. The tubes were centrifuged at 13,000 rpm at 4°C for 5 minutes to repellet the nucleic acid pellet. The ethanol was removed from the nucleic acid pellet using a Pasteur pipette and the pellet was resuspended in 100 µL TE buffer* (10 mM Trizma base, 1 mM Na_2EDTA, pH 8.0). 2 µL of 2 $mgmL^{-1}$ RNAse* (to final concentration to 40 μgmL^{-1}) was added to the nucleic acid solution and incubated at 37°C for 30 minutes. After RNAse treatment, the DNA solution was stored at 4°C.

2.3.3 Southern Blotting of Genomic DNA

2.3.3.1 One-Dimensional Southern Blotting

Approximately 10 µg of genomic DNA were digested with the restriction endonuclease of choice. The DNA was digested overnight at 37°C according to the supplier's instructions. The digested DNA was mixed in 6x DNA loading buffer (0.25% bromophenol blue, 0.25% xylene-cyanol, 15% ficoll) and loaded onto a 0.8 % agarose gel prepared with 0.5 $mgmL^{-1}$ ethidium bromide. The DNA was elecrophoresed overnight at 35 V. Following electrophoresis, the gel was washed twice for 30 minutes in denaturation solution (1.5 M NaCl, 0.5 M NaOH) and then twice for 30 minutes in neutralization solution (1 M ammonium acetate, 20 mM NaOH). The DNA was transferred onto Hybond XL nitrocelluolose membrane overnight in neutralization solution. Following transfer of the DNA the membrane was removed from the gel and crosslinked by baking at 80°C for 2 hours.

The membrane was prehybridized at 42°C for 4 hours in 8 mL prehybridization solution. The random primer-labeled cDNA probe (Section 2.3.3.2) was denatured in an equal volume of deionized formaldyhyde and added to the (pre)hybridization solution and allowed to incubate overnight. The membrane was then washed once for 15 minutes in DNA Membrane Wash Solution 1 (6.6x SCP/1% N-lauroyl sarcosine) at 65°C and then for 90 minutes in DNA Membrane Wash Solution 2 (1.0x SCP/1% N-lauroyl sarcosine) at 65°C. If required, the membrane was washed once again in Membrane Wash Solution 3 (0.2x SCP/1% N-lauroyl sarcosine) at 65°C for 30 minutes. The membrane was sealed in plastic and exposed to autoradiographic film overnight at -75°C.

The probed membranes were stripped by pouring a boiling solution of 0.1% SDS in water onto the blot. The membrane was allowed to soak in the 0.1% SDS solution until the solution cooled to room temperature. If the blot was still radioactive this step was

repeated. The membrane was checked for residual radioactivity by overnight exposure on autoradiographic film. If the membrane gave readings of >1 count per second, it was stripped again. If this did not reduce the signal, the membrane was allowed to decay for an appropriate time until the signal was reduced.

Solutions:

50x Denhardt's Solution

50x Denhardt's solution consists of 1% (w/v) Ficoll 400, 1% (w/v) BSA Pentax Fraction V, and 1% (w/v) Polyvinylpyrrolidon.

20x Sodium Chloride/Phosphate (SCP) Solution

20x SCP solution consists of 2 M NaCl, 60 mM Na_2HPO_4, and 20 mM Na_2EDTA, pH 6.2.

Prehybridization/Hybridization Solution

The (pre)hybridization solution consists of 166.5 mL 20x SCP, 10 mL 20% N-lauroyl sarcosine, 200 μgmL^{-1} NaOH-denatured herring sperm DNA (see Section 2.3.4.), 40 mL 50x Denhardt's Solution, 250 mL formamide, and 10% (w/v) dextran sulfate.

2.3.3.2 Two-Dimensional Neutral/Neutral Southern Blotting

Approximately 100 µg of genomic DNA were digested overnight with *Hin*dIII at 37°C. The digestion volume was reduced from roughly 1.2 mL to 40 µL by rotoevaporation. 20 µL 6X DNA loading buffer was added to the samples and mixed by gentle pipetting. The digested DNA samples were loaded and run overnight at 20 V at room temperature in a 0.4% agarose gel that contained no ethidium bromide. After the DNA was run in the first dimension, the gel was stained in a solution of 0.5 $mgmL^{-1}$

ethidium bromide in order to visualize the DNA. The DNA-containing lanes were cut out and cast into a second gel. The digested DNA from the first dimension was rotated 90°, so that the large molecular weight fragments were on the left side of the tray and the small molecular weight fragments were on the right of the tray. The remainder of the hot 1.0% agarose was poured into the casting tray to cover the DNA in the gel and to form a smooth and uniform gel. The gel was run at 4°C in 0.5 x TBE (at 4°C) for 4 hours at 200-225V. (0.5 x TBE consists of 45 mM Trisma-borate, 1 mM Na_2EDTA).

Transfer of DNA onto membrane, hybridization, washing and stripping of the membranes were performed as described in 2.3.3.1.

Labeling of *R2* cDNA with $^{[32]}P$ α-dCTP is performed as described in Section 2.3.16.). Random primed labeling of *R2* oligonucleotides (*R2-2*, *R2-3*, *R2-4*, and *R2-5*) with $^{[32]}P$ α-dCTP is performed as described for cDNA fragments, however, they were purified using a Bio-Rad Spin 6 column (Bio-Rad) as described by the manufacturer. Once purified, the probes were used for hybridization of 2D Southern blots. Hybridizations with the *R2* oligonucleotides were performed as follows: Membranes were prehybridized for 4 hours in a (pre)hybridization solution (5x Denhardt's solution, 5x SSC, 0.2% SDS) at 42°C. They were hybridized overnight at 42°C in 8 mL of the same fresh solution. Following hybridization, the membranes were washed according to conditions established for each oligonucleotide using test hybridization of DNA slot blots. Membranes probed with each of the four oligonucleotide probes were washed once for 15 minutes at 42°C with Wash Solution 1 (2x SSC, 0.1% SDS) and once for 15 minutes at 42°C with Wash Solution 2 (1x SSC, 0.1% SDS). The membranes were sealed in plastic bags and exposed to autoradiographic film for 14 days at –75°C. Because the

oligonucleotide probes were very short (*i.e.* 20 bp), the incorporation of $^{[32]}$P-dCTP gave only weak signals and so membranes probed with the oligonucleotides required much longer exposure time in order to visualize the signal on radiographic film.

2.3.4 Preparation of Denatured Herring Sperm DNA

Herring sperm DNA (HS-DNA) (1 g) was dissolved in 100 mL of 0.4M NaOH by gentle agitation overnight at room temperature. The solution was boiled on a hot plate for 30 minutes to shear the DNA and then neutralized by titration with glacial acetic acid to a pH of 5.0. The sample was then centrifuged in order to remove debris. Two volumes of 100% ethanol were added to the sample to precipitate the DNA. The suspension was refrigerated at -20°C for 1 hour after which the DNA was collected by centrifugation at 3,200 rpm for 30 minutes at 4°C. The DNA pellet was rinsed with 70% ethanol and allowed to air dry. Excess moisture from the tube was removed using Kleenex and the pellet was dissolved in 50 mL 1 x TE buffer overnight at 4°C. The concentration of the herring sperm DNA was determined by measurement of its absorbance at λ = 260 nm. The DNA was then diluted to a concentration of 10 mgmL^{-1} in 1 x TE buffer and stored at -20°C in 1.0 and 10.0 mL aliquots. A sample of the freshly prepared herring sperm DNA was run out against a previously prepared sample of herring sperm DNA in order to compare quality of denaturation. This was done on a 0.8% agarose gel containing 0.5 mgmL^{-1} ethidium bromide.

2.3.5 Dispersed Cell Assay

Cultured B cells were washed once with RPMI 1640 medium/10% fetal calf serum (FCS), and counted on a hemocytometer. Cell density was adjusted to 10^6 cells mL^{-1} with RPMI 1640 medium/10% FCS and the cell suspension was kept on ice.

Each of five 10 mL tubes containing 5 mL of PBS and 10^5 cells was mixed and poured into one of the manifolds. The cells were trapped on the membrane discs.

The cells on the filters were lysed using an erythrocyte lysis buffer (150 mM NH_4Cl, 7.5 mM $KHCO_3$, 0.1 mM Na_2EDTA). Each filter disc was denatured 3 times, 1 minute each time, on 3MM paper wetted with denaturation solution (0.5 M NaOH, 1.5 M NaCl), and then neutralized 3 times, 1 minute each time, on 3MM paper wetted with neutralization solution (0.5 M Trizma, 1.5 M NaCl, and 1.5 mM Na_2EDTA, pH 7.4). Following neutralization, 200 µL of RNase A (100 μgmL^{-1}) was delivered onto each filter and was allowed to incubate in a humid, 37°C chamber for 60 minutes. 200 µL of 20 μgmL^{-1} Proteinase K was then delivered onto each filter and allowed to incubate in a humid 37°C chamber for 60 minutes. DNA was crosslinked to the nitrocellulose membranes by baking for 2 hours at 80°C. The discs were stored at 4°C.

For hybridization experiments, the discs were prehybridized with 20 mL of DCA (5x Denhardt's Solution (see Section 2.3.3.1), 5x SSC, 0.5% SDS) for 1-4 hours at 65°C. They were then hybridized with 10-20 mL of dispersed cell assay hybridization solution containing the random primer generated probe at 65°C.

The discs were washed once for 15 minutes at 65 °C in DNA Wash Solution 1 (2x SSC, 0.1% SDS). This was followed by a second 15 minute wash at 65°C in DNA Wash

Solution 2 (1x SSC, 0.1% SDS). The discs were exposed to autoradiographic film overnight.

2.3.6 DNA Slot Blots

DNA slot blots were used in order to establish hybridization and wash conditions and temperatures for 2D Southern blots probed with *R2* oligonucleotides. Multiple test strips were prepared, each containing a negative control (100 ng mouse *c-myc* cDNA), a positive control (100 ng *R2* cDNA), and three concentrations (5 µg, 2 µg, and 1 µg) of Pre-B genomic DNA. One slot contained no DNA. Each sample was delivered onto the Nybond N^+ membrane using a Schleicher and Schuell MinifoldII slot blot apparatus after denaturation in an equal volume of saturated NaI (3.75 gmL^{-1}) at 90°C. The total volume of DNA/NaI solution delivered was 50 µL. After delivery of the DNA to the membrane, the membrane was baked at 80°C for two hours.

2.3.7 Hirt Extract For Isolation of Extrachromosomal Elements

Hirt, B. (1967) *J. Mol. Biol.* 26: 365-369.

Solutions:

10^6 cells were lysed per mL of Hirt Extract buffer (10 mM Na_2EDTA, 0.6% SDS). The samples were allowed to stand for 10-20 minutes at room temperature. 5 M NaCl was added to the suspension to give a final concentration of 1 M NaCl. The samples were inverted ten times to mix and stored for a minimum of 8 hours at 4°C. Following incubation at 4°C, the samples were centrifuged at 4 °C at 17,000 rpm for 50 minutes (Using a Beckman JA-10 rotor, 17,000 rpm is equal to 35,000 x *g*). Following

centrifugation, the supernatant containing the extrachromosomal DNA and RNA was collected.

2.3.8 Isolation of Poly (A)+ mRNA

Cultured B cells were harvested and washed twice with ice-cold PBS. 4 mL of STE (100 mM NaCl, 20 mM Trizma pH 7.4, 10 mM Na_2EDTA) + 0.5% SDS was added for every 2-5 x 10^6 cells. The lysed cells were pulled and pushed through a syringe with a G21 needle at least five times. Proteinase K (120 µL 10 $mgmL^{-1}$) was then added to the lysed cells and incubated at 37°C for 1 hour followed by the addition of 410 µL of 5 M NaCl, to give a final concentration of 0.5% NaCl. Oligo (dT) cellulose (50 $mgml^{-1}$) was added to the suspension and it was allowed to incubate on a rotating wheel or a rotating platform overnight at room temperature.

Following overnight incubation, the oligo(dT) was pelleted by centrifugation for 5 minutes at 3200 rpm. The supernatant was discarded and the pellet was washed by resuspending in 10 mL of High Salt Buffer (HSB) (30 mM NaCl, 10 mM Trizma pH 7.4, 5 mM Na_2EDTA) + 0.5% SDS. The oligo (dT) was repelleted by centrifugation at 3200 rpm for 5 minutes and the supernatant was discarded. This washing procedure was repeated two more times. The mRNA was then eluted from the beads by resupending the oligo (dT) pellet in 1 mL of sterile H_2O/0.1% SDS. The oligo (dT) beads were pelleted by centrifugation (3200 rpm, 5 minutes) and the mRNA-containing supernatant was collected. This elution method was repeated two more times with the supernatant being collected each time and pooled with the other previous elutions. The mRNA concentration was determined by measuring 300 µL of the sample in water at λ=260 nm.

3 µL of tRNA (10 $mgmL^{-1}$), 81 µL of 10.0 M ammonium acetate (giving a final concentration of 300 mM ammonium acetate), and 7.0 mL of -20°C 95% ethanol were added to the mRNA and the solution was mixed well by inversion and stored at -20°C.

2.3.8.1 Preparation and Regeneration of Oligo (dT) Cellulose

The preparation of oligo (dT)-coupled cellulose beads involves sequential washes in different buffers in order to prime or regenerate the beads for binding. Prior to initial use, the beads were primed as follows: The beads were washed once with HSB (30 mM NaCl, 10 mM Trizma pH 7.4, 5 mM Na_2EDTA) + 0.1% SDS, then three times with HSB (no SDS). The beads were resuspended for use in HSB (no SDS) at a final concentration of 50 $mgmL^{-1}$. Following use of the oligo (dT), the beads must be regenerated prior to reuse. The beads were first washed twice in 100 mM NaOH, 5mM Na_2EDTA. The beads were then washed five times with H_2O/0.1% SDS and then twice in HSB/0.1% SDS. The regenerated beads were then resuspended in HSB (no SDS) to a final concentration of 50 $mgmL^{-1}$ and stored at 4°C.

2.3.9 Northen Blot Analysis of Poly (A)+ mRNA

Poly (A+) mRNA was electrophoresed in a 1.0% agarose (without ethidium bromide) containing 2.2 M formaldehyde. The appropriate volume of mRNA equivalent to 1 µg was centrifuged for 30 minutes at 4°C at 13,000 rpm. The supernatant was pipetted away and the mRNA pellet was dissolved in RNA loading buffer (50% deionized formamide, 10% 10x MOPS/Na_2EDTA buffer, 6% deionized formaldehyde, 13.3% glycerol, 0.5% bromophenol blue). The mRNA solution was heated for 5 minutes at 65°C and then loaded onto the gel and run overnight at 20V. The gel was washed for

10 minutes in 10x SSC (1x SSC = 0.15 M NaCl, 0.015 M sodium citrate) and then blotted overnight onto Hybond N^+ nitrocellolose membrane in 20x SSC. After blotting, the mRNA was crosslinked to the membrane by baking for 2 hours at 80°C.

The membrane was prehybridized for at least 4 hours at 65°C in 10 mL of Northern Blot hybridization solution (7% SDS, 0.5 M phosphate buffer, 1 mM Na_2EDTA) and then hybridized in 5 mL of Northern Blot hybridization solution with a formamide-denatured random primed cDNA probe. Following overnight hybridization, the membrane was washed for 15 minutes at 65°C in 40 mM phosphate buffer, 1 mM Na_2EDTA, 5.0% SDS. The membrane was then washed from one to three times for 15 minutes at 65°C in 40 mM phosphate buffer, 1 mM Na_2EDTA, 1.0% SDS. Once washed, the membranes were sealed into plastic bags and exposed to autoradiographic film overnight at -75°C. If reprobing of the membranes was required, the membranes were stripped by pouring boiling water containing 0.1% SDS over them and allowing the solution to cool to room temperature. The membranes were then rinsed in 2x SSC and checked by overnight exposure to autoradiographic film.

Solutions:

1 M Phosphate Buffer pH 7.4

1 M phosphate buffer was prepared by dissolving 70g anhydrous Na_2HPO_4 and 4 mL 85% phosphoric acid. The solution was titrated to pH 7.4.

10x MOPS/Na_2EDTA Buffer* MOPS = (3-(N-morpholino)propansulfonic acid

10x MOPS*/Na_2EDTA Buffer consists of 200 mM MOPS, 50 mM sodium acetate, 10 mM Na_2EDTA.

2.3.10 Preparation of Filters and Filtration of [^{32}P]α-dCTP-labeled Probes

Filter columns for radiolabeled cDNA fragments were prepared using Sigma G50 DNA Grade Sephadex beads. A small wad of glass wool was placed into a 1 mL syrette using fine forceps and packed into the tip of the syrette using the plunger from the syrette. A vacuum aspirator hose was attached to the tip end of the syrette. Sephadex swelled in 1x TE buffer was added to the syrette with a 1 mL pipettor until there was 1 mL of Sephadex beads in the syrette. The excess TE was removed by vacuum aspiration. The cap from a conical 15 mL screw-capped tube was removed and an "x" was cut through the centre of the top of the cap. The syrette tip was pushed through the cut in the cap of the conical tube and the cap was screwed onto the tube. The column was centrifuged for 5 minutes on the highest speed of a clinical centrifuge to pack the beads and to remove any remaining liquid from the beads for it would have collected in the conical tube that the syrette it attached to. This excess liquid was disposed of from the conical tube. The labeled probe was delivered to the top of the column in a total of 100-150 µL of dd H_2O and the column was centrifuged for 5 minutes at the highest speed. The eluate containing the radiolabelled probe was collected.

Alternatively, Bio-Rad Spin 6 columns were used according to manufacturer's instructions.

Following purification, 1 µL of the eluate was removed and analyzed by scintillation in a Beckman Scintillation counter set to measure Cherenkov $^{[32]}$P radiation. The signal was routinely in the range of 0.5 –1 x10^6 cpm per 1µL. The probe was denatured with an equal volume of deionized formamide or by boiling in water and added to the prehybridization solution.

2.3.11 Preparation of Whole Cell Protein Extracts for Western Blot Analysis

WEHI231 and MOPC460D cells were passaged 24 hours prior to the extraction of their protein. Pre-B cells were seeded and allowed to grow for 24 hours. They were treated with either 100 nM 4-hydroxytamoxifen or the equivalent volume of 100% ethanol. From this point, cells were harvested for protein either at 1, 3, 6, and 9 hours after treatment, or 0, 6, 9, 12, 24, 48, and 72 hours after treatment. Whole cell extracts were prepared by washing the cells three times in 10 mL of ice-cold PBS, and centrifuging for 5 minutes at 3,000 rpm, at 4°C. The cell pellet was resuspended in 100 µL Whole Cell Extract Buffer + NP-40 (10 mM N-2-Hydroxyethylpiperizine-N'-2-Ethane sulphonic acid (HEPES) buffer pH 7.9, 60 mM KCl, 1 mM $Na2_EDTA$, 0.5% NP-40). 1 mM dithiothreitol (DTT) and 1 mM AEBSF were added to the Whole Cell Extract Buffer immediately before use. The cells were lysed by three cycles of freeze/thaw which consisted of the following: 15 minutes in a dry ice/ethanol bath followed by a quick thaw in a 37°C water bath. The extracts were vortexed vigorously between each thawing and freezing cycle. The cell debris was removed by centrifugation of the sample for 3 minutes at 13,000 rpm. The supernatant was collected, aliquoted in 20 µL volumes and stored at -20°C. The concentration of the protein was determined by using one aliquoted sample. This sample was thawed slowly on ice and 1 µL of the protein sample was added to 999 µL of Bio-Rad protein complexing solution. The absorbance of this resultant solution was measured at $\lambda = 595$ nm and the concentration was established from a standard curve.

2.3.12 Western Blotting Analysis

2.3.12.1 Sample Preparation and SDS Polyacrylamide Gel Electrophoresis

Western analysis was performed with 50 µg of protein sample plus an equal volume of 2x SDS Protein Loading Buffer and separated by SDS polyacrylamide gel electrophoresis (SDS-PAGE). The 2x protein loading buffer was prepared by mixing the following ingredients: 1 mL of 0.5 mL Trizma pH 6.8, 2 mL 10% SDS, 6.2 mg dithithreitol (DTT), 500 µL 98% glycerol, and 0.5% (w/v) Brilliant Blue R 250. The protein, in the loading buffer, was denatured in a boiling water bath for 3 minutes. The denatured samples were loaded onto an 8% SDS polyacrylamide gel and run at 35 V overnight or until the largest protein of the molecular weight marker had run into the resolving gel. The 8% SDS protein gel was prepared as follows: The resolving gel was comprised of 23.3 mL dd H_2O, 13.3 mL 30% bis acrylamide, 12.5 mL 1.5 M Trizma buffer pH 8.8, 500 µL 10% SDS, and polymerized with 24 µL *N, N, N', N'*-Tetramethylethylenediamine (TEMED) and 400 µL 10% ammonium persulphate. A smooth interface was cast by addition of a 2 mL layer of water to the top of the resolving gel solution prior to polymerization. The stacking gel was comprised of 11.1 mL dd H_2O, 3.4 mL 30% bis acrylamide, 5.0 mL 0.5 M Trizma buffer pH 6.8, 200 µL 10% SDS, and polymerized with 10 µL TEMED and 200 µL ammonium persulphate. The gel was run in SDS Running Buffer (100 mM Trizma, 100 mM glycine, and 20% SDS).

Upon completion of electrophoresis, the gel was blotted onto a Hybond Super-C membrane. First the gel and the membrane were wetted in Transfer Buffer (50 mM Trizma base, 40 mM glycine, 0.0375% SDS, and 20% methanol) for 15 minutes. After wetting, the protein was transferred to the membrane using a Bio-Rad semidry transfer

apparatus according to manufacturer's instructions. The transfer was performed at 12 V for 1.5 hours.

2.3.12.2 Antibody Staining Following SDS-PAGE and Blotting

All immunostaining manipulations were performed at room temperature. The membrane was first blocked in a Blocking solution (10% (w/v) skim milk powder, in 0.3% Tween-20 in PBS) for a minimum of one hour on an oscillating shaker. The membrane was then washed twice, 15 minutes each time, on a shaker in PBS/0.3% Tween-20. After this wash, the membrane was incubated with the primary antibody in 0.3% Tween-20 in PBS for one hour. After this incubation the membrane was washed three times, 15 minutes each time, with PBS/0.3% Tween-20 on a shaker. The membrane was then incubated with secondary antibody in PBS/0.3% Tween-20 for 1 hour on a shaker and again washed four times, 15 minutes each time, in PBS/0.3% Tween-20 on a shaker. Appropriate dilution of primary antibodies used was as follows: Mouse 3C7 anti-Myc antibody was diluted 1:1000, mouse anti-Max 256 antibody was diluted 1:20,000 and rabbit anti-R2 was diluted 1:400 in PBS/0.3% Tween-20. Appropriate dilution of Amersham Pharmacia Biotech ECL™ Kit secondary antibodies used was as follows: Anti-mouse horse raddish peroxidase (HRP) and anti-rabbit HRP antibodies were diluted 1: 50,000 in PBS/0.3% Tween-20.

2.3.12.3 The Enhanced Chemiluminescence (ECL) Reaction

All ECL reaction manipulations for the development of anti-body/antigen interactions on Western blots were performed at room temperature. The ECL solutions 1 and 2 were mixed 1:1 and the membrane was immediately incubated in the mixture for 1 minute. The

membrane was wrapped in Saran and exposed to ECL-sensitive film anywhere from 10 seconds to 1 hour, as required.

2.3.12.4 Stripping Of Western Membranes

The membrane was stripped by incubating it in 100 mM glycine (pH 2.5) at room temperature for 10 minutes on a shaker. Before storage or reprobing, the membrane was rinsed with 0.3% Tween-20 in PBS.

2.3.13 DNA/Protein Interaction Experiments

The purpose of DNA/Protein interaction experiments is to determine whether certain DNA sequences will interact with specific proteins or with cell lysate proteins with which they were incubated *in vitro*. Competition experiments were performed to assess the specificity of binding of certain DNA sequences for (a) particular protein(s). These experiments can also be performed with antibodies to disrupt complex formation and thereby elucidate the identity of the protein(s) that bind to a particular DNA sequence under *in vitro* conditions.

2.3.13.1 Annealing of the *R2* Oligonucleotides

The forward and reverse strands of the four *R2* oligonucleotides, *R2-2*, *R2-3*, *R2-4*, and *R2-5* were annealed for the gel shift and competition experiments described in Sections 2.3.13.3, 2.3.13.4, and 2.3.13.5. 1 μg of each single stranded oligonucleotide from a set (*i.e.* forward and reverse strands from *R2-2*) was delivered to a microfuge tube in addition to sterile dd H_2O, to a final volume of 200 μL. The solution was denatured for 5 minutes at 85°C in a heating block and were then allowed to reanneal slowly by cooling to room temperature.

2.3.13.2 5'-End-labeling of Annealed Oligonucleotides with $^{[32]}$P-γ-ATP.

A volume of 2 µL, containing 40 ng of double-stranded oligonucleotide was delivered to a sterile microfuge tube. In addition, 2 µL of 10x Polynucleotide Kinase buffer, 10 µL of sterile dd H_2O, 5 µL of $^{[32]}$P-γ-ATP, and 1 µL of T4 Polynucleotide Kinase were added and the mixture was incubated for 60 minutes at 37°C. Following incubation, 50 µL of dd H_2O was added and the total 70 µL solution was mixed and delivered to a preequilibrated (3 washes with 500 µL of Band Shift Buffer (see Section 2.3.13.2) containing 1 mM DTT) BioRad Spin 6 column and centrifuged at 1,200 rpm for 4 minutes at room temperature. The efficiency of the 5'-end-labeling and the quality of the oligonucleotides was determined by running a 1 µL aliquot of each of the labeled oligonucleotides on a 15% native acrylamide gel (22.5 mL dd H_2O, 25 mL 30% bis acrylamide, 2.5 mL 5x TBE, and polymerized using 50 µL TEMED and 400 µL 10% ammonium persulphate) that was run for 3 hours at 80 V in 0.25x TBE and then exposed to autoradiographic film at 4°C for 1 hour. A 15% acrylamide gel was used because the oligonucleotide probes were very small (*i.e.*20 bp).

2.3.13.3 Bandshift Assays

Protein extracts were thawed on ice just prior to their use. The following ingredients were then mixed: 1-5 µg protein extract, 1 µL (0.50 $\mu g \mu L^{-1}$) denatured herring sperm DNA, and band shift buffer (10 mM N-2-Hydroxyethylpiperizine-N'-2-Ethane sulphonic acid (HEPES) buffer pH 7.9, 60 mM KCl, 1 mM Na_2EDTA, 4 % ficoll, including 1 mM dithiothreitol (DTT)), to a final volume of 20 µL. This solution was incubated for 5 minutes at room temperature. The $^{[32]}$P-γ-ATP-labeled double stranded *R2* oligonucleotide (See Sections 2.3.13.1 and 2.3.13.2) was then added and the solution was

mixed by stirring with a pipette tip. This mixture was allowed to incubate at room temperature for 30 minutes. These samples were then loaded onto a 5% native acrylamide gel comprised of 35.8 mL dd H_2O, 11.7 mL 30% bis acrylamide, 2.5 mL 5x TBE, and polymerized with 50 µL *N, N, N', N'*-Tetramethylethylenediamine (TEMED) and 400 µL 10% ammonium persulphate. The gel was run in 0.25x TBE buffer for 3 hours at 80 V and then dried for 2 hours at 80°C on Hybond XL membrane and two layers of Whatmann 3MM paper. The dried gel was covered with Saran, and exposed to autoradiographic film at -75°C for 12 to 18 hours.

2.3.13.4 Competition Assays

Competition assays were performed in the same way as bandshift assays, except that the radiolabelled oligonucleotide and cell lysate were coincubated with increasing molar excesses (0, 5, 50, and 100-fold) of the competing unlabelled oligonucleotide sequence.

2.3.13.5 Antibody Supershift Assays

Antibody supershift assays were performed in the same way as bandshift assays, except that the radiolabelled oligonucleotide and cell lysate were coincubated with increasing concentrations of a specific antibody.

2.3.14 Protein Staining for Quantitative Fluorescent Immunohistochemistry

All immunostaining manipulations were performed at room temperature. Except where noted, all solutions were prepared in PBS + 50 mM $MgCl_2$, herein referred to as PBS*.

Previously cytospun cells were fixed to microscope slides by a 10 minute incubation in 3.7% formaldehyde and then washed in two washes of PBS*. The cells were then permiabilized by a 12 minute incubation in a solution of 0.2% Triton X-100 in dd H_2O. The slides were then washed in three washes of PBS*. They were subsequently blocked in prewarmed lamb serum for 5 minutes. Primary antibody, appropriately diluted in lamb serum, was then added to the area on the slides containing the cells and allowed to incubate for 45 minutes at room temperature, under a coverslip. The proper dilutions for primary antibodies were as follows: 3C7 anti-Myc antibody (Evan *et al.*, 1985) was diluted 1:1000 and anti-R2 was diluted 1:400 in lamb serum. The slides were washed in three washes of PBS* and then blocked again for 5 minutes at room temperature in prewarmed lamb serum. Appropriately diluted secondary antibody was added to the slides and allowed to incubate for 30 minutes at room temperature, under a coverslip. The secondary antibodies were diluted as follows: Texas Red (TXRD)- conjugated anti-mouse IgG antibody and fluorescein isothiocyanate (FITC)-conjugated anti-rabbit antibody were both diluted 1:400 in lamb serum. The slides were again washed three times in PBS*. The nuclei of the cells were counterstained with DAPI (1 μgmL^{-1} in PBS, no $MgCl_2$) for 5 minutes at room temperature, in the dark, under a coverslip and then mounted in antibleach. The slides were stored at 4°C in the dark if they were not examined immediately.

Antibleach was prepared by mixing 6 g glycerol and 2.4 g Mowiol 4-88 with 6 mL dd H_2O. The mixture was stirred for approximately for 2 hours at room temperature and then mixed with 12 mL of 0.2 M Tris pH 8.5. The solution was then incubated at 50°C until the contents were dissolved, and stirred from time to time. The antibleach

(Mai, 1994) solution was aliquoted and store at -20°C. Prior to use, an aliquot of working solution was prepared by adding 2.5% 1,4 Diazabicyclo(2.2.2)octane (DABCO).

2.3.15 Fluorescent *In Situ* Hybridization (FISH) of Interphase Cells, Metaphase Chromosomes, and Extrachromosomal DNA Molecules

2.1.15.1 Biotin and Digoxigenin Labeling

3 µg of linearized DNA (minimum length of 1 kb) was delivered to a sterile microfuge tube and the volume was adjusted to 15 µL with sterile dd H_2O. The DNA solution was placed in a boiling water bath for 10 minutes and then immediately chilled on ice for at least 2 minutes. The following ingredients were added to the tube while on ice: 2.0 µL hexanucleotide mixture, 2.0 µL dNTP mixture, 1.0 µL Klenow (all ingredients from Digoxigenin (DIG) and Biotin DNA Labelling Kit, Roche Diagnostics). The resultant mixture was incubated overnight at 37°C. After this incubation, 2.0 µL 0.2 M Na_2EDTA, 2.5 µL 4.0 M LiCl, and 75 µL 95% ethanol (-20°C) were added and the mixture was placed at either -75°C for 30 minutes or at -20°C for 2 hours. The sample was then centrifuged for 15 minutes at 13,000 rpm at 4°C, after which the pellet was washed with 70% ethanol (-20°C). The pellet was again centrifuged for 15 minutes at 13,000 rpm at 4°C, dried in a rotoevaporator and dissolved in 50 µL 1x TE buffer. To test the labeling of the probes, 1 µL of each of the samples was set aside to be tested as described in Section 2.3.15.2.

To the remainder of the samples, 551 µL 1x TE buffer, 5.0 µL herring sperm, DNA (10 $mgmL^{-1}$), 5.0 µL t-RNA (10 $mgmL^{-1}$) and 61 µL 3 M sodium acetate (pH 5.5) were added and mixed. The entire volume was mixed and divided into two tubes, 355 µL

each. 840 µL of 95% ethanol (-20°C) was added to each tube and the mixture was incubated on ice for 30 minutes. The tubes were then centrifuged for 15 minutes at 13,000 rpm at 4°C. The pellet was dried by rotoevaporation, dissolved in 50 µL FSP (50% formamide, 2x SSC, 50 mM phosphate buffer pH 7.0), and stored at -20°C.

2.3.15.2 Detection of Digoxigenin- and Biotin-Labeled Probes

Serial dilutions were prepared from the 1 µL sample taken from the labeled probes. The following dilutions were prepared in DNA Dilution Buffer (from DIG and Biotin DNA Labelling Kit, Roche Diagnostics): 1:10, 1:100, 1:1,000, and 1:10,000. A dilution series was also prepared from control samples of digoxigenin- and biotin-labeled DNA. The digoxigenin-labeled control DNA was taken from a Boehringher Mannheim Labeling Kit. There is no biotinylated control DNA provided, thus a suitably labeled sample previously prepared in the lab was used as a control to test biotinylated samples. 1 µL of each dilution of labeled DNA and labeled control sample was spotted onto a small, dry swatch of Hybond N^+ nitrocellulose membrane. The membrane was baked under vacuum at 80°C for 2 hours and then washed on a shaker for 1 minute in Buffer 1 (100 mM maleic acid, 150 mM NaCl, pH 7.5). The membrane was then washed in Buffer 2 (1% Blocking Reagent prepared in Buffer 1) for 30 minutes on a shaker. This membrane was then incubated in anti-DIG-AP, diluted 1:5,000 in Buffer 2, or Streptadivan-AP, diluted 1:25,000 in Buffer 2, on a shaker for 30 minutes and then washed twice in Buffer 3 (100 mM Trizma, 100 mM NaCl, 50 mM $MgCl_2$, pH 9.5). 5 mL of Substrate Solution (from DIG and Biotin DNA Labelling Kit, Roche Diagnostics) was delivered onto the membrane and incubated in darkness until spots were clearly visible. The colourimetric

reaction was stopped by incubating the membrane in TE buffer for 5 minutes. The membrane was then air dried.

2.3.15.3 Metaphase Preparations

Metaphase chromosomes were prepared for analyses by fluorescent *in situ* hybridization (FISH). Cells that were to be analyzed were harvested and 10^5 cells were pelleted in a polypropylene 15 mL conical screw-capped tube. The supernatant was carefully removed. 5 mL of 75 mM KCl were added and the pellet was gently resuspended. This suspension was incubated for 30 minutes at room temperature and then it was centrifuged for 10 minutes at 800 rpm, room temperature. The supernatant was carefully removed and discarded. Freshly prepared methanol:acetic acid (3:1) was added using a pastuer pipette in the following quantities and intervals: One drop was added. One minute later, another drop was added. This was done for a total of 5 drops over 5 minutes. The chromosome fixation continued as follows, with each addition made after a 2 minute interval: 2 drops, 5 drops, 7 drops, 10 drops, 15 drops, 30 drops, 60 drops. After the addition of 60 drops, 1 mL of methanol:acetic acid (3:1) fixative was added and mixed carefully by inverting the tube. The tube was centrifuged for 15 minutes 800 rpm at room temperature. The supernatant was carefully removed and discarded. The chromosome-containing pellet was resuspended in 5 mL of fixative, incubated for 10 minutes at room temperature and centrifuged again for 10 minutes, 800 rpm at room temperature. The resuspension of the chromosomes in methanol:acetic acid followed by centrifugation was repeated twice more, but with 20 and 30 minute intervals of incubation at room temperature. After the final centrifugation, the pellet was then resuspended in 10 mL of methanol:acetic fixative and stored at 4°C.

For analysis the chromosomes were gently mixed with a Pasteur pipette and dropped onto a slide that had been chilled for roughly 20 seconds on dry ice. The slide was placed immediately onto a slide warmer until the solution began to form crystals. The slide was dipped into fresh 50% acetic acid for 1-2 seconds and returned to the slide warmer until all of the liquid had evaporated off. Alternatively, slides were precooled by soaking them briefly in ice water. The methanol:acetic acid-fixed chromosomes were dropped onto the wet slides, rinsed in 50% acetic acid and then dried on the slide warmer. Prepared slides were examined under the microscope (Zeiss Axioplan, 100x magnification) and all areas of the slide where metaphases were located were marked with a diamond scriber.

2.3.15.4 Hybridization of Interphase Nuclear DNA, Metaphase Chromosomes, or Extrachromosomal DNA Molecules

The chromosomes on the slides were fixed in fresh 50% acetic acid 6 times for 20 minutes each time at room temperature. If unable to immediately proceed with the hybridization steps following acid fixation, the slides were then put into a coplin jar filled with 70% ethanol which was then placed at 4°C for a maximum of 2 days. Following acid fixation, the slides were equilibrated in 2x SSC for 10 minutes at room temperature. They were then treated with RNAse (10 μgmL^{-1} in 2x SSC) for 1 hour at 37°C in a humidified atmosphere. The slides were washed three times for 5 minutes in 2 x SSC in a shaking coplin jar at room temperature and then they were incubated in a solution of 50 μgmL^{-1} pepsin, 100 mM HCl for 10 minutes at 37°C. The slides were washed twice for 5 minutes on a shaker in PBS at room temperature, followed by one 5 minute wash in 1x PBS, 50 mM $MgCl_2$, on a shaker at room temperature. Postfixation treatment of the slides was as follows: The slides were soaked in a fresh solution of 1% formaldehyde in PBS, 50 mM

$MgCl_2$ for 10 minutes at room temperature and then washed once for 5 minutes in PBS on a shaker at room temperature. Dehydration of the DNA samples was performed in 70%, 90%, and 100% ethanol, for 3 minutes each at room temperature. The slides were air-dried at room temperature. Denaturation of the samples were performed in a solution consisting of 70% deionized formamide, 2x SSC, pH 7.0 at 70°C for precisely 2 minutes. Immediately following the denaturation step the slides were transferred to -20°C solutions of 70%, 90%, and 100% ethanol for 3 minutes each. The slides were then air-dried at room temperature. Digoxigenin- or biotin-labeled probes were denatured for 5 minutes at 90-95°C. 20-50 ng of probe were delivered in a volume of 20 µL of hybridization solution, to each slide. The probe used for FISH in this thesis work was the *ribonucleotide reductase R2* cDNA (Thelander and Berg, 1986) labeled with digoxigenin. A biotin-labeled mouse chromosome 12 paint was also used to show mouse chromosome 12. The mouse chromosome 12 paint was purchased from Cambio Limited through Cedarlane Laboratories Ltd., (Hornby, ON, Canada) and used according to manufacturer's instructions. The area of the slide where the labelled probe was placed was covered with a coverslip, sealed with rubber cement and then incubated in a humidified atmosphere at 37°C for 12-16 hours. Following hybridization, the coverslips were removed and the slides were washed three times for 5 minutes in 50% formamide, 2x SSC at 42°C. The slides then were washed five times for 2 minutes each in 2x SSC on a shaker at room temperature, and then incubated in lamb serum blocking solution for 10 minutes at room temperature. Diluted primary antibody (200 µL, diluted in lamb serum) was added to the slides, covered with a coverslip and incubated for 30 minutes in a humidified atmosphere at 37°C. The slides were washed three times for 5 minutes in 4x

SSC, 0.1% Tween-20 at 42°C in a shaking water bath. Diluted secondary antibody (200 µL, diluted in lamb serum) was delivered to each slide, and incubated for 30 minutes in a humidified atmosphere at 37°C. The slides were washed three times for 5 minutes in 4x SSC, 0.1% Tween-20 in a shaking water bath at 42°C. The hybridized slides were counterstained with 200 µL per slide of DAPI (1 μgmL^{-1} in PBS) for 5 minutes in darkness. Antibleach was added (50-100 µL) and the slide was covered with a coverslip and examined under a fluorescent microscope.

2.3.16 Fluorescent *In Situ* Hybridization (FISH) of Extrachromosomal DNA Molecules (FISH-EEs)

FISH was carried out according to the protocols described in considerable detail in Section 2.3.15. The following cDNAs were used for FISH-EEs probes: human *c-myc* cDNA (Mai, 1994; Mai *et al.*, 1996), human *cyclin C* cDNA (Mai *et al.*, 1996), mouse *cyclin D2* genomic DNA (Mai *et al.*, 1999), mouse *ribonucleotide reductase R1* and *R2* (*R1* and *R2*) cDNA (Thelander and Berg, 1986), all of which were labeled with digoxigenin. After hybridization, the annealed probe is visualized by incubation with anti-digoxigenin-fluorescein antibody. An additional probe, a mouse *dihydrofolate reductase* (*DHFR*) cDNA (Mai, 1994; Mai *et al.*, 1996), was labeled with biotin, detected with a monoclonal mouse anti-biotin antibody, and visualized by goat anti-mouse-IgG_1-Texas Red.

2.3.16.1 Isolation of Extrachromosomal Elements.

The procedure used for this application is described in detail in Section 2.3.7.

2.3.16.2 Fixation of Extrachromosomal Elements.

The Hirt extracted EEs were mixed with an equal volume of freshly prepared methanol:acetic acid (3:1). The following protocol allowed for the fixation of the EEs onto glass slides, and it guaranteed that the EEs were well spread, but contained within a small area. Briefly: 40 µL of fixed EEs (Hirt extract in fixative) were delivered onto precooled slide (60 seconds on dry ice), and then the slides were immediately moved onto a slide warmer (37°C). When crystals began to appear on the slides, the slides were dipped once into 50% acetic acid and then dried to completion on the slide warmer (37°C). The slide was stained for 2 minutes with modified Giemsa stain (Sigma) and the area onto which the EEs were dropped was located under the microscope (Zeiss Axioplan, 100x magnification) and marked with a diamond scriber.

2.3.16.3 Screening of the Extrachromosomal Elements

DAPI (1µgmL^{-1} in PBS) was used to stain both the DNA in the EEs and any genomic DNA contaminants. Antibleach (see Section 2.3.14.) was added to preserve the fluorescence of the sample and as a mount for the coverslip.

2.3.17 Preparation of cDNA Fragments for FISH, FISH-EEs, Southern and Northern Blot Hybridizations

2.3.17.1. cDNA Preparation and Fragment Isolation

Plasmid DNA constructs containing cDNA fragments of choice were transfected into competent bacteria as described in Section 2.1.4. Bacteria containing the construct of choice were grown up and plasmid DNA was extracted either by Rapid Alkaline Plasmid DNA Isolation (See Section 2.1.2) or by Large Scale Alkaline Plasmid DNA Isolation (See Section 2.1.1). The constructs were digested with the appropriate restriction

endonuclease and the fragment of choice was electrophoretically separated from the plasmid DNA on a 1.0% agarose gel. The restriction endonucleases used for the isolation of the DNA fragments is described in Table 2.3.17.2.

Isolation of cDNA fragments for Southern and Northern analysis is done as follows: Once the fragment was separated by electrophoresis the correct band was cut out of the gel, delivered to dialysis tubing with a minimal amount of 1x TE buffer and electrophoresed out of the gel and into the TE buffer. Isolation of cDNA fragments for FISH and FISH-EEs analyses was completed by finding the appropriate band on the agarose gel, slitting the gel just below the band of interest and running the DNA onto a small piece of DEAE NA45 membrane that had been positioned in the slit. DNA was released from the membrane by overnight incubation of the membrane in 1 M NaCl at 68°C.

Once the fragments were isolated, the DNA was precipitated with 0.6 volumes of isopropanol (-20°C) and 0.3 M sodium acetate at (-20°C) overnight. The DNA was collected by 30 minutes of centrifugation at 13,000 rpm at 4°C. The DNA pellet was washed in ice cold 70% ethanol and resuspended in a small volume of 1x TE buffer. The purity of the isolated fragment was checked by electrophoresing a small aliquot of the isolated fragment on a 1.0% agarose gel.

Table 2.3.17.2. cDNA Fragments Isolated

Probes	Size (bp)	Endonuclease
Rat *Glyceraldehyde-3-Phosphate Dehydrogenase*[a]	1300	*Pst*I
Mouse *Glutathione peroxidase*[b]	700	*Pst*I
Mouse *c-myc* (Exon II)	460	*Pst*I
Mouse *Ribonucleotide reductase R1*[c]	1500	*BamH*I
Mouse *Ribonucleotide reductase R2*[c]	1487	*Pst*I
Mouse *Dihydrofolate reductase*[d]	2000	*Pst*I
Mouse *Cyclin D*[e]	600	*Not*I/*Nco*I
Mouse *Cot-1*[f]	N/A	N/A
Mouse IGF2[g]	1000	*Eco*RI
Human *Cyclin C*[h]	400 + 500	*Eco*RI
Human *c-Myc*[i]	1700	*Hin*dIII/*Bgl*II

[a] Rat *GAPDH*	Dr. Aiping Young
[b] Mouse *GSHPX*	Chambers *et al.*, 1986
[c] Mouse *R1 and R2*	Thelander and Berg, 1986.
[d] Mouse *DHFR*	Mai, 1994.
[e] Mouse *Cot-1*	Canadian Life Technologies (catalogue No. Y01398)
[f] Mouse *Cyclin D*	Mai *et al.*, 1999.
[g] Human *IGF2*	Kitsberg *et al.*, 1993.
[h] Human *Cyclin C*	Mai *et al.*, 1996.
[i] Human *c-Myc*	Mai, 1994; Mai *et al.*, 1996.

2.3.18 Preparation and Use of 4-Hydroxytamoxifen

2.3.18.1 Preparation of 4-Hydroxytamoxifen

A 1:1 E/Z racimate of 4-Hydroxytamoxifen (4-HT) was dissolved in 100% ethanol at a concentration of 10 $mgmL^{-1}$. The dissolved drug was stored in darkness at -20°C. Alternatively, a ≥ 98% Z isomer was purchased and dissolved at a concentration of 10 $mgmL^{-1}$in 100 % ethanol. This preparation was also stored at -20°C and in the dark. The efficacious dose of the drug to be used on cells carrying the Myc-ER™ construct was conducted at different time points after activation in order to follow the activation of the construct. This titration of different doses of drug per mL of culture medium was performed each time a new vial of drug was prepared in order to determine the efficacious dose of the new preparation of 4-HT. The titration experiments were also performed during each activation experiments using the established dose to ensure that the cells were activated for the purpose of the experiment.

2.3.18.2 Titration of 4-Hydroxytamoxifan Efficacy

Pre-B cells were seeded into six 100 mm culture dishes at roughly 10^6 cells per mL. The cells were allowed to incubate at 37°C for 24 hours in 5% CO_2. The doses of 4-HT used in the titration were 0.5 µL, 1.0 µL, 1.5 µL and 2.0 µL of 10 $mgmL^{-1}$ 4-HT per 10 mL of culture medium. The remaining dishes were used as controls and received 0.5, 1.0, and 1.5 µL of 100 % ethanol per 10 mL of culture medium. Measurements of c-Myc-ER™ translocation to the nucleus were made at 0, 1, 2, 4, and 6 hours after activation of the cells with 4-HT and thus cytospins with roughly 250,000 cells per slide were prepared from each of the dishes at those time points. Quantitative Fluorescent Immunohistochemical Analysis (See Section 2.3.14.), using an anti-c-Myc 3C7 antibody

(Evan *et al.*, 1985), was performed in order to measure the translocation of the Myc-ER™ construct from the cytoplasm to the nucleus. Translocation of Myc-ER™ to the nucleus is indicative of successful induction of the cells. Signals of translocated Myc-ER™ were usually 1.5- to 1.8-fold higher than nuclear levels of c-Myc in the non-activated cells. Analysis was performed using a Zeiss Axioplan 2 microscope with a 63x oil immersion lens. The signal intensity was measured using the area density function in the Northern Eclipse 5.0 software package (Empix Imaging Inc).

2.3.19 Histone Immunopurification of Extrachromosomal Elements (HIP-EEs)

2.3.19 Preparation and Blocking of Protein Sepharose Beads

The Protein G sepharose beads used to bind the antihistone antibodies used for the immunopurification of the EEs were prepared as follows: 1 mg of protein G sepharose beads was washed in 5 mL of Buffer A (100 mM KCl, 10 mM Tris pH 7.4, 1 mM Na_2EDTA, 1mM DTT, 1mM AEBSF) by placing on a rotating platform for 10 minutes at room temperature. The beads were centrifuged at 13,000 rpm (16,000 x *g*) for 10 minutes at room temperature and the supernatant was removed and discarded. The beads were washed two more times in Buffer A. The non-specific binding sites on 40 µL of beads were blocked by resuspending the beads in Buffer B (10 mM HEPES pH 7.9, 60 mM KCl, 1mM Na_2EDTA 4% Ficoll, 1mM DTT, 1mM AEBSF, 4% ($^{w}/_{v}$) Bovine Serum Albumin).

2.3.19.2 Immunopurification of Extrachromosomal Elements

This procedure was used to perform the purification of the Hirt-extracted histone-bound EEs from the impurities found in the Hirt-extracted EE sample. Freshly extracted

EEs were dialyzed against 0.5x TE buffer overnight at 4°C. They were then incubated in 500 µL Buffer B on a rotating platform for 10 minutes at room temperature. 1 µg of anti-core histone antibody per µg of EEs was added and the mixture was incubated for 30 minutes at room temperature on a rotating platform. The blocked beads were added to the antibody-treated EEs and incubated overnight on a rotating platform at room temperature. Following this incubation, the EE/beads were centrifuged at 13,000 rpm for 10 minutes at room temperature and the supernatant was removed. The EE/beads were then washed, three times, with 300 µL of Buffer A. The bound histone-containing EEs were eluted by adding 300 µL of 100 mM glycine (pH 2.3) to the beads and inverting the tube 5 - 10 times to mix. The sample was then centrifuged at 13,000 rpm for 10 minutes at room temperature and the supernatant (eluate) was removed and collected. The eluate was immediately neutralized to pH 7.2 using 1 M Tris pH 8.0. The elution step was repeated once more. The sample was concentrated to approximately 40 µL by rotoevaporation.

2.3.20 Microscopic Examinations

Image acquisition and analyses of FISH and FISH-EEs and preparations and fluorescence quantitative immunohistochemical analyses of cellular protein levels was performed on a Zeiss Axiophot microscope equipped with a Photometrics charge capture device (CCD) camera and IPLAb Spectrum software v.3.1 software (Scanalytics). Alternatively, images acquired for immunostaining and for HIP-EEs analysis were gathered on a Zeiss Axioplan 2 microscope equipped with a Hamamatsu CCD camera and Empix Northern Eclipse 5.0 software (Empix Imaging Inc, Mississauga, Canada).

2.3.21 Photography

Photography of the FISH, FISH-EEs and HIP-EEs images for publication was performed using a Nikon F-601 camera equipped with a 60 mm macro lens. Colour matching was done using Kodak Ecktachrome 400 ASA slide film. Prints were made using Fuji NPH135 400 ASA print film. The prints were colour-matched and custom-developed at Light Visions (Winnipeg, Manitoba).

2.4 SUPPLIES

Amersham Pharmacia Biotech

Hybond Super-C Transfer Membrane (0.45μ)	(20 cm x 3m)	(Code: RPN 203G)
Hybond N+ Nylon Hybridization Membrane	(30 cm x 3m)	(Code: RPN 203B)
Hybond XL Nylon Hybridization Membrane	(30 cm x 3m)	(Code: RPN 303S)
Oligolabeling Kit	(40 reactions)	(Code: 27-9250-01)
Rainbow Marker	(250 μL)	(Code: RPN 756)
Protein G Sepharose		
Redivue™ [^{32}P]-α-dCTP	(250 μCi)	(Code: A0075)
[^{32}P]-γ-ATP	(250 μCi)	(Code: PB1018)

Beckton Dickinson

Mouse Monoclonal Anti BrdU antibody	(Catalogue No.: 347583)

Bio-Rad

Acrylamide/Bis (30%)	(Catalog No. 161-0159)
Ammonium Persulfate	(Catalog No. 161-7000)
Spin-6 Filtration Columns	(Catalog No. 732-6002)
Protein Determination Solution	(Catalog No. 500-0006)

Canadian Life Technologies (Canadian Life Technologies)

Cell Culture Medium and Supplements

β-Meraptoethanol (50 mL; 55 mM in DPBS)	(Catalogue No.: 21985-023)

Buffered Phenol (Catalogue No.: 15513-047)

Fetal Bovine Serum (Catalogue No.: 26140-079)

L-Glutamine (100 mL; 200 mM) (Catalogue No.: 25030-081)

MEM Sodium Pyruvate (100 mL; 100 mM) (Catalogue No.: 11360-070)

Penicillin (5,000 Units mL^{-1})/Streptomycin (5,000 μgmL^{-1}) (100 mL)

(Catalogue No.: 150-70-063)

RPMI 1640 Medium with L-Glutamine (500 mL) (Catalogue No.: 11875-093)

Selectamine™ RPMI 1640 Medium (1 L) (Catalogue No.: 17402-017)

Miscellaneous

Ethidium Bromide (ultrapure) (1 mL; 10 $mgmL^{-1}$) (Catalogue No.: 15585-011)

Agarose (Catalogue No.: 15510-027)

Cedarlane Laboratories Limited:

Mouse Chromosome 12 Paint (biotinylated) (Cambio: 1187-12MB-01)

Fisher Scientific:

Miscellaneous:

Polyvinylpyrrolidon (100 g) (Catalogue No.: BP-431-100)

By Manufacturer

Corning

Polystyrene sterile 15 mL conical screw-capped tubes (500)

(Catalogue No.: 05-538-51D)

Polypropylene sterile 15 mL conical screw-capped tubes (500)

(Catalogue No.: 05-538-51D)

Polypropylene sterile 50 mL conical screw-capped tubes (500)

(Catalogue No.: 05-539-7)

Costar

5 mL disposable pipettes	(Catalogue No.: 303 110)
10 mL disposable pipettes	(Catalogue No.: 303 110J)

Difco

Bacto Agar	(454 g)	(Catalogue No.: DF-0140-0010)
Tryptone Peptone	(500 g)	(Catalogue No.: DF-0123-17)
Yeast Extract	(500 g)	(Catalogue No.: DF-127-1-9)

Falcon

Polypropylene Blue Max Jr. 15 mL conical screw-capped tubes (500)

(Catalogue No.: 14-959-70C)

Nalgene

115 mL filters (0.45 µm)	(Catalogue No.: 09-740-47C)
500 mL filters (0.45 µm)	(Catalogue No.: 09-740-37P)
1000 mL filters(0.45 µm)	(Catalogue No.: 09-740-22G)
Syringe filters (0.45 µm)	(Catalogue No.: 09-740-37J)

Schleicher & Schull

25 mm Nitrocellulose Discs: BA 83, 0.2 µM, Ø25mm.

Shandon

Cytospin Filter Cards (200 per box) (Catalogue No.: 190005)

Fluka

Bovine Serum Albumen	(Catalogue No.: 05480)
Dabco (1,4 Diazabicyclo(2.2.2)octane)	(Catalogue No.: 33480)
Ethyl Alcohol	(Catalogue No.: 02857)
Methyl alcohol	(Catalogue No.: 65542)
Formaldehyde	(Catalogue No.: 47629)

Invitrogen

Easy-DNA Kit (Genomic DNA Isolation Kit)	(Catalogue No.: K1800-01)

O. Kindler

Microscope slides

Coverslips 25 x 25 mm^2

Coverslips 24 x 60 mm^2

New England Biolabs

T4 Polynucleotide Kinase	(Catalogue No.: 201S)

Roche Diagnostics (formerly **Boehringer Mannheim**)

Restriction Endonucleases

BamH I	(10,000 units; 40 units μL^{-1})	(Catalogue No.: 798 975)
EcoR I	(10,000 units; 40 units μL^{-1})	(Catalogue No.: 200 310)
EcoR V	(10,000 units; 40 units μL^{-1})	(Catalogue No.: 1 040 197)
Hind III	(10,000 units; 40 units μL^{-1})	(Catalogue No.: 789 983)
Pst I	(10,000 units; 40 units μL^{-1})	(Catalogue No.: 798 991)

Digoxigenin and Biotin Labeling Reagents

Hexanucleotide Mixture (10x)	1277 081 or from Labeling Kit 1175 033

dNTP Mixture (DIG)(10x) 1277 065 or from Labeling Kit 1175 033

dNTP Mixture (BIOTIN (10x))

dATP	1.0 mM	27-2050-01
dCTP	1.0 mM	27-2060-01
dGTP	1.0 mM	27-2070-01
dTTP	0.65 mM	27-2080-01
Biotin dUTP	0.35 mM	1-093070

Substrate Solution Labeling Kit 1175 041

Klenow enzyme 1008 404 or from Labeling Kit 1175 033

Anti-DIG-AP polyclonal anti-sheep, anti-DIG-Fab fragment-AP)
Labeling Kit 1175 033

Streptadivan-AP 1089 161.

Miscellaneous

Molecular Weight Marker II (50 µg; 250 μgmL^{-1}) (Catalogue No.: 236 250)

Proteinase K (100 mg) (Catalogue No.: 745 723)

Pefabloc® SC (AEBSF) (100 mg) (Catalogue No.: 1 429 868)

Random Primed DNA Labeling Kit (50 reactions) (Catalogue No.: 1 004 760)

RNase A (100 mg) (Catalogue No.: 109 169)

tRNA (100 mg) (Catalogue No.: 109 541)

Sarstedt Inc.

1-200 µL pipette tips (Catalogue No.: 70.760.002)

100-1000 µL pipette tips (Catalogue No.:70.762)

Sigma

Drugs

Bacterial Culture:

Ampicillin (50 mg) (Catalogue No.: A-2804)

Cell Culture:

4-hydroxytamoxifen [(E) and (Z) isomers 50:50] (10 mg)

Purchased from RBI Scientific (Catalogue No.: T-176)

4-hydroxytamoxifen (≥ 98 % Z) (Catalogue No.: H-7904)

Miscellaneous Chemicals and Reagents

4'6'diamidino-2-phenylindol (DAPI)	(1 g)	(Catalogue No.: D-9542)
Ammonium Acetate (crystalline)	(2.5 kg)	(Catalogue No.: A-1542)
Ammonium Chloride (crystalline)	(100 g)	(Catalogue No.: A-4514)
Boric Acid	(1 kg)	(Catalogue No.: B-7901)
Brilliant Blue (Coomassie)	(5 g)	(Catalogue No.: B-0770)
Brilliant Blue R	(10 g)	(Catalogue No.: B-7920)
Bromodeoxyuridine	(50 mg)	(Catalogue No.: B-9285)
Chloroform	(500 mL)	(Catalogue No.: C-2432)
Demicolcine (Colcemide)	(5 mg)	(Catalogue No.: D-7385)
Dextran sulfate (sodium salt)	(250 g)	(Catalogue No.: D-8906)
Dithiothreitol (DTT)	(1 g)	(Catalogue No.: D-9779)
Ethylenediamine tetraacetic acid (Na_2EDTA)		(Catalogue No.: E-6511)
Ficoll	(100 g)	(Catalogue No.: F-4375)
Formamide	(500 mL)	(Catalogue No.: F-7503)

Glycerol	(500 mL)	(Catalogue No.: G-6279)
Glycine	(2.5 kg)	(Catalogue No.: G-4392)
Herring sperm DNA (Type XIV: herring testes)		(Catalogue No.: D-6898)
Hydrochloric scid	(500 mL)	(Catalogue No.: H-7020)
Isoamyl alcohol	(500 mL)	(Catalogue No.: I-3643)
Isopropanol	(1 L)	(Catalogue No.: I-0398)
Lauryl sulphate (SDS)	(500 g)	(Catalogue No.: L-3771)
Lithium chloride	(500 g)	(Catalogue No.: L-9650)
Lysozyme	(25 g)	(Catalogue No.: L-6876)
Magnesium chloride (crystalline)	(500 g)	(Catalogue No.: M-3634)
Maleic acid (repurified)	(500 g)	(Catalogue No.: M-0375)
Mimosine	(1 g)	(Catalogue No.: M-0253)
Modified Giemsa stain	(500 mL)	(Catalogue No.: GS-500)
MOPS (3-(N-morpholino)propansulfonic acid)		(Catalogue No.: M-1254)
N,N,N',N'-Tetramethylethylenediamine (TEMED)		(Catalogue No.: T-8133)
N-lauroyl sarcosine	(250 g)	(Catalogue No.: L-9150)
Oligo-(dT) cellulose	(1 g)	(Catalogue No.: O-3131)
Pepsin (1:60,000)	(5 g)	(Catalogue No.: P-7012)
Phosphoric Acid (85%)	(500 mL)	(Catalogue No.: P-6560)
Polyethylene glycol 8000	(1 kg)	(Catalogue No.: P-4463)
Polyoxyethylenesorbitan (Tween-20)	(100 mL)	(Catalogue No.: P-1379)
Potassium Acetate	(500 g)	(Catalogue No.: P-5708)
Potassium Bicarbonate	(500 g)	(Catalogue No.: P-9144)

Potassium Chloride	(500 g)	(Catalogue No.: P-3911)
Propidium idodide	(25 mg)	(Catalogue No.: P-4170)
Potassium Phosphate	(500 g)	(Catalogue No.: P-0662)
Quinacrine Mustard		(Catalogue No.: Q-2876)
RNA(transfer)Type X (yeast)	(500 units)	(Catalogue No.: R-9001)
Sephadex G25 (Superfine DNA grade)	(50 g)	(Catalogue No.: S-5772)
Sodium Acetate	(500 g)	(Catalogue No.: S-2889)
Sodium Bicarbonate	(500g)	(Catalogue No.: S-6297)
Sodium Carbonate	(500g)	(Catalogue No.: S-7795)
Sodium Chloride	(5 kg)	(Catalogue No.: S-3014)
Sodium Citrate	(1 kg)	(Catalogue No.: S-4146)
Sodium Hydroxide	(500 g)	(Catalogue No.: S-5881)
Sodium Phosphate	(500 g)	(Catalogue No.: S-9390)
Triton X-100	(1 L)	(Catalogue No.: T-9284)
Trizma Base	(1 kg)	(Catalogue No.: T-6791)
Xylene Cyanole FF	(10 g)	(Catalogue No.: X-4126)

CHAPTER 3

RESULTS

Chapter 3. RESULTS

This chapter is divided into four sections. Each section represents thesis work that has been published or thesis work that has been submitted for publication. Chapter 3.1 describes FISH-EEs a new method wherein fluorescent *in situ* hybridization (FISH) is used as a method of probing for genes found on Extrachromosomal Elements (EEs). Chapter 3.2 describes the c-Myc dependent rearrangement and amplification the R*ibonucleotide reductase R2* gene. Chapter 3.3 describes the isolation of histone-bound EEs using anti-core histone antibodies for the immunopurification of potentially active EEs. Chapter 3.4 describes the c-Myc dependent replication-driven amplification of the r*ibonucleotide reductase R2* gene.

Chapter 3.1.

Preface

Chapter 3.1 is the full paper format of a manuscript published in the electronic journal *Technical Tips Online*: Theodore I. Kuschak, James T. Paul, Jim A. Wright, J. Frederic Mushinski, and Sabine Mai (1999). FISH on purified extrachromosomal DNA molecules Technical Tips Online,<http://www.biomednet.com/db/tto> t01669.

This paper was the first to describe the advantages and potential uses of FISH-EEs, fluorescent *in situ* hybridization (FISH) as a means of studying Extrachromosomal Elements (EEs).

FISH on purified extrachromosomal DNA molecules

Theodore I. Kuschak, James T. Paul, Jim A. Wright, J. Frederic Mushinski, and Sabine Mai

keywords: fluorescent *in situ* hybridization, extrachromosomal elements (EEs), genomic instability

Corresponding author:

S. Mai: Manitoba Institute of Cell Biology, University of Manitoba, Department of Physiology, Department of Human Genetics

100 Olivia Street

Winnipeg MB R3E 0V9 Canada

phone: 204-787-2135

FAX: 204-787-2190

e-mail: smai@cc.umanitoba.ca

3.1.1. INTODUCTION

To facilitate the isolation of extrachromosomal circular DNA molecules (extrachromosomal elements, EEs) from tissue culture cells, we have adapted the Hirt protocol (Ref. 1), which was originally designed to isolate polyoma virus particles. Such preparations of EEs are frequently contaminated with varying amounts of genomic DNA and/or apoptotic DNA fragments (Ref. 2). To address this problem, Gaubatz and Flores describe the use of exonuclease III treatment of the samples, since this enzyme removes linear DNA molecules in these preparations (Ref. 3). However, exonuclease III also digests open and nicked circular extrachromosomal DNA molecules. Thus, this procedure can eliminate some of the EEs, and interfere with obtaining a true representative analysis of the total population of EEs in a cell.

To circumvent this problem, we have designed a method of analysis of EEs that allows their representative examination using fluorescent *in situ* hybridization (FISH), which we have termed FISH-EEs, and does not require the use of exonuclease III.

These are the general advantages of FISH-EEs as described here: (i) Allows analysis of total heterogenous population of EEs in cell lines using the Hirt procedure (Ref. 1), (ii) Generates libraries of EEs DNA from target cells, (iii) Allows examination of genes involved in genomic instability, and (iv) It is fast, reproducible and most importantly, gives a complete representation of EEs and their genomic information in cell lines and allows the adaptation to tumor samples.

In the present work, we have chosen genes that are frequently found on EEs due to c-Myc deregulation in the cells, such as *dihydrofolate reductase (DHFR), ribonucleotide reductase R2* and *cyclin D2* (Ref. 4-7). *Cyclin C* has been used as

negative control, since it appears to be genomically stable irrespective of c-Myc protein levels (Ref. 5). We have also included as a positive control, COLO320DM, which has constitutive c-Myc upregulation due to *c-myc* amplification on EEs (Ref. 8).

3.1.2. METHODS AND MATERIALS

3.1.2.1. Isolation of EEs. Our procedure is a modification of the protocol of Hirt (Ref. 1). Briefly; 1-5x10^7 cells are lysed in 0.6%SDS/0.01M EDTA (pH 7.5) for 20 minutes at room temperature. The lysate is then brought to a final concentration of 1M NaCl and left overnight at 4°C. The insoluble NaCl/SDS/chromatin fraction is pelleted by centrifugation at 17,000 rpm for 30 minutes at 4°C. The supernatant is the so-called Hirt extract and is collected. It contains the bulk of the EEs, but it may also contain contamination with small linear fragments of genomic DNA (Ref. 2) and apoptotic DNA fragments.

3.1.2.2. Fixation of EEs. The Hirt extract is mixed with an equal volume of freshly prepared methanol:acetic acid (3:1). This mixture can be stored at 4°C for months.

3.1.2.3. Dropping of EEs onto slides and their fixation. The following protocol allows the fixation of the EEs onto glass slides, and it guarantees that the EEs are well-spread, but contained within a small area. Briefly: 40 ml of fixed EEs (Hirt extract in fixative) are dropped onto precooled slides (20 seconds on dry ice), and the slides are immediately moved onto a slide warmer (37°C). When almost dry, the slides are dipped into 50%

acetic acid and then dried to completion on the slide warmer (37°C). The area onto which the EEs were dropped is marked with a diamond pen.

3.1.2.4. Analysis of the EEs sample under the fluorescent microscope. 4'6' diamidino-2-phenylindole (DAPI) (1mg/ml in PBS) is used to stain both the DNA in the EEs and any genomic DNA contaminants. Anti-bleach (Ref. 4,5) is added to preserve the fluorescence of the sample and as a mount for the cover slip. Under a 63x oil immersion objective and a UV filter, the sample is examined using a fluorescent microscope. DAPI-stained EEs are visible as distinct dots, while genomic DNA appears as DAPI-stained fibres (Fig. 3.1.1).

3.1.2.5. FISH analysis of EEs (FISH-EEs). FISH is carried out according to previously published protocols (Refs. 4,5,9). Briefly: the slides are treated with RNAse and pepsin as described for metaphase chromosomes and interphase cells. DNA probes are labeled with haptens by random priming as described, and hybridizations are performed in 50% formamide/2 x SSC/50 mM phosphate pH 7/10% dextran sulfate overnight at 37°C in a humidified incubator. Post-hybridization washes are carried out as follows: 3 x 5 minutes at 42°C in 50% formamide/2 x SSC; 5 x 2 minutes at room temperature in 2 x SSC. Prior to the use of antibodies, the slides are blocked in 100% serum. Anti-hapten antibodies, conjugated with fluorescein (FITC) or Texas Red (TXRD), are used to visualize the hapten-labeled probes. The antibody incubation is carried out for 30 minutes at 37°C. The unbound antibodies are washed off at 42°C in 4 x SSC/0.1% Tween 20 for 3 x 5 minutes. DAPI (1mg/ml in PBS, 5 minutes) is used to stain the DNA and the slides are mounted in anti-bleach. In the examples shown in Fig. 3.1.2, we have used the following

probes: human *c-myc* cDNA (Ref. 4,5), human *cyclin C* cDNA (Ref. 5), mouse *cyclin D2* genomic DNA (Ref. 7), mouse *ribonucleotide reductase R1* and *R2* (*R1* and *R2*) cDNA (Ref. 10), all of which were labeled with digoxigenin. After hybridization, the annealed probe is visualized by incubation with anti-digoxigenin-fluorescein antibody (Boehringer Mannheim). An additional probe, a mouse *dihydrofolate reductase* (*DHFR*) cDNA (Ref. 4,5), was labeled with biotin, detected with a monoclonal mouse anti-biotin antibody (Boehringer Mannheim), and visualized by goat anti-mouse-IgG-Texas Red (Southern Biotechnology, Ass., Inc.).

Table 3.1.1.

Table of Products Used

4-hydroxytamoxifen (4HT)	Research Biochemicals International
sheep anti-digoxigenin fluorescein	Boehringer Mannheim
monoclonal mouse anti-biotin antibody	Boehringer Mannheim
goat anti-mouse-IgG-Texas Red	Southern Biotechnology Ass., Inc.
DAPI	Sigma
microscope	Zeiss Axiophot
CCD camera	Photometrics
IPLab Spectrum (version 3.1)	Signal Analytics

References

1. Hirt, B. (1967) J. Mol. Biol. 26, 365-369.
2. Regev, A., Cohen, S., Cohen, E., Bar-Am, I. and Lavi, S. (1998) Oncogene 17, 3455-3461.
3. Gaubatz, J. W. and Flores, S. C. (1990) Analyt. Biochem. 184, 305-310.
4. Mai, S. (1994) Gene 148, 253-260.
5. Mai, S., Hanley-Hyde, J. and Fluri, M. (1996) Oncogene 12, 277-288.
6. Kuschak, T.I., Taylor, C., McMillan-Ward, E., Israels, S., Henderson, D.W., Mushinski, J.F., Wright, J.A. and Mai, S. (1999) Submitted.
7. Mai, S., Hanley-Hyde, J., Rainey, G. J., Kuschak, T.I., Taylor, C., Fluri, M., Stevens, L. M., Henderson, D. W. and J. F. Mushinski. (1999) Curr. Topics in Microbiol. Immunol. In press. 1999.
8. Quinn, L.A., Moore, G.E., Morgan, R.T. and Woods, L.K. (1979) Cancer Research 39, 4919-4924.
9. Fukasawa, K., Wiener, F., Vande Woude, G. and Mai, S. (1997) Oncogene 15, 1295-1302.
10. Thelander, L. and Berg, P. (1986) Mol. Cell. Biol. 6, 3433-3442.

Figures.

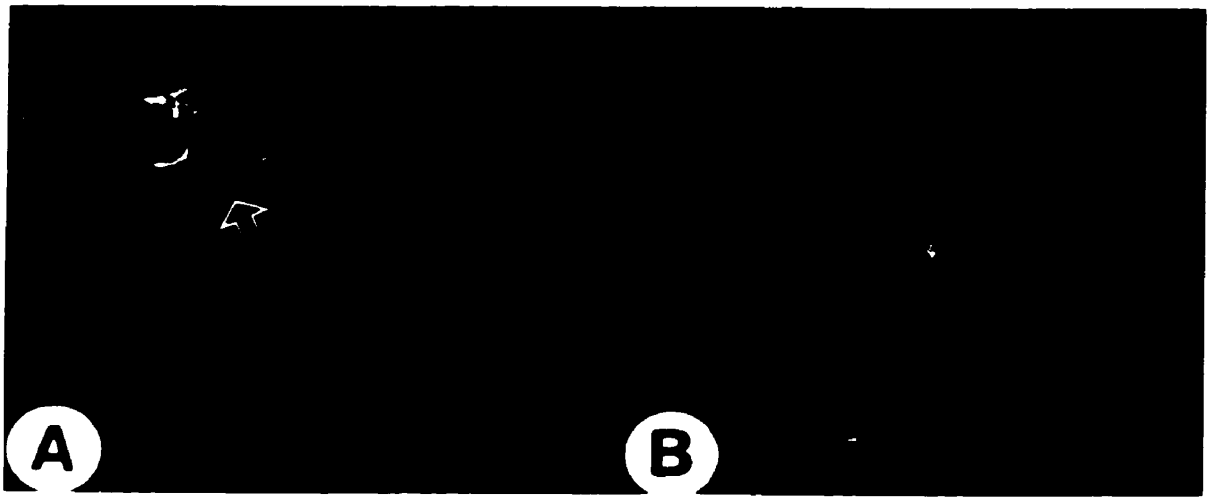

Fig. 3.1.1.

DAPI-stained extrachromosomal elements (EEs) were prepared as described above. Dots represent EEs that are present in both **Figs. 3.1.1.A** and **B**. The arrow in **Fig. 3.1.1.A** points to contaminating genomic DNA, which has a filamentous appearance. **Fig. 3.1.1.B** is a preparation of EEs that has no genomic contamination.

Fig. 3.1.2.

Panel A. EEs isolated from COLO320DM (9) and hybridized with *c-myc* **(B,C)** (4) or *cyclin C* **(E,F)** (5).

A: EEs isolated from COLO320DM and counterstained with DAPI.

B: Same EEs hybridized with digoxigenin-labeled *c-myc* and visualized with anti-digoxigenin-fluorescein antibody. *C-myc* signals appear green.

C: Overlay of **A** and **B**. Note that some green signals (small arrow) do not colocalize with DAPI signals in image **A**, due to: (i) *c-myc* antibody amplification of the hybridization signal seen in image **B**, (ii) different sizes of the EEs, (iii) different exposure times, and/or iv) background. **A** large arrow shows an example of colocalization of DAPI counterstain and *c-myc* hybridization signals. Colocalized signals considered to be authentic EEs that bear *c-myc* sequences, appear greenish-white.

D: EEs isolated from COLO320DM and counterstained with DAPI.

E: Same EEs hybridized with digoxigenin-labeled *cyclin C*, visualized with anti-digoxigenin-fluorescein antibody. *Cyclin C* signals would appear green if there was hybridization.

F: Overlay of D and E.

Figure 3.1.2.

Panel B. EEs isolated from 4HT-activated mouse pre-B cells and hybridized with *DHFR* (B,C), *cyclin D2* (E,F), *ribonucleotide reductase R1* (H,I), and *ribonucleotide reductase R2* (K,L).

A: EEs isolated from 4HT-activated preB cells and counterstained with DAPI.

B: Same EEs hybridized with biotin-labeled *DHFR*, visualized with anti-biotin antibody, followed by anti-mouse-IgG-Texas Red. *DHFR* signals therefore appear red.

C: Overlay of A and B. Note that some red signals (small arrow) do not colocalize with DAPI signals in image A, due to: (i) *DHFR* antibody amplification of the hybridization signal seen in image B, (ii) different sizes of the EEs and, (iii) different exposure times, and/or iv) background. A large arrow shows an example of colocalization of DAPI counterstain and *DHFR* hybridization signals. Colocalized signals appear pinkish.

D: EEs isolated from 4HT-activated mouse pre-B cells and counterstained with DAPI.

E: Same EEs hybridized with digoxigenin-labeled *cyclin D2*, visualized with anti-digoxigenin-fluorescein antibody. *Cyclin D2* signals therefore appear green.

F: Overlay of D and E. Note that some green signals (small arrow) do not colocalize with DAPI signals in image D, due to: (i) *cyclin D2* antibody amplification of the hybridization signal seen in image B, (ii) different sizes of the EEs and, (iii) different exposure times, and/or iv) background. A large arrow shows an example of colocalization of DAPI counterstain and *cyclin D2* hybridization signal. Colocalized signals appear greenish-white.

Figure3.1.2. Panel B Continued.

G: EEs isolated from 4HT-activated mouse pre-B cells and counterstained with DAPI.

H: Same EEs hybridized with digoxigenin-labeled *R1*, visualized with anti-digoxigenin-fluorescein antibody. *R1* signals therefore appear green.

I: Overlay of G and H. A large arrow shows an example of colocalization of DAPI counterstain and *R1* hybridization signal. Colocalized signals appear greenish-white.

J: EEs isolated from 4HT-activated mouse pre-B cells and counterstained with DAPI.

K: Same EEs hybridized with digoxigenin-labeled *R2*, visualized with anti-digoxigenin-fluorescein antibody. *R2* signals therefore appear green.

L: Overlay of J and K. Note that some green signals (small arrow) do not colocalize with DAPI signals in image J, due to: (i) *R2* antibody amplification of the hybridization signal seen in image B, (ii) different sizes of the EEs and, (iii) different exposure times, and/or iv) background. A large arrow shows an example of colocalization of DAPI counterstain and *R2* hybridization signal. Colocalized signals appear greenish-white.

Acknowledgements.

This work was supported by the Leukemia Research Fund of Canada.

Affiliations.

T.I.K., J.T.P., and S.M.: Manitoba Institute of Cell Biology, University of Manitoba, 100 Olivia Street, Winnipeg, MB R3E 0V9, Canada. J.A.W.: Manitoba Institute of Cell Biology, University of Manitoba, and GeneSense Technologies, Inc. Sunnybrook Health Sciences Centre, 2075 Bayview Avenue, Toronto, ON, Canada, M4N 3M5. J.F.M.: Laboratory of Genetics, NIH/NCI, Building 37, Room 2B26, Bethesda, Maryland 20892-4255, USA.

Preface

Chapter 3.2

Chapter 3.2 is the full paper format of a manuscript published in the journal *GENE*: Theodore I. Kuschak, Cheryl Taylor, Eileen McMillan-Ward, Sara Israels, Darren W. Henderson, J. Frederic Mushinski, Jim A. Wright, and Sabine Mai (1999). The *ribonucleotide reductase R2* gene is a non-transcribed target of c-Myc-induced genomic instability. *Gene* **238**: 351-365.

This paper was the first to demonstrate c-Myc dependent rearrangement as well as chromosomal and extrachromosomal amplification of the *ribonucleotide reductase R2* gene. More importantly, this paper was the first to define two classes of c-Myc amplification targets, namely one class wherein amplification results in overexpression of the gene product and a second class, wherein amplification of the gene has no effect on the expression levels of the gene product.

The *ribonucleotide reductase R2* gene is a non-transcribed target of c-Myc-induced genomic instability

Theodore I. Kuschak [1,2], Cheryl Taylor [1], Eileen McMillan-Ward [1,3], Sara Israels [1,3], Darren W. Henderson [4], J. Frederic Mushinski [4], Jim A. Wright [1,2,5,8], and Sabine Mai [1,6,7]

1. Manitoba Institute of Cell Biology and the Manitoba Cancer Treatment and Research Foundation, 100 Olivia St., Winnipeg, Manitoba, CANADA, R3E 0V9.

2. Department of Microbiology, University of Manitoba, Winnipeg, Manitoba, CANADA, R3T 2N2.

3. Department of Pediatrics, University of Manitoba, Winnipeg, Manitoba, CANADA, R3E 0V9.

4. Molecular Genetics Section, Laboratory of Genetics, National Institutes of Health National Cancer Institute, Bethesda, MD, 20892-4255, USA.

5. Department of Biochemistry and Molecular Biology, University of Manitoba, 730 William Avenue, Winnipeg, Manitoba, CANADA, R3E 0V9.

6. Department of Human Genetics, University of Manitoba, 770 Bannatyne William Avenue, Winnipeg, Manitoba, CANADA, R3E 0W3.

7. Department of Physiology, University of Manitoba, 730 William Avenue, Winnipeg, Manitoba, CANADA, R3E 0V9.

8. GeneSense Technologies, Inc. Sunnybrook Health Sciences Centre, 2075 Bayview Avenue, Toronto, Ontario, CANADA, M4N 3M5

*corresponding author:
Sabine Mai, Ph.D.
Manitoba Institute of Cell Biology and
The Manitoba Cancer Treatment and Research Foundation,
100 Olivia St., Winnipeg, Manitoba, CANADA, R3E 0V9
Phone: 204-787-2135
FAX: 204-787-2190
e-mail: smai@cc.umanitoba.ca

Abbreviations:

4-HT: 4-hydroxytamoxifen; bp: base pair(s); cDNA: DNA complementary to RNA; DABCO: diazabicyclo[2.2.2]-octane; DAPI: 4',6' diamidino-2-phenylindole; *DHFR*: gene encoding *dihydrofolate reductase* DTT: dithiothreitol; FITC: fluorescein isothiocyanate; EEs: Extrachromosomal Elements; EM: Electron Microscope; FISH: fluorescent *in situ* hybridization; *GAPDH:* gene encoding *glyceraldehyde-3-phosphate dehydrogenase*; *GSHPX:* gene encoding *glutathione peroxidase*; HEPES: N-2-Hydroxyethylpiperizine-N'-2-Ethane sulphonic acid; HU: hydroxyurea; IU: international unit(s); kDa: kilodalton(s); LTR: long terminal repeat; MOPS: (3-[N-Morpholino]propanesulphonic acid; NA_2EDTA: Ethylaminediaminetetraacetic acid, disodium salt; *ODC*: gene encoding *ornithine decarboxylase*; PBS: phosphate buffered saline (0.15 M NaCl, 1.4 mM NaH_2PO_4, 4.3 mM NaH_2PO_4, 0.015 M Na_3 citrate); *R2*: gene encoding *ribonucleotide reductase R2*; SCP: sodium citrate phosphate buffer; SDS: sodium dodecyl sulfate; Tween-20: Polyoxyethylenesorbitan; TXRD: Texas Red; SSC: standard sodium citrate (0.015 M sodium citrate, 0.15 M sodium chloride).

Key words:

ribonucleotide reductase R1, gene amplification, extrachromosomal elements, tumorigenesis, oncogenes

ABSTRACT

The c-Myc oncoprotein is highly expressed in malignant cells of many cell types, but the mechanism by which it contributes to the transformation process is not fully understood. Here, we show for the first time that constitutive or activated overexpression of the *c-myc* gene in cultured mouse B lymphocytes is followed by chromosomal and extrachromosomal amplification as well as rearrangement of the *ribonucleotide reductase R2* gene locus. Electron micrographs and fluorescent *in situ* hybridization (FISH) demonstrate the c-Myc-dependent generation of extrachromosomal elements, some of which contain *R2* sequences. However, unlike other genes that have been shown to be targets of c-Myc-dependent genomic instability, amplification of the *R2* gene is not associated with alterations in *R2* mRNA or protein expression. These data suggest that c-Myc dependent genomic instability involves a greater number of genes than previously anticipated, but not all of the genes that are amplified in this system are transcriptionally upregulated.

3.2.1. INTRODUCTION

Ribonucleotide reductase is a highly regulated, cell cycle-controlled enzyme that is essential for DNA synthesis and repair. It is the only enzyme responsible for the reduction of ribonucleotides to their corresponding deoxyribonucleotides. Under normal conditions, it provides the cell with a balanced supply of deoxyribonucleotide precursors essential for DNA synthesis and repair (Wright, 1989).

The active mammalian enzyme is composed of two dissimilar subunits, R1 and R2, which are encoded by different genes and are differentially regulated during the cell cycle. While levels of the R1 subunit do not vary during the cell cycle, there is an S-phase-correlated increase in the amount of R2 protein. The activity of ribonucleotide reductase and implicitly, DNA synthesis and cell proliferation, are controlled during the cell cycle by the synthesis and degradation of the R2 subunit (Wright, 1989). The R2 component, which is rate-limiting, is a phosphoprotein, and it is capable of being phosphorylated by the CDC2 and CDK2 protein kinase mediators of cell cycle progression (Chan *et al.*, 1993). Ribonucleotide reductase can, in addition, be regulated by an S-phase-independent mechanism that is important for DNA repair (Hurta and Wright, 1992).

Previous studies have reported that expression of ribonucleotide reductase, and the R2 subunit in particular, is increased in drug-resistant cells (Wright, 1989), and in cell lines that have been exposed to tumor promoters (Chen *et al.*, 1993) and growth-inhibiting factors such as transforming growth factor-β1(TGF-β1) (Hurta and Wright, 1995). Elevated levels of ribonucleotide reductase R2 protein have been described in some malignancies (Wright, 1989 and references therein). Fan *et al.* (1996) report that R2 is a novel "tumor progressor" that controls the malignant potential of tumor cells in oncogene-mediated mechanisms.

c-Myc is a multifunctional oncoprotein (for review, see Lüscher and Larsson, 1999). It is known to play pivotal roles in the cell cycle and in cell cycle progression (Heikkila *et al.*, 1987; Karn *et al.*, 1989), replication (Classon *et al.*, 1987) and development (Paria *et al.*, 1992). Furthermore, it is involved in transformation, neoplasia and tumor progression (for recent review, see Claassen and Hann, 1999 and references therein), and apoptosis (for review, see Prendergast, 1999 and references therein). The c-Myc protein expression is tightly regulated during normal cellular proliferation (Heikkila *et al.*, 1987; Karn *et al.*, 1989; Hanson *et al.*, 1994). c-Myc has been reported to be involved in the transcriptional regulation of specific cyclins, such as *cyclins E, A*, and *D1*, cyclin dependent kinases (cdks), the phosphatase *cdc25a* (for review, see Obaya *et al.*, 1999) as well as the telomerase reverse transcriptase (TERT) (Wu *et al.*, 1999). An increased half-life of c-Myc is associated with immortalization and transformation (see Claassen and Hann, 1999 and references therein). It has also been shown that elevated c-Myc levels disrupt proliferation control. Moreover, the deregulation and overexpression of the protein is frequent in murine and human tumors, where the *c-myc* gene is often found to be amplified, rearranged, and/or translocated (Yokota *et al.*, 1986)

The deregulation of c-Myc is emerging as an important component in promoting or enhancing genomic instability. c-Myc deregulation results in locus-specific gene amplification (Denis *et al.*, 1991; Mai, 1994; Mai *et al.*, 1996a, 1999) and karyotypic instability (Mai *et al.*, 1996b). Felsher and Bishop (1999) describe increases in genomic instability and tumorigenicity in Rat1A cells that transiently overexpress c-Myc.

The present study was initiated to address two points. First, we wished to resolve the question of whether c-Myc plays a role in the initiation of genomic instability of the *R2*

gene. Second, we wished to determine whether overexpression of c-Myc plays a role in the elevated expression of R2 protein found in some malignant cells. We demonstrate for the first time, that chromosomal and extrachromosomal amplification as well as rearrangements of the *R2* gene locus are associated with the overexpression of c-Myc. We then demonstrate that the amplification of the *R2* gene locus has no effect on *R2* mRNA or protein levels in any of the c-Myc-overexpressing cells tested. The instability of the *R2* gene is therefore associated with c-Myc dependent genomic instability, however in this experimental system, the *R2* gene appears to be a non-transcribed target of c-Myc deregulation.

3.2.2. METHODS AND MATERIALS

3.2.2.1. Fluorescent In Situ Hybridization (FISH)

Metaphase spreads and fluorescent *in situ* hybridizations were performed as described in Mai *et al.* (1996a). The *R2* probe used was a 1487-bp *Pst* I (Roche Diagnostics)-fragment of the mouse *R2* coding region (Thelander and Berg, 1986). Evaluation of metaphase spreads and interphase nuclei was performed using a Zeiss Axiophot microscope and a CCD camera (Photometrics). Image analysis was performed using IPLab Spectrum H-SU2 (Signal Analytics, USA) and Gene Join (Yale University, USA) on a Power Macintosh 8100 computer. 100-150 metaphases and interphases were evaluated in three independent experiments. Amplification was measured with IPLabSpectrum/Multiprobe (Signal Analytics, USA), using the line measurement function. B lymphoid cells (ABM Pre-B lymphocytes (Mai *et al.*, 1999), WEHI 231 cells and MOPC 460D cells (Mai *et al.*1996a)), were cultured in RPMI 1640 medium, supplemented with 10 % (v/v) fetal bovine serum, 1 % (v/v) sodium pyruvate, 50 IU mL^{-1} penicillin, 50 µg mL^{-1} streptomycin, and 5.5 x 10^{-5} M

β-mercaptoethanol, and 2mM glutamine. MOPC 460D cells were also supplemented with 100 μL of IL-6 hybridoma supernatant per 10 mL of culture medium, kindly provided by Dr. Karasuyama, (Basel Institute for Immunology, Switzerland). All cell lines were cultured in a humidified atmosphere with 5 % CO_2 at 37°C. All medium and supplemental ingredients were supplied by Gibco/BRL.

In this series of experiments, we used ABM cells, a Pre-B cell line in which c-Myc activity can be experimentally upregulated. This cell line was created as described in Mai *et al.* (1999). The ABM Pre-B cells were seeded and activated 24 hours after seeding with 100 μM 4-hydroxytamoxifen (4-HT) (Research Biochemicals International, Natick, MA) dissolved in 100 % ethanol. These 4-HT-activated cells were designated Pre-B+. The non-activated Pre-B cells, designated Pre-B-, received an equal volume of 100 % ethanol.

3.2.2.2. Southern Blotting and Dispersed Cell Assay Analyses of the R2 locus

Genomic DNA was prepared from cultured cells using the Easy DNA Kit (Invitrogen). 10 μg DNA samples were digested overnight with 40 units of one of the following (Roche Diagnostics) restriction endonucleases, *BamHI*, *EcoRI*, *EcoRV*, *Hin*dIII, and *Pst*I, electrophoretically separated and blotted onto Hybond XL membrane (Amersham Pharmacia Biotech). Following blotting, the membrane was baked at 80°C for 2 hours. The membrane was hybridized at 42°C in 10 mL of hybridization solution (6.6x SCP: sodium citrate phosphate buffer: 0.66 M NaCl, 0.2 Na_2HPO4, 6.6 mM Na_2EDTA)/ 0.4 % (v/v) N-lauroyl sarcosine/ 200 μgmL^{-1} denatured herring sperm DNA/ 4x Denhardt's Solution /50 % (v/v) formamide) and random primer labeled probes (described below). Membranes were washed once for 15 minutes at 65°C in 6.6x SCP/1.0 % N-lauroyl sarcosine (v/v) and once for 90 at 65°C in 1.0x/1.0 % N-lauroyl (v/v) sarcosine. Membranes were exposed to

Hyperfilm™ MP high performance autoradiographic film (Amersham Pharmacia Biotech) at -75°C. (All reagents for Denhardt's and wash solutions were purchased from Sigma).

Dispersed Cell Assays (Lavi, 1981) were performed with slight modifications (Mai, 1994). This experiment was carried out 4 times. Each trial of this experiment was performed with 5 filter discs for each cell type tested. Proteinase K and RNaseA were purchased from Roche Diagnostics. Membranes were exposed to Hyperfilm™ MP high performance autoradiographic film (Amersham Pharmacia Biotech) at -75°C. Nitrocellulose filters used for DCA assays were manufactured by Protran. The gene for the *R2* subunit was probed with the 1487 bp *Pst*I (Roche Diagnostics) fragment of the *R2* coding region. Accuracy of loading for Southern blot analysis and Dispersed Cell Assays was confirmed by probing the discs for *glutathione peroxidase* (*GSHPX*) (kindly provided by Dr. Aiping Young) using a *Pst*I-digested 700 bp fragment. 50 ng of each probe was random primer-labeled with ^{32}P-α-dCTP (Amersham Pharmacia Biotech) to specific activity of 1-2 x10^9 dpm μg^{-1} using an Oligolabelling Kit (Amersham Pharmacia Biotech). Densitometric analysis was performed on a phosphorimager (Molecular Dynamics).

3.2.2.3. Electron Micrography and FISH on Extrachromosomal Elements

Extrachromosomal DNA isolated by the Hirt method (Hirt, 1967) was diluted to a concentration of approximately 1 μgmL^{-1} in 20 mM $MgCl_2$/30 mM triethanolamine buffer. Aliquots of these DNA samples were then placed on formvar/carbon coated grids, fixed with 0.1 % gluteraldehyde in White's saline (Israels and Gerrard, 1996) and negatively stained with 3 % uranyl acetate. Grids were allowed to air dry and then shadowed with tungsten to enhance resolution (Grey, 1994). All grids were examined in a

Philips Model 420 transmission electron microscope at 80 kV.

3.2.2.4. Northern Blot Analyses

Poly (A)+ mRNA was extracted from cultured cells using oligo-(dT) cellulose (Sigma). One µg samples of the RNA were loaded onto a denaturing gel (1 % agarose, 2.2 M formaldehyde) and blotted onto Hybond N^+ membrane (Amersham Pharmacia Biotech), and baked at 80°C for 2 hours. The membrane was hybridized at 65°C in 40 mM phosphate buffer/ 7 % SDS (Sodium Dodecyl Sulphate) (w/v)/ 1 mM Na_2EDTA solution with random primer labeled probes (described below). The membrane was washed in 40 mM phosphate/1mM Na_2EDTA/5.0 % (w/v) SDS buffer for 15 minutes at 65°C followed by a 15-minute wash at 65°C in 40 mM phosphate/1mM Na_2EDTA/1.0 % (w/v) SDS buffer. The membrane was exposed to Hyperfilm™ MP high performance autoradiographic film (Amersham Pharmacia Biotech) at -75°C for image acquisition. The gene for *R2* subunit was probed as previously described. The *c-myc* gene was probed using a 460 bp *Pst*I fragment of mouse exon II (kindly provided by Dr. Konrad Huppi, NIH). Equal loading for northern blot analysis was confirmed by probing for *GAPDH* using a 1.3 kb *Pst*I fragment (kindly provided by Dr. Aiping Young). *Pst*I was purchased from Roche Diagnostics. 50 ng of each radioactively labeled probe was prepared as described in Figure 2.

3.2.2.5. Western Blot Analysis

Whole cell protein extracts were prepared from Pre-B+ cells. Logarithmically growing cells were washed twice with ice-cold PBS, resuspended (100 µL/10^6 cells), in Protein Extract Buffer [(10 mM HEPES, pH 7.9, 60 mM KCl, 1 mM Na_2EDTA, 1mM DTT, 1mM AEBSF (Pefabloc®SC) (Roche Diagnostics)], and subjected to three 15-minute cycles of freezing (95 % ethanol/dry ice) and thawing (37°C water bath). Following

centrifugation (5 minutes/ 13,000 rpm/ 4°C) to remove cell debris, the extracts were aliquoted, frozen at -20°C, and concentrations were measured. The proteins were analyzed on an 8 % (v/v) SDS-PAGE with 100 µg of whole cell protein extract loaded per lane. Protein was transferred to Hybond-C Super (Amersham Pharmacia Biotech) using a BIORAD semi-dry transfer apparatus. For detection of R2 protein, the rabbit polyclonal anti-R2 antibody was used diluted 1:400 units in 0.3 % (v/v) Tween-20 (polyoxyethylenesorbitan) in PBS. This anti-R2 antibody was generated by injection of the whole recombinant R2 protein into a New Zealand rabbit (Chan *et al.*, 1993 and references therein). Measurement of loading accuracy was performed by immunostaining of the blot with anti-Max 256 antibody (generously provided by Dr. Achim Wenzel, Heidelberg) diluted to 200 $pg\mu L^{-1}$. Secondary antibody chemiluminescence reactions for western analysis were performed using an ECL™ kit (Amersham Pharmacia Biotech) according to instructions and visualized on Hyperfilm™ ECL™ high performance chemiluminescence film. Exposures to film for both R2 and Max were 60 seconds.

3.2.2.6. Quantitative Fluorescent Immunohistochemical Analysis

Prior to immunohistochemical staining and analysis, cells were cytospun onto microscope slides at a density of 10^5 per slide. Slides were stained with appropriate antibodies as follows: Cells were fixed on the slides in a solution of 3.7 % deionized formaldehyde in PBS containing 50 mM $MgCl_2$ for 10 minutes, followed by three washes in PBS + 50 mM $MgCl_2$. The cells were permeabilized in 0.2 % (v/v) Triton X-100 (Sigma) for 12 minutes. Following three washes in PBS + 50 mM $MgCl_2$, the slides were blocked for 5 minutes in fetal bovine serum (Gibco/BRL) and then stained with primary antibodies for 45 minutes. Following three washes in PBS + 50 mM $MgCl_2$, the slides were again blocked

for 5 minutes in serum and then incubated in the dark for 30 minutes with the appropriate secondary fluorescent-conjugated antibodies. Following three washes in PBS + 50 mM $MgCl_2$, slides were stained with 4', 6' diamidino-2-phenylindole (DAPI, 1 µg/ml) and fixed in antibleach (12 % glycerol, 4.8 % Mowiol 4-88 (Hoechst), 2.4 % 1,4 diazabicyclo[2.2.2]-octane (DABCO) (Fluka), in 0.2 M Tris/ HCl, pH = 8.5). Stained cells were stored in the dark at 4°C. 94 -164 cells were measured for fluorescence intensity for each set of cells stained. The antibody used for immunohistochemical analysis of R2 protein expression was as described in western blot analysis. Immunohistochemical analysis of c-Myc expression was measured using an anti-c-Myc antibody, 3C7 (1 $pg\mu L^{-1}$) (kindly provided by Dr. Achim Wenzel, Heidelberg)

3.2.3. RESULTS AND DISCUSSION

3.2.3.1. c-Myc deregulation affects R2 genomic stability

To test whether c-Myc played a role in *R2* genomic (in)stability, we studied two established mouse B lymphocytic cell lines, WEHI 231 and MOPC 460D, and a Pre-B cell line (Table 3.2.1., Figure 3.2.1.), under conditions of normal c-Myc expression and activated or constitutive c-Myc overexpression. In those cells we determined *R2* gene copy numbers in both interphases and metaphases by fluorescent *in situ* hybridization (FISH) (Mai, 1994; Mai *et al.*, 1996a).

We first compared two cells lines that express different levels of the c-Myc protein: WEHI 231, a low c-Myc expressing mouse B lymphoblastoid tumor, and MOPC 460D, a mouse plasmacytoma that constitutively overexpresses the c-Myc oncoprotein (Mai *et al.*, 1996a). There was no evidence of instability in the active *R2* gene when examined WEHI

231 cells by FISH (Figure 3.2.3.1. (a)). Figure 3.2.3.1. (a) indicates a single green fluorescent hybridization *R2* signal (which appears light blue or white when overlaid with the 4',6' diamidino-2-phenylindole- (DAPI) counterstained DNA image) on the active *R2* locus in WEHI 231 cells, indicating no alteration of the locus. The arrow indicates the location of the single, endogenous *R2* locus and it shows that none of the three *R2* pseudogenes are able to hybridize with the *R2* cDNA FISH probe (Thelander and Berg, 1986). On the other hand, the *R2* gene was amplified and rearranged in MOPC 460D. The fluorescent probe can been seen hybridizing to at least 16 spots on the chromosomes as well as extrachromosomal elements in these high c-Myc expressing cells (Figure 3.2.3.1. (b and c)). Since there was no hybridization of the *R2* pseudogenes in the WEHI 231 cells, it is likely that the *R2* signals in the MOPC 460D cells represent chromosomally amplified sequences derived from the active *R2* gene locus as well as extrachromosomally amplified *R2*, but not pseudogenes. The chromosomal and extrachromosomal *R2* gene amplification was seen in all of the 100 individual cells examined with IPLab Spectrum software.

To determine whether the above findings of the amplified *R2* gene locus were the direct result of c-Myc overexpression, we examined the *R2* gene in Pre-B- and Pre-B+ cells. In this cell line we detected evidence of c-Myc-dependent genomic instability of the *R2* gene within 72 hours of Myc-ER^{TM} activation. Figure 3.2.3.1. (d-f) comprises images representative of the majority of the cells at the 72 hour time point. FISH analyses for Pre-B- cells (Figure 3.2.1. (d)) showed a single green fluorescent *R2* hybridization signal (appears white after overlay), indicating unaltered copies of the *R2* locus. Based on the control hybridization (Figure 3.2.1. (c)) that shows only a single signal and not the other three *R2* pseudogenes on chromosomes 4, 7, and 13, it is unlikely that the *R2* probe is

able to detect pseudogenes in either the Pre-B- or Pre-B+ cells in the FISH experiments. The Pre-B+ cells (Figure 3.2.1. (e-f)) show amplification of the *R2* gene as indicated by the increased number of green (appearing as white) fluorescent signals of the probe. The additional FISH signals suggest both chromosomal and extrachromosomal sites of amplification. Figure 3.2.1. (f) shows metaphase chromosomes in which fluorescent signals in the Pre-B+ cells appear to be primarily chromosomal. Amplification is also extrachromosomal, as shown in Figure 3.2.3. Panel B (a) and (b), which shows fluorescent green *R2* hybridization signals (appearing white when overlayed) co-localizing on DAPI-stained (blue) extrachromosomal elements (EEs). We examined 100 interphase and metaphase spreads from Pre-B- and Pre-B+ cells. We found no *R2* gene amplification in the Pre-B- cells, but found chromosomal and extrachromosomal amplification of the *R2* locus in all 100 of the Pre-B+ cells examined. Rearrangements of the *R2* locus were also detected by FISH analysis (Figure 3.2.1. (f)), indicating c-Myc-dependent rearrangement of the *R2* gene locus. FISH analysis shows an increase in copy number of the *R2* locus in cells that overexpress c-Myc as compared with cells where c-Myc is not deregulated. The latter consistently show a single endogenous copy of the *R2* gene, while the former show multiple chromosomal or extrachromosomal copies of the *R2* locus.

3.2.3.2. Southern and DCA analyses confirm FISH R2 amplification data

We performed Southern blot analysis as an additional assay to assess c-Myc dependent (in)stability of *R2* (Fig 3.2.2. (a-d)). All cell lines shown in Table 3.2.1. were analyzed by digestion with five restriction endonucleases and probed first with *R2* and then, following stripping of the membrane, with *glutathione peroxidase (GSHPX).* Figure 3.2.2. (a) is a hybridization of the blot of the low and high c-Myc expressing cell lines, WEHI 231

and MOPC 460D. The hybridization revealed darker *R2*-hybridizing bands in virtually every lane of the MOPC 460D samples, depicting the amplification of the *R2* locus. The *GSHPX* hybridization indicated bands of virtually the same intensity in the DNA from the two tumors (Figure 3.2.2. (b)). Furthermore, comparison of WEHI 231 and MOPC 460D genomic DNA, digested with *EcoR*V and hybridized with *R2* shows a band, marked by the open arrow (Figure 3.2.2. (a)), which is present in the MOPC 460D DNA, but not in the low c-Myc-expressing WEHI 231 cell DNA. This open arrow indicates rearrangement of the *R2* locus in the high c-Myc expressing cells. Fig 3.2.2. (c) and (d) depicts a similar comparison of Pre-B cells without 4-HT activation of Myc-ER^{TM} with Pre-B cells after three days of 4-HT Myc-ER^{TM} activation. The *GSHPX* control hybridization showed bands of virtually the same intensity in the DNA from the two groups of cells (Figure 3.2.2. (d)). This experiment revealed increases in the *R2* signal in the Myc-activated cells. In addition, comparison of Pre-B- and Pre-B+ *R2* hybridization signals also demonstrated rearrangement of the *R2* locus in the later (Figure 3.2.2. (c)). Comparisons of *Eco*RI- and *Hin*dIII-digested genomic DNA from Pre-B- and Pre-B+ cells shows an extra *R2* hybridizing band in the Pre-B+ cells (Figure 3.2.2. (c)). Thus, results of the Southern blotting experiments confirm the amplification and the rearrangements detected by FISH analysis. Overexpression of c-Myc either through constitutive or activated overexpression results in the amplification and rearrangement of the *R2* gene locus.

Although, the Southern blot technique is effective in detecting gene rearrangements and chromosomal amplifications, it is usually inadequate for detection of extrachromosomal elements (Hahn, 1993). We wished to confirm the genomic instability of the *R2* locus found during FISH analysis by using the Dispersed Cell Assay (DCA) (Lavi, 1981). This method

involves probing the DNA of cells lysed directly on a nitrocellulose membrane. In this way, all genetic material, whether chromosomal or extrachromosomal, is studied simultaneously. Our DCA data confirmed that the *R2* gene is amplified in MOPC 460D, that constitutively overexpress c-Myc, and in the Pre-B+ cells, but not in WEHI 231 or the Pre-B- cells which express low levels of c-Myc protein (data not shown).

3.2.3.3. Isolation and FISH Analysis of Extrachromosomal DNA

To assess by an additional approach whether the *R2* amplification identified by FISH and DCA analyses in the c-Myc overexpressing B lymphoid cells involved the generation of *R2*-bearing EEs, we isolated extrachromosomal DNA from each of the cell types described above, using the method described by Hirt (Hirt, 1967). To ensure that the DNA in this Hirt-extracted suspension was not contaminated with genomic DNA, all samples were scanned by electron microscopy (EM) and photographed. The electron micrography (Figure 3.2.3. Panel A (a-d)) showed circular DNA with <1 % contamination by linear strands of genomic DNA in each sample (not shown). EEs derived from c-Myc overexpressing cells were circular and markedly larger than the circular DNA molecules found in low c-Myc expressing cells. WEHI 231-derived extrachromosomal DNA ranged in size from 0.03 to 0.05 μm, while the MOPC 460D-derived extrachromosomal DNA circles were 0.05 to 0.15 μm in diameter. Similarly, Pre-B- EEs ranged in size from 0.03 to 0.07 μm, while Pre-B+ EEs ranged in size from 0.07 to 0.22 μm in diameter or larger. In addition, extrachromosomal DNA from c-Myc overexpressors showed what appear to be DNA replication bubbles (shown by the black arrow) (Figure 3 Panel A (d)).

We then performed FISH analysis on the EEs (FISH-EEs) extracted from Pre-B+ cells (Kuschak *et al.*, 1999) (Figure 3.2.3. Panel B (a) and (b)). This method was developed

because it offers several advantages over more conventional methods such as Southern blotting, and over standard FISH procedures. FISH-EEs allows for the isolation and analysis of the total heterogenous population of EEs present in cell preparations and it enables one to examine cells for extrachromosomal genes.

EEs from Pre-B+ cells harvested 72 hours after 4-HT activation, were hybridized with an *R2* probe. The digoxigenin-labeled *R2* probe colocalized on a small number of individual DAPI-stained extrachromosomal DNA molecules (Figure 3.2.3. Panel B (a) and (b)), indicating that there are a large number of EEs generated in the Pre-B+ cells, but only a small percentage of the DAPI-stained EEs in the sample hybridized with the *R2* probe. These data suggest that the *R2* gene is only one of many targets of c-Myc-dependent genomic instability.

3.2.3.4. c-Myc deregulation has no effect on R2 mRNA levels

To examine the effect of c-Myc overexpression on *R2* mRNA expression, we performed northern blot analysis on Poly (A)+ mRNA extracted from low c-Myc expressing WEHI 231 cells and constitutive c-Myc expressing MOPC 460D cells, 24 hours after seeding. *R2* mRNA levels were 4.7-fold higher in WEHI 231 than in MOPC 460D cells at 24 hours after seeding (data not shown). This was surprising in that MOPC 460D cells showed an increase in *R2* gene copy number by FISH, DCA, and Southern analyses.

Examination of the *R2* message in Pre-B- and Pre-B+ cells was performed at two different time frames after Myc-ER^{TM} activation with 4-HT. (Figure 3.2.4. (a) and (b)). We performed the early time frame northern analysis at 3, 6, and 9 hours after activation to determine whether *R2* was a transcriptional target affected immediately following c-Myc deregulation. 4-HT-activated Pre-B cells displayed no changes in *c-myc* mRNA

transcription levels (Figure 3.2.4. (a)) as is expected, indicating that 4-HT does not affect transcription levels of *c-myc* mRNA. Rather, activation of the Myc-ER™ construct is reflected in its translocation to the nucleus. Immunohistochemical analysis of these cells following 4-HT addition to the culture indicated a transient maximum translocation of the Myc-ER™ to the nucleus 2-4 hours following activation, followed by a steady decrease to pre-activation levels (data not shown). Activation of Myc-ER™ was followed by insignificant changes in steady-state levels of *R2* mRNA (Figure 3.2.4. (a)), indicating that *R2* is not an immediate target of c-Myc transactivation.

We then examined whether 72 hours of 4-HT activation of c-Myc-ER™ in Pre-B+ cells affects levels of *R2* mRNA (Figure 3.2.4 .(b)). The 72 hour time point was the peak of *R2* instability, but *R2* mRNA levels of Pre-B+ cells remained unchanged (Figure 3.2.4. (b)). This indicates that there was also no long-term or post-amplification effect of Myc-ER™ activation on transcription of *R2*. While *R2* gene amplification did occur following c-Myc overexpression, neither the *R2*-containing EEs, nor the chromosomally amplified and rearranged *R2* gene locus is able to increase the levels of *R2* message. No significant changes were detected by densitometric analysis (not shown) since changes that are not at least 2-fold higher or lower than the respective control samples were not regarded as relevant.

There are at least two possibilities that may explain this phenomenon and these are part of ongoing studies. For example, it is possible that transcription of *R2* mRNA from the extrachromosomal DNA circles is abrogated by inappropriate *R2* amplicon structure because of the loss of key sequences required for the initiation of transcription. Only those that are functionally "complete" may be expressed. Second, one might assume that there are

other targets of c-Myc dependent amplification in the vicinity of the *R2* gene. In mice, the active *ornithine decarboxylase* (*ODC*) gene also lies on 6.00 cM of chromosome 12, while the active *R2* gene is found one Morgan away (Mouse Genome Database, <http://www.informatics.jax.org/>, June, 1999). *R2* and *ODC* are part of the same amplification unit, mapped to the same region (p24----p25) of chromosome 2 in humans (Yang-Feng *et al.*, 1987). Mouse and human *R2* and *ODC* genes display coamplification following drug selection experiments. Selection of R2-overexpressing cells often results in the amplification of *ODC* (Yang-Feng *et al.*, 1987) while selection for ODC overexpressors leads to the amplification and in some cases, the overexpression of the R2 subunit (Ask *et al.*, 1993). The examples above are drug-mediated. However, one cannot rule out the possibility that the same coamplification phenomenon may occur following c-Myc deregulation. Both the *R2* gene (Kuschak, unpublished data) and the *ODC* gene (Bello-Fernandez *et al.*, 1993) contain Myc/Max-binding E-box motifs, as do other targets of c-Myc in genomic instability, such as *DHFR* (Mai and Jalava, 1994; Mai *et al.*, 1996a) and *cyclin D2* (Mai *et al.*, 1999). ODC may confer a growth advantage (Polvinen *et al.*, 1988) and has been shown to transform cells (Tabib and Bachrach, 1998).

3.2.3.5. c-Myc deregulation has no effect on R2 protein levels.

This study has shown that there are no changes in *R2* mRNA levels, either due to c-Myc transactivation, or due to c-Myc-dependent amplification of the *R2* gene. In order to examine whether R2 protein levels were affected by c-Myc overexpression, we performed western blot analysis (Figure 3.2.5.) and measured R2 protein levels in Pre-B+ cells at the same time points as were studied by northern blotting. Accuracy of protein loading was determined by staining with anti-Max 256. No changes were observed in R2 protein levels

in the 9 hours following activation of c-Myc overexpression.

We also performed immunohistochemical analysis with the WEHI231 and MOPC460D cells 24 hours after seeding as well as with Pre-B- and Pre-B+ cells. This is a more sensitive method since it is analyzed on the level of individual cells. In these experiments we used quantitative fluorescent immunohistochemical analysis coupled with fluorescence intensity line measurements which allowed us to quantify expression levels and to differentiate between individual cells that might be expressing different amounts of R2 protein.

When analyzing 100 WEHI 231 and 100 MOPC 460D cells, we observed low levels of c-Myc protein in WEHI 231cells (Figure 3.2.6. Panel A (a) and Figure 3.2.7. (a)), in agreement with previous work (Mai *et al.*, 1996a), while 88.6 % of MOPC 460D cells (Figure 3.2.6. Panel A (b) and Figure 3.2.7. (a)) displayed c-Myc protein levels that were 2- to 6-fold higher than those observed in WEHI 231. We also measured the R2 protein levels in WEHI 231 and MOPC 460D using immunohistochemical staining and immunofluorescent line measurements. R2 protein levels in both WEHI 231 and MOPC 460D were the same 24 hours after seeding (Figure 3.2.6. Panel A (c) and (d)); Figure 3.2.7. (b)). This data conflicts with our expectations of higher R2 protein levels in WEHI 231, which showed roughly 5-fold higher levels of *R2* message in WEHI 231. The reasons for this difference are unknown.

We performed long-term R2 protein experiments (72 hours after Myc-ER^{TM} activation) in Pre-B cells in order to determine the levels of R2 protein following amplification of the *R2* locus. The Pre-B line exhibits transient c-Myc activation (and upregulation) 72 hours after stimulation with 4-HT (Figure 3.2.7. (c)). While Myc-ER^{TM}

activation levels are not as high at 72 hours as they are 3 to 4 hours after activation, they appear to be slightly higher than c-Myc levels found in Pre-B- cells. This finding is not surprising due to the continual production of the Myc-ER^{TM} construct by the cells and residual 4-HT levels remaining in the medium. Using quantitative fluorescent immunohistochemistry and fluorescent intensity measurements, we evaluated 100 Pre-B- and 100 Pre-B+ cells using IPLab Spectrum software. We measured c-Myc expression levels in Pre-B- cells (Figure 3.2.6. Panel B (a); Figure 3.2.7. (c)) and Pre-B+ cells (Figure 3.2.6. Panel B (b); Figure 3.2.7. (c)). A portion of the Pre-B+ cell population measured showed c-Myc levels that were higher than those observed in Pre-B- cells (Figure 3.2.6. Panel B (b); Figure 3.2.7. (c)). R2 protein levels were not significantly altered in any of the cells overexpressing c-Myc compared with their respective controls (Figure 3.2.6. Panel B (c) and (d); Figure 3.2.7. (d)).

As previously noted, elevated levels of the ribonucleotide reductase R2 enzyme have been described in some malignancies (Wright, 1989 and references therein). Furthermore, previous work has suggested that R2 is a "malignancy determinant" in mechanisms of tumor progression. Fan *et al.* (1996) suggest that deregulation of *R2* leads to the activation of the Raf/Ras/MAPK signaling pathway, which affect downstream targets, such as the *c-myc*. Furthermore, based on growth of R2/Myc clones in soft agar and tumor growth in syngeneic mice, Fan *et al.* (1998) reported that R2 overexpression and c-Myc deregulation cooperate in the cellular transformation process.

Our work focused on the immediate effects of transient overexpression of the c-Myc oncoprotein on the *R2* locus. It centered on the consequence of a single (regulatable) change (c-Myc overexpression in the cell) within the context of its direct effects on the *R2* gene.

This study allowed us to examine two questions, the effects of c-Myc overexpression on *R2* gene amplification and rearrangements, and the effect of c-Myc overexpression on mRNA and protein levels of cells, prior to and following amplification of the *R2* gene in cultured B lymphoid cells.

Based on our data, we conclude that initiation of c-Myc-dependent genomic instability involves the *R2* gene by affecting only its gene copy number. There is no evidence in this study to indicate that c-Myc protein deregulation is directly involved in deregulation of *R2* gene expression. *R2* is only one of a number of identified targets of c-Myc-dependent genomic instability. *DHFR* (Mai *et al.*, 1996a) and *cyclin D2* (Mai *et al.*, 1999) are known targets of c-Myc-dependent genomic instability, but there are likely to be other, as yet unidentified genes, whose stability is affected by c-Myc deregulation. Selective pressure may allow for the maintenance of specific genes with a role in the generation of the transformed phenotype. We conclude that initiation of genomic instability and cellular transformation are distinct events.

Conclusions

(a) In this study, we have shown that tumor cells that constitutively overexpress c-Myc exhibit chromosomal and extrachromosomal amplifications as well as rearrangement of the active *ribonucleotide reductase R2* (*R2*) gene. In contrast, there was no evidence of genomic alterations of the *R2* gene in low c-Myc expressing cells.

(b) To examine whether the instability of the *R2* gene was a c-Myc dependent event or the result of general genomic instability, we analyzed cells in which c-Myc expression could be experimentally regulated. Activation of the Myc-ER^{TM} construct

in a mouse Pre-B cell line (AMB-Pre-B), was followed by chromosomal and extrachromosomal amplification as well as rearrangement of the *R2* gene, demonstrating c-Myc-dependent instability of the *R2* gene locus.

(c) c-Myc-induced instability of the *R2* gene locus was not associated with transcriptional alteration of *R2*. Both *R2* mRNA and protein levels were unaltered irrespective of c-Myc protein levels.

(d) *R2* is the first non-transcribed target of c-Myc-dependent genomic instability to be described. This finding is of general importance for our understanding of the mechanisms of c-Myc-induced instability and neoplasia. c-Myc-dependent genomic instability appears to involve two classes of genes: genes which remain functionally unaltered, such as *R2*, and genes whose overexpression follows their amplification *i.e. DHFR* (Lücke-Huhle *et al.*, 1997) and *cyclin D2* (Mai *et al.*, 1999). Thus, c-Myc operates on a pool of functionally distinct target genes. Potential changes in the expression of such genes and selective pressure will determine their role in cellular proliferation, mutagenesis, or survival during the multi-step process of transformation.

REFERENCES

Ask, A., Persson, L., Rehnholm, A., Frostesjo, L., Holm, I., and Heby, O., 1993. Development of resistance to hydroxyurea during treatment of human myelogenous leukemia K562 cells with α-difluoromethylornithine as a result of coamplification of genes for ornithine decarboxylase and ribonucleotide reductase R2 subunit. Cancer Res. 53, 5262-5268.

Bello-Fernandez, C., Packham, G., Cleveland, J.L., 1993. The ornithine decarboxylase gene is a transcriptional target of c-Myc. Proc. Natl. Acad. Sci. USA 90, 7804-7808.

Chan, A.K., Litchfield, D.W., and Wright, J.A., 1993. Phosphorylation of ribonucleotide reductase R2 protein: in vivo and in vitro evidence of a role for p34cdc2 and CDK2 protein kinases. Biochemstry 32, 12835-12840.

Chen, F.Y., Amara, F.M., and Wright, J.A., 1993. Mammalian ribonucleotide reductase R1 mRNA stability under normal and phorbol ester stimulating conditions: involvement of a cis-trans interaction at the 3' untranslated region. EMBO J. 12, 3977-3986.

Claassen, G.F. and Hann, S.R., 1999. Myc-mediated transformation: the repression connection. Oncogene 18, 2925-2933.

Classon, M., Henrikson, M., Klein, G., and Hammaskjold M-L., 1987. Elevated c-myc expression facilitates the replication of SV40 DNA in human lymphoma cells. Nature 330, 272-274.

Denis, N., Kitzis, A., Kruh, J., Dautry, F., and Crocos, D., 1991. Stimulation of methotrexate resistance in dihydrofolate reductase gene amplification by c-myc. Oncogene 6, 1453-1457.

Fan, H., Villegas, C., and Wright, J.A., 1996. Ribonucleotide reductase R2 component is a novel malignancy determinant that cooperates with activated oncogenes to determine transformation and malignant potential. Proc. Natl. Acad. Sci. USA 93, 14036-14040.

Fan, H., Villegas, C., Young A, and Wright, J.A., 1998. The mammalian ribonucleotide reductase R2 component cooperates with a variety of oncogenes in mechanisms of cellular transformation. Cancer Res. 58, 1650-1653.

Felsher, D.W. and Bishop, J.M., 1999. Transient excess of MYC activity can elicit genomic instability and tumorigenesis. Proc. Natl. Acad. Sci. USA. 96, 3940-3944.

Grey, C.W., 1994. Electron Microscopy of Protein-Nucleic Acid Complexes. Enhanced High Resolution Shadowing. In: Methods in Molecular Biology. Vol. 22 Microscopy, Optical Spectroscopy, and Macroscopic Techniques. Jones C., and Thomas A.H. (Eds.) Humana Press Inc., Totowa, N.J., Haase, S.B., Heinzel, S.S., and Calos, M.P.

Hahn, P.J., 1993. Molecular biology of double-minute chromosomes. Bio Essays 15, 477-484.

Hanson, K.D., Shichiri, M., Follansbee, M.R., and Sedevy, J.M., 1994. Effects of c-myc expression on cell cycle progression. Mol. Cell. Biol. 14, 5748-5755.

Heikkila, R., Schwab, G., Wickstrom, E., Loke, S.L., Pluznik, D.H., Watt, R., and Neckers, L.M., 1987. A c-myc antisense oligodeoxynucleotide inhibits entry into S phase but not progress from Go to G1. Nature 328, 445-449.

Hirt, B., 1967. Selective Extraction of Polyoma DNA from Infected Mouse Cell Cultures. J. Mol. Biol. 26, 365-369.

Hurta, R.A.R., and Wright, J.A., 1992. Alterations in the activity and regulation of

mammalian ribonucleotide reductase by chlorambucil, a DNA damaging agent. J. Biol. Chem. 267, 7066-7071.

Hurta, R.A.R., and Wright, J.A. 1995. Malignant transformation by H-ras results in aberrant regulation of ribonucleotide reductase gene expression by transforming growth factor-β1. J. Cell. Biochem. 57, 543-556.

Israels, S.J. and Gerrard, J.M., 1996. Immunohistochemical and Electron Microscopic Studies of Platelets. *Platelets: A Practical Approach.* (Eds. Watson, S.P. & and Authi, K.S.) IRL Press at Oxford University Press.

Karn, J., Watson, W., Lowe, A.D., Green, S.M., and Vedeckis, W., 1989. Regulation of cell cycle duration by c-myc levels. Oncogene 4, 773-787.

Kuschak, T.I., Paul, J.T., Mushinski, J.F., Wright, J.A., and Mai, S., 1999. FISH on purified extrachromosomal DNA molecules. Technical Tips Online, <http://www.biomednet.com/db/tto> t01669.

Lavi, S., 1981. Carcinogen-mediated amplification of viral DNA sequences in Simian virus 40-transformed Chinese hamster embryo cells. Proc. Natl. Acad. Sci. USA. 78, 6144-6148.

Lücke-Huhle, C., Mai, S. and Moll, J., 1997. c-Myc overexpression facilitates radiation-induced DHFR gene amplification. Int. J. Radiat. Biol., 71, 167-175.

Lüscher, B. and Larsson, L-G., 1999. The basic region/helix-loop-helix/leucine zipper domain of Myc proto-oncoproteins: Function and regulation. Oncogene, 18, 2955-2966.

Mai, S. and Jalava, A., 1994. c-Myc binds to 5' flanking sequence motifs of the dihydrofolate reductase gene in cellular extracts: role in proliferation. Nucleic Acids Res.

22, 2264-2273.

Mai, S., 1994. Overexpression of c-myc preceeds amplification of the gene encoding dihydrofolate reductase Gene 148, 253-260.

Mai, S., Hanley-Hyde, J., and Fluri, M., 1996a. c-Myc overexpression associated DHFR gene amplification in hamster, rat, mouse, and humans cells. Oncogene 12, 277-288.

Mai, S., Fluri, M., Siwarski, D., Huppi, K., 1996b. Genomic instability in MycER-activated Rat1A-MycER cells. Chromosome Res. 4, 365-371.

Mai, S., Hanley-Hyde, J., Rainey, G. J., Kuschak, T.I., Fluri, M., Taylor, C., Littlewood, T., Mischak, H., Stevens, L.M., Henderson, D.W., and Mushinski, J.F., 1999. Myc-dependent genomic instability at the murine cyclin D2 locus resulting in increased cyclin D2 mRNA and protein. Neoplasia, In Press.

Mouse Genome Database (MGD), Mouse Genome Informatics, The Jackson Laboratory, Bar Harbor, Maine. World Wide Web (URL: http://www.informatics.jax.org/). June, 1999).

Obaya, A.J., Mateyak, M., and Sedivy, J.M., 1999. Mysterious liaisons: the relationships between c-Myc and the cell cycle. Oncogene 18, 2934-2941.

Paria, B.C., Dey, S.K., and Andrews, G.K., 1992. Antisense c-myc effects on preimplantation mouse embryo development. Proc. Natl. Acad. Sci. USA 89, 10051-10055.

Polvinen, K., Sinervirta, R., Alhonen, L., and Janne, J., 1988. Overproduction of ornithine decarboxylase confers an apparent growth advantage to mouse tumor cells. Biochim. Biophys. Res. Commun. 155, 373-378.

Prendergast, G.C., 1999. Mechanisms of apoptosis by c-Myc. Oncogene 18, 2967-2987.

Tabib, A. and Bachrach, U., 1998. Polyamines induce malignant transformation in cultured NIH 3T3 fibroblasts. Int. J. Biochem. Cell. Biol. 30, 135-146.

Thelander, L. and Berg, P., 1986. Isolation and characterization of expressable cDNA clones encoding the M1 and M2 subunits of mouse ribonucleotide reductase. Mol. Cell. Biol. 6, 3433-3442.

Wright, J.A., 1989. Altered mammalian ribonucleotide reductase from mutant cell lines. In: Encycl. Pharmacol. Therapeut. 128, 89-111.

Wu, K.J., Grandori, C., Amacker, M., Simon-Vermot, N., Polack, A., Lingner, J., and Dalla-Favera, R., 1999. Direct activation of TERT transcription by c-MYC. Nat. Genet. 21, 220-224.

Yang-Feng, T.L., Barton, D.E., Thelander, L., Lewis, W.H., Srinivasan, P.R., Francke, U., 1987. Ribonucleotide reductase M2 subunit sequences mapped to four different chromosomal sites in humans and mice: functional locus identified by its amplification in hydroxyurea-resistant cell lines. Genomics 1, 77-86.

Yokota, J., Tsunetsugu-Yakota, Y., Battifora, H., Le Fevre, C., and Cline, M.J., 1986. Alterations in myc, myb, and ras Ha proto-oncogenes in cancers are frequent and show clinical correlation. Science 231, 261-265.

FIGURE LEGENDS

Figure 3.2.1. The Amplification and Rearrangement of the *R2* Gene Locus in c-Myc-Overexpressing Mouse B Lymphocytes is Detected by FISH

FISH analysis performed with a digoxigenin-labeled *R2* probe and a FITC-conjugated anti-digoxigenin antibody (Roche Diagnostics). **(a)** WEHI 231 cells. The arrow shows an endogenous single copy *R2* gene. **(b)** and **(c)** FISH performed with MOPC 460D cells and a digoxigenin-labeled *R2* probe. **(d)** FISH analysis of Pre-B- cells. The arrows show a single copy *R2* gene. **(e)** and **(f)** Pre-B+ cells with a digoxigenin-labeled *R2* probe (Roche Diagnostics).

Figure 3.2.1. The Amplification and Rearrangement of the *R2* Gene Locus

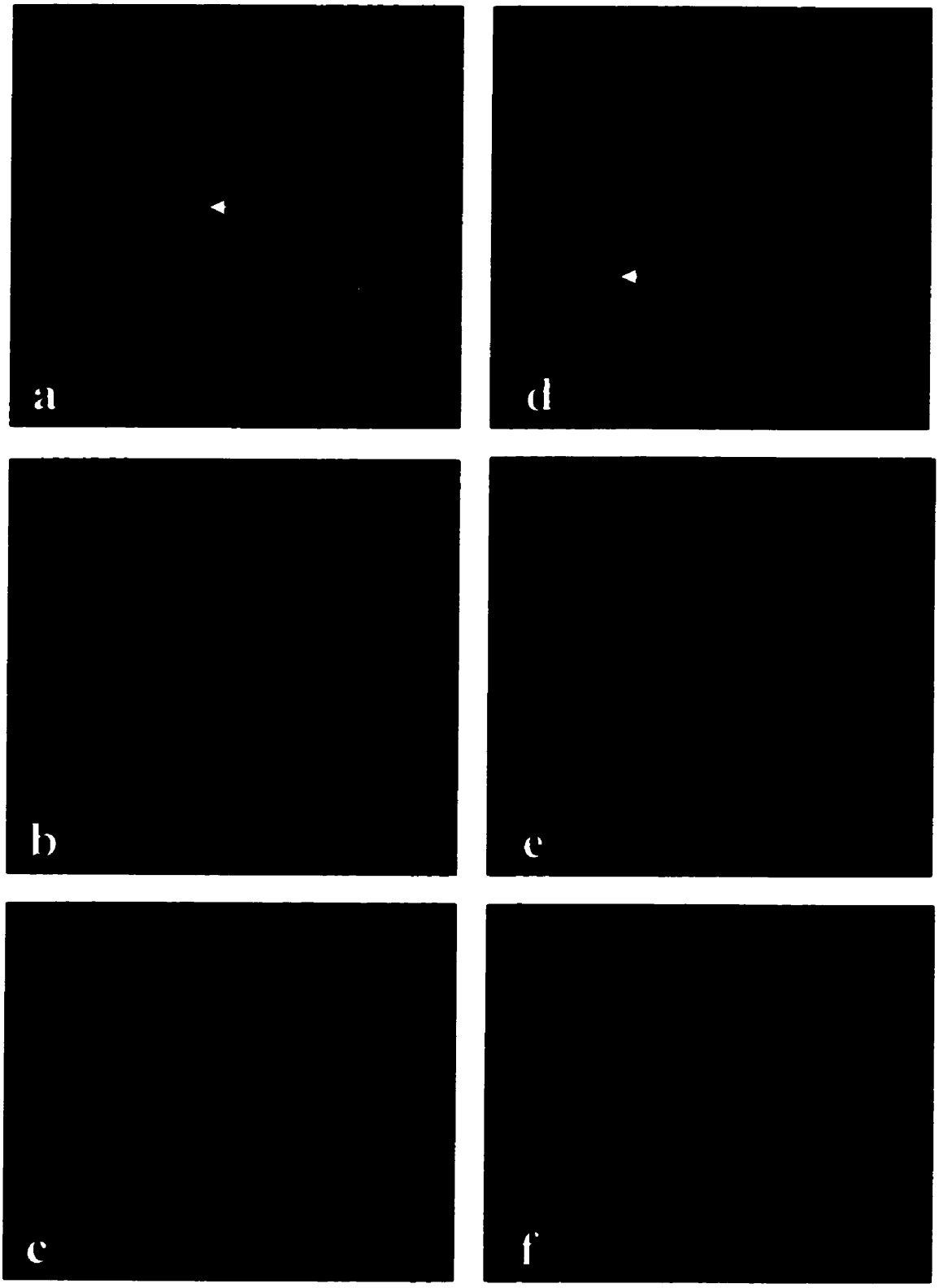

Figure 3.2.2.

Amplification and Rearrangement of the *R2* Locus in c-Myc-Overexpressing Mouse B Lymphocytes is Detected by Southern Blot and Dispersed Cell Assay Analyses.

(a) *Bam*HI, *Eco*RI, *Eco*RV, *Hin*dIII, and *Pst* I digested genomic DNA prepared from WEHI 231 (lanes 1-5) and MOPC 460D (lanes 6-10). Enzymes were purchased from Roche Diagnostics. **(b)** *glutathione peroxidase* (*GSHPX*) control hybridizations. *R2* hybridizations **(a)** showed detectable differences in all of the lanes of WEHI 231 and MOPC460D DNA. *Hin*dIII and *Pst*I showed amplification, and *Eco*RV revealed both amplification and rearrangement of the *R2* loci of c-Myc overexpressors. In **(a)**, amplification is indicated by small, black arrows, and rearrangement is shown by large, open arrows.

(c) *Bam*HI, *Eco*RI, *Eco*RV, *Hin*dIII, and *Pst*I-digested genomic DNA prepared from Pre-B-cells (lanes 1-5), and 4-HT-activated PreB+ cells (lanes 6-10). **(d)** shows *glutathione peroxidase* (*GSHPX*) control hybridizations. Relative to the *GSHPX* loading control, *Pst*I-digested DNA showed only *R2* gene amplification in the c-Myc overexpressing cells, while *BamH*I-, *Eco*RI-, *Hin*dIII-, and *Eco*RV-digested genomic DNA showed amplification and rearrangement of the *R2* locus in high c-Myc expressing cells. In **(c)**, amplification is indicated by small, black arrows, and rearrangements are shown by large, open arrows.

Figure 3.2.2. Southern Analysis shows Amplification and Rearrangement of *R2*

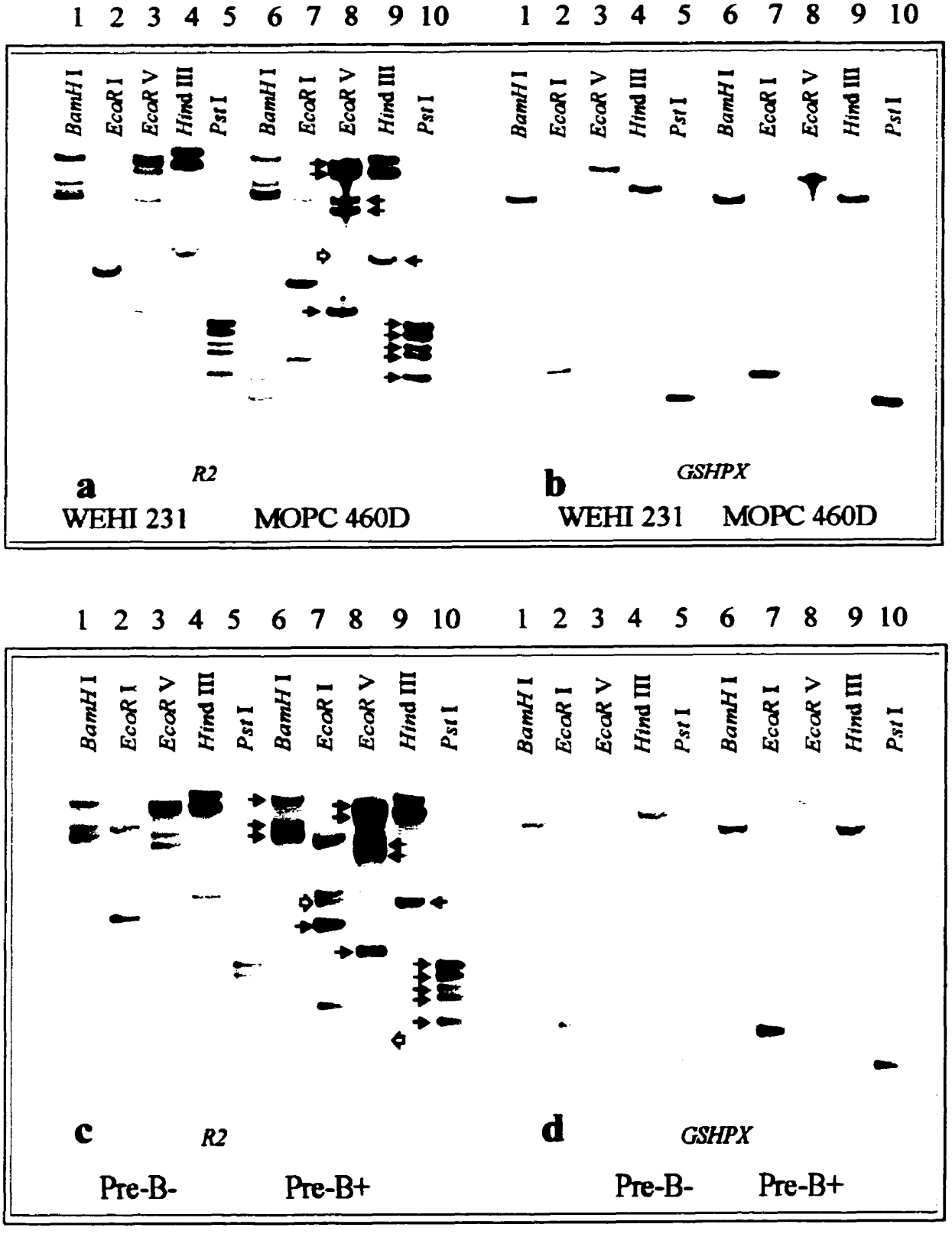

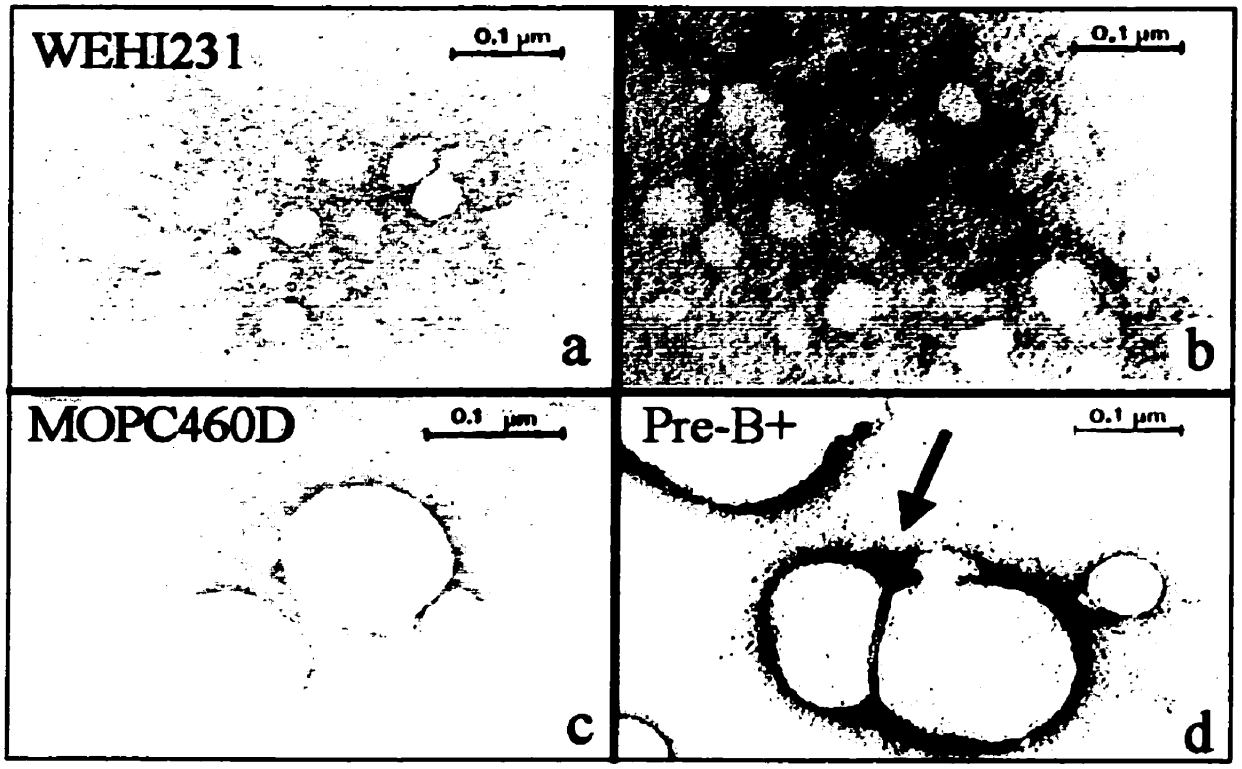

Figure 3.2.3. Panel A (a-d)

Figure 3.2.3. Panels A and B.

Extrachromosomal Elements are shown in Pre-B+ Lymphocytes by Electron Micrographs; *R2* Hybridization with EEs shown by FISH.

Panel A (a-d) Electron micrographs of extrachromosomal DNA prepared from **(a)** WEHI 231, **(b)** MOPC 460D, **(c)** Pre-B- and **(d)** PreB+ cells. The arrow in **Panel A (d)** indicates a putative replication bubble in the Pre-B+ EEs.

Figure 3.2.3. Panel B (a) and (b) FISH analysis of the Pre-B+ cells. **Panel B (a)** shows Hirt-extracted extrachromosomal DNA stained blue with 4'6'diamidino-2-phenylindol) (DAPI) (Sigma) (1 μgmL^{-1} in PBS) and **Panel B (b)** is a composite overlay which shows the green FITC-labeled (Roche Diagnostics) anti-digoxigenin labeled *R2* probe and extrachromosomal DNA counter-stained with DAPI (blue). The FITC-conjugated secondary antibodies are green when viewed alone, but appear white following image overlay with the blue DAPI counter-stained EEs. The arrows in **Panel B (b)** indicate co-localization of DAPI signals (blue) with *R2* signals shown by FITC-conjugated antibodies (white due to overlay).

Figure 3.2.3. Panel B (a-b) FISH Analysis of Pre-B+ Cells

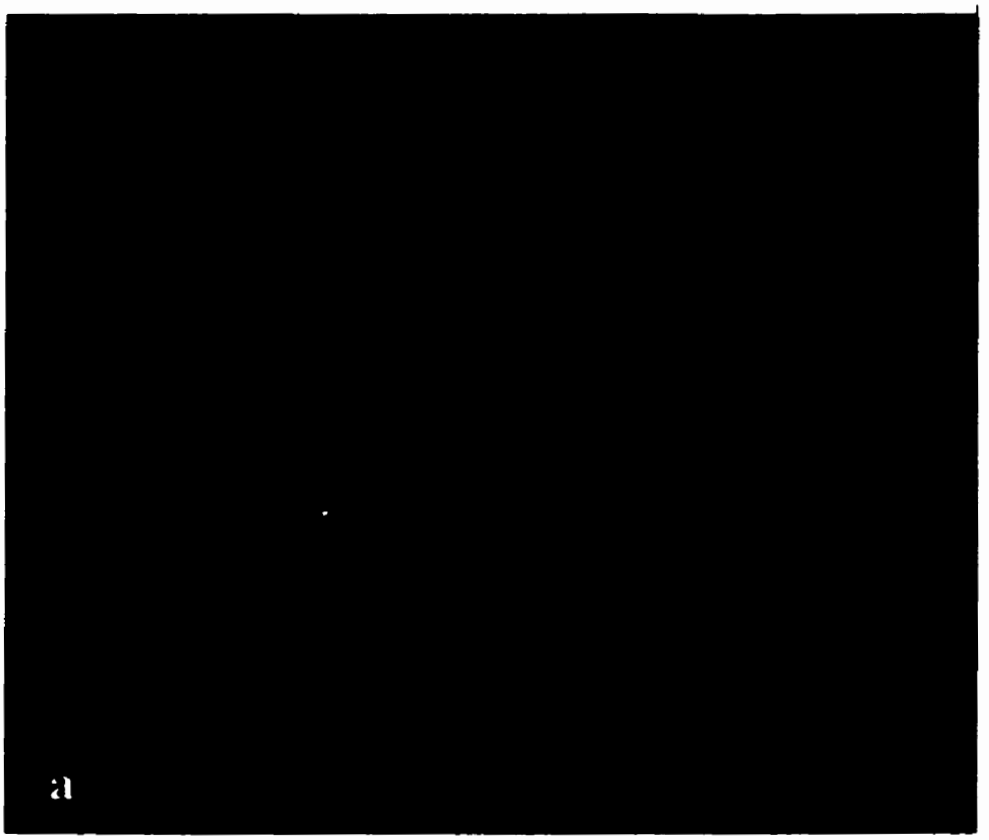

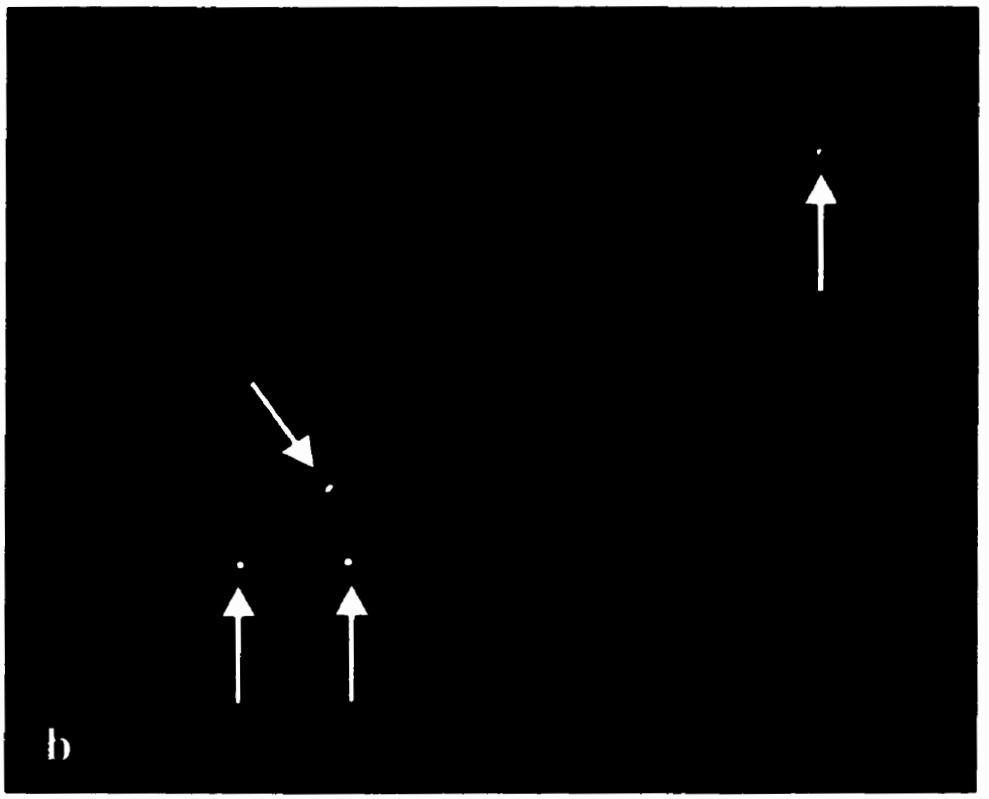

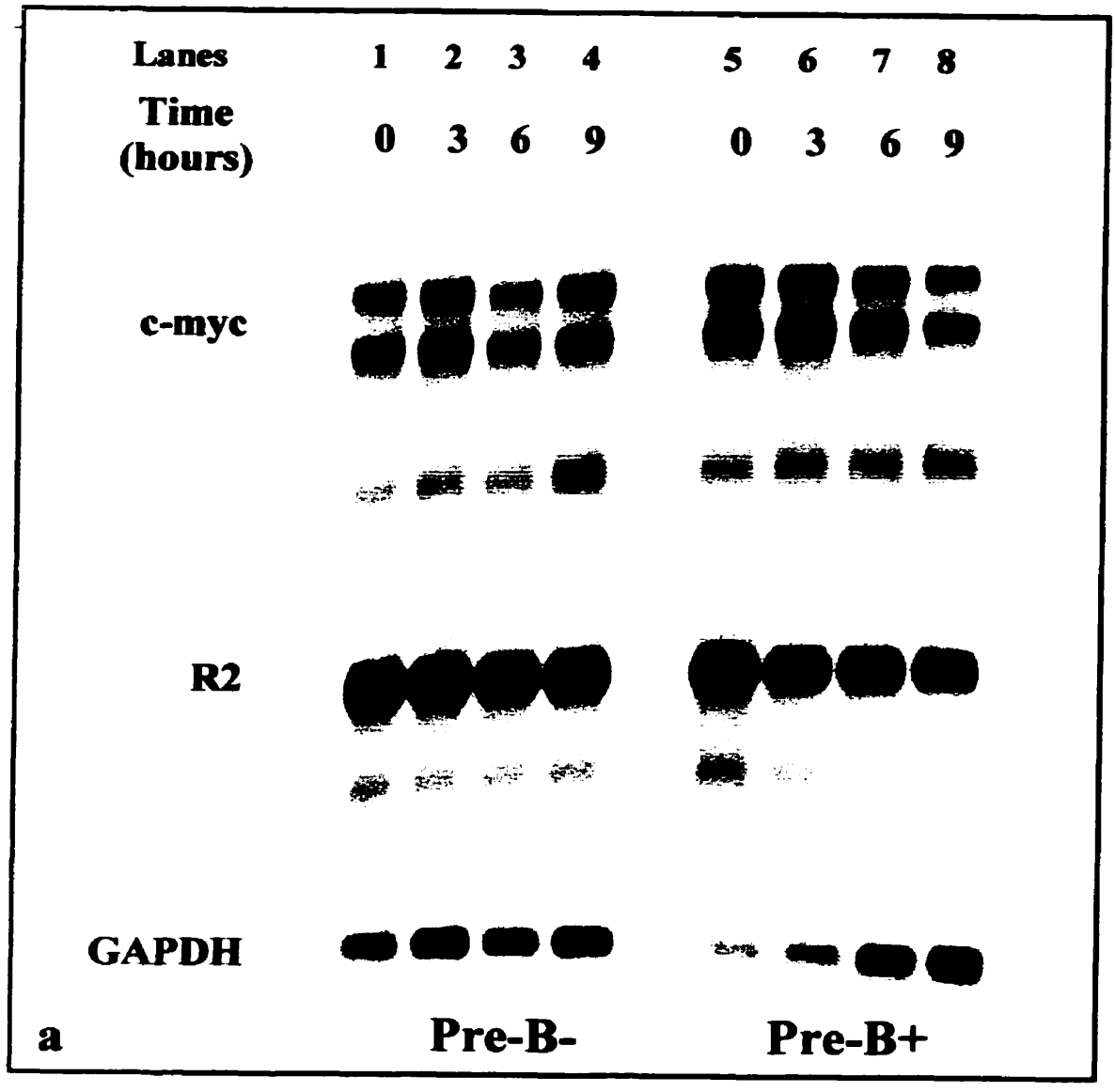

Figure 3.2.4.

There are No Changes in *R2* mRNA Levels Following Transient c-Myc Overexpression.

(a) Northern analysis of Pre-B- (lanes 1-4) and Pre-B+ (lanes 5-8) cells from 0, 3, 6, and 9 hours.

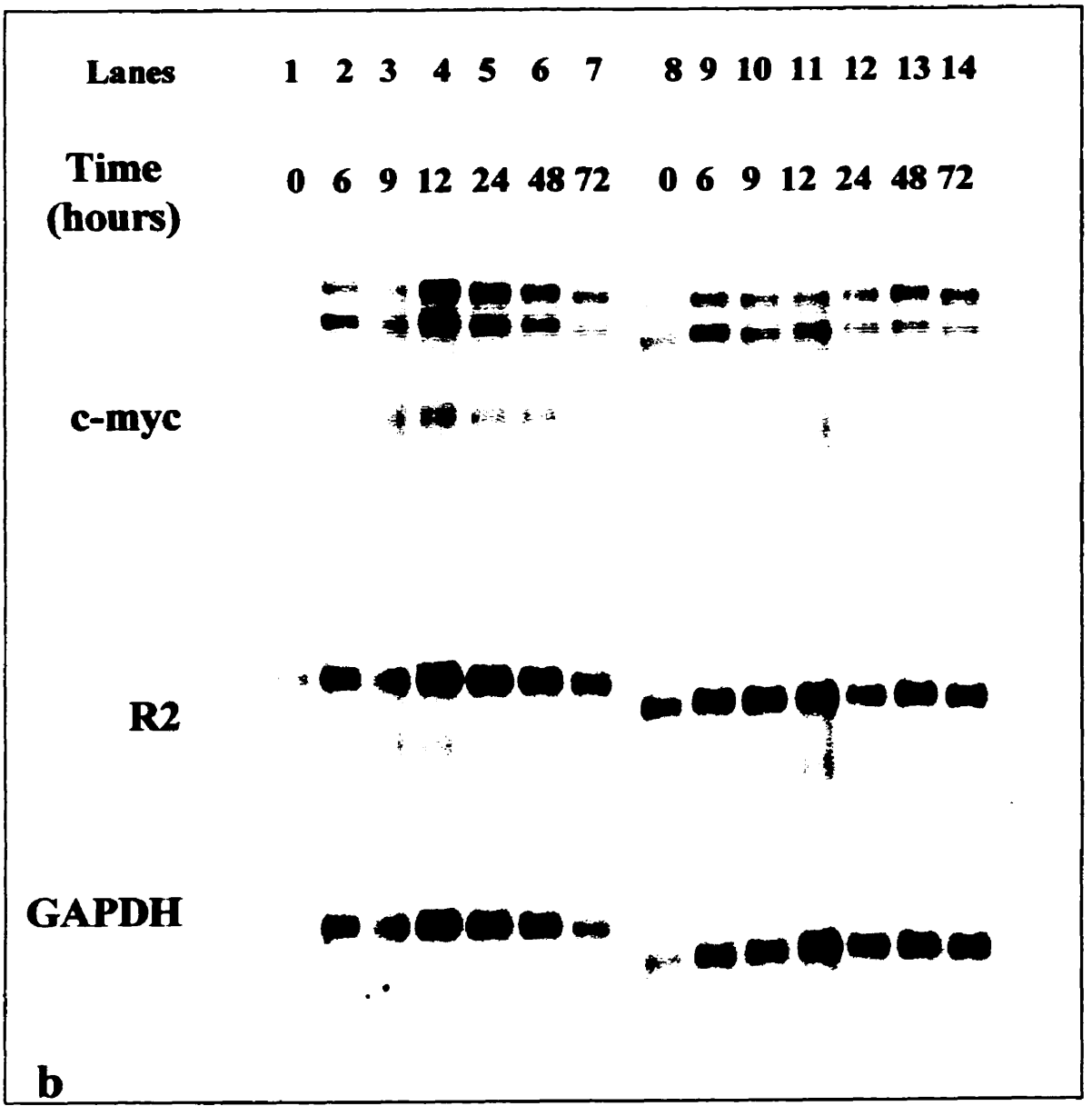

Figure 3.2.4. (b) Northern analysis of Pre-B- (lanes 1-7) and Pre-B+ (lanes 8-14) cells at 0, 6, 9, 12, 24, 48, and 72 hours. The blots are probed with the genes for *c-myc*, *R2*, and *GAPDH*, as indicated in the figure.

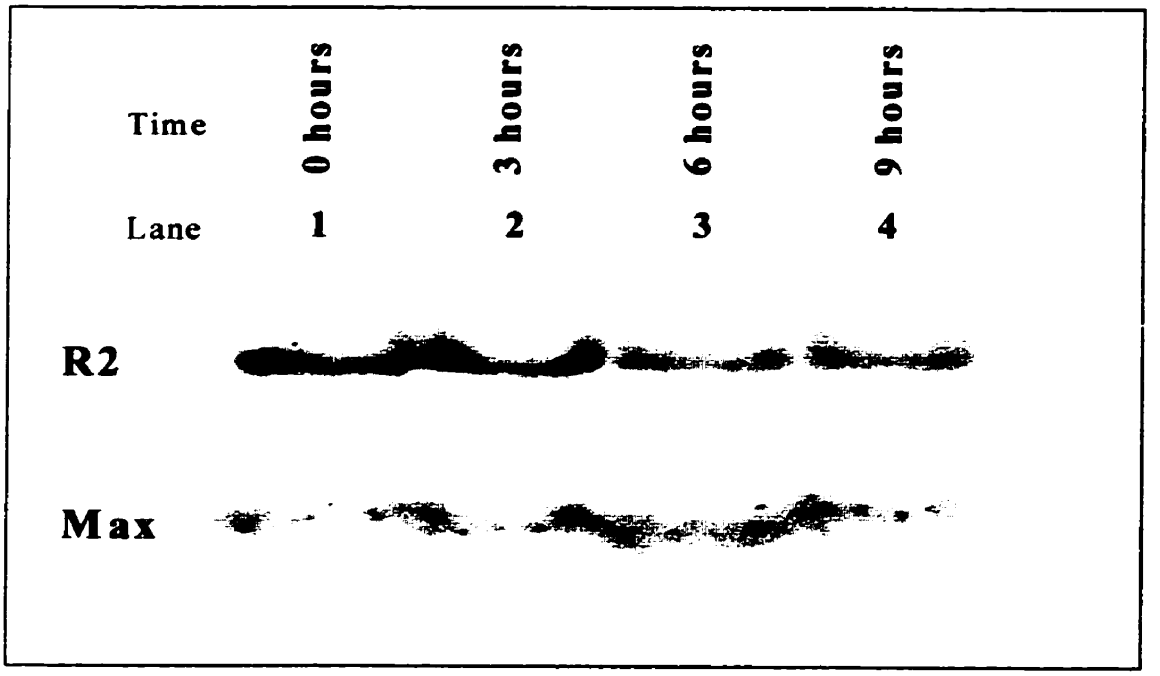

Figure 3.2.5.

Western Blot Analysis shows that R2 Protein Levels Remain Unchanged Following Activation of c-Myc Overexpression

Western blot analysis on an 8 % acrylamide gel shows the 45 kDa R2 protein expression levels in 4-HT-activated PreB+ cells at 0, 3, 6, and 9 hours (lanes 1-4). Accuracy of loading was controlled by hybridization with α-Max 256 antibody. (The anti-Max 256 was a generous gift from Dr. Achim Wenzel, and the anti-R2 antibody was generated by injection of the whole recombinant R2 protein into a New Zealand Rabbit (Chan *et al.*, 1993 and references therein).

Figure 3.2.6. Panels A and B.

Quantitative Fluorescent Immunohistochemistry shows no changes in R2 Protein Levels after c-Myc-Instability of the *R2* Gene

Panel A (a) shows immunohistochemical staining of WEHI 231 and **Panel A (b)** of MOPC 460D cells with anti-c-Myc antibody. **Panel A (c)** shows immunohistochemical staining of WEHI 231 and **Panel A (d)** of MOPC 460D cells with a rabbit polyclonal anti-R2 antibody (Chan *et al.*, 1993). **Panel B (a)** shows the immunohistochemical staining of Pre-B- cells and **Panel B (b)** of Pre-B+ cells with anti-c-Myc antibody. **Panel B (c)** shows immunohistochemical staining Pre-B- cells and **Panel B (d)** of Pre-B+ cells with the polyclonal rabbit anti-R2 antibody.

Figure 3.2.6. Panel A (a-d)

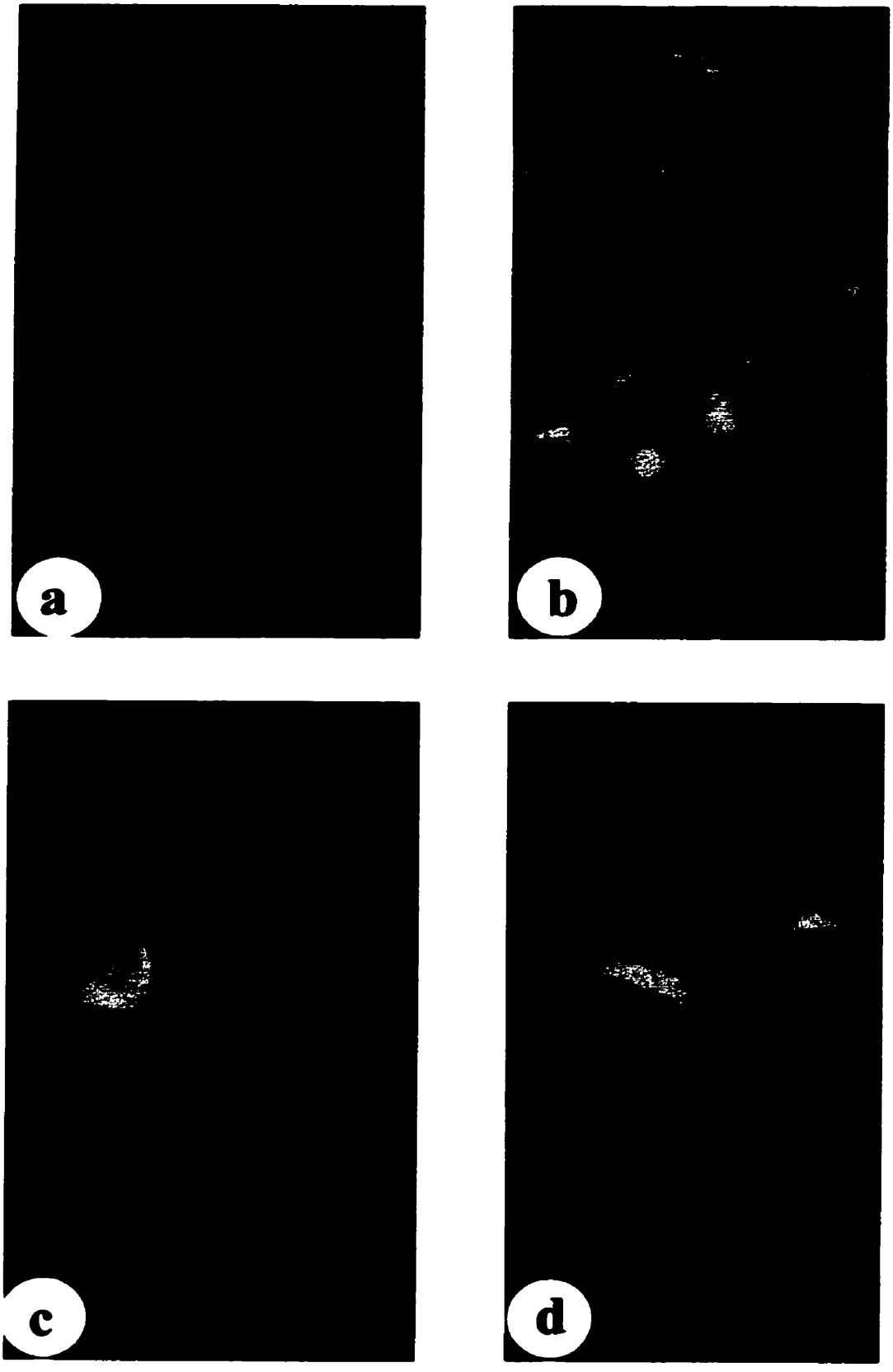

Figure 3.2.7.

c-Myc and R2 Protein Expression Levels Measured by Quantitative Fluorescent Immunohistochemistry.

Figure 3.2.7. (a-d) describes the percentage of cells per fluorescent intensity range following immunohistochemical staining. **(a)** Relative c-Myc expression levels in WEHI 231 and MOPC 460D cells. **(b)** Relative R2 expression levels in WEHI 231 and MOPC 460D cells. **(c)** Relative c-Myc expression levels of Pre-B cells grown in the absence (Pre-B-) and presence (Pre-B+) of 4-HT. **(d)** Relative R2 expression levels of Pre-B- and Pre-B+ cells.

Figure 3.2.7. c-Myc and R2 Protein Expression Levels

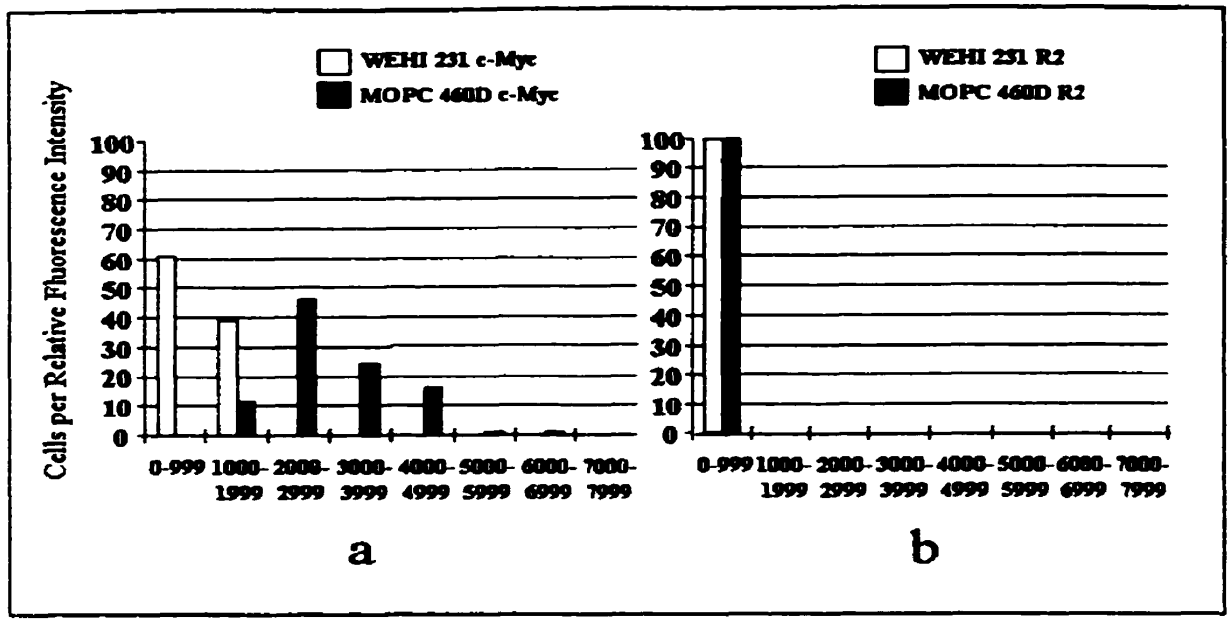

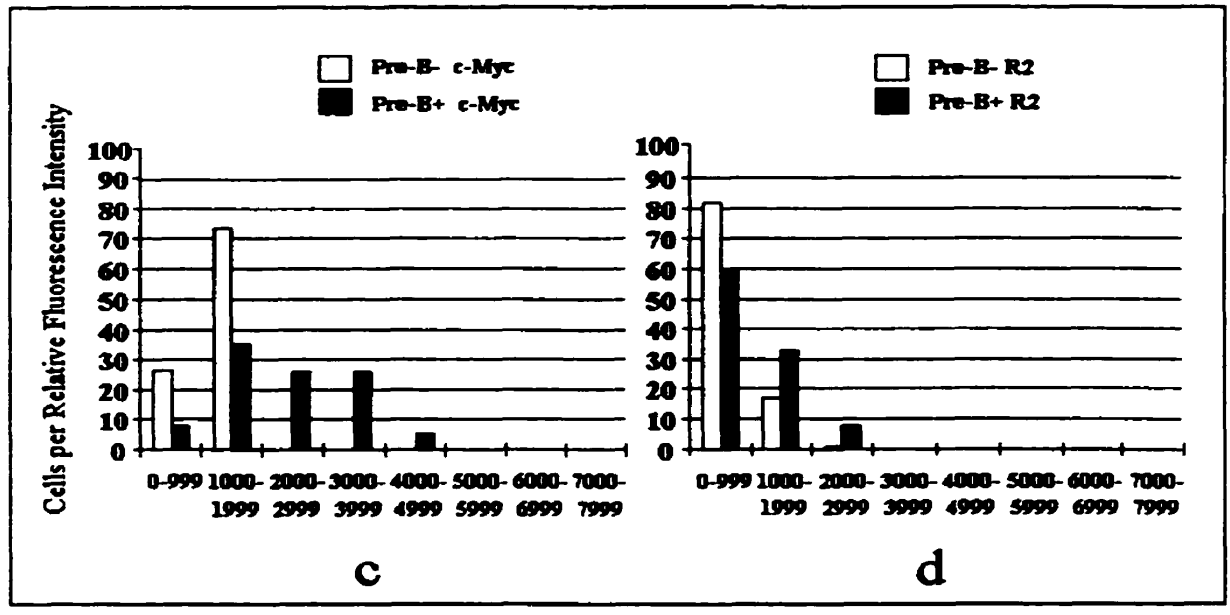

Table 1

Cell Lines Used in this Study.

Cell Line	Cell Type	c-Myc Protein Level
WEHI 231	mouse lymphoblastoid tumor	low
MOPC 460D	mouse plasmacytoma	constitutively deregulated
AMB Pre-B	mouse Pre-B lymphocyte line	regulateable

Ackowledgements:

S.M. is supported by grants from the Manitoba Cancer Research and Treatment Foundation and the National Science and Engineering Research Council of Canada. J.A.W. is supported by grants from the Medical Research Council of Canada and the National Science and Engineering Research Council of Canada. J.F.M is supported by the National Institutes of Health, Bethesda, Maryland. T.I.K. is the recipient of the *David and Mona Copp Graduate Studentship from the* Manitoba Cancer Research and Treatment Foundation.

Chapter 3.3

Preface

Chapter 3.3 is the full paper format of a manuscript submitted for publication. The authors are: Theodore I. Kuschak, Brenda C. Kuschak, Jim A. Wright, and Sabine Mai (2000). Isolation of Extrachromosomal Elements by Histone Immunoprecipitation.

This paper describes the isolation of histone-bound extrachromosomal DNA molecules by immunoprecipitation. This enrichment process is significant since it allows for the study of a potentially representative population of active extrachromosomal DNA from cultured cells as well as normal primary tissue and tumor samples.

Isolation of Extrachromosomal Elements by Histone Immunoprecipitation.

Theodore I. Kuschak[1,2,3,§], Brenda C. Kuschak[1,2,§], Jim A. Wright[3,6], and Sabine Mai[1,2,4,5,†]

[1]Manitoba Institute of Cell Biology, CancerCare Manitoba, 100 Olivia Street, Winnipeg, Manitoba, CANADA R3E 0V9.

[2]The Genomic Centre for Cancer Research and Diagnosis, Manitoba Institute of Cell Biology, CancerCare Manitoba, 100 Olivia Street, Winnipeg, Manitoba, Canada, R3E 0V9.

[3]Department of Microbiology, University of Manitoba, Winnipeg, Manitoba, Canada, R3T 2N2.

[4]Department of Physiology, University of Manitoba, 432 Basic Medical Sciences Building, 770 Bannatyne Avenue, Winnipeg, Manitoba, Canada, R3E 0W3.

[5]Department of Biochemistry and Medical Genetics, University of Manitoba, 336 Basic Medical Sciences Building, 770 Bannatyne Avenue, Winnipeg, Manitoba, Canada, R3E 0W3.

[6]Lorus Therapeutics, Inc. 7100 Woodbine Avenue, Suite 215. Markham, Ontario, CANADA, L3R 5J2

[§] Both authors contributed equally to this work.

[†]Corresponding Author:
Sabine Mai, Ph.D.
Tel: 204-787-2135
Fax: 204-787-2190
e-mail: smai@cc.umanitoba.ca

- **Key Words:** extrachromosomal, double minutes, oncogenes, drug resistance, amplification, tumorigenesis, enrichment, histones.

ABSTRACT

We describe a gentle and effective method for rapid and reproducible isolation of histone-bound extrachromosomal DNA molecules (extrachromosomal elements; EEs). This method facilitates the harvest of a specific population of EEs following their isolation from cultured cells, primary tissues and tumor cells by the Hirt method (3). Wiener *et al.* (11) showed that active histone is bound to EEs and demonstrated that these histone-bound EEs carry actively transcribing *c-myc* genes. The method described here exploits the presence of histones on EEs, and serves as a first-step purification procedure, allowing for cloning or multi-variant analysis of an immunopurified sample of EEs. We islolated EEs from 4-hydroxytamoxifen-activated Myc-ER™ regulatable Pre-B ABM cells. Following one round of immunoprecipitation, we demonstrate purification of histone-bound EEs. We confirmed that our purification enriched for EEs that carry genes by using FISH-EEs (4) where we probed non-enriched and immunopurified EEs with a *dihydrofolate reductase* (*DHFR*) cDNA probe, known to detect extrachromosomal amplification in these Myc-activated cells (4, 6, 7). We demonstrate the enrichment of immunoprecipitated *DHFR*-containing extrachromosomal DNA molecules.

3.3.1. INTRODUCTION

To facilitate the isolation of functional extrachromosomal circular DNA molecules (or EEs) extracted from tissue culture cells or clinical samples, we have further adapted the Hirt protocol (3) that was originally designed to isolate polyoma virus particles. Preparations of EEs are frequently contaminated with varying amounts of genomic DNA and/or apoptotic DNA fragments (9). The contamination of EEs with genomic and apoptotic DNA was addressed by Gaubatz and Flores (2), who described the use of exonuclease III, an enzyme that removes linear DNA molecules from these preparations. Exonuclease III also digests open and nicked circular extrachromosomal DNA molecules, potentially eliminating some of the EEs. Therefore, the use of this enzyme may compromise the isolation of a true and representative population of potentially transcriptionally or replicationally active EEs from a cell.

Wiener *et al.* (11) described a population of EEs that were able to actively transcribe *c-myc* mRNA. Moreover, these functional EEs carried active histone proteins. We have used the presence of histones on functional EEs to develop a method enabling the isolation of EEs that carry genes, leaving behind genomic and apoptotic contaminants from cells, as well as histone-free EEs. The value of this purification is demonstrated by the enrichment in the population of EEs that carries genes. In these experiments our immunopurified EEs showed an enriched population of EEs that carry *DHFR* gene sequences.

The advantage of this immunoprecipitation method is that, as a first post-extraction purification step, it allows for a number of analytical procedures to be conducted on a pure heterogeneous, but non-contaminated population of EEs derived

from cultured cells, primary tissue, or tumor samples. The immunopurified EEs can be cloned and used to create libraries. Moreover, purified EEs can be used to study genomic instability and mechanisms of gene amplification through procedures such as FISH-EEs, mRNA FISH, electron microscopy, cloning, and Southern blotting.

3.3.2. MATERIALS AND METHODS

3.3.2.1. Cell Culture

A mouse AMB Pre-B cell line used for the generation and isolation of extrachromosomal DNA purification. This is a Myc-regulatable cell line that carries a Myc-ER™ that is activated by the addition of 100 nM 4-hydroxytamoxifen (4-HT) (Sigma-Aldrich Canada, Winston, ON, Canada). (For simplicity, 4-HT-activated cells are referred to as Pre-B+ cells.) The origin of Pre-B cells (9) and their culture conditions (5) have been described.

3.3.2.2. Isolation of EEs

We began our experiments by isolating EEs Pre-B+ cells. Our procedure for EE isolation is based on the protocol of Hirt (3) and modified as described previously (4). The Hirt extract contains the bulk of the EEs and the total cellular RNA, but it may also be contaminated with small linear fragments of genomic DNA, and apoptotic DNA fragments which has been estimated to comprise 0.5 – 1.0% of the total amount of EEs isolated (9). Extrachromosomal DNA consists of a heterogeneous population of small polydispersed circles that can contain highly repetitive and mid-repetitive, as well as gene family sequences (1). Following isolation, all manipulations of EEs were performed in sterile, siliconized micro-centrifuge tubes (Fisherbrand, Fisher Scientific, Pittsburgh, PA, USA).

3.3.2.3. Purification of Histone-Containing Extrachromosomal DNA Molecules

We pretreated the Protein G sepharose beads (Amersham Pharmacia Biotech, Inc, Baie d'Urfé, PQ, Canada), used for the immunopurification of the EEs. We washed 1 mg of Protein G sepharose beads in 5 mL Buffer A (100 mM KCl, 10 mM Trizma pH 7.4, 1

mM Na_2EDTA, 1mM DTT, 1mM AEBSF) by placing on a rotating platform for 10 minutes at room temperature. (KCl, Trizma base, and Na_2EDTA were purchased from Sigma-Aldrich Canada, Winston, ON, Canada; DTT was purchased from FLUKA through Sigma-Aldrich Canada, Winston, ON, Canada. AEBSF was purchased from Roche Diagnostics, Laval, PQ, Canada). The beads were centrifuged at 13,000 rpm (16,000 x *g*) for 10 minutes at room temperature and the supernatant was removed and discarded. This washing procedure was performed a total of 3 times. The non-specific binding sites on 40 µL of beads were blocked by resuspending the beads in 300 µL of Buffer B (Buffer A + 4% ($^{w}/_{v}$) Bovine Serum Albumin) (FLUKA purchased through Sigma-Aldrich Canada, Winston, ON, Canada). The binding of the sheep anti-core histone antibody to the Protein G sepharose beads is shown in Figure 1.

Immunopurification of extrachromosomal elements was used to perform the isolation of the Hirt-extracted histone-bound EEs from the impurities found in the Hirt-extracted EE sample. Freshly extracted EEs were dialyzed against 1x TE buffer (10 mM Trizma base, 1 mM Na_2EDTA, pH 8.0) overnight at 4°C (Trizma base and Na_2EDTA were purchased from Sigma-Aldrich Canada, Winston, ON, Canada). The EEs were then incubated in 500 µL Buffer B on a rotating platform for 10 minutes at room temperature. We added 1µg of anti-core histone antibody per µg of EEs and incubated the mixture for 30 minutes at room temperature on a rotating platform. The blocked beads were then added to the antibody-treated EEs and incubated overnight on a rotating platform at room temperature. Following this incubation, the EE/beads were centrifuged at 13,000 rpm for 10 minutes at room temperature to remove any unbound material. The EE/beads were washed three times with Buffer A to remove any residual unbound material. We eluted

the bound histone-containing EEs by adding 300 µL of 100 mM glycine (Sigma-Aldrich Canada, Winston, ON, Canada) (pH 2.3) to the beads and mixing gently by inverting the tube 5-10 times. The tube was centrifuged at 13,000 rpm for 10 minutes at room temperature and the supernatant (eluate) was removed and collected. This eluate was immediately neutralized to pH 7.2 using 1 M Trizma, pH 8.0. The elution step was repeated once more and the two collected eluates were pooled together. The sample was concentrated to approximately 40 µL by roto-evaporation.

3.3.2.4. Analyses of Immunopurified Extrachromosomal Elements

The following protocol allows the fixation of the EEs onto glass microscope slides and it ensures that the EEs are contained within a small area. Briefly: 40 µL of Hirt extract (3) or immunopurified and concentrated EEs are diluted 1:1 in a fixative solution (freshly prepared 3:1 methanol:actetic acid) and then delivered onto pre-cooled slides (60 seconds on dry ice) (O. Kindler, Germany). The slides are immediately moved onto a slide warmer (37°C). The fixation procedure continues as described previously (4). (Methanol was purchased from FLUKA through Sigma-Aldrich Canada, Winston, ON, Canada and acetic acid was purchased through Sigma-Aldrich Canada, Winston, ON, Canada.)

We visualized non-immunopurified and immunopurified Hirt-extracted EEs by immunohistochemical staining (5). For this procedure, we used a sheep anti-core histone antibody (Sigma-Aldrich Canada, Winston, ON, Canada) diluted 1:200 and incubated for 30 minutes at room temperature. This was followed by incubation with a secondary antibody, a donkey anti-sheep IgG-FITC antibody (Sigma-Aldrich Canada, Winston, ON, Canada) diluted 1:400 in lamb serum (Gibco/BRL, Life Technologies, Inc., Burlington,

ON, Canada) and incubated for 30 minutes at room temperature. Immunofluorescent analysis of histone-bound EEs was performed as previously described (5), the only modification being the omission of the permiabilization step. 4',6' diamidino-2-phenylindole (DAPI) (Sigma-Aldrich Canada, Winston, ON, Canada) (1μgmL^{-1} in PBS) is used to counter-stain both the DNA in the EEs and any genomic DNA contaminants. Anti-bleach (6) is added to preserve the fluorescence of the sample and to function as a mount for the cover slip. We analyzed the immunostained EEs using a Zeiss Axioplan2 microscope (Carl Zeiss Canada, Inc., Ottawa ON, Canada) under a 63x oil immersion objective and a UV filter. The images were acquired using *Northern Eclipse 5.0* software (Empix Imaging Inc., Mississauga, ON, Canada) and a Sony (model XC75) CCD camera. Adaptive thresholding tools (*Northern Eclipse* version 5.0 from Empix Imaging Inc., Mississauga, ON, Canada) were used to remove all dots from the DAPI-stained images that were ≤ 5 x 5 pixels in size at a magnification when we used a 0.63x oil immersion objective lens and a 0.63x adapter.

FISH-EEs (4) was performed on Hirt-extracted EEs and on immunopurified EEs using a *DHFR* probe (6). We analyzed the EEs using a Zeiss Axiophot microscope (Carl Zeiss Canada, Inc., Ottawa ON, Canada) under a 63x oil immersion objective, a 1x magnification adapter, and a UV filter. The images were acquired using IPLab software (Scanalytics, Fairfax VA, USA) Photometrics (CH250/a) CCD camera equipped with a KAF-1400-50 sensor chip (1317 x 1035 pixels, Kodak).

3.3.3. RESULTS

The isolation of the histone-bound population of extrachromosomal DNA extracted from Pre-B+ cells (4) was performed by immunoprecipitation. Pre-B+ cells contain a 4-HT-responsive Myc–ER™ construct and have been activated with 4-HT to overexpress c-Myc (5). This induces the activation of EEs from c-Myc overexpressing Pre-B+ cells. These EEs were isolated, first by Hirt extraction, and then followed by immunoprecipitation of histone-bound EEs (5, 7).

3.3.3.1. Binding of Anti-Core Histone Antibody to Protein G Sepharose Beads

Sheep anti-core histone antibody (Sigma Chemical Company, St. Louis Mo.) was bound to Protein G sepharose beads (Amersham Pharmacia Biotech) according to manufacturer's instructions. Briefly, the anti-histone antibody was eluted from the Protein G sepharose beads by incubating in 100 mM glycine buffer, pH 2.3. The eluate was immediately neutralized to pH 7.2 using 1 M Trizma Buffer, pH 8.0. Figure 3.3.1. shows the successful binding and elution of the sheep anti-core histone antibody from the Protein G sepharose beads.

Immunostaining shows Enrichment of Histone-Bound EEs following HIP-EEs

Figure 3.3.2. (a-f) shows immunohistochemical staining for the presence of histone proteins on EEs. Non-immunopurified EEs (Figure 3.3.2. (a-c)) are compared with immunoprecipitated EEs (Figure 3.3.2. (d-f)). In this figure, large white arrows indicate co-localized DAPI and FITC signals and small white arrows indicate FITC signals that do not co-localize with a light blue DAPI signal (see Figure 3.3.2. (f)). 3.3.2. (a-c) shows the relative proportion of histone-bound EEs in a sample of non-purified EEs. Figure 3.3.2. (a) shows a large population of extrachromosomal elements, shown by pale blue or

white DAPI signals. Figure 3.3.2. (b) shows light yellow or white signals from FITC-conjugated donkey anti-sheep antibody, indicating the presence of EEs bound by histone proteins. Figure 3.3.2. (c) is the overlay of (a) and (b), where light yellow FITC signals are over-layed with the pale blue DAPI-stained EEs. These over-layed signals are visible as distinct light yellow or white dots. In the antibody-purified population (Figure 3.3.2. (d-f)), we observed an enrichment in histone-bound EEs. Figure 3.3.2. (d), shows a sparse population of DAPI-stained extrachromosomal DNA, seen as blue dots. Figure 3.3.2. (e) shows an equally sparse population of pale yellow dots generated by the FITC-conjugated donkey anti-sheep antibody, and corresponding to extrachromosomal DNA after immunopurification of histone-bound EEs. Figure 3.3.2. (f) illustrates the overlay of Figure 3.3.2. (d) and (e). In this figure, the majority of DAPI signals co-localize with FITC signals, and appear as pale blue or white dots (see large white arrows). Figure 3.3.2. (f) also shows FITC signals where there is no co-localization with DAPI signals (see small white arrows). The reason for this is likely that DAPI intercalates into the DNA, but its signal was not amplified further. In contrast, the sheep anti-core histone antibody was amplified by the donkey anti-sheep secondary antibody, giving a greater relative signal intensity in comparison to the DAPI signal intensity.

The data show that there are fewer DAPI signals in the immunopurified sample (Figure 3.3.2. (d-f)), indicating fewer EEs in the immunopurified sample, as compared to the non-immunopurified EEs. However, of the EEs isolated by immunopurification, the majority is co-localized with bright yellow or white signals indicative of histone protein. This demonstrates an enrichment of histone-bound EEs.

FISH-EEs shows Enrichment of *DHFR* Sequences on EEs following HIP-EEs

To assess the value of this EE immunopurification method, we assayed for the enrichment of an extrachromosomally amplified gene. It was demonstrated previously that c-Myc deregulation results in amplification of *DHFR* in mouse, rat, hamster, and human cell lines (6, 7). We showed by the FISH-EEs method, that *DHFR* was present on extrachromosomal DNA from Pre-B+ cells (4). We hypothesized that the enrichment of the Hirt-extracted EEs by our immunopurification method should increase the relative ratio of *DHFR*-containing EEs when comparing non-immunoprecipitated with immunoprecipitated EE sample populations.

Figure 3.3.3. (a-f) illustrates the comparison of *DHFR*-containing EEs from non-immunopurified EEs (Figure 3.3.3. (a-c)) with *DHFR*-containing EEs from immunopurified EEs (Figure 3.3.3. (d-f)). In Figure 3.3.3. (f), large white arrows indicate co-localized DAPI and FITC signals, small white arrows indicate FITC signals that do not co-localize with DAPI signals, and open arrows indicate DAPI signals where there is no co-localized FITC signal. Figure 3.3.3. (a-c) shows the results of FISH-EEs experiments where we probed a non-immunoprecipitated population of Hirt-extracted EEs with a digoxigenin-labeled *DHFR* cDNA probe. Figure 3.3.3. (a) shows a large population of DAPI-stained EEs, shown as pale blue or white dots. Figure 3 (b) shows a sparse population of EEs detected by a digoxigenin-labeled *DHFR* cDNA probe and amplified by a FITC-conjugated anti-digoxigenin antibody. These signals appear as small green, or larger pale yellow dots. The overlay of Figure 3.3.3. (a) and (b) shows the co-localization of DAPI and FITC signals and appear as pale yellow or white dots. Figure 3.3.3. (a-c) indicates a very small number of *DHFR* FISH-EEs signals relative to a very

large number of DAPI signals in the non-immunopurified EE population. (Figure 3.3.3. (d-f)) shows the results of FISH-EEs experiments conducted with immunopurified EEs. Figure 3.3.3. (d) illustrates that there is smaller number of DAPI-stained EEs in the population isolated by immunopurification, than in the non-purified sample shown in (Figure 3.3.3. (a)). These signals appear as pale blue or white dots. Figure 3.3.3. (e) shows a greater number of EEs that hybridize to a *DHFR* probe than in the non-purified sample (Figure 3.3.3. (b)), appearing as pale yellow signals. The overlay of Figures 3.3.3. (d) and (e) shows a higher proportion of *DHFR*-stained EEs that co-localize to DAPI-stained EEs (Figure 3.3.3. (f)). In Figure 3.3.3. (f), large white arrows indicate *DHFR* signals that co-localize with DAPI signals. This overlay shows an increased proportion of *DHFR*-containing EEs in comparison to the non-purified EE sample. Small white arrows in Figure 3.3.3. (f) show FITC signals that do not co-localize with DAPI signals. As described above, this is likely due to the relatively poor signal intensity of DAPI in comparison with the amplified *DHFR* signal amplified by a secondary antibody (see MATERIALS AND METHODS). Figure 3.3.3. (f) shows in increase in the number of co-localized DAPI-FITC signals in comparison with the proportion of DAPI-FITC co-localized signals in the non-purified sample shown in Figure 3.3.3. (c). In addition, in Figure 3.3.3. (f) we also observed a number of DAPI signals that did not show co-localization with a FITC signal (see open arrow). These are likely histone containing EEs that do not contain *DHFR* sequences, but may contain sequences from other gene families (5, 8, 9).

Overall, these data indicate enrichment in the number of EEs that carry *DHFR* sequences, and presumably sequences of other c-Myc target genes, such as

ribonucleotide reductase R1 and *R2* genes (4, 5), *cyclin D2* (9), and potentially other, as yet unidentified genes.

3.3.4. DISCUSSION

The immunopurification of the active population of extrachromosomal DNA molecules is advantageous in studying functional EEs since it enriches for a potentially active population of EEs, removing the non-histone-bound and presumably inconsequential population of EEs from the extrachromosomal DNA population. The value of this method as a means of isolating potentially functional EEs from a large population of extrachromosomal DNA amplicons was assessed by two methods.

We began by analyzing non-immunopurified and immunopurified EEs by immunostaining for histone protein and comparing the ratio of DAPI-stained DNA molecules that co-hybridized with the signal from an anti-histone antibody (Figure 3.3.2. (a-f)). We saw an enrichment of histone-bound EEs in the immunopurified samples. Nearly all of the EEs in the sample of immunopurified EEs showed co-localization with FITC, indicating that the majority of the EEs in the purified samples contained histone proteins. The results of the immunostaining assay shows that this method is successful in isolating histone-bound EEs from a large pool of EEs that do not contain histone protein.

The second method of assessment was the comparison of the number of EEs that hybridize with a gene of interest, in this case *DHFR* (Figure 3.3.3. (a-f)). The experiment shows that immunopurified EEs carry a larger relative number of *DHFR* sequences, indicating an overall enrichment of specific extrachromosomal amplicons. Figure 3.3.3. (f) shows that although there is an increase in the proportion of EEs that hybridize with a *DHFR* probe, there are also a number of EEs where no FITC signal is seen to co-localize

with DAPI stained EEs. This is expected since previous work has shown that a number of genes can be found on EEs from Myc-ER™-activated mouse Pre-B+ cells. These include *ribonucleotide reductase R1* and *R2* (4, 5), *cyclin D2* (8), as well as *DHFR* (7) sequences. It is likely that there are others as well.

In conclusion, we have shown that our method for immunopurification of EEs is useful as a means of studying extrachromosomal gene amplification phenomena as well as amplification-mediated expression of oncogenes, drug-resistance genes, and potentially others. A body of literature is accumulating describing the role of extrachromosomal DNA molecules in tumor initiation and progression. The immunopurification of EEs is a novel tool that is ideally suited as a first step purification of EEs for a variety of studies in cultured cells, primary cells, and tumor samples. These analyses and procedures include generating libraries of EEs from cells, analyses of EEs by electron microscopy, fluorescent *in situ* hybridization (FISH-EEs) (4, 5, 7, 8), mRNA FISH (10, 11), cloning, and Southern blotting.

ACKNOWLEDGEMENTS

T.I.K. is the recipient of the G.H. Sellers Graduate Studentship from the Manitoba Institute of Cell Biology and CancerCare Manitoba. This research was funded by grants to S.M. and J.A.W. from National Science and Engineering Research Council and the Medical Research Council. *The Genomic Centre for Cancer Research and Diagnosis* is a Canada Foundation for Innovation (CFI)-funded Regional/National research facility. We thank Kevin Coonan from Empix Imaging Inc., (Mississauga, ON, Canada) for custom-design and installation of imaging software applications.

REFERENCES

1. **Cohen, S., Regev, A., and Lavi, S.** 1997. Small polydispersed circular DNA (spc DNA) in human cells: association with genomic instability. Oncogene *14*: 977-985.

2. **Gaubatz, J. W. and Flores, S. C.** 1990. Purification of eucaryotic extrachromosomal circular DNAs using exonuclease III. Analyt. Biochem. *184*, 305-310.

3. **Hirt, B.** 1967. Selective Extraction of Polyoma DNA from Infected Mouse Cell Cultures. J. Mol. Biol. *26*: 365-369.

4. **Kuschak, T.I., Paul, J.T., Wright, J.A., Mushinski, J.F., and Mai, S.** 1999. FISH on purified extrachromosomal DNA molecules. TTO http:// biomednet.com/db/tto. T01669.

5. **Kuschak, T.I., Taylor, C.T., Mushinski, J.F., Henderson, D.W., Israels, S., McMillan-Ward, E., Wright, J.A., Mai, S.** 1999. The *ribonucleotide reductase R2* gene is a non-transcribed target of c-Myc-induced genomic instability. Gene *238*: 351-365.

6. **Mai, S.,** 1994. Overexpression of c-myc precedes amplification of the gene encoding dihydrofolate reductase. Gene *148*: 253-260.

7. **Mai, S., Hanley-Hyde, J., and Fluri, M.** 1996. c-Myc overexpression associated *DHFR* gene amplification in hamster, rat, mouse and human cell lines. Oncogene *12*: 277-288.

8. **Mai, S., Hanley-Hyde J., Rainey J., Kuschak, TI, Fluri M., Taylor C., Littlewood T.D., Mischak H., Stevens L.M., Henderson D.W., and Mushinski**

J.F. 1999. Chromosomal and extrachromosomal instability of the *cyclin D2* gene is induced by Myc overexpression. Neoplasia, *1*: 241-252.

9. **Regev, A., Cohen, S., Cohen, E., Bar-Am, I. and Lavi, S.** 1998. Telomeric repeats on small polydisperse circular DNA (spcDNA) and genomic instability. Oncogene *17*: 3455-3461.

10. **Szeles A., Kerstin, I., Falk, S.I., and Klein, G.** 1999. Visualization of alternative Epstein-Barr Virus expression programs by fluorescent *in situ* hybridization at the cell level. J. Virol. *73*: 5064-5069.

11. **Wiener, F., Kuschak, T.I., Ohno, S., and Mai, S.** 1999. Deregulated expression of c-Myc in a translocation-negative plasmacytoma on extrachromosomal elements that carry *IgH* and *myc* genes. Proc. Natl. Acad. Sci. USA. *96*: 13967-13972.

FIGURES

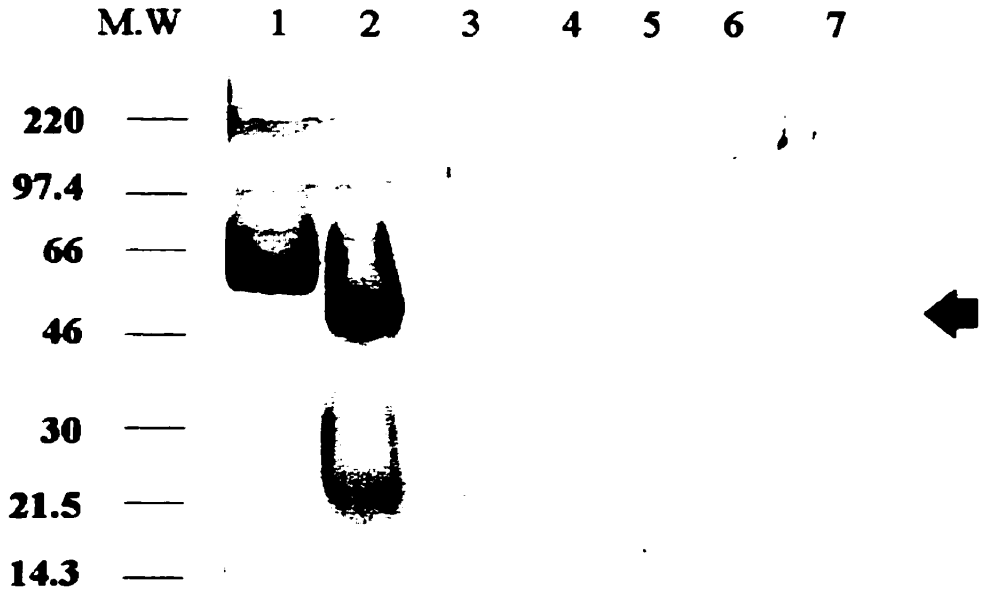

Figure 3.3.1.

Binding and elution of sheep anti-core histone antibody to protein G beads. Lane 1 was loaded with 4% ($^{w}/_{v}$) bovine serum albumin. Lane 2 was loaded with 20 μg sheep anti-core histone antibody. Lane 3 contains unbound sheep anti-core histone antibody from the ProteinG sepharose beads. Lanes 4-6 were loaded with washes 1-3, where the Protein G sepharose beads were washed with Buffer A. Lane 7 contains sheep anti-core histone antibody following elution with 100 mM glycine (pH 2.3) and neutralization with Trizma pH 8.0. (Each lane was loaded with 300 μL of sample that had been roto-evaporated to a final volume of 20 μL.) The black arrow indicates bands corresponding to sheep anti-core histone antibody following elution from Protein G sepharose beads using 100 mM glycine, pH 2.3 and immediate neutralization with 1 M Trizma pH 8.0.

Figure 3.3.2. (a-f)

Immunoprecipitation of EEs with anti-core histone antibody isolates histone-bound extrachromosomal elements. Figure 3.3.2. (a-f) shows the relative proportion of histone-bound EEs in non-purified EEs from Pre-B+ cells. (a) shows DAPI-stained non-purified Hirt-extracted EEs (b) shows anti-core histone antibody immunostaining of EEs (green dots). (c) shows the over-lays of (a) and (b). Figure 3.3.2. (d-f) shows the relative proportion of histone-bound EEs in purified EEs. (d) shows DAPI-stained immunopurified Hirt-extracted EEs, (e) shows anti-core histone antibody immunostaining of immunopurified EEs. (f) shows the over-lays of (d) and (e). Large white arrows in (f) indicate co-localized DAPI and FITC signals. Small white arrows indicate FITC signals without co-localized DAPI signals. See RESULTS for details.

Figure 3.3.3. (a-f)

Immunoprecipitation of EEs with anti-core histone antibody enriches for extrachromosomal elements that carry *DHFR* sequences. Figure 3.3.3. (a-c) shows the relative proportion of non-immunopurified EEs that carry *DHFR* gene sequences. (a) shows, DAPI-stained non-immunopurified Hirt-extracted EEs. (b) shows EEs probed by FISH-EEs using a FITC-conjugated anti-digoxigenin digoxigenin-labeled *DHFR* probe. (c) shows the over-lays of (a) and (b). Figure 3.3.3. (d-f) shows the relative proportion of immunopurifed EEs that carries *DHFR* gene sequences. (d) shows DAPI-stained immunopurified Hirt-extracted EEs, and (e) shows immunopurified EEs that carry *DHFR* gene sequences. (f) shows the over-lays of (d) and (e). Large white arrows in (f) indicate co-localized DAPI and FITC signals. Small white arrows indicate FITC signals without co-localized DAPI signals. Open white arrows show EEs where a light blue DAPI signal is seen without a FITC co-localized signal. See RESULTS for details.

Chapter 3.4

Preface

Chapter 3.4 describes my study that aims to elucidate the mechanism of c-Myc-dependent amplification of the mouse *ribonucleotide reductase R2* gene locus, specifically at the stage of its initiation.

This body of work is the first to describe the c-Myc-dependent replication-driven mechanism through which the amplification of the *ribonucleotide reductase R2* gene is initiated. c-Myc appears to initiate illegitimate re-replication-events during the course of a single cell cycle. This manuscript contributes to the field of genomic instability, and specifically the understanding of the role that c-Myc plays in locus-specific gene amplification. It is the first to show that the mechanism of c-Myc-induced amplification of a target gene *ribonucleotide reductase R2* (and perhaps other genes) is a replication-driven phenomenon that is reminiscent of the *onionskin* model initially described by Varshavsky (1981) and later by Mariani and Schimke (1984) as well as others.

c-Myc Deregulation Over-rides Replication Control: Induction of *Ribonucleotide Reductase R2* Re-replication in a Single Cell Cycle

Theodore I. Kuschak [1, 2, 3], Cheryl Taylor [1, 2], Jim A. Wright [1, 3, 4, 5], and Sabine Mai* [1, 2, 4]

1. Manitoba Institute of Cell Biology, and CancerCare Manitoba, 100 Olivia St., Winnipeg, Manitoba, CANADA, R3E 0V9.
2. The Genomic Centre for Cancer Research and Diagnosis, and CancerCare Manitoba, 100 Olivia St., Winnipeg, Manitoba, CANADA, R3E 0V9.
3. Department of Microbiology, University of Manitoba, Winnipeg, Manitoba, CANADA, R3T 2N2.
4. Department of Biochemistry and Medical Genetics, University of Manitoba, 336 Basic Medical Sciences Building, 770 Bannatyne Avenue, Winnipeg, Manitoba, Canada, R3E 0W3
5. Lorus Therapeutics, Inc. 7100 Woodbine Avenue, Suite 215. Markham, Ontario, CANADA, L3R 5J2

*To whom correspondence should be addressed:

Sabine Mai, Ph.D.
Manitoba Institute of Cell Biology, CancerCare Manitoba, University of Manitoba
100 Olivia St., Winnipeg, Manitoba, CANADA, R3E 0V9.
Tel: 204-787-2135
FAX: 204-787-2190
e-mail: smai@cc.umanitoba.ca

Key words: *ribonucleotide reductase*, replication, genomic instability, E-box, c-Myc

Abbreviations

2D: two-dimensional; 4-HT: 4-hydroxytamoxifen; bp: base pair(s); BrdU: bromodeoxyuridine; cDNA: DNA complementary to RNA; DABCO: diazabicyclo[2.2.2]-octane; DAPI: 4',6' diamidino-2-phenylindole; *DHFR*: gene encoding *dihydrofolate reductase* DTT: dithiothreitol; FITC: fluorescein isothiocyanate; EEs: extrachromosomal elements; EM: electron microscope; FISH: fluorescent *in situ* hybridization; HEPES: N-2-hydroxyethylpiperizine-N'-2-ethane sulphonic acid; international unit(s); kDa: kilodalton(s); LTR: long terminal repeat; Na_2EDTA: Ethylaminediaminetetraacetic acid, disodium salt; PBS: phosphate buffered saline (0.15 M NaCl, 1.4 mM NaH_2PO_4, 4.3 mM NaH_2PO_4, 0.015 M Na_3 citrate); *R2*: gene encoding *ribonucleotide reductase R2*; SCP: sodium citrate phosphate buffer; SDS: sodium dodecyl sulphate; SSC: standard sodium citrate (0.015 M sodium citrate, 0.15 M sodium chloride); TBE: trizma borate Na_2EDTA; TE: trizma Na_2EDTA; TXRD: texas red; QM; quinacrine mustard.

ABSTRACT

During c-Myc-dependent *ribonucleotide reductase R2* amplification, chromosomal and extrachromosomal amplicons are generated within 72 hours. The mechanism of c-Myc-induced *R2* amplification is unknown. We have examined four non-canonical E-box sequences present in the region flanking Exon VIII of mouse *R2*. These E-box sequences bind c-Myc/Max heterodimers *in vivo*. We demonstrate initiation of c-Myc-dependent *R2* re-replication 24 hours after Myc-ER™ activation in synchronized Pre-B cells *in vivo*. All four E-boxes are within the *R2* replication initiation zone and are part of c-Myc-driven re-replication. In cells where c-Myc deregulated we show enhanced BrdU uptake into Band A of mouse chromosome 12 that contains *R2*, suggesting that *R2* amplification is initialized during illegitimate *R2* re-replication. We describe a c-Myc-dependent, replication-driven mechanism for the initiation of *R2* gene amplification.

3.4.1. INTRODUCTION

Tumor cells can arise in healthy tissue following the accumulation of DNA lesions that may contribute a growth advantage to these cells (reviewed in Bishop, 1987; Vogelstein and Kinzler, 1993; Knudson, 1996). Genetic lesions can occur in the form of numerical chromosome aberrations, translocations, deletions, point mutations, as well as locus specific gene amplification. These lesions are capable of altering the expression of oncogenes and tumor suppressor genes. Genomic instability is also seen in repair- and tumor suppressor-deficient cells (Donner and Preston, 1996; Fukasawa *et al.*, 1997).

The focus of this work is gene amplification. Gene amplification is not found in normal cells (Fidler and Hart, 1982; Nowel, 1976; Tlsty *et al.*, 1989; Tlsty, 1990). When it does occur, gene amplification can be intrachromosomal and can be seen as Homogeneously Staining Regions (HSRs) or as Double Minutes (DMs) (Cowell, 1982; Schimke, 1988, 1992; Hamlin *et al.*, 1991; Stark, 1993). In many cases, these amplicons have been shown to carry oncogenes (Sanchez *et al.*, 1998; Kaira *et al.*, 1998), and drug resistance genes (reviewed in Von Hoff, 1991).

Gene amplification has been studied in *in vitro* models, where a large number of drug-resistant clones have been selected and isolated using a variety of cell cycle inhibiting drugs (Schimke 1988, Hamlin *et al.*, 1991; Knudson, 1986). The most common method of generating drug-resistant clones is through gene amplification by using drug selection methods that will amplify a target gene (Johnston *et al.*, 1983; Tlsty *et al.*, 1989). Gene amplification is thought to occur either through replication- or through segregation-driven mechanisms. Significant progress has been made in studying the early events that occur in drug-dependent gene amplification (Ma *et al.*, 1993; Singer *et al.*,

2000) however, the early events in oncogene-dependent gene amplification, are less well known, as is exemplified by a poor understanding of c-Myc dependent gene amplification.

c-Myc deregulation is now recognized as an important factor in initiating and promoting genomic instability that results in locus-specific gene amplification (Denis *et al.*, 1991; Mai, 1994; Mai *et al.*, 1996a, 1999, Kuschak *et al.*,1999a) and karyotypic instability (Mai *et al.*, 1996b; Felsher and Bishop, 1999).

c-Myc dependent gene amplification is associated with the binding of c-Myc/Max heterodimers to E-box motifs located on c-Myc target genes. c-Myc/Max heterodimers in cell-free extracts of proliferating cells were shown to bind to two adjacent 5'-flanking E-box motifs of the gene encoding murine *dihydrofolate reductase* (*DHFR*) (Mai and Jalava, 1994; Wells *et al.*, 1996) and four E-box motifs located in the 5'-flanking region of the murine *cyclin D2* gene (Mai *et al.*, 1994). In the *DHFR*-related studies, binding of c-Myc/Max heterodimers was correlated with cellular proliferation and DNA synthesis. Regulatable overexpression of c-Myc precedes enhanced binding of c-Myc/Max heterodimers to the 5'-flanking E-box motifs in both *DHFR* and *cyclin D2* genes and results in their amplification (Mai, 1994; Mai and Jalava, 1994; Mai *et al.*, 1996a, 1999). The amplification of the *DHFR* and *cyclin D2* genes results in enhanced expression of DHFR (Lücke-Huhle *et al.*, 1997) and cyclin D2 protein (Mai *et al.*, 1999). Our recent work (Kuschak *et al.*, 1999a) showed that under conditions of c-Myc deregulation, the *ribonucleotide reductase R2* gene locus is rearranged as well as chromosomally and extrachromosomally amplified.

This study focuses on the mechanism of c-Myc-dependent amplification of the mouse *R2* gene. We examined a cluster of four non-canonical E-box motifs spanning a region of 155 bp in intron VII, exon VIII, and at the exon VIII-intron VIII boundary of the *R2* gene. Our goal was to answer three questions. First, we wished to determine whether c-Myc/Max heterodimers are able to bind the four motifs located in the *R2* locus. Our data indicate that the *R2* E-box-containing oligonucleotides incubated in cell lysate from proliferating mouse NIH 3T3 cells, are able to bind c-Myc/Max heterodimers in *in vitro* gel shift experiments and the complex formation is disrupted in Myc-antibody experiments. We also showed complex formation with each of the E-box sequences using GST-Myc and GST-Max fusion proteins. Second, we wished to establish whether the Myc/Max-binding E-box regions serve as initiation zones for the initiation of DNA replication. We showed that each of the E-box motifs located in the regions flanking Exon VIII of the *R2* gene locus was part of the replication initiation zone in the mouse *R2* gene. Third, we wished to demonstrate a mechanism for c-Myc-dependent amplification of the *R2* gene locus. Using 2-dimensional gel electrophoresis followed by Southern analysis, we demonstrate c-Myc-dependent re-initiation of the *R2* replication cycle of the *R2* locus within 24 hours. To assess replication *in vivo*, we also assessed BrdU incorporation into the *R2*-containing band A of mouse metaphase chromosome 12. We showed increased incorporation of BrdU into band A of mouse chromosome 12 and this is indicative of a c-Myc-dependent increase in *R2* replication and amplification of the area where the *R2* gene is located.

Together, these data suggest a c-Myc-dependent, replication-driven initiation of *R2* amplification. This mechanism is reminiscent of the *onionskin* amplification model

initially proposed by Varshavsky (1981) and later substantiated (Mariani and Schimke, 1984; Stillman, 1996; Kearsey *et al.*, 1996). These data are the first to demonstrate an illegitimate re-replication phenomenon that occurs immediately following the regulatable transient deregulation of c-Myc.

3.4.2. METHODS AND MATERIALS

3.4.2.1. Cell Culture

3.4.2.1.1. Culture conditions and medium

In this study, we used a Pre-B cell line with a regulatable Myc-ER™ construct that can be experimentally upregulated by the addition of 4-hydroxytamoxifen (4-HT). This cell line was created as described in Mai *et al.* (1999) and was cultured as described in Kuschak *et al* (1999a).

Pre-B cells were synchronized in Select-amine™ (Canadian Life Technologies) isoleucine-depleted RPMI 1640 medium for 45-48 hours, followed by incubation for 12 hours in whole cell medium containing 400 μM L-mimosine (Sigma) (Wang *et al*, 1998).

3.4.2.1.2. Myc-ER™ activation

Synchronized Pre-B cells were activated immediately after seeding into whole cell medium. The 4-HT (Sigma), containing a minimum of 98% (Z) isomer, was dissolved 10 $mgmL^{-1}$ in 100 % ethanol and was used at a concentration of 0.5-1.0 μL per 10 mL of culture medium. The 4-HT-activated cells were designated Pre-B+. The non-activated Pre-B cells, designated Pre-B-, received an equal volume of 100 % ethanol.

Activation of the Myc-ER™ construct by 4-HT was monitored by preparation of cytospins from activated and non-activated control cells at 0, 1, 2, 4, and 6 hours after

activation. Cells were immunostained (Kuschak *et al.*, 1999a) using a Pan Myc (Genosys Clone M-911-94) primary antibody (1:1000) and the protein binding was visualized using a Texas Red (TXRD)-conjugated anti-mouse antibody IgG_1 (Southern Biotechnology Associates, Birmingham, USA). Measurements of increased nuclear c-Myc signal density (data not shown), was indicative of translocation of the Myc-ER™ construct from the cytoplasm to the nucleus and thus, successful Myc-ER™ activation. Photographs were made on a Carl Zeiss Axioplan2 (Carl Zeiss Canada) microscope using a 63x oil immersion lens. Images were captured on a digital (CCD) camera (Sony XC75). Density measurements were made using the area signal density application (Northern Eclipse, version 5.0 software package, Empix Imaging Inc., Mississauga, ON, Canada). Cells were used for experiments only if successful Myc-ER™ activation was shown.

3.4.2.2. DNA/Protein Interaction Experiments

3.4.2.2.1. Preparation of oligonucleotides containing Ribonucleotide Reductase R2 E-box motifs

E-box motif-containing *R2* oligonucleotides *R2-2*, *R2-3*, *R2-4*, and *R2-5* (Figure.3.4.1.) were prepared by Dr. Jose Garcia-Sanz (Basel Institute for Immunology, Basel, Switzerland) based on the *R2* gene cDNA sequence described in Thelander and Berg (1986). Preparation of *DHFRI* and *DHFRm* oligonucleotides (used as positive and negative controls, respectively), were prepared as described in Mai (1994). Oligonucleotides were labeled using a T4 polynucleotide kinase 5'-end labeling reaction (New England Biologicals) and γ-[^{32}P]-dATP (Amersham Pharmacia Biotech). Figure

3.4.1. illustrates the location of the E-boxes within the mouse *R2* gene that were examined during this study.

3.4.2.2.2. Gel Retardation Experiments

Gel retardation assays were performed on a 5% native polyacrylamide gel. Protein extracts were prepared from logarithmically growing NIH3T3 cells and protein concentrations were determined by the Bradford method (1976). We incubated the four ^{32}P-5'-end-labeled *R2* oligonucleotides and the ^{32}P-end-labeled *DHFRI* oligonucleotide in the absence or presence of 5 µg of NIH3T3 whole cell extracts. Assays were performed on a 5% native acrylamide gel. Gels were exposed overnight to Hyperfilm™ MP High Performance film (Amersham Pharmacia Biotech) at -75°C.

3.4.2.2.3. R2 Oligonucleotide Competition Experiments

Competition assays were performed on 5% native acrylamide gel. Protein concentrations used were as described for Gel Retardation Experiments (3.4.2.2.2.). Several independent competition assays were performed in which each of the four ^{32}P – 5'-end-labeled *R2* oligonucleotides was incubated with 5 µg of protein from NIH3T3 cell lysates plus 0 or 5-, 50-, and 100-fold molar excess of the other unlabeled oligonucleotides (*R2-2*, *R2-3*, *R2-4*, or *R2-5*, respectively). These competition experiments were also performed with the point-mutated, unlabeled *DHFR* oligonucleotide, *DHFRm*. Electrophoresis experiments were performed on a 5% native acrylamide gel and exposed as described above.

3.4.2.2.4. Antibody Experiments

We incubated each of the four ^{32}P-γ-dATP-5'-end-labeled *R2* oligonucleotides *R2-2, R2-3, R2-4, R2-5* with 1 μg NIH3T3 protein plus increasing concentrations (0, 1, 2, 5, 7, 10, 12, and 15 μg) of Pan-Myc Clone M-911-94 (Genosys), or 12 μg of control antibodies [anti-c-Fos (Clone (4)-G, Santa Cruz), anti-USF-1 (Clone 20, Santa Cruz) or anti-Mxi-1 (anti-Mad 2, Clone 17, Santa Cruz)]. The reactions were electrophoresed on a 5% native acrylamide gel was exposed as described above.

3.4.2.2.5. Gel Shifts with GST-Myc and GST-Max Fusion Proteins

Other gel shift experiments were performed using isopropyl β-D thiogalactoside-(IPTG) induced glutathione transferase (GST) Myc and Max fusion proteins generated in *E.coli* bacteria. Their growth and induction are described in Mai and Mårtensson (1995). Each of the four *R2* oligonucleoides was end-labeled (described above), and incubated in the presence of either (i) 1 μg of cell lysate from non-induced bacteria, (ii) 1 μg of bacterial cell lysate from GST-Myc-expressing bacteria, (iii) 1 μg of bacterial lysate from GST-Max-expressing bacteria, or (iv) 1 μg of cell lysate from each of GST-Myc- and Max-expressing bacteria, respectively. The reactions were run on a native 8% acrylamide gel and the gels were exposed to Kodak BIOMAX MR Scientific Imaging film at –75°C.

3.4.2.3. 2-Dimensional Gel Electrophoresis

3.4.2.3.1. 2D Electrophoresis of Pre-B- and Pre-B+ Genomic DNA

Genomic DNA was isolated from synchronized, non-activated or 4-HT activated cells by standard procedures. The DNA was phenol:chloroform (1:1), then chloroform extracted (Chloroform was purchased from Fisher Scientific, Trizma buffer–saturated

phenol (pH 8.0) was purchased from Canadian Life Technologies). The DNA was treated with 100 μg mL^{-1} RNaseA (Roche Diagnostics) for 1 hour at 37°C and re-extracted as described above. DNA concentrations were measured spectrophotometrically at λ = 260 nm. 100 μg of each DNA sample was digested overnight at 37°C with *Hin*dIII restriction endonuclease (Roche Diagnostics) and then rotoevaporated to a final volume of approximately 40 μL. The samples were electrophoresed under neutral/neutral conditions in two dimensions. The first dimension was run overnight at 20V into a 0.4% agarose (Canadian Life Technologies), room temperature, and the second dimension was run into a 1.0% agarose gel at 200 V, at 4°C for 4 hours (see Dijkewel *et al.*, 1991). The gels were washed and blotted as described in Kuschak *et al.* (1999a).

3.4.2.3.2. Probing of 2D Gel Blots

The probes used for the analysis of *R2* replication forks were as follows: A 1487 bp *Pst*I *R2* cDNA (Thelander and Berg, 1986) fragment was radiolabeled by random priming (Roche Diagnostics) using α-[^{32}P]-dCTP from Amersham Pharmacia Biotech. The *R2* oligonucleotides (Figure 1) (kindly provided by Dr. Josie Sanz-Garcia, Basel Institute for Immunology, Basel Switzerland), corresponding to regions of the *R2* gene containing E-box motifs were ligated into longer segments using DNA ligase enzyme (New England Biologicals) and labeled by random priming with α-[^{32}P]-dCTP (Amersham Pharmacia Biotech). Southern blots probed with the *R2* cDNA were hybridized as described in Kuschak *et al.* (1999a). Hybridization of these blots with radiolabeled oligonucleotide probes was performed at 42°C in a (pre)hybridization solution (5x Denhardt's Solution, 5x SSC, 0.1% SDS). The blots were washed at 42°C for 15 minutes in 2x SSC, 0.1% SDS followed by a 15 minute wash at 42°C in 1x SSC,

0.1% SDS. Probed membranes were exposed to Hyperfilm™ MP High Performance film (Amersham Pharmacia Biotech.) at -75°C.

3.4.2.4. Bromodeoxyuridine Incorporation Analyses

3.4.2.4.1. BrdU Incorporation into Cultured Cells

Bromodeoxyuridine (BrdU) incorporation assays to assess DNA replication in whole cells following c-Myc deregulation were conducted in synchronized, non-activated Pre-B cells. Prior to cytospinning cells onto slides for immunostaining, the cells were treated with 10 μM bromodeoxyuridine (Sigma) for 15 minutes under normal culture conditions. BrdU incorporation assays were conducted following 45-48 hours incubation in ILE- medium and after 12 hours of incubation in medium containing 400 μM L-mimosine. BrdU incorporation was assessed in these synchronized cells that were incubated in the presence of 4-HT or the equivalent volume of 100% ethanol for 0, 24, 48, and 72 hours. The incorporation of BrdU into the replicating DNA was assayed by immunostaining with a mouse monoclonal anti-BrdU antibody (Becton Dickenson) described below in Section 3.4.2.4.3. Parallel cytospins were prepared at all synchronization stages and at all time points described above to assess c-Myc levels during cell cycle synchronization and after Myc-ER activation. Myc levels were assessed by immunohistochemical staining as described in Section 3.4.2.1.2.

3.4.2.4.2. BrdU Incorporation into Chromosomes

Metaphase chromosomes were prepared (as described by Mai *et al.*, 1999) from non-activated and 4-HT-activated Pre-B cells following synchronization 24 hours after addition of ethanol (control) or 4-HT. This time point was selected following the results of the 2D gel electrophoresis showing that the *R2* gene re-replicates 24 hours after c-Myc

deregulation. Prior to metaphase chromosome preparation the cells were incubated in the presence of 10 μM BrdU for 30 minutes under normal cell culture conditions, after which they were pelleted, washed, and resuspended in B cell medium for an additional 24 hours. They were allowed to incubate in medium for another 24 hours in order to allow the chromosomes which had incorporated BrdU to reach metaphase in the cell cycle. The cells were then harvested and metaphase chromosomes were prepared (Mai, 1999).

3.4.2.4.3. Immunostaining of Whole Cells for BrdU Incorporation

A modified protocol of Leonhardt *et al.* (1992) was used for quantitative fluorescent immunostaining of BrdU. The staining was performed using monoclonal anti-BrdU (Becton Dickinson) diluted 1:5 in lamb serum that was diluted to 5% ($^{v}/_{v}$) in PBS + 1.5 mM $MgCl_2$ + 1 mM $CaCl_2$, pH 7.4 ($PBS^{\dagger}$). The signal was amplified by staining with a secondary anti-mouse IgG_1 TXRD-conjugated antibody (Southern Biotechnology Associates, Birmingham, USA) diluted 1:400 in 5% serum in $PBS^{\dagger}$. Photographs were made on a Carl Zeiss Canada Axioplan 2 microscope (Carl Zeiss Canada) using a 63x oil immersion lens. Images were acquired on a Sony (XC75) charge coupled device (CCD) camera. Roughly 100-500 live cells were counted from each sample. Cells incorporating BrdU were counted and percentages were calculated as a function of the total number of live cells in the field.

3.4.2.4.5. Chromosome Painting and Immunostaining of Metaphase Chromosomes for BrdU Incorporation.

Metaphase chromosomes that were incubated with BrdU were painted with a biotinylated mouse chromosome 12-specific paint and also immunostained to detect BrdU incorporation into the chromosomes. Chromosome 12-specific paint (Cambio,

Cambridge, UK) was applied according to manufacturer's recommendations and then detected with mouse anti-biotin antibody (Boehringer Mannheim, Mannheim, Germany) (10 ngμL^{-1}). The signal was again amplified by staining with a Texas Red (TXRD)-conjugated goat anti-mouse IgG_1 antibody (2.5 ngμL^{-1}) (Southern Biotechnology Associates, Birmingham, USA).

Images of the TXRD-stained chromosomes 12 and DAPI-stained metaphase chromosome spreads were acquired using a Carl Zeiss Axiophot microscope and a Photometrics CCD camera (model CH250/a), as described for acquisition of fluorescent *in situ* hybridization images in Kuschak *et al.* (1999a). Following image acquisition, the chromosomes were stained for BrdU incorporation as described in section 3.4.2.4.3. for whole cells except that no formaldehyde fixation was required and 0.2% Triton X-100 treatment was omitted. BrdU was detected using FITC-conjugated anti-BrdU (Becton Dickinson, San Jose, USA) primary antibody (diluted 1:5), followed by secondary staining with rabbit anti-FITC (Cambio, Cambridge, UK) (25 ngμL^{-1}). The latter was detected by tertiary antibody staining using FITC-conjugated goat anti-rabbit IgG (H and L) antibody (Pierce, Rockford, USA) (25 ng μL^{-1}).

3.4.2. RESULTS

To examine the role of the c-Myc protein on the *ribonucleotide reductase R2* gene we conducted a series of experiments to learn about interaction of c-Myc with the *R2* gene and especially with the E-box sequences flanking Exon VIII. Specifically we wanted to know whether c-Myc could physically interact with the R2 gene and whether the E-box motifs were putative c-Myc/Max binding sites. We studied interactions of

protein lysates from proliferating NIH 3T3 cells with each of the *R2* oligonucleotides and studied the specificity of their interaction. Moreover, we determined that c-Myc was able to interact with the *R2* oligonucleotides in *in vivo* experiments. We also showed interaction with each of the oligonucleotides with GST-Myc and GST-Max fusion proteins.

The aims of our experiments were also to establish the mechanism of c-Myc dependent amplification of the *ribonucleotide reductase R2* gene locus. Henriksson and Lüscher (1996) and Li and Dang (1999) describe a role for c-Myc in proliferation and DNA replication. Classon *et al.* (1987) demonstrated that c-Myc facilitates SV40 DNA replication in human lymphocytes. Since SV40 viral DNA replication is controlled by cellular machinery, c-Myc plays a role in the replicative process. Our previous work showed the c-Myc deregulation resulted in *R2* amplification and our current gel shift experiments showed c-Myc interaction with *R2* oligonucleotides. For this reason we examined the possibility of a replication-driven mechanism as opposed to a segregation-driven mechanism of *R2* amplification. We chose to examine the re-replication and amplification mechanism using bromodeoxyuridine incorporation experiments (Leonhardt *et al.*, 1992) and 2D gel electrophoresis and Southern analysis experiments (Wang *et al,*. 1998). Bromodeoxyuridine incorporation data revealed that Pre-B+ cells took up more BrdU 24 and 48 hours after c-Myc deregulation than did the Pre-B- cells. Moreover, we showed a significant difference in the amount of BrdU taken into Pre-B+ cell band A of mouse chromosome 12, where the *R2* gene is located. Using 2D gel electrophoresis we showed the initiation of re-replication of the *R2* gene locus within 24

hours of transient c-Myc deregulation. Moreover, we showed that each of the *R2* oligonucleotides was part of the re-replication initiation zone for *R2* re-replication.

3.4.2.1. DNA/Protein Interaction Experiments

3.4.2.1.1. Gel Retardation Experiments Demonstrate Protein Interaction with R2 Oligonucleotides

Gel shift experiments were performed in order to assess whether or not any of the non-canonical E-box sequences found in the region flanking Exon VIII were capable of forming specific DNA/protein complexes. Cell lysate was prepared from proliferating NIH3T3 and incubated with each of the four *R2* oligonucleotides. Figure 3.4.2 (a) shows a representative gel shift analysis where, in the presence of cell lysate from proliferating NIH3T3, each of the *R2* oligonucleotides (Figure 3.4.1.) and a positive control, *DHFRI* (Mai and Jalava, 1994), is bound by protein(s). Black arrows indicate formation of complexes between the oligonucleotides and the NIH 3T3 protein. No complexes were formed in the absence of cell lysate.

3.4.3.1.2. R2 Oligonucleotides Successfully Compete for Protein Binding

Competition experiments with ^{32}P-5'-end-labeled *R2-3* and each of the *R2* oligonucleotides were performed in order to assess the capacity of each of the oligonucleotides to bind the same proteins specifically. Figure 3.4.2.(b) is a representative figure showing the incubation of ^{32}P-5'-end-labeled *R2-3* oligonucleotide in the presence or absence of NIH3T3 protein and either 0, or 5-, 50-, and 100-fold molar excess of unlabeled *R2-2*, *R2-3*, *R2-4*, and *R2-5*, respectively. The DNA/protein complex, or lack there of following competition, is indicated by the black arrow. This figure also shows *R2-3* in competition with a point-mutated unlabeled *DHFR* oligonucleotide,

DHFRm. Note the ability of each of the *R2* oligonucleotides and *DHFRI*, but not *DHFRm* (Mai and Jalava, 1994), to successfully compete away proteins that bind *R2-3*. Competition assays performed with each of the four *R2* oligonucleotides showed that each was able to successfully compete away protein from the radio-labeled probe, as is true for each of the other *R2* oligonucleotides (data not shown).

3.4.3.1.3. DHFRI/Protein Complexes are Disrupted by R2 Oligonucleotides

Competition experiments with ^{32}P-5'-end-labeled *DHFRI* and each of the *R2* oligonucleotides were performed in order to assess the capacity of each of the oligonucleotides to bind the same proteins specifically. Figure 3.4.2.(c) shows the incubation of ^{32}P-5'-end-labeled *DHFRI* oligonucleotide in the presence or absence of NIH3T3 protein and either 0, or 5-, 50-, and 100-fold molar excess of unlabeled *R2-2*, *R2-3*, *R2-4*, *R2-5*, and the point mutated *DHFRm* (Mai and Jalava, 1994), respectively. This experiment showed that molar excesses of each of the *R2* oligonucleotides, except for *DHFRm*, were able to disrupt complex formation between *DHFRI* and the cell lysate. The DNA/protein complex, or lack thereof following competition, is indicated by the black arrow.

3.4.3.1.4. c-Myc Antibody Disrupts R2 Oligonucleotide/Protein Complex Formation in Gel Shift Experiments

Gel shift experiments following functional depletion of c-Myc were performed using an anti-c-Myc antibody in order to determine if c-Myc was one of the proteins that forms complexes with the *R2* oligonucleotides. Figure 3.4.2. (d) shows the formation of a DNA/protein complex when the oligonucleotide *R2-3* is incubated in the presence of 1 μg of NIH3T3 cell lysate alone (lane 3). The figure shows the of disruption of a *R2-3*/protein

complex in increasing amounts of anti-c-Myc antibody, but not when the complex is incubated in the presence of anti-Mxi-1, anti-c-Fos, or anti-USF. Formation of DNA/protein complexes are indicated by the black arrow. These data are similar in experiments with each of the *R2* oligonucleotides and show that in each experiment, the *R2* oligonucleotides form a complex with a protein or proteins, one of which is c-Myc, but not with proteins such as Mxi-1, c-Fos, or USF. In the experiment with *R2-3*, the protein complex is completely disrupted following the addition of ≥7 μg of anti-c-Myc antibody. Complexes with *R2-2*, *R2-4*, and *R2-5* are disrupted following coincubation of ≥7 μg, ≥5 μg, and ≥7 μg of anti-c-Myc antibody, respectively (data not shown). In addition to this it is important to note that no complex disruption was seen in the control antibody incubations with anti-Mxi-1, anti-USF, or anti-c-Fos, demonstrating specificity of interaction of the c-Myc protein with the E-box sequence.

3.4.3.1.5. GST-Myc and GST-Max Fusion Proteins Bind to R2 Oligonucleotides

Gel shift experiments with GST-Myc and GST-Max fusion proteins were performed in order to confirm the capacity for each of the *R2* oligos to interact with c-Myc and Max proteins alone. Figure 3.4.2.(e) shows the incubation of the *R2* oligonucleotides in the presence of DH5α *E.coli* bacteria that were grown in the presence or absence of ITPG-induced GST-Myc or GST-Max fusion proteins, or both Myc and Max fusion proteins together. Each gel shift shows that each of the fusion proteins alone (lanes 3 and 4) are able to form a DNA protein complex (shown by the black arrow) as are the Myc and Max fusion proteins together (lane 5). These data are consistent for *R2-3*, *R2-4*, and *R2-5*. Each of which form complexes in the presence of GST-Myc alone, GST-Max alone and in the presence of both GST fusion proteins. The complex formation

in lane 5, where the oligonucleotide is incubated in the presence of both GST-Myc and GST Max is weak in each experiment. The experiment was repeated at least 5 times however, complexes were not as strong as complexes in lanes with GST-Myc or GST-Max alone. This is unusual and not presently understood, since strong complexes with GST-Myc and GST Max have been seen in the presence of both canonical and non-canonical E-box sequences (Mai and Mårtensson ,1995).

3.4.3.2. *R2* Replication in Synchronized Pre-B- and Pre-B+ Cells.

3.4.3.2.1. Assessment of Nuclear c-Myc Levels in Synchronized Pre-B- and Pre-B+ Cells

Figure 3.4.3 Panel A illustrates c-Myc levels in c-Myc-inducible Pre-B cells incubated in the absence or presence of 4-HT. Figure 3.4.3. Panel A (a) and (b) show representative Pre-B- and Pre-B+ cells, respectively, immunostained with a mouse pan-Myc antibody and visualized by amplification with a Texas Red- (TXRD) conjugated goat anti-mouse IgG_1 antibody. These cells are photographed 1 hour after activation with ethanol (control cells) and 4-HT. Figure 3.4.3. Panel A (c) illustrates the results of three immunostaining experiments for nuclear c-Myc levels. As expected from G_1/S arrest, the immunostaining assays indicated that c-Myc was present in the nuclei of cells in spite of their arrest and synchronization following incubation in isoleucine-depleted and mimosine-containing media. Following seeding into complete medium c-Myc levels temporarily decreased, followed by increases in nuclear c-Myc levels that occur between 1 and 4 hours after release into whole cell medium. Following this increase of the c-Myc levels in the 1-4 hours time range, the levels diminish through the 6 hour time point.

Figure 3.4.3. Panel B illustrates the results of three experiments of immunostaining for nuclear c-Myc levels from the ILE- medium through to the 72 hour time point. Immunostaining revealed that c-Myc was present in the nuclei of cells in spite of their arrest and synchronization following incubation in isoleucine-depleted and mimosine-containing media, (6149 ± 189 and 4230 ± 416 relative fluorescent intensity (RFI) units, respectively). The levels of c-Myc in the Pre-B- and Pre-B+ cells at 0 hours were nearly equivalent (5188 ± 366 *vs.* 4774 ± 16 RFI, respectively). At 24 hours and at 48 hours, nuclear c-Myc levels in the Pre-B- cells were lower than in the Pre-B+ cells (5976 ± 358 and 7880 ± 675 *vs.* 5044 ± 231 RFI and 6539 ± 1640 RFI, respectively). At 72 hours, the c-Myc levels in the Pre-B- cells had increased, while nuclear c-Myc levels in the Pre-B+ cells had diminished 7837 ± 1134 vs. 6296 ± 1538 RFI, respectively). For time points measured up to 48 hours after c-Myc activation, our data indicate that nuclear c-Myc levels in 4-HT activated cells were elevated, however, only the levels at 24 hours are significantly different. Using a Student's t test, we computed a value of $p<0.005$ with 3 degrees of freedom, indicating that the differences in nuclear c-Myc levels in the 4-HT-activated cells are significantly different from the c-Myc levels in the non-activated cells at the 24 hour time point. The 0, 48, and 72 hour time points were not significantly different.

Figure 3.4.4. Panels A and B illustrate the results of the BrdU incorporation experiments beginning at the time of seeding into whole medium at 0 hours through to the 72 hour time point. Representative photos shown in Figure 3.4.4. Panel A (a) and (b) depict the difference between L-mimosine-treated cells that were not replicating their DNA and those that are replicating their DNA. Figure 3.4.4. Panel A (a) shows no BrdU

incorporation into cells following 12 hour incubation in L-mimosine-containing medium. In contrast, Figure 3.4.4. Panel B (b) shows synchronized cells 24 hours after activation with 4-HT.

Figure 3.4.4. Panel B summarizes the BrdU incorporation data. These data show the average intensity of fluorescent signals that are indicative of BrdU incorporation over each of the experimental time points, beginning with BrdU incorporation following incubation in isoleucine-depleted medium, through to the 72 hour time points in both Pre-B- and Pre-B+ cells. The plots show that there is no BrdU following the arrest and synchronization steps (Figure 3.4.4. Panel B (a) and (b)), and little at the point where the cells are seeded into whole medium (Figure 3.4.4. Panel B (c) and (d)). Our Student's t test analysis of bromodeoxyuridine incorporation data revealed that Pre-B+ cells took up more BrdU 24 hours after c-Myc deregulation than Pre-B- cells did and that the difference in uptake was significant ($p<0.005$) (Figure 3.4.4. Panel B (e) and (f)). At 48 hours, Pre-B+ cells also showed greater BrdU uptake than Pre-B- cells ($p<0.001$) (Figure 3.4.4. Panel B (g) and (h)). At 72 hours after seeding into whole medium the Pre-B- and Pre-B+ cells all contained BrdU signal, though the intensities are lower in each case. There are no significant differences in the amount of BrdU incorporated into Pre-B- and Pre-B+ cells at the 72 hour time point (Figure 3.4.4. Panel B (i) and (j)).

3.4.3.3. 2-Dimensional Gel Electrophoresis and Southern Analysis of Pre-B- and Pre-B+ Cells

3.4.3.3.3.1. 2D Gel Electrophoresis and Southern Analysis of Synchronized Pre-B- and Pre-B+ Genomic DNA

Genomic DNA isolated from cells harvested from synchronized Pre-B- and Pre-B+ cells at 0, 24, 48, and 72 hours after seeding into whole medium was digested with *Hin*dIII and electrophoresed in two dimensions as described in the methods. *Hin*dIII was chosen for these experiments since it leaves the active *R2* gene uncut following digestion (Thelander and Berg, 1986). Figure 3.4.5. Panel A (a-f) shows 2D gel electrophoresis and Southern analyses of Pre-B- (a-d) and 4-HT-activated (e-h) Pre-B+ cells at 0, 24, 48, and 72 hours after synchronizing and introduction into whole medium. The membranes were probed with an *R2* cDNA fragment. This panel of figures indicates that the *R2* gene in both Pre-B- and Pre-B+ cells replicates within 24 hours of resuspension into whole medium. The black arrows in the figures indicate replication and re-replication forks. The Pre-B- cells show no replication at 0 hours (Figure 3.4.5. Panel A (a)) and a single replication fork can be seen from the active *R2* gene in Figure3.4.5. Panel A (b). Pre-B- cells show continued replication at 48 (Figure 3.4.5. Panel A (c)), and 72 hours (Figure 3.4.5. Panel A (d)). The Pre-B+ cells show no replication at 0 hours (Figure 3.4.5. Panel A (e)). The Pre-B+ cells show multiple replication forks (black arrows) at 24 hours (Figure 5 Panel A (f)) and continued replication at 48 hours (Figure 3.4.5. Panel A (g)), and 72 hours (Figure 3.4.5. Panel A (h)). The 0 hour time points in both Pre-B- and Pre-B+ are identical, showing no replication, as expected. Of interest is the fact that the 72 hour time point in the Pre-B- cells resembles the Pre-B- and Pre-B+ 0 hour time points

however, the 72 hour time point of the Pre-B+ cells shows amplification and a definite increase in the amount of *R2* signal detected. This indicates that the non-activated Pre-B cells had undergone a single DNA replication cycle per cell cycle and have what appears to be unaltered amounts of *R2* gene copies in the cell. In contrast, the 4-HT-activated Pre-B+ cells have initiated illegitimate rereplication of their *R2* gene locus at 24 hours. The continual and progressive increase in the amount of *R2* signal observed at the 48 and 72 hours shows that the *R2* gene locus was not only re-replicated at the 24 hour time point, but that it is also amplified. This is in agreement with our previous findings (Kuschak *et al.*, 1999a). We probed the membranes with a control gene, *insulin growth factor 2* (*IGF2*)(data not shown) (Kitsberg *et al.*, 1993). This gene was selected as a control because the maternal and paternal alleles replicate at different times during the cell cycle. Our hybridization indicates that *IGF2* does not replicate at the same time as *R2* (data not shown).

Next, we assessed whether the *R2* E-box motifs (Figure 3.4.1.) are part of the DNA replication initiation zones in the *R2* gene. Each of the membranes from the 2D gel electrophoresis and Southern blot of Pre-B- and Pre-B+ cell genomic DNA harvested at 0, 24, 48, and 72 hours was probed with each of the *R2* oligonucleotides (Figure 3.4.1.). The 2D gel electrophoresis experiments and Southern blots for *Hin*dIII-digested Pre-B- genomic DNA is shown in Figure 3.4.5. Panel B (a-d). The 2D gel electrophoresis experiments and Southern analyses for *Hin*dIII-digested Pre-B+ genomic DNA are shown in Figure 3.4.5. Panel B (e-h). Each of the four oligonucleotides was used to probe the membranes, but only *R2-5* is shown here as a representative of these results. Figure 3.4.5. Panel B (a)) shows that there was no replication at the 0 time point. At the 24 time point

there was no evidence of replication originating from any of the E-box motifs probed with the *R2* oligonucleotides (Figure 3.4.5. Panel B (b)). There was no evidence of DNA replication at the 48 and 72 hours ((Figure 3.4.5. Panel B (c) and (d)). In contrast, probing of the Pre-B+ 2D gel electrophoresis Southern blots clearly showed that there are multiple replication forks originating in the regions flanking Exon VIII of the *R2* gene ((Figures 3.4.5. Panel B (e-f)). The probing of the Pre-B+ 0 time point membrane also showed no replication. Figure 3.4.5. Panel B (f) clearly shows multiple replication forks originating from the region probed by each of the *R2* oligonucleotides and represented by oligonucleotide *R2-5*. There was no evidence of replication occurring at the 48 and 72 hour time points of the Pre-B+ membranes ((Figures 3.4.5. Panel B (g, h)).

3.4.3.4. BrdU Incorporation into Chromosomes to Assess Gene Amplification

Synchronized Pre-B cells were treated with ethanol (control) or 4-HT immediately after release into whole medium. After 24 hours, these cells were pulsed for 30 minutes with 10 μM BrdU and then resuspended in fresh medium for another 24 hours after which they were harvested for chromosome preparation. Based on our 2D gel electrophoresis experiment data, we expect to see a greater uptake of BrdU into Band A, the region of chromosome 12 in mouse Pre-B+ cells where the *R2* locus is located (Figure 3.4.6. (a)).

We assessed the effect of Myc-ER™ activation on the replicative profile of the Pre-B+ cell as compared to the non-activated Pre-B- population. We counted metaphases in a total population of approximately 800 Pre-B- and Pre-B+ cells. Our counts showed a metaphase index of 1.7% in the Pre-B- cells and a metaphase index of 3.4% in Pre-B+ cells. The two-fold increase of metaphase numbers is indicative of transient c-Myc

deregulation (data not shown) and further substantiates the role of c-Myc in proliferation (Henriksson and Lüscher, 1996) and replication (Li and Dang, 1999).

Our analysis of chromosomal BrdU incorporation into Band A of mouse chromosome 12 revealed a broad range of uptake in the chromosomes we examined in Pre-B- and Pre-B+ cells. Some chromosomes 12 showed nearly equivalent, but never equal, uptake of BrdU into both chromatids of chromosome 12 in many of the Pre-B- and Pre-B+. Others showed large differences between the chromatids of a single chromosome (Figure 3.4.6. (d)) metaphases. A number of Pre-B- (Figure 3.4.6. (b) and (d)) and Pre-B+ (Figure 3.4.6. (c) and (d)) metaphases showed greater differences in BrdU uptake between chromatids, suggesting a preferential uptake of BrdU into one of the two chromatids. The chromatids displaying increased BrdU uptake are shown by the white arrows in Figure 3.4.6. (b) and (c) and in the graphs shown in Figure 3.4.6. (d). Line measurements of BrdU intensities analyzed by non-parametric Krushall Wallis test comparing the normalized ratios showed significantly higher BrdU incorporation into Band A of Pre-B+ alleles than Pre-B- alleles ($p<0.048$). These data suggest that the deregulation of c-Myc results in significantly higher incorporation of BrdU into cells where the c-Myc protein levels are deregulated. Especially significant is the increased BrdU incorporation into Band A of chromosomes 12 of cells where c-Myc is transiently overexpressed. These data are consistent with the *R2* re-replication data demonstrated in our current work as well as with our previous studies (Kuschak *et al.*, 1999a).

3.4.4. Discussion

Genomic instability is considered to be a major driving force of multistep carcinogenesis. It plays a crucial role in the initiation and progression of a variety of

different cancers and that most cancers may be genetically unstable. Gene amplification is the most extensively studied form of genomic instability and has been described frequently in cultured cells and in tumors that have been treated with drugs (Stark 1993; Schimke *et al.*, 1978). The amplification of genes has also been demonstrated following constitutive growth factor expression in cultured cells (Huang and Wright, 1994; Huang, *et al.*, 1994, Huang *et al.*, 1995), or after DNA damage (Tlsty *et al.*, 1989; Lücke-Huhle *et al.*, 1987, 1991; Lavi 1981).

c-Myc is a multifunctional protein that plays a pivotal role in the cell. c-Myc deregulation has been previously shown to cause the locus-specific amplification of a number of target genes, namely *DHFR* (Mai, 1994, Mai *et al.*, 1996), *Cyclin D2*, (Mai *et al.*, 1999), *CAD* (Fukasawa *et al.*, 1997), and *ribonucleotide reductase R2* (Kuschak *et al.*, 1999a).

Our previous study (Kuschak *et al.*, 1999a) showed that the *R2* gene was chromosomally and extrachromosomally amplified and rearranged within 72 hours of inducible and transient deregulation of c-Myc. This study describes the mechanism of c-Myc-dependent amplification of the *ribonucleotide reductase R2* gene. We have shown, for the first time, that the c-Myc induced amplification of *R2* occurs through a replication driven mechanism. This is suggestive of a re-replication mechanism reminiscent of the *onionskin* model proposed by Varshavsky (1981) and later by others (Mariani and Schimke, 1984; Stillman, 1996 and Kearsey *et al.*, 1996). Moreover, we demonstrate that a cluster of 4 non-canonical E-box motifs located in the flanking regions of ExonVIII in the *R2* gene are a part of the initiation zone of *R2* re-replication. It suggests that the interaction of c-Myc/Max heterodimers with the non-canonical E-box motifs in the *R2*

gene in *in vitro* assays and the involvement of these motifs in the initiation zone of *R2* re-replication may be linked. Bromodeoxyuridine incorporation into metaphase chromosomes indicates a significant increase in the uptake of BrdU into Band A of mouse chromosome 12 in c-Myc deregulated cells.

The controlled expression of c-Myc is followed by the initiation of DNA replication. c-Myc and Max heterodimers bind to the E-box motifs (Blackwell *et al.*, 1993) and take part in the replication of the *R2* gene locus in a controlled manor. When the replication has been initiated in S phase, c-Myc levels would be declining and their potential to influence replication would be insignificant. In contrast, if c-Myc were constitutively expressed or transiently deregulated, as it is in our model, the replication cycle of *R2* might continue. The initial binding and replication would give rise to two daughter strands of DNA, which would also have E-box motifs following the generation of a replication bubble. The E-box motifs on these two daughter strands would be bound by c-Myc/Max heterodimers, and the replication would begin again (*i.e.* re-replication), giving rise to another set of replication initiation bubbles. The latter set of replication bubbles may be "on top" of the initial replication bubbles (for review see Stark *et al.*, 1989; Stark and Wahl, 1989), or they may be an onionskin, as proposed by Varshavsky (1981) and later by Mariani and Schimke, 1984; Stillman, 1996; Kearsey *et al.*, 1996. The cycle could continue, generating multiple re-replication bubbles within the *R2* gene locus. The deregulated expression of c-Myc would allow for sustained interaction of c-Myc with E-box motifs in the presence of all of the licensing factors that are required (and normally present) for DNA replication (for reviews see Chevalier and Blow, 1996; Thommes and Blow, 1977; Tada and Blow, 1998). It is possible that when normal DNA replication has

been completed, several cycles of replication of c-Myc target genes such as *R2* have occurred simultaneously. When the normal replication has been completed and the cell is ready to divide, the licensing factors that are present for the replication are depleted and the aberrant replication process is also terminated. Thus, within the time the cell has legitimately replicated the majority of its DNA once, several cycles of illegitimate DNA re-replication have also occurred, giving rise to the amplification of the *R2* gene locus and potentially other c-Myc dependent amplification targets. *R2* is an early gene in the replication cycle and its initial replication cycle is completed well before the rest of the genome has completed its replication. It may have the opportunity to replicate at least once more before the cell completes the normal round of DNA replication. Overall, this suggests a re-replication phenomenon that can initiate with a small deviation in c-Myc levels.

In conclusion, these data indicate that the transient deregulation of c-Myc is followed by the earliest events examined to date in the amplification process of the mouse *ribonucleotide reductase R2* gene. Our data show evidence of re-replication of the *R2* gene locus within 24 hours of c-Myc deregulation. Overall, we demonstrate a role for c-Myc in the initiation of *ribonucleotide reductase R2* amplification that occurs through a replication-driven mechanism.

REFERENCES

Bishop JM. (1987). *Science* 235: 305-311.

Blackwell, T.K., Huang, J., Ma, A., Kretzner, L., Alt, F.W., Eisenman, R.N., and Weintraub, H. (1993). *Mol. Cell. Biol.* 13: 5216-5224

Bradford, M.M. (1976). *Anal Biochem.* 72: 248-254.

Chevalier, S. and Blow, J.J. (1996). *Curr. Opin. Cell. Biol.* 8: 815-821.

Classon, M., Henrikson, M., Klein, G., and Hammaskjold M-L. (1987). *Nature* 330: 272-274.

Cowell, J.K. (1982). *Annu. Rev. Genet. 16*: 21-59.

Denis N, Kitzis A, Kruh J, Dautry F and Crocos D. (1991) Oncogene, 6, 1453-1457.

Dijkwel, P.A., Vaughn, J.P., and Hamlin, J.L. (1991). *Mol. cell. Biol.* 11: 3850-3859.

Donner, E.M. and Preston, R.J. (1996). *Carcinogenesis* 17: 1161-1165.

Fidler and Hart, I.R. (1982). Oncodev. Biol. Med. 4: 161-176.

Felsher, D.W., and Bishop, J.M. (1999). *Proc. Natl. Acad. Sci. USA*. 96: 3940-3944.

Hamlin, J.L., Leu, T.H., Vaughn, J.P., Ma, C., and Dijkwel, P.A. (1991). *Prog. Nucleic Acids Res. Mol. Biol.* 41: 203-239.

Huang A, and Wright JA. (1994). Exp. Cell. Res.,213, 335-339.

Huang A, Jin H, Wright JA. (1994). Oncogene, 9, 491-499.

Huang A, Jin H, Wright JA. (1995) *Cancer Res.*, 55, 1758-1762.

Johnston, R.N., Beverley, S.M., and Schimke, R.T. (1983). *Proc. Natl. Acad. Sci. USA* 80: 3711-3715.

Kaira, P., James, C.D., and Leffak, M. (1998). *Gene* 221: 101-108.

Kearsey, S.E., Labib, K., and Maiorano, D. (1996). *Curr. Opin. Genet. Dev.* 6: 208-214.

Kitsberg, D., Selig, S., Brandeis, M., Simon, I., Keshet, I., Driscoll, D.J., Nicholls, R.D.,and Cedar, H. (1993). *Nature* 364: 459-463.

Knudson, A.G., Jr. (1986). *Annu. Rev.Genet.* 20: 231-251.

Knudson, A.G. (1996). *J. Can. Res. Clin. Oncol.* 122: 135-140.

Kuschak, T.I., Taylor, C., McMillan-Ward, E., Israels, S., Henderson, D.W., Mushinski, J.F., Wright, J.A., and Mai, S. (1999a). *Gene* **238**: 351-365.

Kuschak, T.I., Paul, J.T., Mushinski, J.F., Wright, J.A., and Mai, S. (1999b). Technical Tips Online, <http://www.biomednet.com/db/tto> t01669.

Lavi, S., 1981. *Proc. Natl. Acad. Sci. USA.* 78, 6144-6148.

Lücke-Huhle C and Herrlich P. (1991). Int. J. Cancer, 47, 461-465.

Lücke-Huhle C, Mai S and Moll J. (1997). *Int. J. Radiat. Biol.* 71: 167-175.

Ma C, Martin S, Trask B, Hamlin JL. (1993). *Genes Dev.* 7: 605-620.

Mai S. (1994). *Gene*, 148, 253-260.

Mai, S., Hanley-Hyde, J., and Fluri, M. (1996) Oncogene, 12: 277-288.

Mai, S., Hanley-Hyde J., Rainey J., Kuschak, TI, Fluri M., Taylor C., Littlewood T.D., Mischak H., Stevens L.M., Henderson D.W., and Mushinski J.F. (1999) *Neoplasia*, 1: 241-252.

Mai, S. and Jalava, A. (1994). *Nucl. Acids Res.* 22: 2264-2273.

Mai, S. and Mårtensson, I-L. (1995). *Nucl. Acids. Res.* 23: 1-9.

Mariani, B.D. and Schimke, R.T. (1984). *J. Biol. Chem.* 259: 1901-1910.

Nowel, P.C., (1976). *Science* 194: 23-28.

Prody, C.A., Dreyfus, P., Zamir, S.M., Zakut, H., and Soreq, H. (1989) *Proc. Natl. Acad. Sci. USA* 86: 690-694.

Sanchez, A.M., Barrett, J.T., and Schoenlein, P.V. (1998). *Cancer Res.* 58: 3845-3854.

Schimke, R.T. (1988). *J. Biol. Chem.* 263: 5989-5992.

Schimke, R.T. (1992). *Mut. Res.* 276: 145-149.

Singer, M.J., Mesner, L.D., Friedman, C.L., Trask, B.J., and Hamlin J.L. (2000). *Proc. Natl. Acad. Sci. USA.* 97: 7921-7926.

Smith, K.A., Agarwal, M.L., Chernov, M.V., Chernova, O.B., Deguchi, Y., Ishizaka, Y., Patterson, T.E., Poupon, M.F., and Stark, G.R. (1995). *Philos. Trans. R. Soc. London B* 347: 49-56.

Stark, G.R., Debatisse, M., Guilotto, E., and Wahl, G.W. (1989). *Cell* 57: 901-908.

Stark, G.R and Wahl, G.W. (1989). *Annu. Rev. Biochem.* 53: 447-491.

Stark, G.R. (1993). *Adv. Cancer Res.* 61: 87-113.

Stillman, B. (1996). Science. 274:1659-6164.

Tada, S. and Blow, J.J. (1998). *Biol Chem.* 379: 941-949.

Thommes, P. and Blow, J.J. (1997). *Cancer Surv.* 29: 75-90.

Thelander L and Berg P. (1986) *Mol. Cell. Biol.* 6: 3433-3442.

Tlsty, T.D., Margolin B.H., and Lum, K. (1989). *Proc. Natl. Acad. Sci. USA* 86: 9441-9445.

Tlsty, T.D. (1990). *Proc. Natl. Acad. Sci. USA* 87: 3132-3136.

Varshavsky, A. (1981). *Proc. Natl. Acad. Sci. USA* 78: 3673-3677.

Vogelstein, B. and Kinzler, K.W. (1993). *Trends Genet.* 9: 138-141.

Von Hoff, D. (1991). *Cancer Treat Res.* 57: 1-11.

Wang, S., Dijkwel, P.A., and Hamlin, J. (1998). *Mol. Cell. Biol.* 18: 39-50.

Wells J, Held P, Illeye S and Heintz NH. (1996). *Mol. Cell. Biol.* 16: 634-647.

Wright, J.A., Smith, H.S., Watt, F.M., Hancock, M.C., Hudson, D.L., and Stark, G.R. (1990). *Proc. Natl. Acad. Sci. USA* 87: 1791-1795.

FIGURE LEGENDS

Figure 3.4.1. The *R2* gene locus carries non-canonical E-box motifs.

Legend: The schematic shows the structure of the *R2* gene and location of E-box motifs (*R2-2*, *R2-3*, *R2-4*, and *R2-5*). The expanded area shows the 5'-end of Intron VII, Exon VIII, and the 3'-end of Intron VIII. The array of E-box sequences spans a total length of 155 bp. The 25-bp oligonucleotide sequences containing the E-box motifs are represented by the double headed arrows and are drawn relative to their location within the *R2* gene. *R2-2* is in intron VII and spans 4161-4185 bp with the E-box sequence beginning at nucleotide 4170 bp. *R2-3*, which overlaps with the 3'-end of *R2-2*, is located between 4781-4805 bp, and the E-box sequence begins at 4189 bp. *R2-4* bridges the intron VII/Exon VIII boundary spanning from 4816-4840 bp. The E-box motif, beginning at bp 4826, is contained within exon VIII. The *R2-5* oligonucleotide spans 4916-4940 bp, bridging the exon VIII/intron VIII boundary. This E-box sequence is divided in half by the exon VIII/intron VIII boundary, beginning at 4922 bp. The distances between the four E-box sequences are 20, 38 and 97 bp respectively.

Figure 3.4.1. The *R2* gene locus carries non-canonical E-box motifs.

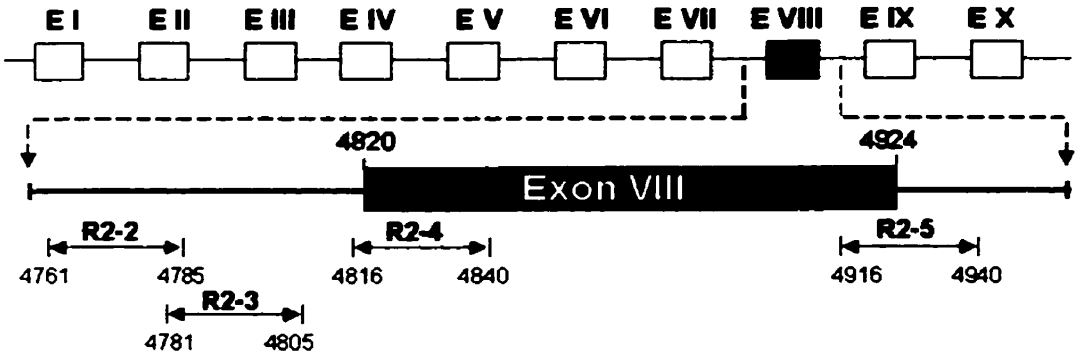

R2-2: 5'-TAAGTCATG**CATGTG**AACAGTAGAG-3'

R2-3: 5'-TAGAGCCC**CACGGTG**ACCTTGAACG-3'

R2-4: 5'-CTAGGGTTTA**CACTGTG**ACTTTGCC-3'

R2-5: 5'-ATAGAG**CAGGTG**AGTGACTGCGTGC-3'

Figure 3.4.2. (a) **Binding study shows that R2 oligonucleotides form DNA/protein complexes with NIH3T3 lysate.**

protein	−	+	−	+	−	+	−	+	−	+
hot oligo	R2-2		R2-3		R2-4		R2-5		DHFRI	
lane	1	2	3	4	5	6	7	8	9	10

Legend: This figure shows the binding of the four ^{32}P-5'-end-labeled *R2* oligonucleotides and the ^{32}P-5'-end-labeled *DHFRI* oligonucleotide to proteins present in the NIH3T3 cell extract. The *R2* oligonucleotides were loaded in the absence (lanes 1, 3, 5, 7) or presence of 5 μg of cell extract (lanes 2, 4, 6, and 8). *DHFRI* was loaded into lanes 9 and 10 in the absence (lane 9) and presence (lane 10) of protein. The arrow indicates the position of a DNA/protein complex that is common to all four *R2* oligonucleotides and the *DHFRI* oligonucleotide. Reactions were performed at room temperature and run on a 5% native acrylamide gel (see Method and Materials).

Figure 3.4.2. (b) ***R2*** **oligonucleotides successfully compete for proteins in competition assays.**

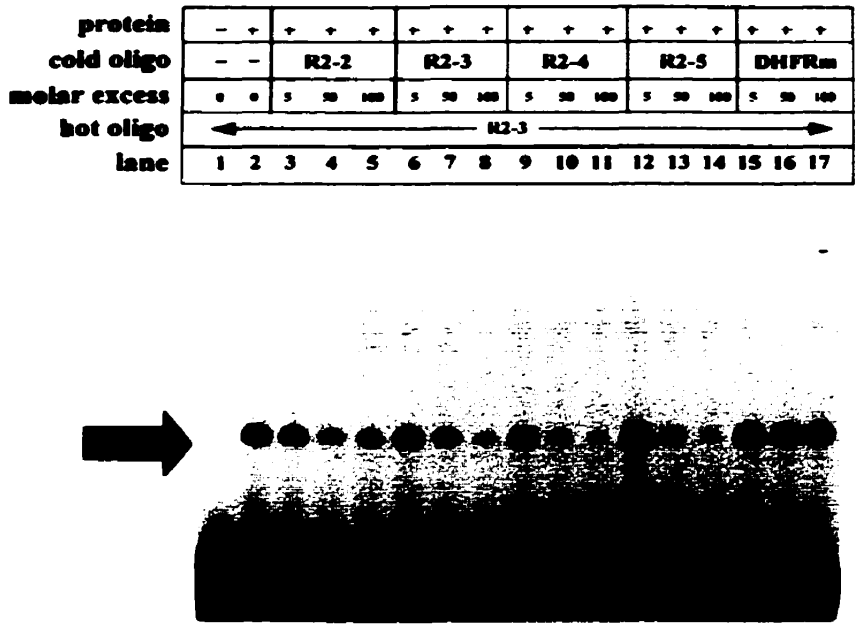

Legend: This figure is representative of several independent competition assays in which each of the four ^{32}P-5'-end-labeled *R2* oligonucleotides was incubated with 5 μg of protein from NIH3T3 cell lysates and increasing amounts of the other three unlabeled oligonucleotides. This figure shows the incubation of ^{32}P-5'-end-labeled *R2-3* oligonucleotide with protein and each of the other *R2* oligonucleotides. Lane 1 shows the migration of *R2-3* alone. Lane 2 shows the *R2-3* oligonucleotide in the presence of protein extract alone. Lanes 3-5 show *R2-3* (and protein extract) in competition with 5-, 50-, and 100-fold molar excess of unlabeled *R2-2*. Similarly, lanes 6-8, 9-11, and 12-14 show *R2-3* in competition with 5-, 50-, and 100-fold molar excess of unlabeled *R2-3*, *R2-4* and *R2-5*, respectively. Lanes 15-17 show *R2-3* in competition with a point-mutated unlabeled *DHFR* oligonucleotide, *DHFRm*. Reactions were incubated at room temperature and run out on 5% native acrylamide gel (see Methods and Materials).

Figure 3.4.2. (c) ***R2* oligonucleotides successfully compete proteins away from *DHFRI* oligonucleotide.**

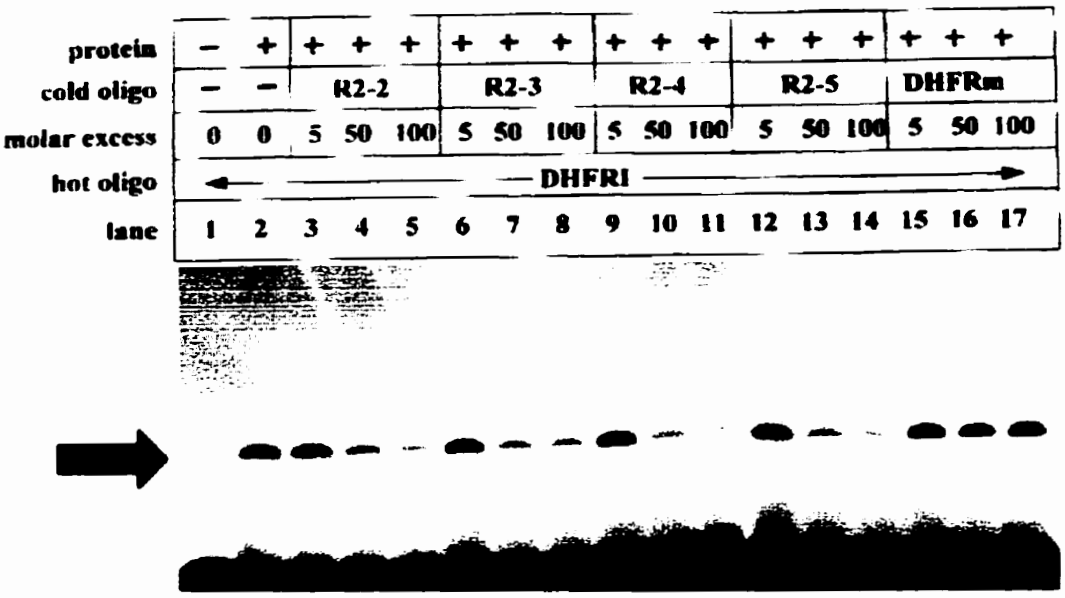

Legend: This figure shows the result of incubating ^{32}P-5'-end-labeled oligonucleotide *DHFRI* with 5 μg NIH3T3 protein, the four *R2* oligonucleotides, and the point mutated *DHFR* oligonucleotide, *DHFRm*. *DHFRI* and *DHFRm* are oligonucleotides that have been previously characterized (Mai, 1994). Lane 1 shows the incubation of the *DHFRI* with neither cold oligonucleotide competitors, nor protein extract. Lane 2 shows the *DHFRI* in the presence of protein extract alone. Lanes 3-5 show *DHFRI* in competition with protein extract and 5-, 50-, and 100-fold molar excess of unlabeled *R2-2*. Similarly, lanes 6-8, 9-11, 12-14 and 15-17 show *DHFRI* (and protein extract) in competition with 5-, 50-, and 100-fold molar excess of unlabeled *R2-3*, *R2-4*, *R2-5*, and *DHFRm*, respectively. The arrow indicates complex formation. Reactions were incubated at room temperature and run out on 5% native acrylamide gel (see Methods and Materials).

Figure 3.4.2. (d) Anti-c-Myc antibody disrupts *R2* oligonucleotide/protein complex formation.

Legend: Figure 3.4.2.(d) shows a gel shift assays with oligonucleotide *R2-3* and is representative of similar assays with oligonucleotides *R2-2*, *R2-3*, *R2-4*, and *R2-5*, respectively. Figure 2d depicts gel shift assays where protein complexes formed by NIH3T3 cell lysate and ^{32}P-γ-dATP-labeled *R2* oligonucleotides are disrupted by incubation with increasing concentrations of anti-c-Myc antibody. Lane 1 contains radiolabeled *R2* probe alone. Lane 2 contains anti-c-Myc antibody alone. Lanes 3-11 contains an *R2* oligonucleotide, 1 μg NIH3T3 lysate and 0, 1, 2, 5, 7, 10, 12 or 15 μg of anti-c-Myc antibody. Lanes 12-17 are incubated with control antibodies. Lanes 12 and 13 are incubated with an *R2* oligonucleotide, and 12 μg of anti-Max antibody. Lane 12 contains no protein and lane 13 contains 1 μg NIH3T3 cell lysate. Similarly, lanes 14 and 15 are incubated with an *R2* oligonucleotide, and 12 μg of anti-Mxi-1 antibody. Lane 14 contains no protein and lane 15 contains 1 μg NIH3T3 cell lysate. Similarly, lanes 16 and 17 are incubated with an *R2* oligonucleotide, and 12 μg of anti-Fos antibody. Lane 16 contains no protein and lane 17 contains 1 μg NIH3T3 cell lysate. In each of the figures, the black arrow indicates complex formation and the lack of a band signifies disruption of complex formation between c-Myc/Max and the *R2* oligonucleotide by the anti-c-Myc antibody.

Figure 3.4.2. (d) **Anti-cMyc antibody disrupts *R2* oligonucleotide/protein complex formation**

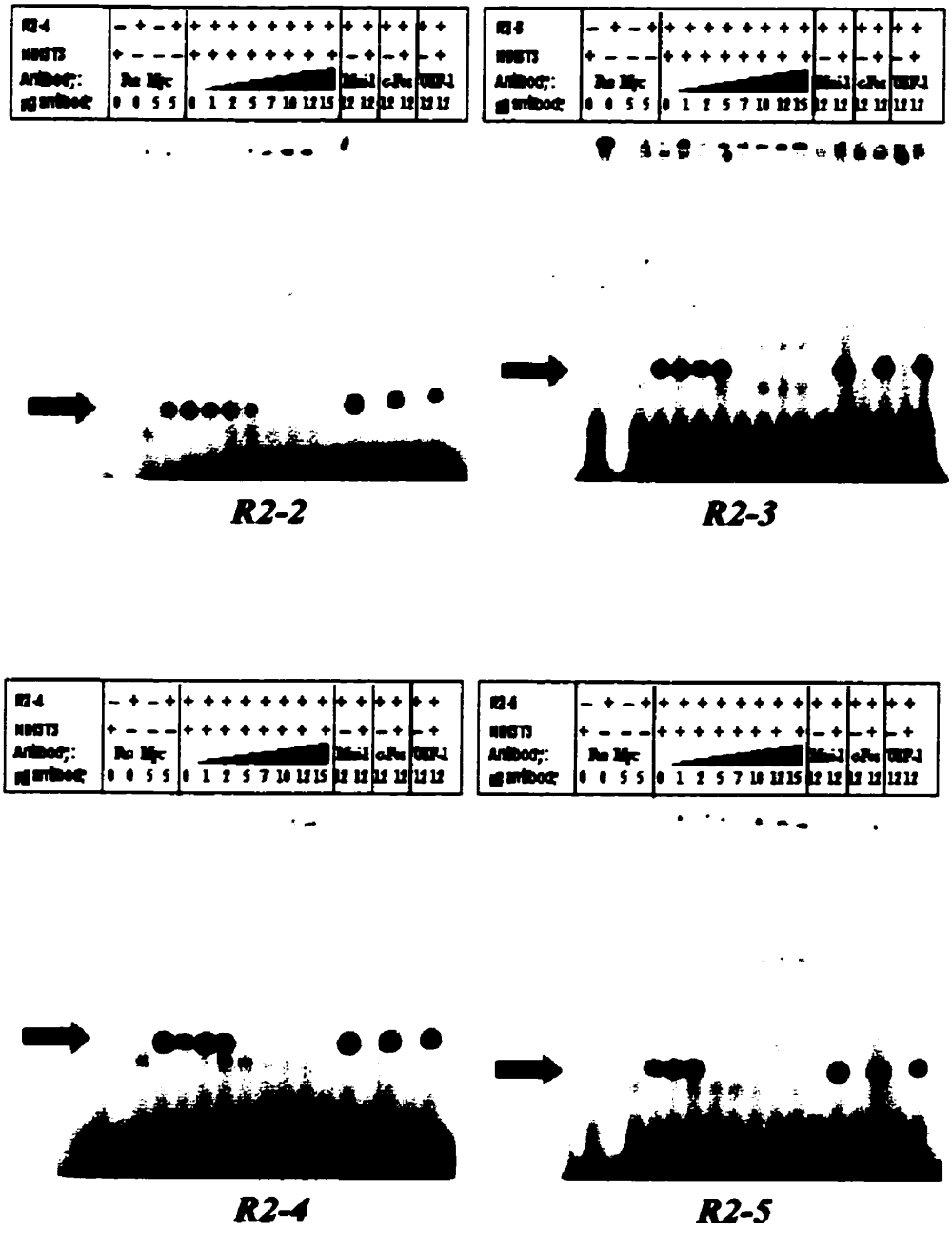

Figure 3.4.2. (e) ***R2* oligonucleotides form complexes with GST-Myc and GST-Max fusion proteins.**

Legend: This figure shows a gel shift with each of the four *R2* oligonucleotide and GST-Myc and GST-Max fusion proteins. The *R2* oligonucleotide was incubated alone (lane 1), or with 1 μg of DH5-α *E.coli* (lane 2) or 1 μg GST-Myc fusion protein (lane 3), or 1 μg GST-Max fusion protein (lane4) or 1 μg of each of GST-Myc and GST-Max fusion proteins (lane 5). The black arrow indicates complex formation between the *R2* oligonucleotide and either Myc (lane 3), Max (lane 4) or Myc/Max (lane 5).

Figure 3.4.2. (e) **Gel Shift Assay with GST-Myc and GST-Max Fusion Proteins**

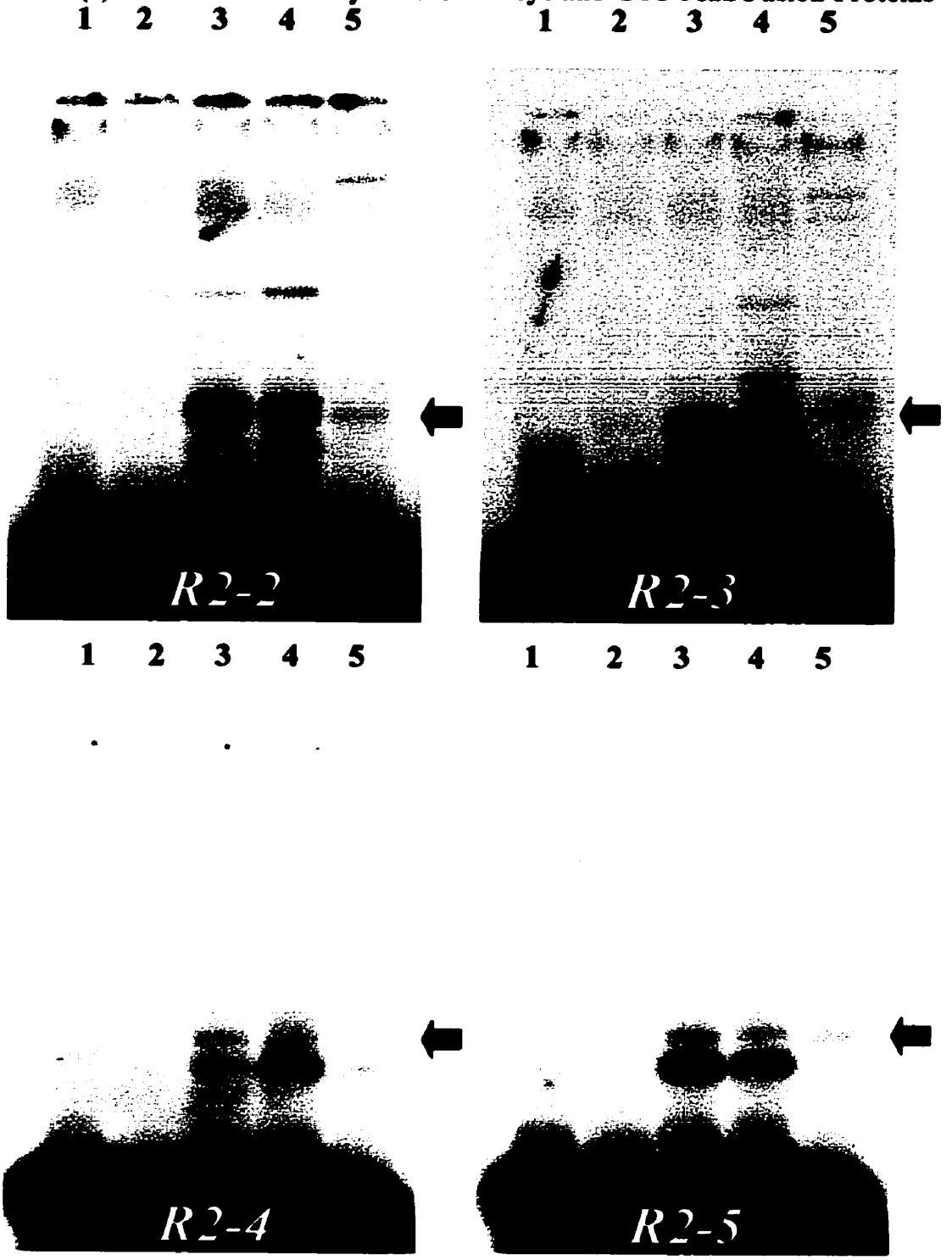

Figure 3.4.3. Panel A (a) and (b) Nuclear c-Myc levels are elevated in Pre-B+ cells.

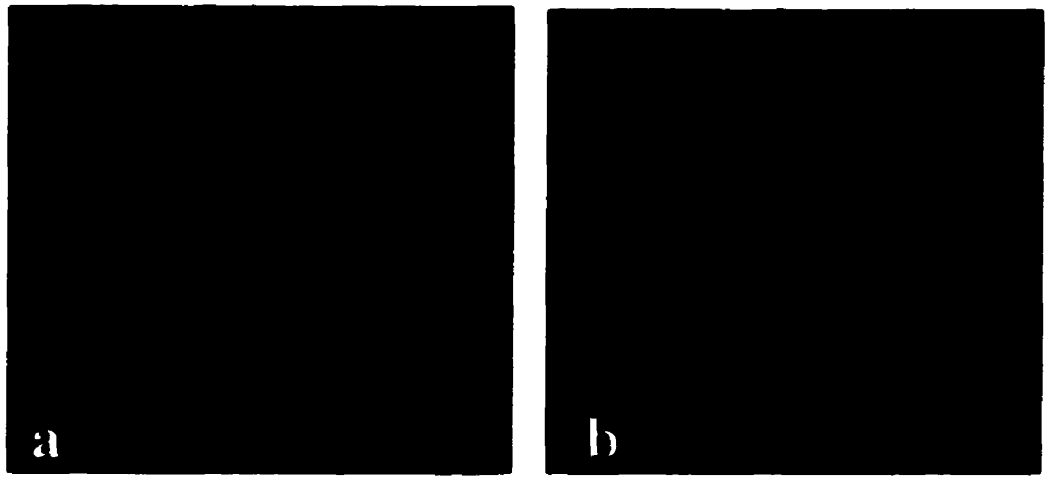

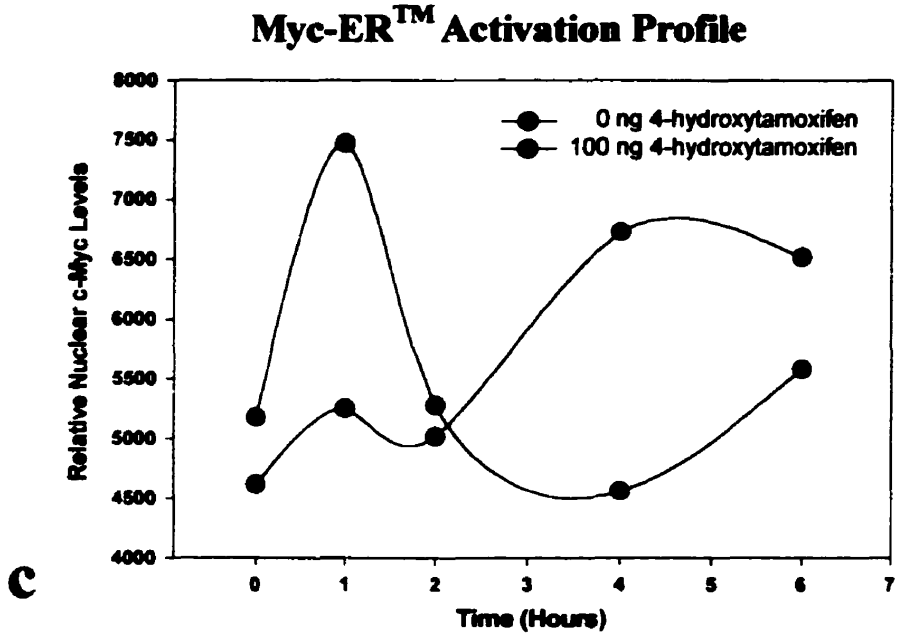

Legend: Figure 3.4.3. Panel A shows nuclear c-Myc levels after ethanol or 4-HT activation. c-Myc levels are visualized as a red signal in the nucleus of each cell at 1 hour after treatment with ethanol (Pre-B-) shown in (a) or 100 nM 4-HT (Pre-B+) shown in (b). Nuclear c-Myc profiles in Pre-B- cells and Pre-B+ cells at 0, 1, 2, 4, and 6 hours after treatment with ethanol or 4-HT are shown in Figure 3.4.3. Panel A (c).

Figure 3.4.3. Panel B **Nuclear c-Myc levels during and after synchronization and up to 72 Hours after Myc-ER™ activation.**

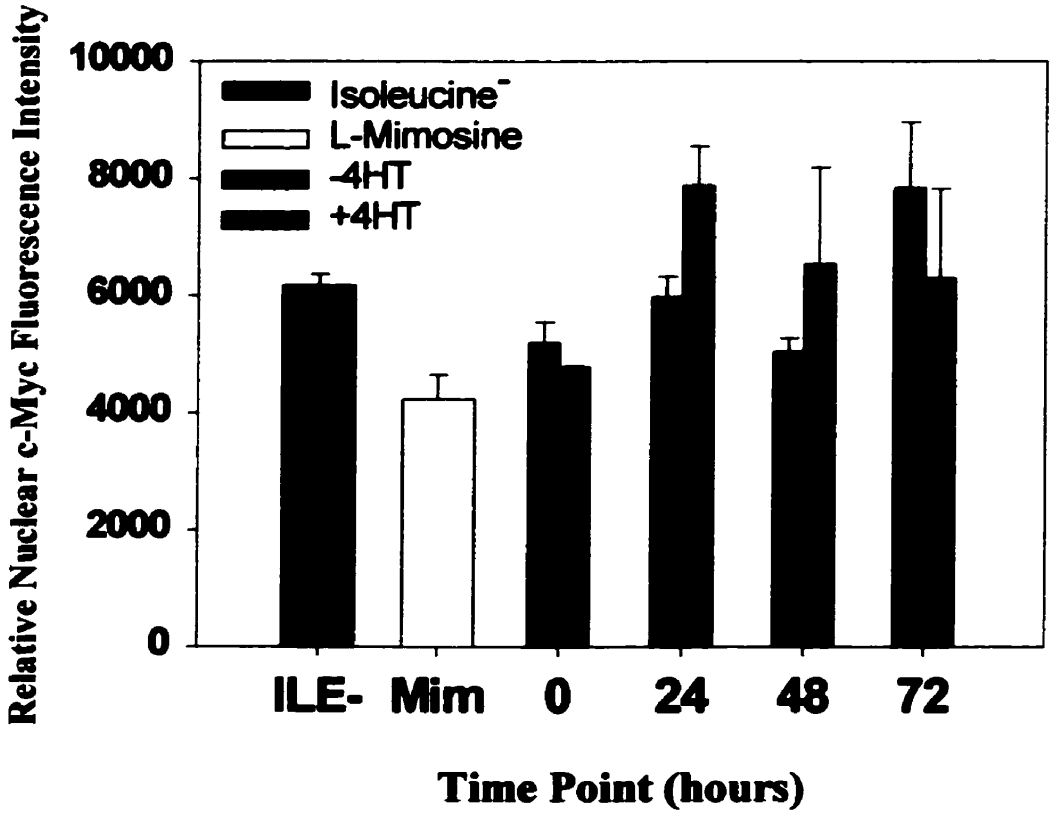

Legend: Figure 3.4.3. Panel B illustrates nuclear c-Myc levels during the synchronization steps and during the 0, 24, 48, and 72 hour time points for Pre-B- and Pre-B+ cells. A student t test of triplicate assays from each time point indicates that none of the c-Myc levels are significantly different between Pre-B- and Pre-B+ at 0, 24, at 72 hours. However, nuclear c-Myc values are significantly higher in Pre-B+ cells than in Pre-B- cells ($p<0.005$) at the 24 hour time point.

Figure 3.4.4. Panel A **BrdU incorporation: L-Mimosine-synchronized cells show no DNA replication, but Pre-B+ cells show DNA replication 24 hours after Myc-ER™ activation.**

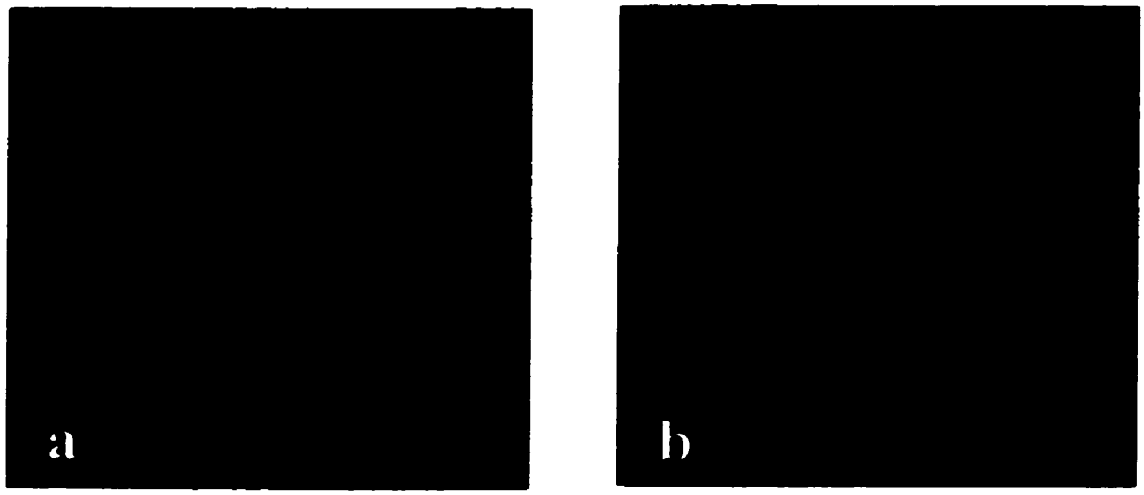

Legend: Figure 3.4.4. Panel A shows representative BrdU incorporation results for cells that are synchronized and not replicating their DNA following incubation in 400 mM L-mimosine (a) and cells at the 24 hour time point and are in normal medium and have been activated with 4-HT (b). Cells where no BrdU has been incorporated appear with blue nuclei, indicating the presence of DAPI, which stains only the DNA. Cells where BrdU has been incorporated appear with punctate red dots.

Figure 3.4.4. Panel B BrdU incorporation profiles

Legend: Figure 3.4.4. Panel B (a-j) are scatter plots which depict the BrdU incorporation levels into individual cells. Each dot represents a cell and its relative average fluorescence intensity level that is indicative of BrdU incorporation. (a) depicts BrdU incorporation levels of cells after 45-48 hours of incubation in isoleucine-depleted medium and (b) depicts BrdU incorporation levels of cells after 12 hours of incubation in medium containing 400μM L-mimosine. (c) and (d) depict relative BrdU intensity levels into Pre-B- and Pre-B+ cells, respectively at cells at 0 hours after delivery into whole medium and mock activation with ethanol. Similarly, (e) and (f), (g) and (h), and (i) and (j) illustrate average relative BrdU intensity levels in Pre-B- and Pre-B+ cells at 24, 48, and 72 hour time points, respectively.

1.4. Panel B BrdU incorporation profiles

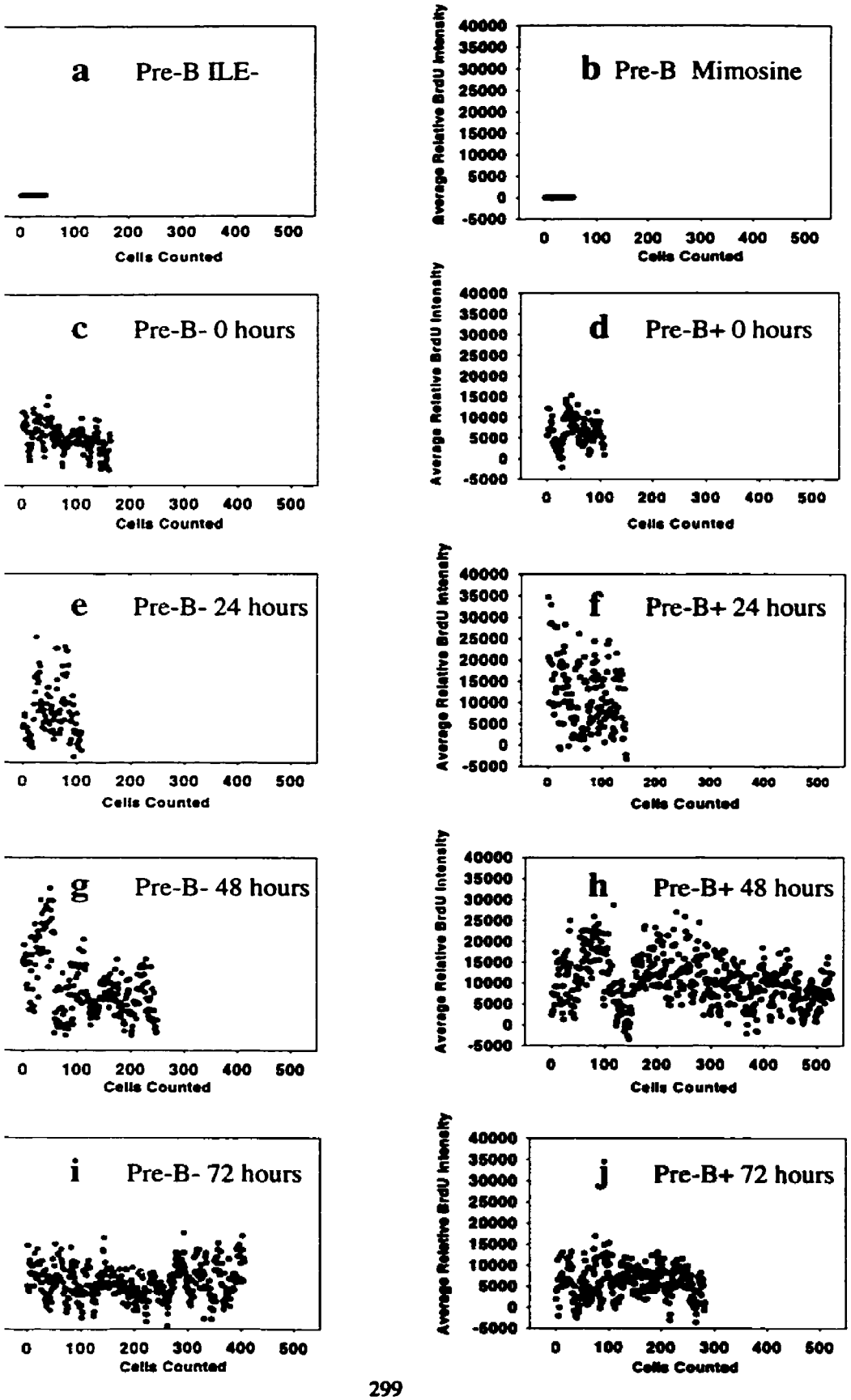

Figure 3.4.5. Panel A 2D gel electrophoresis and Southern analysis of synchronized Pre-B+ cell genomic DNA shows R2 re-replication at 24 hours.

Legend: This figure shows 2D gel electrophoresis and Southern analyses of non-activated (a-d) and 4-HT-activated (e-h) Pre-B cells at 0, 24, 48, and 72 hours after synchronizing and introduction into whole medium. The membranes were probed with a 1487 bp *PstI R2* cDNA fragment. The red arrows in the figures indicate replication and re-replication forks at 24 hours in the Pre-B- and Pre-B+ cells, respectively. Following hybridization and washing, the membranes were exposed to film for 7 days at –75 °C.

Figure 3.4.5. Panel A **2D gel electrophoresis probed with *R2* cDNA**

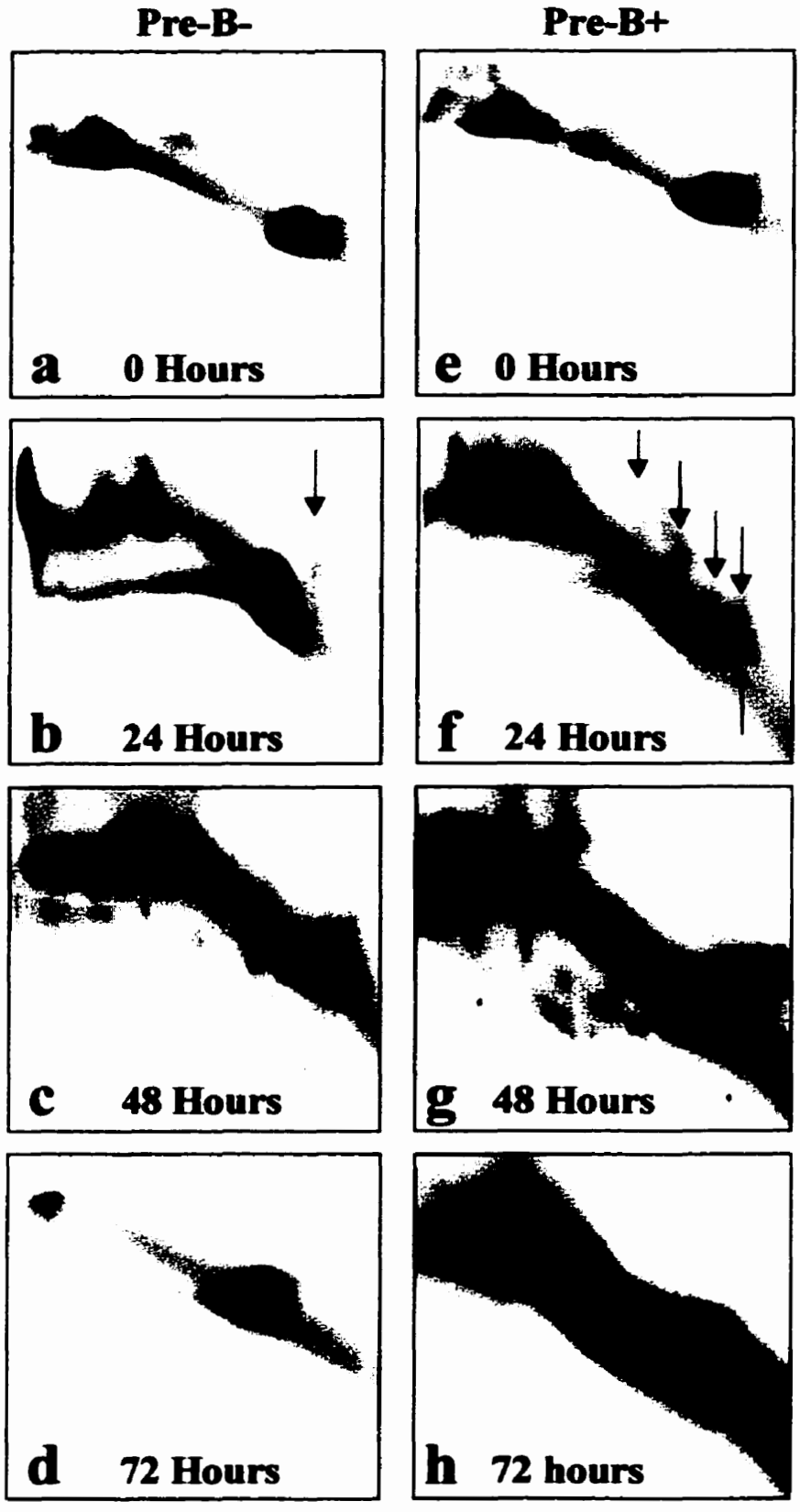

Figure 3.4.5. Panels B-E Pre-B- and Pre-B+ genomic DNA Southern blots separated by 2D gel electrophoresis and probed with *R2* oligonucleotides.

Figure 5 Panel B (a-h) shows 2D gel electrophoresis and Southern analyses of Pre-B- (a-d) and 4-HT-activated (e-h) Pre-B+ cells at 0, 24, 48, and 72 hours after synchronizing and introduction into whole medium. These membranes were probed with radiolabeled *R2-2*. The red circles indicate the area of multiple replication forks in Pre-B+ cells at the 24 hour time point. These membranes were also hybridized with *R2-3*, *R2-4*, and *R2-5* and are shown in Figure 5 Panels C (a-h), D (a-h), and E (a-h), respectively. In each of these panels, the red circles indicate multiple replication forks in the Pre-B+ DNA at 24 hours following activation with 4-HT. Following hybridization and washing, the membranes were exposed at –75 °C for two weeks, since the probes were random-primed 20-mers that gave very weak signals. For this reason, the autoradiograms were scanned and the brightness and contrast was adjusted in each case to show the hybridization signals.

Figure 3.4.6. (a) The location of the *R2* gene on the ideogram of mouse chromosome 12

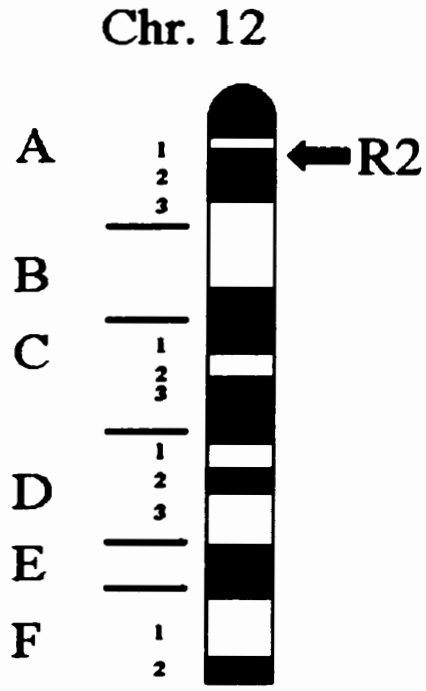

Legend: Figure 3.4.6. (a) shows an ideogram of mouse chromosome 12. The *ribonucleotide reductase R2* gene, indicated by the arrow, is located in Band A of chromosome 12.

This figure was modified from ***Resources for Molecular Cytogenetics***, University of Bari, Italy, (http://bioserver.uniba.it/fish/Cytogenetics/welcome.html).

Figure 3.4.6. (b) and (c) Texas Red- and BrdU-stained mouse chromosomes 12: Mouse Pre-B+ chromosomes 12 show increased BrdU incorporation into Band A

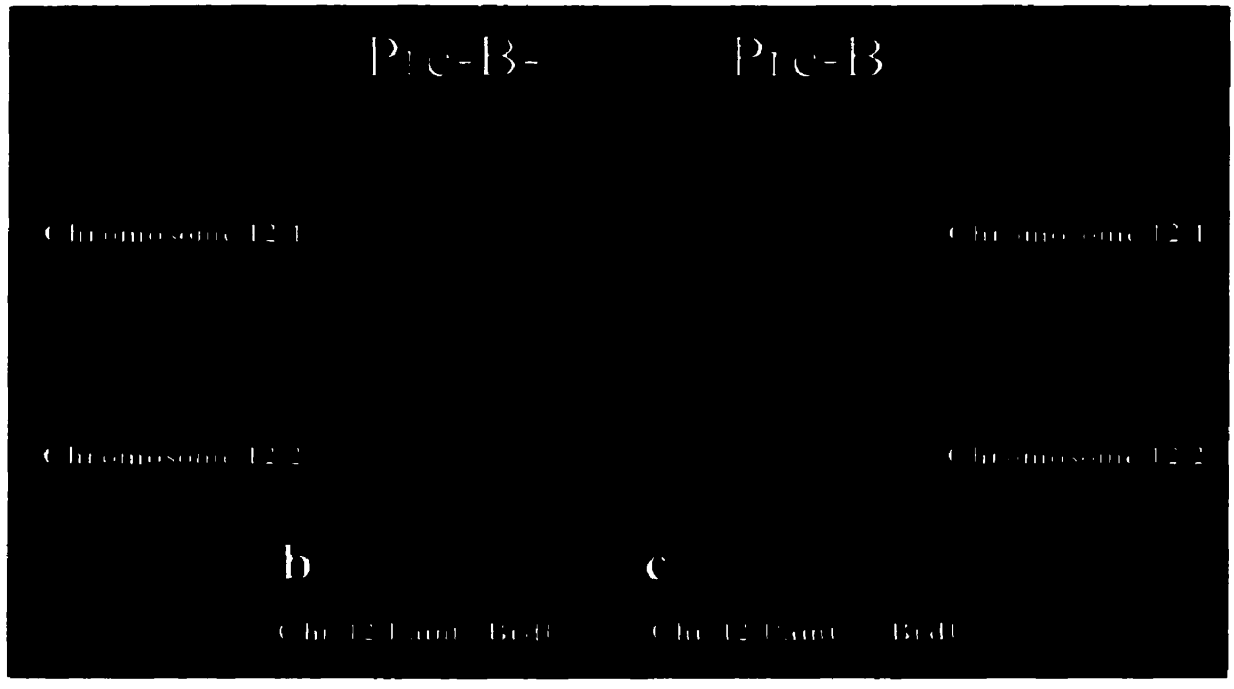

Legend: Figure 3.4.6. (b) and (c) are representative BrdU-labeled metaphase chromosomes 12 that were pulsed with BrdU for 30 minutes, 24 hours after synchronization and treatment with either 100 % ethanol (b) or 4-HT (c), and then harvested 24 hours after pulse and seeding into fresh medium. Each of the two chromosomes 12 in the metaphase is shown with Texas Red. The chromosome 12 staining is visualized with a Texas Red-conjugated goat anti-mouse IgG_1 that detects mouse anti-biotin. White arrows indicate areas of increased BrdU (green) uptake into the actively replicating alleles on one chromatid of chromosomes 12.1 in Pre-B- cells and chromosome 12.2 of Pre-B+ cells. The *R2* locus is in the area of the chromosome indicated by the white arrows. Line measurements of BrdU intensities analyzed by non-parametric Kruskall Wallis test comparing the normalized ratios showed significantly higher BrdU incorporation into Pre-B+ alleles than Pre-B- alleles ($p<0.048$).

Figure 3.4.6. (d) BrdU incorporation profiles for active and inactive alleles of mouse chromosomes 12 from Pre-B- and Pre-B+ cells

Legend: This figure illustrates BrdU incorporation levels into Band A of each pair of chromatids of chromosome 12. In this graph, two bars represent the BrdU intensity level in each chromosome, one for each chromatid. Of the two, the chromatid incorporating the lesser amount of BrdU (based on fluorescent intensity measurements) was assigned a value of >1. The other was (based on its fluorescent signal intensity) was given a value as a ratio of 1. Thus, each chromosome is depicted where one chromatid incorporates BrdU equivalent to 1 unit and the other chromatid incorporates some factor of 1. Pre-B- chromatids incorporating lower amounts of BrdU are shown with yellow fill and Pre-B- chromatids incorporating more BrdU are shown with black fill. Pre-B+ chromatids incorporating less BrdU are shown in green fill, while those incorporating more BrdU are shown in red fill. Line measurements of BrdU intensities analyzed by non-parametric Kruskall Wallis test comparing the normalized ratios showed significantly higher BrdU incorporation into Pre-B+ alleles than Pre-B- alleles ($p<0.048$).

Figure 3.4.6. (d) BrdU uptake ratios in bands A of chromosome 12 chromatids

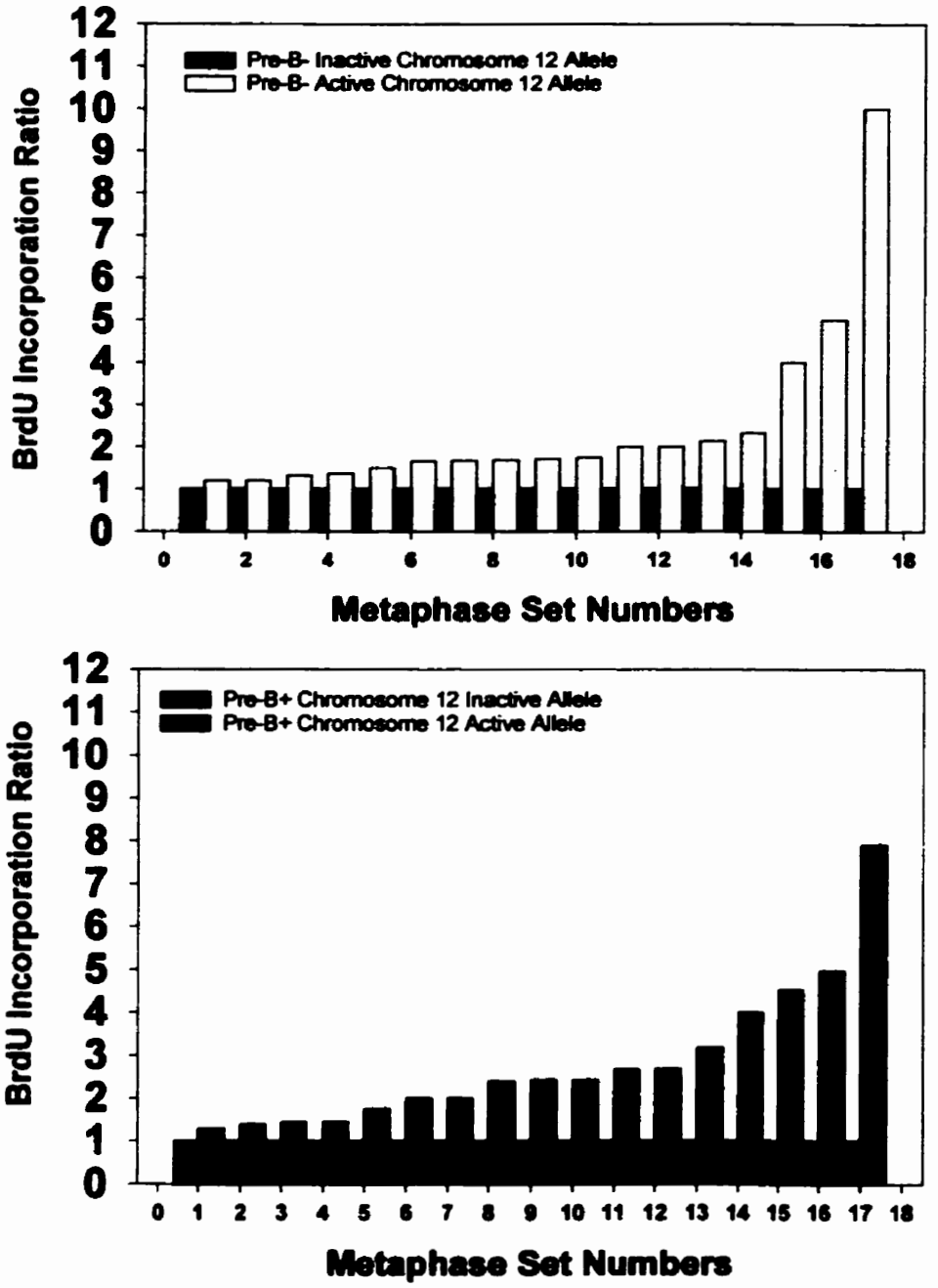

Chapter 4

DISCUSSION

DISCUSSION

This thesis work contributes to our understanding of how the deregulation of c-Myc affects targets such as the *ribonucleotide reductase R2* gene. The study focuses on the early *R2* amplification events (0-72 hours) that follow c-Myc deregulation. It has revealed the that *R2* is another c-Myc target gene and has described not only the consequences of the c-Myc deregulation at the level of the *R2* gene, but in regard to expression of the gene product. Furthermore, it has reveled a possible mechanism of c-Myc-dependent *R2* amplification. These data are summarized and discussed below.

For many years, c-Myc has been regarded as a complex transcription factor. It has been studied for a number of decades and is now known to be a multifaceted protein with diverse roles. It plays roles in cell cycle progression and cell growth as well as in the development of organisms. In these functions, c-Myc is critical. Moreover, it has been shown to play roles in apoptosis, tumor initiation and tumor progression leading to neoplasia. Recent work is revealing yet another role for c-Myc: When deregulated, c-Myc can act on target genes to cause their amplification, thus contributing to genomic instability. Thus far, c-Myc dependent amplification has been shown in *DHFR* (Mai, 1994), *CAD* (Fukasawa *et al.*, 1997), and *cyclin D2* (Mai *et al.*, 1999). This thesis work describes the role of c-Myc in the amplification of the *ribonucleotide reductase R2* gene.

Transient and constitutive c-Myc deregulation show consistently that c-Myc plays a pivotal role in amplifying the *R2* gene locus, chromosomally and extrachromosomally. Moreover, it plays a role in rearrangement of the *R2* gene locus. However, contrary to our initial hypothesis and to previously studied c-Myc-mediated gene amplification phenomena such as *dihydrofolate reductase* (*DHFR*) (Lücke-Huhle *et al.*, 1997) and

cyclin D2 (Mai *et al*, 1999), there is no corresponding increase in *R2* mRNA or protein expression levels. It is likely that the *R2* gene is not able to transcribe its message or make its product. It is possible that the gene has been truncated and is missing critical sequences that are required for successful transcription. It is also possible that though the gene is amplified it is not the actual target of gene amplification, and is itself amplified as a bystander gene that is located next to the preferred target. Such a target may be the *ornithine decarboxylase* (*ODC*) gene located 100 cM away. These possibilities are currently under investigation. Although this possibility has not been investigated, it is also possible that the amplification *R2* may result in over-expression of the mRNA and protein products, but that an alteration in the amplicons' DNA sequences and control regions may alter the stability of the mRNA. A reduction in mRNA stability would result in no net change in mRNA or protein.

In more detailed analysis of the interaction of c-Myc with the *R2* gene, I was able to demonstrate an *in vitro* physical interaction of the c-Myc protein with E-box motifs that are located in the regions flanking Exon VIII. Gel shift analyses demonstrated that the c-Myc/Max heterodimers do in fact bind non-canonical E-box motifs found in the areas flanking Exon VIII of the *R2* gene. These results were suggestive of a c-Myc-driven amplification process that may function through interaction with the *R2* E-box motifs and lead to the examination of the mechanism of c-Myc-dependent gene amplification.

Data obtained from two-dimensional (2D) gel electrophoresis suggest that c-Myc deregulation results in re-replication of the *R2* gene locus. In cells with normal c-Myc expression, the *R2* gene showed a single replication fork. In contrast, cells wherein c-Myc expression was deregulated, multiple *R2* replication forks were generated at the 24 hour

time point. This suggests a c-Myc dependent re-replication phenomenon, reminiscent of the *onionskin* phenomenon described initially by Varshavsky, (1981) and later by Mariani and Schimke (1984). This work is the first to demonstrate a c-Myc dependent re-replication phenomenon. Previous studies involved the amplification of genes using cell cycle arresting drugs such as methotrexate, which eventually selectively amplified a target gene such as *DHFR*. The demonstration that c-Myc is able to amplify its target genes through a replication-driven mechanism is novel.

The degree of involvement of the *R2* E-box motifs was also in question. Probing each of the 2D Southern membranes with labeled 20 bp *R2* E-box oligonucleotides revealed that each E-box motif was part of the *R2* replication initiation zone. This suggests that the *in vitro* interaction of c-Myc with the *R2* E-box motifs and the subsequent amplification of the *R2* gene locus that begins on or near the E-box motifs flanking Exon VIII, may be related.

We propose a model that may be appropriate for the mechanism of c-Myc dependent amplification of the *R2* gene. This model is reflects the fact that c-Myc is required for DNA replication and cellular proliferation, but that over-expression of c-Myc is known to over-ride proliferation control as well as lead to gene amplification. We envision that the timely endogenous expression of c-Myc is a part of replication initiation. c-Myc binds to the E-box motifs and takes part in the replication of the gene locus in a controlled manner as is expected in normal cells. When the replication has been initiated in S phase, c-Myc levels would be declining and Myc's potential to influence replication would be diminished (Figure 4.1.(a)). In contrast however, if c-Myc were constitutively expressed, the replication cycle of *R2* might continue. It might be that c-

Myc can function as a re-replication licensing factor that is able to over-ride other replication constraints that are able to restrict the cell to a single replication cycle under conditions where c-Myc expression is not altered. This model is illustrated in Figure 4.1.(b). The initial binding and replication would give rise to two daughter strands of DNA, each of which would also have E-box motifs bound by c-Myc/Max proteins. The cycle could continue, generating multiple re-replication bubbles within the *R2* gene locus, each bound by c-Myc and Max. These bubbles might be the *onionskin* type (Varshavsky, 1981), or they may be bubble-on-bubble (Stark and Wahl, 1989; Stark *et al.*, 1989). *R2* is an early gene in the DNA replication cycle. It may be that when normal DNA replication has been completed, several rounds of re-replication of c-Myc target genes such as *R2* have occurred simultaneously, giving rise to the amplification of the *R2* gene locus and potentially other c-Myc dependent amplification targets.

Figure 4.1.(b) shows a number of possibilities for the creation of different types of amplicons. The amplified DNA may form homogeneously staining regions (HSRs) as well as extrachromosomal DNA molecules however, the mechanisms that lead to chromosomal or extrachromosomal amplicons following re-replication of the DNA have not yet been elucidated. The HSRs may form through insertion of the amplified DNA into the *R2* locus or into other chromosomal sites, possibly through their integration into repetitive sequence areas. Alternatively, the formation of the extrachromosomal amplicons may be generated by the breakage of amplified DNA sequences away from the re-replicated and amplified locus. This breakage may occur at fragile sites or repetitive sequence DNA, followed by the creation of circular extrachromosomal elements. The

breaking away of amplicons that give rise to extrachromosomal DNA may result in deletions on the chromosome ((Figure 4.1.b)).

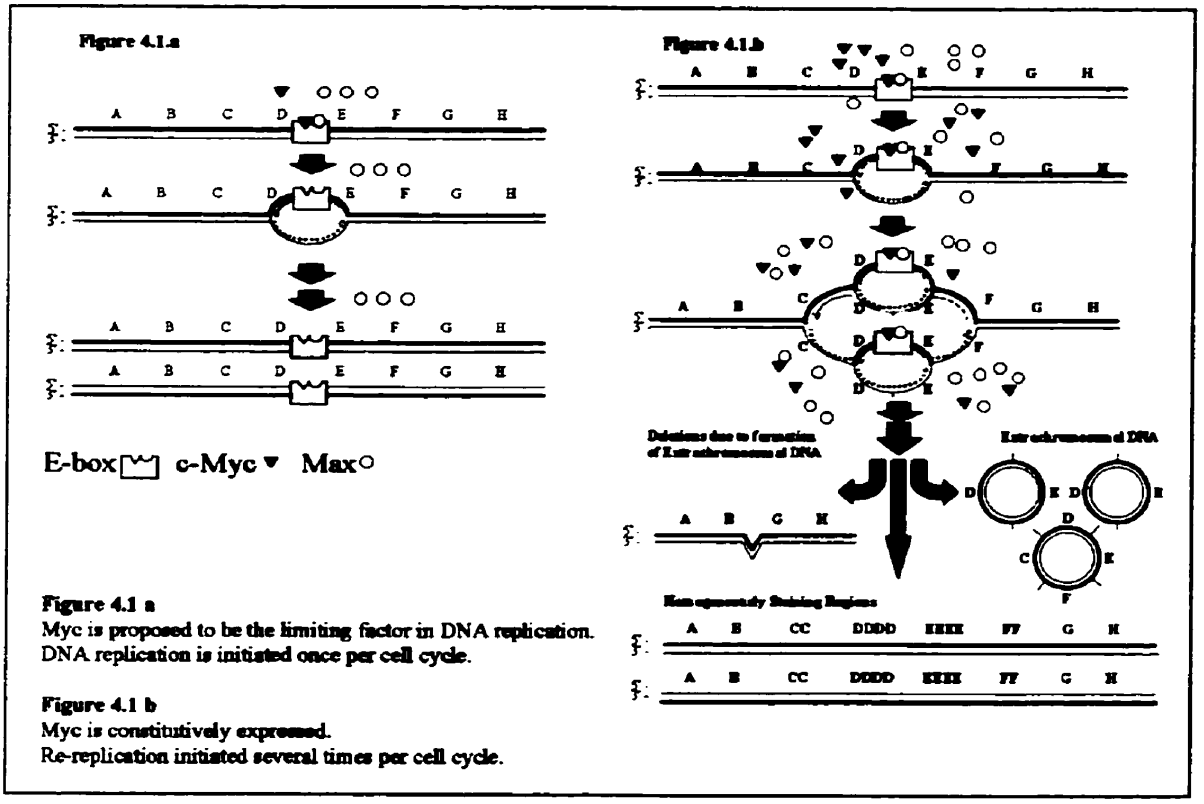

Figure 4.1 a
Myc is proposed to be the limiting factor in DNA replication.
DNA replication is initiated once per cell cycle.

Figure 4.1 b
Myc is constitutively expressed.
Re-replication initiated several times per cell cycle.

Does the model address the amplification that is seen in our data within 72 hours of transient c-Myc deregulation? Considering the replication of a single *R2* allele, two rounds of *R2* re-replication at the 24 hour time point give rise to 4 copies of the *R2* gene by the time the cell has divided once. Two subsequent rounds of re-replication of the existing (amplified) *R2* loci at the 48 hour time point may give rise to as many as 16 copies of the *R2* gene locus within 72 hours. Our initial study of c-Myc dependent *R2* amplification showed that in some metaphase cells there are as many as 16 chromosomal and extrachromosomal copies of *R2* at the 72 hour time point (Kuschak *et al.*, 1999a). (See Figure 4.1.(b)).

There are a number of studies that describe roles for c-Myc in cell proliferation and DNA replication and amplification. Classon *et al.* (1987) demonstrated that c-Myc facilitates SV40 DNA replication in human lymphocytes. Since SV40 viral DNA replication is controlled by cellular machinery, c-Myc plays a role in the replicative process. Mai *et al.* (1996) showed that prolonged periods of Myc-ER in activation, Rat1A-Mycer cells resulted in irreversible chromosomal aberrations that included numerical changes, chromosome breakage, the formation of circular chromosomal structures, chromosome fusions, and extrachromosomal elements. Li and Dang (1999) propose a model involving c-Myc deregulation that may explain our findings. In colcemid-treated cells, the overexpression of c-Myc is proposed to uncouple DNA synthesis from mitosis. Spindle disruption is shown to cause hypophosphorylation of the retinoblastoma protein. c-Myc is shown to by-pass the hypophosphorylated retinoblastoma protein and thereby induce endoreduplication of DNA. In a different study, c-Myc over-expressing cells were pre-selected with low doses of *N*-(phosphonacetyl)-L-aspartate (PALA). The pre-selection generated a population of cells that showed co-amplification of *N-myc* and *carbamyl-phosphate synthetase, aspartate transcarbamyloase, dihydroorotase* (*CAD*) genes. Treatment of these cells with higher doses of PALA showed that due to N-Myc over-expression following pre-selection with low doses of PALA, these cells were able to over-ride p53 checkpoint controls and were able to withstand higher doses of PALA due to the *N-myc* and *CAD* gene co-amplifications. The analysis of the data showed that c-Myc over-expression abrogates PALA-induced p53-mediated cell cycle arrest and facilitates the co-amplification of *N-myc* and *CAD* (Chernova *et al.*, 1998).

There are other future experiments that would reveal important information about c-Myc dependent gene amplification of *R2*. Briefly, these involve a number of relevant questions. First, the study of the actual evolution of the *R2*-bearing extrachromosomal elements following c-Myc deregulation and the generation of re-replication forks. Second, there is the question of why certain EEs are functional and others, such as *R2*, are not. Finally, there is the question of an *in vivo* component for these studies. What will the study of an Eμ-myc mouse tell us about the fate of the *R2* gene following constitutive c-Myc deregulation in the B cells of a transgenic mouse? These questions are discussed in more detail in **FUTURE DIRECTIONS**.

CONCLUSIONS

CONCLUSIONS

The c-Myc oncoprotein is associated cellular proliferation, apoptosis, tumorigenesis, tumor progression and neoplasia. The multifaceted protein is now more frequently recognized as a key factor associated with gene amplification and genomic instablity. Gene amplification and genomic instability in general, are is pivotal steps that play a role in tumorigenesis, tumor progression, and neoplasia. Previous studies have clearly demonstrated the role of c-Myc deregulation in the amplification and in the subsequent overexpression of c-Myc amplification-target genes. The genes that have been established as amplification targets of c-Myc are *DHFR* and *cyclin D2*. In each case, the amplification of the target genes was the result of transient deregulation of c-Myc that was followed by amplification and overexpression of the gene product. My current work has examined the effect of c-Myc deregulation on the genomic (in)stability of the *ribonucleotide reductase R2* gene in a cultured mouse Pre-B lymphocyte model. This study sought to answer two main questions.

First, this thesis work examined the effect of transient and constitutive c-Myc overexpression on the genomic (in)stability of the r*ibonucleotide reductase R2* gene in cultured Pre-B cells. It also sought to establish whether any observed c-Myc-dependent effects on *R2* genomic stability resulted in altered *R2* mRNA and protein expression in these cells. It demonstrated that transient and constitutive deregulation of c-Myc resulted in chromosomal and extrachromosomal amplification as well as in the rearrangement of the *ribonucleotide reductase R2* gene locus. Unexpectedly, there was no alteration in *ribonucleotide reductase R2* mRNA or protein. *R2* is the first c-Myc amplification target

gene that shows no alteration in the level of its mRNA or protein. This work is described in detail in Chapter 3.2.

Second, the study sought to answer more detailed questions about the relationship between c-Myc and the *ribonucleotide reductase R2* gene and to examine the mechanism of the c-Myc-dependent amplification of the *R2* gene locus. First, we examined the *R2* gene sequence and found a putative E-box motifs. One cluster of four E-boxes was investigated further. We first wished to determine whether the four non-canonical E-box motifs found flanking the Exon VIII region of the *ribonucleotide reductase R2* gene are c-Myc/Max binding motifs and whether these domains played a role in c-Myc-dependent gene amplification of *R2* in cultured Pre-B cells. Using gel shift analyses, antibody supershift analyses and gel shift experiments with GST-Myc and GST-Max fusion proteins, we demonstrated that each of the four synthetic oligonucleotides carrying the sequences of the *R2* E-boxes were able to bind Myc and Max under *in vitro* conditions. This part of the study demonstrates that the *R2* gene is a legitimate c-Myc target that carries non-canonical E-box motifs in the flanking regions of Exon VIII that are able to bind c-Myc/Max heterodmers *in vitro*.

I then examined the ability of the c-Myc protein to interact with the *R2* gene and the effect of c-Myc deregulation on the replication profile of the *ribonucleotide reductase R2* gene in a cultured B cell model. As a result of these studies we propose a mechanism of c-Myc dependent replication-driven amplification of *R2*. Transiently deregulated expression of c-Myc protein results in the reinitiation of DNA synthesis and the illegitimate rereplication of the *R2* gene locus within 24 hours of c-Myc deregulation, leading to the initiation of *R2* amplification within the course of a single cell cycle. Prior

to this study, reinitiation of DNA synthesis and illegitimate DNA replication has been shown only in drug-mediated gene amplification models. This study is the first to suggest illegitimate reinitiation in a replication-driven model following transient c-Myc deregulation Multiple replication initiation cycles are reminiscent of data described earlier by Varshavsky in 1981 and later by Mariani and Schimke in 1984. This study is described in detail in Chapter 3.4.

While this study focuses on the c-Myc dependent amplification of a single c-Myc amplification target, *ribonucleotide reductase R2*, it is conceivable that other c-Myc target genes may be amplified or coamplified by a similar mechanism. It suggests that the deregulation of the c-Myc protein may result in the illegitimate rereplication of c-Myc targets within a single cell cycle.

During the course of this work, a method called FISH-EEs (Fluorescent *In Situ* Hybridization of Extrachromosomal Elements) was developed to better study extrachromosomal elements (EEs) using fluorescent *in situ* hybridization (FISH). This work is described in detail in Chapter 3.1. Additional experiments have been completed that allow for the purification of histone-bound EEs using a method called Isolation of Extrachromosomal Elements by Histone Immunoprecipitation. This work is described in Chapter 3.3 and has been submitted for publication.

FUTURE DIRECTIONS

FUTURE DIRECTIONS

It is clear at this point that much of what we understand about genomic instability involves gene amplification. The study of genomic instability and gene amplification alone is rich in its potential to reveal valuable information concerning pathways and mechanisms that play a role in tumorigenesis and tumor development. Moreover, the study of c-Myc-dependent mechanisms of gene amplification is an exciting field that is revealing much about c-Myc and its involvement in amplification resulting in either altered or unaltered target gene expression. There are a number of important questions and issues that must be addressed.

Extrachromosomal DNA

Although it is certainly not a new area of study, among the most exciting is the revived focus on extrachromosomal DNA molecules. Of special interest is the area of their generation. This thesis work has suggested that c-Myc deregulation results in the amplification of the *R2* gene locus through illegitimate rereplication that occurs through a replication-driven phenomenon as early as 24 hours after c-Myc is deregulated. It has also been shown that the result of this rereplication is the chromosomal and extrachromosomal amplification of the *R2* gene locus as well as its rearrangment. What remains unclear are the steps or mechanisms that tie together the initial steps of amplification (*i.e.* the generation of rereplication forks) with the generation of extrachromosomal elements which carry *R2* sequences. This is an interesting step that will reveal the mechanisms that operate in the transition between the rereplication at the chromosomal level and the generation of extrachromosomal DNA molecules. For example, are extrachromosomal DNA molecules generated following intrachromosomal

amplification, or are they a product of deletions within a chromosome? Are they generated through rereplication of a gene locus, where multiple copies of a gene are re-replicated, some becoming chromosomally integrated while others are broken away from the replication bubble(s) and form autonomous amplicons capable of replicating and transcribing? Have the EEs undergone recombination events?

The function of the extrachromosomal DNA in cells is a critical issue. Of primary importance is the understanding of gene expression regulation in extrachromosomal elements. The first real indication of their functional and role in tumorigenesis and tumor progression has come only recently when it was shown that extrachromosomal DNA molecules are able to transcribe mRNA and play a pivotal role in tumorigenesis and tumor progression, contributing to the neoplastic phenotype of the translocation-negative plasmacytoma DCPC21 mouse (Wiener *et al.*, 1999).

In order to study a representative population of EEs that actually play a role in the cell, methods must be developed that will facilitate the study of properly purified populations of representative extrachromosomal DNA molecules, beyond what has been accomplished thus far. The isolation and/or enrichment of representative and functional extrachromosomal DNA amplicons should be the first step in their study. Currently a number of projects are underway that will result in the enrichment of pure, gene-harbouring extrachromosmal DNA, isolated from both culture- as well as from patient- and animal-derived cells. Enrichment of a pure fraction of functional extrachromosomal elements will allow for more facile multifacited manipulation and/or study of these molecules and their role(s) in tumorigenesis and tumor progression. Purified EEs can be used to study genomic instability and mechanisms of gene amplification through

procedures such as FISH-EEs, mRNA FISH, electron microscopy, micro-array technology, cloning, and Southern blotting.

Functional Analysis of Individual Extrachromosomal DNA Amplicons

The functional analysis of extrachromosomal DNA molecules is paramount if one is to elucidate their role in tumorigenesis and tumor progression. Central to understanding the effects of extrachromosomal amplicons is the study and defining of the potential of individual extrachromosomal amplicons to catalyze a single, initiating step that will utlimately alter the path of a cell from normal regulation to tumorigenesis and neoplasia. This information can come only from the isolation of c-Myc dependent generation of EEs, their purification and transfection into primary B cells. Following transplantation, the functional capacity of particular populations of EEs to generate tumors can be assessed.

Other studies must be conducted in order to understand the generation of extrachromosomal DNA molecules and to functionally characterize them. Additional studies currently underway in a cultured cell model seek to address the question of coamplification of "bystander" genes along with the *R2* gene, as well as the potential for transcription of "bystander" genes that are associated with the extrachromosomal *R2* amplicon. More specifically it will be important to establish reasons on the molecular level why certain amplicons result in enhanced gene expression and why others are inconsequential in this respect. For this reason it necessary to examine minimal sequence requirements for successful expression from extrachromosomal DNA amplicons. Comparison of data from these types of studies with sequences of disfunctional extrachromosomal amplicons such as those which carry the *R2* gene will likely reveal a

great deal about the amplification process as well as the sequence requirements for successful expression from these amplicons. It may be that non-transcribing EEs lack positional information in the nucleus that is required for their transcription.

It will also be prudent to establish what types of molecules are associated with EEs. For example, it would be interesting to determine whether Myc/Max heterodimers play a role in the expression or further amplification of extrachrosmosomal DNA initially generated by c-Myc deregulation. Experiments should also be conducted in order to determine whether Myc/Max heterodimers as well as Max/Max homodimers in any way modulate transcription of traditional c-Myc transcription targets that may be found on extrachromosomal elements. Also, one might examine whether c-Myc/Max heterodimers bind and mediate the further amplification of extrachromosomal c-Myc-dependent amplification target genes such as *dihydrofolate reductase (DHFR), ribonucleotide reductase R2,* or *Cyclin D2*. Since it is known that extrachromosomal elements are able to transcribe mRNA, it will be important to confirm which transcription related proteins are present on these amplicons during transcription. For example, are transcription-related molecules such as histone acetyltransferase as well as other transcription related proteins associated with amplicons that have been shown to transcribe? In a similar direction, it is known that extrachromosomal DNA amplicons are able to replicate autonomously. What molecules are associated with the replicating extrachromosomal amplicon? It would be interesting to confirm the presence of a number of replication-related proteins, such as MCM and cdc family proteins. The elucidation of the molecular and functional nature of extrachromosomal elements would be of great value in explaining the mechanism of extrachromosomal DNA function(s) such as they relate to tumorigenesis and neoplasia.

In vivo Studies of Gene Amplification

The greatest shortcoming of this thesis work is the fact that the study has been conducted only in cultured cells. The most important contributions to understanding the function(s) of c-Myc on the amplification process of established or putative target genes will be learned only from *in vivo* studies.

An important *in vivo* extension of this thesis work, *i.e.* the issue of c-Myc deregulation and its effects on *R2*, is best served by studies performed in the mouse. One study that is currently underway, is the examination of the effects of c-Myc deregulation in the B lymphocytes of the Eμ-myc mouse. The study seeks to examine the effects of c-Myc deregulation within the B cell compartment on c-Myc target genes such as *R2* and others, such as *DHFR*, and *cyclin D2*. A study of the effects of c-Myc deregulation from the embryonic stage to (*i.e.* E9.5, when c-Myc deregulation is initiated in the Eμ-myc mouse embryo) to the time of near-death in these mice will afford a great deal of understanding of the mechanisms of amplification and possible changes in expression and replication of c-Myc target genes. Such as study would clarify the earliest of events that occur in c-Myc target genes once c-Myc is deregulated. For example, how soon does the deregulation of c-Myc begin to generate genomic instability in the form of chromosomal, extrachromosomal amplification or aneuploidy in the mouse B cell? Myc-dependent amplification of the *DHFR* gene has been examined in the mouse however, no such experiments have been conducted in assessing the effects of c-Myc deregulation on *ribonucleotide reductase R2* or *cyclin D2*. Certainly, no studies have been conducted in the area of c-Myc-dependent genomic instability in the mouse embryo. One will also be able to establish the temporal order of genetic events as a function of c-Myc deregulation

at the earliest stages. For example, which if any af the c-Myc target genes are deregulated in the mouse embryo first? Does this deregulation have consequences in the expression of the gene? If there are mRNA and protein expression changes following c-Myc-dependent amplification of a target gene, are these expression changes due to chromosomal or extrachromosomal amplicons? Finally, questions regarding the generation and function of EEs as discussed above must be studied in the mouse model.

The study of non-lymphoid models of neoplasia must also be conducted in *in vitro* and *in vivo* environments.

APPENDICES

APPENDICES

This section of the thesis includes two appendices, namely A and B. The appendices include two papers where I contributed experimental data during the course of my Ph.D. studies and where I was among the authors. These papers are included in this thesis because they are related to my work on c-Myc-dependent genomic instability, however, are not part of my thesis/practicum work.

Appendix A

Preface

Appendix A is the full paper format of a manuscript published in the journal *Neoplasia*: Sabine Mai, Joan Hanley-Hyde, G. Jonah Rainey, Theodore I. Kuschak, James T. Paul, Trevor D. Littlewood, Harald Mischak, Lisa M. Stevens, Darren W. Henderson, and J. Frederic Mushinski (1999). Chromosomal and extrachromosomal instability of the *Cyclin D2* gene is induced by *Myc* overexpression. *Neoplasia* **1**: 241-252.

This paper is the first to describe c-Myc dependent instability of the *Cyclin D2* gene and the subsequent overexpression of *Cyclin D2* protein and mRNA.

Chromosomal and extrachromosomal instability of the *cyclin D2* gene is induced by *Myc* overexpression

Sabine Mai[1,2], Joan Hanley-Hyde[3], G. Jonah Rainey [3,4], Theodore I. Kuschak[1], James T. Paul[1], Trevor D. Littlewood[5], Harald Mischak[6], Lisa M. Stevens[3,7], Darren W. Henderson[3], and J. Frederic Mushinski [3,8]

[1]Manitoba Institute of Cell Biology, University of Manitoba, Winnipeg, MB, Canada R3E OV9

[2]The Basel Institute for Immunology, Grenzacherstraße 487, CH-4005 Basel, Switzerland

[3]Molecular Genetics Section, Laboratory of Genetics, National Cancer Institute, Bethesda MD 20892-4255

[4]Present address: Dept. of Biochemistry, Tufts University Medical Center, Boston, MA 02111

[5]Imperial Cancer Research Fund, 44 Lincoln's Inn Fields, London, UK WC2A 3PX

[6]Institute for Clinical Molecular Biology and Tumor Genetics, GSF, Munich, Germany

[7]Degree candidate: Molecular & Cell Biology Program, University of Maryland, College Park, MD

[8]Corresponding author at Building 37, Room 2B26, NIH; 37 CONVENT DR MSC-4255; BETHESDA MD 20892-4255. Tel: 301-496-5260; Fax: 301-402-1031; e-mail: mushinsj@pop.nci.nih.gov

Running Title: Myc-dependent genomic instability of *cyclin D2*

Key Words: Myc, cyclin D2, genomic instability, expression, extrachromosomal elements

Abstract

We examined the expression of *cyclins D1, D2, D3* and *E* in mouse B-lymphocytic tumors. *Cyclin D2* mRNA was consistently elevated in plasmacytomas, which characteristically contain *Myc*-activating chromosome translocations and constitutive c-*Myc* mRNA and protein expression. We examined the nature of *cyclin D2* overexpression in plasmacytomas and other tumors. Human and mouse tumor cell lines that exhibited c-*Myc* dysregulation displayed instability of the *cyclin D2* gene, detected by Southern blot, fluorescent *in situ* hybridization (FISH) and in extrachromosomal preparations (Hirt extracts). *Cyclin D2* instability was not seen in cells with low levels of c-Myc protein. To unequivocally demonstrate a role of c-Myc in the instability of the *cyclin D2* gene, a Myc-estrogen receptor chimera was activated in two mouse cell lines. After 3-4 days of Myc-ER™ activation, instability at the *cyclin D2* locus was seen, in the form of extrachromosomal elements, determined by FISH of metaphase and interphase nuclei and of purified extrachromosomal elements. At the same time points, northern and western blots detected increased *cyclin D2* mRNA and protein levels. These data suggest that Myc-induced genomic instability may contribute to neoplasia by increasing the levels of a cell cycle-regulating protein, *cyclin D2*, via intrachromosomal amplification of its gene or generation of extrachromosomal copies.

The abbreviations used are: cdk, cyclin-dependent kinase; Dhfr, dihydrofolate reductase; DAPI, 4', 6' diamidino-2-phenylindole; PI, propidium iodide; 4HT, 4-hydroxytamoxifen; R1, ribonucleotide reductase R1 subunit; R2, ribonucleotide reductase R2 subunit; FISH, fluorescent *in situ* hybridization; EEs, extrachromosomal elements; A-MuLV, Abelson murine leukemia virus; GAPDH, glyceraldehyde-3-phosphate-dehydrogenase.

INTRODUCTION

The oncoprotein Myc plays a crucial role in transformation of a wide variety of cell types (1-3). In a subset of these tumors, and particularly in neoplasms of B lymphocytes, c-*Myc* expression is constitutively upregulated as a result of one of three processes associated with genomic instability: i) gene amplification (4-5); ii) retroviral (6) or transposon (7) insertion; or iii) chromosomal translocation of c-*Myc* to immunoglobulin (Ig) loci. The last process has been observed in chicken bursal lymphomas, human Burkitt and other non-Hodgkin's B-cell lymphomas, mouse plasmacytomas and rat immunocytomas (8-10). In several forms of neoplasia, c-*Myc* gene copy numbers and protein levels have been used as prognostic markers (11). The molecular basis for the link between c-*Myc* overexpression and transformation has not been fully elucidated in these systems.

Previous studies have suggested that Myc contributes to neoplasia by affecting cell cycle progression (12-15). c-*Myc* expression is tightly controlled in normal cells at transcriptional, post-transcriptional, translational and post-translational levels (3). In diploid primary cells, c-*Myc* is upregulated in G1 and downregulated shortly after the entry into the S-phase (16; 17). c-*Myc* antisense oligonucleotides have been shown to block the transition from G1 to S (18). Cells with c-*Myc* overexpression have shown shortened G1-phases (19; 20). On the other hand, cells with one disrupted c-*Myc* allele had a prolonged G1-phase (21), and disruption of both c-*Myc* alleles in a cell line prolonged the G2-phase as well (22), prolonging the cell cycle duration significantly and proving lethal *in vivo* (23).

The regulated expression of cyclins and cyclin-dependent kinases (cdks) is critical to the normal progression through the cell cycle of untransformed cells. In contrast, immortalized and transformed cells often exhibit dysregulated expression of cyclins, cdks and cdk inhibitors. It was reported earlier that Myc plays a role in the expression of

cyclins A, D1, and *E* (12-14). Moreover, c-*Myc* expression and cell cycle progression are linked through the activation of G1 cyclins and cdks (15). It has been reported that Myc, when heterodimerized with Max, transactivates the *Cdc 25* gene, which encodes a cdk-activating phosphatase, suggesting a mechanism through which Myc could influence the cell cycle (24).

The focus of our work has been on Myc-dependent genomic instability. We recently demonstrated that c-*Myc* overexpression is associated with the non-random amplification and rearrangement of the *dihydrofolate reductase* gene (*Dhfr*, Refs. 25; 26) and the gene encoding the *R2* subunit of *ribonucleotide reductase* (*R2*, Kuschak *et al.*, submitted).

In the present study, we show evidence of Myc-dependent genomic instability of the *cyclin D2* gene, with an increase in intrachromosomal copy numbers or extrachromosomal elements bearing *cyclin D2* sequences. Both amplification events occur concomitant with an increase in *cyclin D2* gene products. These findings link c-*Myc* overexpression and cell cycle regulation for the first time at the level of genomic instability of this G1 cyclin. Based on these findings, we propose a model of Myc-dependent genomic instability and neoplasia.

MATERIALS AND METHODS

Cell lines and tissue culture. Human breast ductal adenocarcinoma T47D and mouse B lymphoma WEHI 231, were obtained from the American *Type Culture* Collection, Rockville, MD. Mouse plasmacytomas, MOPC 265 and MOPC 460D, the human colorectal carcinoma line, COLO320HSR, and primary human fibroblasts, GL30/92T, have been previously described (26-28). The spectrum of mouse B-lymphocytic cell lines has been presented in detail earlier (29). Cells were propagated in RPMI 1640 (Biofluids, Inc., Rockville, MD) supplemented with 10% heat-inactivated (30 minutes, 56°C) fetal bovine serum (Gibco/BRL, Germantown, MD), 2 mM glutamine, 100 U/ml penicillin and 100 μg/ml streptomycin. Culture medium for B-lymphoid cell lines also contained 50 μM 2-mercaptoethanol. We generated an *in vitro* line of mouse pre-B lymphocytes by transformation of BALB/c bone marrow cells with A-MuLV (30). These cells were subsequently transfected with LXSN-bcl-2, a mouse *bcl-2*-expressing vector (31), and pBabePuroMyc-ER^{TM}, an expression vector (32) with which the human Myc protein can be activated by 100 nM 4-hydroxytamoxifen (4HT, Research Biochemicals International, Natick, MA). We also produced a line of mouse fibroblasts in which Myc could be upregulated by 4HT due to stable transfection of pBabePuroMyc-ER^{TM} into ψ2 cells (33).

Cloning and sequencing of mouse *cyclin D2* cDNA and 5' genomic flank. A cDNA library of the mouse pre-B cell, 18-81, in lambda ZAP-2, was screened under relaxed conditions with Cyl1 (34), a partial cDNA for murine *cyclin D1*, a generous gift of Dr. Charles Sherr. Several clones that encoded mouse *cyclin D2* were isolated, rescued as pBlueScript clones, characterized and sequenced. A probe derived from the clone with the longest (1255 bp) insert was sequenced and found to have a coding region identical to the mouse *cyclin D2* cDNAs in the literature (35). This probe was used to screen a partial

EcoRI library of BALB/c liver DNA in EMBL-4 arms, a generous gift of Drs. Linda Byrd and Konrad Huppi. One positive clone that contained a 17.1-kb insert was isolated, purified and digested to completion with EcoRI. Only one of the 3 EcoRI fragments that were generated from 2 internal EcoRI sites, a 5.4-kb fragment, hybridized with the 5' end of the *cyclin D2* cDNA probe, and it was subcloned into pBlueScript for further study. Partial sequencing of this fragment revealed that the 3' 505 base pairs were identical to the 5' portion of our *cyclin D2* cDNA [and that of Kiyokawa *et al.* (35)]. The 3' 194 base pairs contained an AUG followed by an open reading frame, and the adjacent 301 upstream base pairs contained the 5' untranslated sequence of the cDNA. The remainder was considered 5' flank in which regulatory motifs might be located. A more complete sequence of the mouse 5' flank is being generated and will be reported elsewhere.

Probes. A 700-bp PstI-fragment of our mouse *cyclin D2* cDNA was used to probe Southern and northern blots, and the 5.4-kb genomic clone (see above) was used as a probe for fluorescent *in situ* hybridization (FISH). A strategy similar to that described above was used to isolate cDNAs for mouse *cyclins D1* and *D3* (38, generous gifts from Paul Hamel, University of Toronto). Each was used as an 800-bp EcoRI/HindIII fragment that contained the entirety of the coding region. Each of the cyclin D cDNAs has a 100-bp region that is 90% identical. Thus repeated and sequential hybridization of RNA blots was necessary to determine which bands were unique to the cyclin D member being probed. Only the unique RNA bands are shown in the figures. The human *cyclin D2* cDNA was a kind gift from Gordon Peters (39). It was used as a 1.2-kb NotI-XhoI-fragment. The *R1* probe was a 1.5-kb BamHI fragment of mouse *ribonucleotide reductase R1 subunit* cDNA (40). The cDNA clone for mouse c-*Myc*, pMc-Myc54 (41), was the kind gift of Kenneth B. Marcu, from which a 0.6-kb Hind III-Sst I fragment was used as an exon I-specific probe and a 1.0-kb Sst I-Hind III fragment was used as an exons 2+3 probe for the *Myc* sequences expressed in pBabePuroMyc-ER^{TM} (32).

Mouse *cyclins C* and *E* probes were gifts of Steven Reed. They were used as 1.1- and 2.5-kb EcoRI fragments, respectively, for hybridization. The cDNA for *GAPDH* was the kind gift of Dr. Marc Piechaczyk (42).

Assays for genomic instability: gene amplification and extrachromosomal elements. Gene dosage was examined using Southern blot analysis (36) and FISH of metaphase and interphase chromosomes (26; 37). Evaluation of metaphase spreads and interphase nuclei was performed using a Zeiss Axiophot microscope and a CCD camera (Optikon/Photometrics). 100 - 150 metaphases and interphases were evaluated in each of three independent experiments. Extrachromosomal fluorescent signals were considered specific when they also stained with 4', 6' diamidino-2-phenylindole (DAPI) (1 μg/ml) or propidium iodide (PI) (1 μg/ml).

RNA isolation and northern blotting. Total RNA or Poly(A)$^+$ RNA was isolated from cells as previously reported (29). 5 μg of Poly(A)$^+$ RNA or 15 μg of total RNA were fractionated on a 1 % agarose gel containing formaldehyde. The RNA was transferred to a Hybond-N membrane (Amersham, Arlington Heights, IL) by capillary blotting and hybridized with ^{32}P-labeled cDNA probes as indicated in the figure legends. Radioisotopic labeling was performed with the Nick Translation System (GIBCO/BRL, Germantown, MD) according to the manufacturer's protocol. The membranes were hybridized overnight with $3x10^6$ dpm/ml probe, washed with 0.1 x SSC, 0.1% SDS at 20°C and exposed to X-ray film overnight at -80°C. For sequential hybridization of the same blot with different probes, membranes were stripped with boiling water.

Western blotting. Western blots were performed on lysates of pre-B cell cultures as previously described (43) except that protein concentration was determined using the BCA Protein Assay (Pierce), and 10 μg were loaded per lane. The immunoreactive bands

were identified by the ECL Western blotting detection system (Amersham, Arlington Heights, IL). The anti-cyclin D2 (M-20) was purchased from Santa Cruz Biotechnology (Santa Cruz, CA). The anti-actin (clone AC-40) was from Sigma ImmunoChemicals (St. Louis, MO). The HRP-Goat anti-Rabbit IgG and HRP-Goat anti-Mouse IgG and IgM were purchased from Axell (Westbury, NY).

Extrachromosomal elements. Cells were subjected to a procedure designed to separate chromosomal from non-chromosomal DNA (44). Cells were suspended at 1-5 x 10^7 per ml and lysed in 0.6% SDS/0.01 M EDTA at room temperature for 10-20 minutes. Then 5 M NaCl was added to bring the suspension to 1 M NaCl, and precipitation was allowed to proceed at 4°C overnight. The supernatant from a centrifugation at 35,000 x *g* for 30 min at 4°C ("Hirt extract") was applied to glass slides for FISH (see next section) or to grids for electron microscopy (EM) examination. For EM, Hirt extracts were diluted to a concentration of ca. 1 µg/ml in 20 mM $MgCl_2$/ 30 mM triethanolamine (45). Aliquots were placed on formvar/carbon-coated grids, fixed with 0.1 % glutaraldehyde in White's saline (46) and negatively stained with 3% uranyl acetate. Grids were allowed to air dry and then shadowed with tungsten to enhance resolution. Grids were examined in a Philips Model 420 transmission electron microscope at 80 kV.

FISH on purified extrachromosomal elements. EEs were isolated according to a modification (47) of the protocol by Hirt (44). They were diluted 1:1 in freshly prepared methanol: acetic acid (3:1) and dropped onto slides. Fixations were carried out as described earlier (25; 26). FISH was performed following RNAse and pepsin treatments. DAPI was used to stain the DNA of the EEs. Hybridization signals were considered specific if they colocalized with DAPI-stained EEs. Hybridizations were carried out with a panel of probes including *Dhfr* and *Ribonucleotide Reductase Subunit 2 (R2)* that had been shown to be present on EEs of 4HT-activated pre-B lymphoma cells (47). Relative

fluorescence intensities were measured with IPLab Spectrum software, version 3.1 (Signal Analytics).

RESULTS

Northern blot analysis of *cyclin D2* expression in murine B-lymphocytic lines with different degrees of B-cell maturation. Figure App.A.1 shows a blot of poly(A)$^+$ RNA from a series of mouse B-cell lymphoma cell lines of increasing maturation from left to right (29). This blot was sequentially hybridized with four murine G1 cyclin probes. The *cyclin D3* probe revealed strong 2.3-kb bands in 4 cell lines of early B lymphocytes, but barely detectable levels in plasmacytomas. The *cyclin D1* probe showed a very strong 3.9-kb band in the myeloid-pro-B line in lane 1, strong bands in two B-cell lines, lanes 5 and 8, but very low levels in the remaining RNA samples. *Cyclin E* transcripts were virtually undetectable (not shown). When normalized to the *glyceraldehyde phosphate dehydrogenase (GAPDH)* control hybridization signals, the highest level of expression of the predominant *cyclin D2* mRNA species (6.5-kb) was seen in the four plasmacytomas (lanes 11-14). In addition, several smaller *cyclin D2* mRNA species are prominent, chiefly in these four lanes. Plasmacytomas are known to be rich in *Myc* mRNA (48), and this is the case for these four lanes. There is not a clear correlation between levels of *Myc* and *cyclin D2* mRNA, but a similar pattern of high levels of *Myc* and *cyclin D2* mRNA was also seen in blots of RNA from 45 additional plasmacytomas (data not shown). This series included plasmacytomas with t(12;15) and t(6;15) translocations and tumors without translocations, but with *Myc* upregulation due to stable integration of *Myc*-expressing recombinant retroviruses (28).

Established mouse and human tumors with c-*Myc* overexpression have Southern blot evidence of amplification of the *cyclin D2* locus. The stability of the *cyclin D2* locus was characterized in two mouse B-lymphoid lines, MOPC 460D, a

plasmacytoma that constitutively overexpresses c-*Myc* due to *Myc/Ig* chromosome translocation (28), and WEHI 231, a lymphoblastoid tumor with low Myc protein levels (26). Southern blot analyses showed that the *cyclin D2* gene was chromosomally amplified in MOPC 460D (Fig. 2, upper left panel, filled arrowheads), but not in WEHI 231 cells. Mouse *ribonucleotide reductase subunit R1 (R1*, Fig. 2, lower panels) and *cyclin* C (not shown), genes that are retained as single-copy genes irrespective of Myc protein levels, were used as reference genes.

These analyses were extended to human cell lines: the colon carcinoma line COLO320HSR, a classic example of c-*Myc* gene amplification and overexpression (28-fold higher Myc protein levels than GL30/92T primary human fibroblasts); and the breast cancer line T47D, which expresses 11 times higher c-Myc protein levels than GL30/92T, a fibroblast of normal genotype (26). COLO320HSR and T47D displayed chromosomally amplified bands of *cyclin D2* gene hybridization in Southern blots (Figure App.A.2., upper right panel, filled arrowheads), compared to the control *R1* hybridizations (Figure App.A.2., lower right panel) while primary human fibroblasts did not shown *cyclin D2* amplification. In T47D, the c*yclin D2* gene is partially deleted from the chromosomes as indicated by missing genomic bands in the Southern blot (see open arrowheads in Figure App.A.2). Such deletions appear to reflect an additional form of genomic instability of this locus in cells that overexpress *Myc*.

***Cyclin D2* amplification involves the generation of extrachromosomal elements in COLO320HSR and MOPC 460D.** 4', 6' diamidino-2-phenylindole (DAPI) or propidium iodide (PI) staining of metaphase chromosome spreads of COLO320HSR showed the presence of extrachromosomal elements (EEs). FISH studies of these preparations showed amplified signals of the *cyclin D2* gene on chromosomes and the EEs (Figure App.A.3A). A similar analysis of the BALB/c plasmacytoma MOPC 460D also showed EEs that contained *cyclin D2* sequences (Figure App.A.3B).

Extra- and intrachromosomal amplification is gene-specific. EEs contain only a subset of gene sequences. The Southern blot data showed amplification of *cyclin D2* but not of the negative controls, *cyclin C* or *R1*. Similarly, FISH studies of COLO320HSR and MOPC 460D showed no extrachromosomal elements that hybridized with *cyclin C* (data not shown).

Induced upregulation of Myc activity in mouse pre-B cells results in *cyclin D2*-containing extrachromosomal elements and increased *cyclin D2*- mRNA and protein after three days. A mouse pre-B cell line derived from bone marrow cells by transformation with A-MuLV was stably transfected with pBabePuroMyc-ER™, an inducible *Myc* expression vector that constitutively expresses Myc-ER™, a chimeric protein that contains human c-Myc, linked to a mutated estrogen receptor (32). The Myc of the chimera is activated by addition of 4-hydroxytamoxifen (4HT). After three days of stimulation by 4HT, numerous EEs could be seen in metaphase chromosome spreads following Giemsa staining of chromatin (not shown) and DAPI staining of DNA (Figure App.A.3D.). Some of the EEs were shown by FISH analysis to carry *cyclin D2* sequences. This evidence of genomic instability involving the *cyclin D2* gene was not seen in the same cells without tamoxifen stimulation (Figure App.A.3C.) nor in 4HT-treated pre-B cells that lack Myc-ER™ (data not shown).

Northern blots were prepared from total RNA from the A-MuLV-transformed pre-B cells before and after stable introduction of pBabePuroMyc-ER™, and after different periods of stimulation by 4HT. Figure App.A.4. shows the results of successive hybridizations of this blot with *cyclin D2* and other germane probes. *Cyclin D2* message expression is clearly elevated after 4 and 6 days of Myc activation by 4HT, when compared to the ethidium bromide-stained 28S ribosomal RNA bands in each lane. Transcripts from the retroviral pBabePuroMyc-ER™ in the stably transfected line, shown in the right panels, are detected with a *Myc* exon 2+3 probe. As often happens (3)

endogenous c-*Myc* expression (shown by a 2.4-kb band that hybridizes with *Myc* exon 1 probe) decreased after 4HT activation of the exogenous Myc-ER (which lacks exon 1). There was no detectable mRNA for *cyclin D1* (not shown), and no significant change in mRNA level of *cyclin D3* was seen during the treatment with 4HT.

Western blots of lysates from the 4HT-treated cells described in the preceding paragraph were probed with anti-cyclin D2 antibody and, as a loading control, with anti-actin antibody. As shown in Fig. 4B, cyclin D2 protein levels gradually rose in parallel with the levels of *cyclin D2* mRNA after Myc activation by 4HT in the pBabePuroMyc-ER™-containing cells but not in the pre-B cells that lack this vector. Thus, both elevated *cyclin D2* mRNA and protein levels appear simultaneously with the *cyclin D2* genomic amplification, not prior to it.

Induced upregulation of Myc activity in mouse fibroblasts also leads to the generation of *cyclin D2*-containing extrachromosomal elements and increased *cyclin D2* mRNA. A mouse fibroblast line, derived by transfection of ψ2 cells with pBabePuroMyc-ER™, was stimulated with 4HT to induce increased Myc activity. After three days of stimulation by 4HT, numerous *cyclin D2*-containing EEs could be seen in metaphase chromosome spreads and in interphase nuclei (Figures App.A. 3G and H). This evidence of genomic instability and of *cyclin D2* gene amplification were not seen in the same cells without prolonged tamoxifen stimulation (Figure App.A.3F). A control FISH study of 4HT-stimulated ψ2 cells that do not bear the Myc-ER™ expression vector showed no *cyclin D2*-hybridizing EEs (Fig. 3E).

Northern blots were prepared from total RNA from the fibroblasts with and without stable integration of pBabePuroMyc-ER™, and after different periods of stimulation by 4HT. Figure 5C shows the results of successive hybridization of this blot with *cyclin D2* and other probes. As with the pre-B cells, *cyclin D2* message expression is clearly elevated after several days of Myc activation by 4HT, when compared to the

GAPDH loading control. Thus the fibroblast data parallel the results seen in pre-B cells, with increased *cyclin D2* expression accompanying, but not preceding, appearance of *cyclin D2*-containing extrachromosomal elements.

Myc-induced extrachromosomal elements are DNA-containing circles, some of which bear *cyclin D2* sequences. Figure 5 shows electron microscopic images of the EEs found in "Hirt extracts" (44) prepared from pre-B cells bearing pBabePuroMyc-ER™ before (Figure App.A.5A) and after (Figures App.A.5 B – D) three days of 4HT treatment. These initial studies using electron microscopy repeatedly and reproducibly yielded the unusual images shown here. Their significance is only beginning to be understood, and our tentative interpretations are as follows. Figure App.A.5A shows small extrachromosomal DNA-containing small irregular, asymmetrical circular elements (diameter, <0.10 μm), believed to contain repetitive sequence motifs only, which is characteristic of normal cells (49). Figures App.A.5B-D are electronmicrographs taken at the same magnification as the upper panel, showing an example of the larger (diameter, 0.15 - 0.35 μm), more discrete circles that are found after 4HT-activation of pBabePuroMyc-ER™-bearing pre-B cells and which are thought to contain amplified genes

To confirm the presence of *cyclin D2* on EEs in 4HT-treated cells, we developed a method to examine the total population of EEs purified by the Hirt procedure (47). This protocol involved affixing EEs isolated by the method of Hirt (44) to glass slides that were then processed for FISH and counterstained with DAPI. FISH hybridization signals are considered specific only if they colocalize with DAPI-stained EEs. When FISH was performed on the slides, we found that about 10% of the EEs contained *cyclin D2*-sequences (Figures. App.A. 6 B, C (indicated by large white arrows). The sizes of the *cyclin D2*-hybridizing EEs were shown to be 10 - 20 pixels, using IPLab software analysis of the fluorescence images. The finding that only a fraction of the DAPI-positive

spots hybridized to the *cyclin D2* probe was evidence for the specificity of this hybridization. FISH studies of Hirt extracts of normal cells, showed only a few, extremely tiny DAPI-staining dots (pixel size <5, data not shown), similar to those seen in uninduced pre-B cells (Figure App.A.5A), which did not hybridize with the *cyclin D2* probe. These data establish that *cyclin D2* hybridizes specifically to a subset of the EEs seen in nuclei, metaphases and on microscopic preparations of EEs. We conclude from these data that *cyclin D2* is one of an unknown number of targets of c-Myc-induced genomic instability found on EEs.

DISCUSSION

A direct role for Myc in *cyclin D2* gene amplification in this study was first suspected when a coupling was observed between *Myc* overexpression and amplification of the *cyclin D2* gene in established tumors. This is not unprecedented, since earlier work has demonstrated that Myc can influence replication (50). Amplification of *cyclin D2* was first seen in Southern blots of two human cell lines, COLO320HSR and T47D, which were known to have c-*Myc* amplification and overexpression. Similar evidence of *cyclin D2* amplification was also found in mouse plasmacytomas that did not have c-*Myc* gene amplification but which did have constitutive expression of c-*Myc* due to chromosomal translocations.

The *cyclin D2* amplification that was detected in mouse plasmacytomas was accompanied by enhanced mRNA and protein levels on RNA and protein blots. More transcripts were found in plasmacytomas than in other B-cell lines that did not have c-*Myc*-activating chromosome translocations. Such increased expression of other members of the G1 cyclins, *cyclins D1, D3* and *E* was not found in plasmacytomas, indicating that this was a special attribute of *cyclin D2*.

To directly implicate Myc levels in the induction of *cyclin D2* amplification, we studied the effects of inducible overexpression of *Myc* in mouse pre-B cells using a tamoxifen-activated pBabePuroMyc-ER™ chimeric expression vector. Since amplification of genes occurs gradually, over successive replication cycles, we did not study the potential short-term effects of c-*Myc* upregulation of the *cyclin D2* gene via transcription activation. Instead, we concentrated on the state of the locus and its expression over several days of 4HT stimulation. 4HT had no effect on the *cyclin D2* of parental A-MuLV-transformed pre-B cells. FISH studies showed no evidence of genomic instability, and mRNA expression remained very low. In the cells with an activated Myc-ER™ chimera, extrachromosomal elements, which have also been referred to as double-minutes, polydispersed circular DNA, episomes and extrachromosomal DNA (49; 51 - 53), that hybridized with the *cyclin D2* probe, appeared after three to four days, indicating increased genomic instability. At these same time points, blots of RNA and cell lysates isolated from these cells began to show increased expression of *cyclin D2* mRNA and protein.

The data obtained to date do not require upregulation of either RNA transcription or changes in RNA stability. It is possible that simple *status-quo* rates of expression could yield increased steady-state levels of mRNA and protein if the template were increased, such as by the amplification that we have demonstrated. Such a mechanism could also be responsible for the high levels of *cyclin D2* mRNA in plasmacytomas, secondary to their constitutive expression of high levels of c-Myc mRNA and protein. It is interesting to note that Southern blots of DNA from pre-B cells after 3 days of 4HT-induction did not show increased *cyclin D2* hybridization signals (data not shown) like those that were seen in well-established tumor cells that have experienced high Myc levels for many generations. This finding is not surprising, since extrachromosomal DNA is generally not visualized in conventional Southern blots (54; 55). Moreover, extrachromosomal DNA molecules tend to be unstable, because they usually do not

contain centromeres and may be lost during mitosis. With time, some have been shown to integrate into the chromosomes to take the appearance seen in established cell lines (52; 56; 57).

We do not yet know whether the EEs are the source of the increased *cyclin D2* mRNA that appears simultaneously with the appearance of these elements. We have determined, however, that both the number of *cyclin D2*-containing EEs per cell and the level of *cyclin D2* mRNA decreased when 4HT was removed for four days from cultures of pre-B cells and fibroblasts that had been stimulated with 4HT for 6 days (data not shown). Preliminary studies have indicated that the EEs contain protein and DNA, because they stain with Giemsa and DAPI and disappear when treated with DNAase. Some preparations of DNA from EEs can be digested with restriction endonucleases, and we are presently optimizing the isolation of EEs with undegraded DNA to attempt its cloning and sequencing. In addition, we will examine whether the EEs are transcribed to yield cyclin D2 mRNA.

A causal connection between Myc levels and *cyclin D2* amplification is probably not limited to B lymphocytic tumors, because we saw amplified *cyclin D2* in human colorectal and breast carcinomas. In addition, we also found a gradual increase in *cyclin D2* expression in mouse fibroblasts when *Myc* is overexpressed and activated by 4HT treatment of cells that bear the Myc-ER™ expression vector.

We do not yet know why *cyclin D2* is amplified when *Myc* expression is high. We found four CACGTG Myc/Max-binding E-box motifs upstream of exon one of the *cyclin D2* gene (to be published in full elsewhere), and we speculate that these E boxes may play a role in targeting such genes for Myc-induced amplification.

This Myc-associated genomic instability may be the cause of the frequent aneuploidy and instability seen in long-term cultures (57) or extensively passaged experimental tumors. More specifically, it has been reported that tumor-specific non-random chromosomal translocations become increasingly difficult to recognize with

repeated passages of plasmacytoma lines induced by *Myc*-activating chromosome translocations, due to accumulations of additional, presumably random, chromosomal aberrations (58). Although it has been shown that excess Myc activity can elicit overall karyotypic instability (57) and increased tumorgenicity (59), it is important to emphasize that our data show that Myc-associated gene amplification is locus-specific. Extra-and intrachromosomal amplification has been demonstrated previously for *Dhfr* (26) and in this paper for *cyclin D2*, but we have also determined that high *Myc* expression produces no such amplification in the genes encoding ornithine decarboxylase, syndecan-2, GAPDH or cyclin C (26).

Is it possible to construct a hypothetical model for how the genes that are amplified in the presence of *Myc* overexpression might work together toward neoplasia? We propose that increased Myc activity leads to a redundant expression of genes that promote cell cycle progression and cell proliferation. This effect produces a potent combination favoring induction, promotion or progression of neoplastic transformation if apoptotic pathways are bypassed. Overexpression of *Myc* has been shown to shorten the G1 phase of the cell division cycle (19; 20), which favors further mutations by curtailing the period available for cells to assess and repair DNA damage before it is duplicated in S phase. Such mutations might allow the cells to escape apoptosis, which is frequently associated with increased Myc activity. A similar effect would be expected from overexpression of *cyclin D2*, an important G1 cyclin. High levels of such cyclins could also foreshorten G1 and rush cells prematurely into S by titrating out cdk inhibitors such as p21 and p27. Perhaps such changes are responsible for the transformed characteristics that are induced by overexpression of *cyclin D1* in fibroblasts (60). *Cyclin D1* amplification and overexpression is a well-known step in various cancers (61 - 63). Amplification and/or overexpression of *cyclin D2* may have similar effects. Overexpression of *cyclin D2*, along with *D1* and *D3*, has been found in mouse skin neoplasms and has been associated with tumor progression (64). Similar to our finding of

cyclin D2 gene amplification in COLO320HSR, Leach *et al.* (65) reported that this cyclin gene was amplified in a subgroup of colorectal carcinomas. What is more, inappropriate expression of *cyclin D2* also occurs as a result of retroviral integration in retrovirus-induced rodent T-cell lymphomas (66). Finally, the expression of G1 cyclins and their control of the cell division cycle is known to vary between normal and transformed cells (38).

Another gene that is amplified by *Myc* overexpression is *Dhfr*. It is a key enzyme of folate metabolism, and it is essential for DNA synthesis. High levels of the product of this gene may contribute to maintenance of cell proliferation. High copy number of *Dhfr* genes and overexpression of the enzyme, *e.g.*, following amplification, have been correlated with the metastatic potential of tumor cells in a rat carcinoma model (67). Thus we propose that Myc induces a locus-specific instability, and additional steps of selection will determine which cell(s) become malignant clone(s). This makes it possible, and indeed likely, that such cells that survive in this new regulatory setting will accumulate additional genomic alterations and will have an increased potential to complete the multi-step process of neoplastic transformation. This concept has recently received support by experiments that demonstrated that c-Myc-induced instability allowed the outgrowth of tumors in athymic mice following their subcutaneous inoculation with fibroblasts that exhibited Myc-mediated instability (59).

In summary, *cyclin D2* is one of a growing list of genes targeted for genomic instability by high Myc levels. We are in the process of determining the magnitude (number of genes involved) of the genomic instability induced by *Myc* overexpression.

ACKNOWLEDGMENTS

We thank our colleagues for many valuable discussions, probes and cell lines and libraries of clones. We thank Ms. E. McMillan-Ward for electron microscopy. This work has been supported by grants to S. M. from the National Science and Engineering Research Council (NSERC), the Manitoba Health and Research Council (MHRC), and the Thorlakson Foundation Fund. The Basel Institute for Immunology was founded and is supported by F. Hoffmann-La Roche, Basel, Switzerland.

REFERENCES

1. Cole MD (1986). The myc oncogene: its role in transformation and differentiation. *Ann. Rev. Genet.* **20**, 361-384.

2. Erisman MD, Scott JK, Watt RA, and Astrin SM (1988). The c-myc protein is constitutively expressed at elevated levels in colorectal carcinoma cell lines. *Oncogene* **2**, 367-378.

3. Marcu KB, Bossone SA, and Patel AJ (1992). Myc function and regulation. *Ann. Rev. Biochem.* **61**, 809-860.

4. Citri Y, Braun J, and Baltimore D (1987). Elevated myc expression and c-myc amplification in spontaneously occurring B lymphoid cell lines. *J. Exp. Med.* **165**, 1188-1194.

5. Feo S, Liegro CD, Jones T, Read M, and Fried M (1994). The DNA region around the c-myc gene and its amplification in human tumour cell lines. *Oncogene* **9**, 955-961.

6. Hayward WS, Neel BG, and Astrin SM (1981). Activation of a cellular onc gene by promoter insertion in ALV-induced lymphoid leukosis. *Nature* **290**, 475-480.

7. Morse B, Rotherg PG, South VJ, Spandorfer JM, and Astrin SM. (1993). Insertional mutagenesis of the myc locus by a LINE-1 sequence in a human breast carcinoma. *Nature* **333**, 87-90.

8. Taub R, Kirsch I, Morton C, Lenoir GM, Swan D, Tronick S, Aaronson S, and Leder P. (1982). Translocation of the c-myc gene into the immunoglobulin heavy chain locus in human Burkitt lymphoma and murine plasmacytoma cells. *Proc. Natl. Acad. Sci. USA.* **79**, 7837-7841.

9. Shen-Ong GLC, Keath EJ, Piccoli SP, and Cole MD (1982). Novel myc oncogene RNA from abortive immunoglobulin-gene recombination in mouse plasmacytomas. *Cell* **31**, 443-480.

10. Pear WS, Wahlstrom G, Nelson SF, Axelson H, Szeles A, Wiener F, Bazin H, Klein G, and Sumegi J (1988). 6;7 chromosomal translocation in spontaneously arising rat immunocytomas: evidence for c-*myc* breakpoint clustering and correlation between isotype expression and the c-*myc* target. *Mol. Cell Biol.* **8**, 441-451.

11. Yokota Y, Tsunetsugu-Yokota Y, Battifora CL, and Cline MJ (1986). Alterations in myc, myb, ras Ha proto-oncogenes in cancers are frequent and show clinical correlation. *Science* **231**, 261-265.

12. Jansen-Duerr P, Meichle A, Steiner P, Pagano M, Finke K, Botz J, Wessbecher J, Draetta G, and Eilers M (1993). Differential modulation of cyclin gene expression by MYC *Proc. Natl. Acad. Sci. USA* **90**, 3685-3689.

13. Daksis JI, Lu RY, Facchini LM, Marhin WW, and Penn LJZ (1994). Myc induces cyclin D1 expression in the absence of de novo protein synthesis and links mitogen-stimulated signal transduction to the cell cycle. *Oncogene* **9**, 3635-3645.

14. Philipp A, Schneider A, Vaestrik I, Finke K, Xiong Y, Beach D, Alitalo K, and Eilers M (1994). Repression of cyclin D1: a novel function of MYC. *Mol. Cell Biol.* **14**, 4032-4043.

15. Steiner P, Philipp A, Lukas J, Godden-Kent D, Pagano M, Mittnacht S, Bartek J, and Eilers M (1995). Identification of a Myc-dependent step during the formation of active G1 cyclin-cdk complexes. *EMBO J.* **14**, 4814-4826.

16. Waters CM, Littlewood TD, Hancock DC, Moore JP, and Evan GI (1991). c-myc protein expression in untransformed fibroblasts. *Oncogene* **6**, 797-805.

17. Mai S and Jalava A (1994). c-Myc binds to 5' flanking sequence motifs of the dihydrofolate reductase gene in cellular extracts: role in proliferation. *Nucl. Acids Res.* **22**, 2264-2273.

18. Heikkila R, Schwab G, Wickstrom E, Loke SL, Pluznik DH, Watt R, and Neckers LM (1987). c-myc antisense oligodeoxynucleotide inhibits entry into S phase but not progress from G0 to G1. *Nature* **328**, 445-449.

19. Karn J, Watson JV, Lowe AD, Green SM, and Vedeckis W (1989). Regulation of cell cycle duration by c-myc levels. *Oncogene* **4**, 773-787.

20. Alexandrow MG and Moses HL (1998). c-myc-enhanced S phase entry in keratinocytes is associated with positive and negative effects on cyclin-dependent kinases. *J Cell Biochem* **70**, 528-542.

21. Hanson KD, Shichiri M, Follansbee MR, and Sedivy JM. (1994). Effects of c-myc expression on cell cycle progression. *Mol. Cell Biol.* **14**, 5748-5755.

22. Mateyak MK, Obaya AJ, Adachi S, and Sedivy JM (1997). Phenotypes of c-Myc-deficient rat fibroblasts isolated by targeted homologous recombination. *Cell Growth Differ.* 8, 1039-1048.

23. Davis AC, Wims M, Spotts GD, Hann SR, and Bradley A (1993). A null c-myc mutation causes lethality before 10.5 days of gestation in homozygotes and reduced fertility in heterozygous female mice. Genes Dev. 7: 671-682.

24. Galaktionov K, Chen X, and Beach D (1996). Cdc25 cell-cycle phosphatase as a target of c-myc. *Nature* **382**, 511-517.

25. Mai S (1994). Overexpression of c-myc precedes amplification of the gene encoding dihydrofolate reductase. *Gene* **148**, 253-260.

26. Mai S, Hanley-Hyde J and Fluri M. (1996) c-Myc overexpression-associated DHFR gene amplification in hamster, rat, mouse and human cell lines. *Oncogene* **12**, 277-288.

27. Jaffe BM, Eisen HN, Simms ES and Potter M (1969). Myeloma proteins with anti-hapten antibody activity: epsilon-2,4- dinitrophenyl lysine binding by the protein produced by mouse plasmacytoma MOPC-460. *J. Immunol.* **103**, 872-878.

28. Mushinski JF (1988). c-*myc* activation and chromosomal translocation in BALB/c plasmacytomas. In *Cellular Oncogene Activation* (ed. Klein) pp. 181-211. Marcel Dekker, New York and Basel.

29. Mushinski JF, Davidson WD, and Morse HC (1987). Activation of cellular oncogenes in human and mouse leukemia-lymphomas: spontaneous and induced oncogene expression in murine B lymphocytic neoplasms. *Cancer Invest.* **5**, 345-368.

30. Rosenberg N and Baltimore D (1976). A quantitative assay for transformation of bone marrow cells by Abelson murine leukemia virus. *J. Exp. Med.* **143**, 1453-1463.

31. Gurfinkel N, Unger T, Givol D, and Mushinski JF (1987). Expression of the bcl-2 gene in mouse B lymphocytic cell lines is differentiation stage specific. *Eur. J. Immunol.* **17**, 567-570.

32. Littlewood TD, Hancock DC, Danielian PS, Parker MG, and Evan GI. (1995). A modified oestrogen receptor ligand-binding domain as an improved switch for the regulation of heterologous proteins. *Nucl. Acids Res.* **23**, 1686-1690.

33. Mann R, Mulligan RC, and Baltimore D (1983). Construction of a retrovirus packaging mutant and its use to produce helper-free defective retrovirus. *Cell* **33**, 153-159.

34. Matsushime H, Roussel MF, Ashmun RA, and Sherr CJ (1991). Colony-stimulating factor 1 regulates novel cyclins during the G1 phase of the cell cycle. *Cell* **65**, 701-713.

35. Kiyokawa H, Busquets X, Powell CT, Ngo L, Rifkind RA, and Marks PA (1992). Cloning of a D-type cyclin from murine erythroleukemia cells. *Proc. Natl. Acad. Sci. USA* **89**, 2444-2447.

36. Southern EM (1975). Detection of specific sequences among DNA fragments separated by gel electrophoresis. *J. Biol. Chem.* **253**, 5852-5860.

37. Mai S, Hanley-Hyde J, Coleman A, Siwarski D, and Huppi K (1995). Amplified extrachromosomal elements containing c-Myc and Pvt 1 in a mouse plasmacytoma. Genome. *Genome* **38**, 780-785.

38. Hamel PA and Hanley-Hyde J (1997). G1 cyclins and control of the cell division cycle in normal and transformed cells. *Cancer Investigation* **15**, 143-152.

39. Sinclair AJ, Palmero I, Peters G, and Farrell PJ (1994). EBNA-2 and EBNA-LP cooperate to cause G0 to G1 transition during immortalization of resting human B lymphocytes by Epstein-Barr virus. *EMBO J* **13**, 3321-3328.

40. Thelander L and Berg P (1986). Isolation and characterization of expressible cDNA clones encoding M1 and M2 subunits of mouse ribonucleotide reductase. *Mol. Cell Biol.* **6**, 3433-3442.

41. Stanton LW, Watt R, and Marcu KB (1983). Translocation, breakage and truncated transcripts of c-myc oncogene in murine plasmacytomas. *Nature* **303**, 401-406.

42. Fort P, Marty L, Piechaczyk M, El Sabrouty S, Dani C, Jeanteur P, and Blanchard JM (1985). Various rat adult tissues express only one major mRNA species from the

43. Mischak H, Goodnight J, Kolch W, Martiny-Baron G, Schaechtle C, Kazanietz MG, Blumberg PM, Pierce JH, and Mushinski JF (1993). Overexpression of protein kinase C-δ and-ε in NIH 3T3 cells induces opposite effects on growth, morphology, anchorage dependence, and tumorigenicity. *J. Biol. Chem.* **268**, 6090-6096.

44. Hirt B (1967). Selective extraction of polyoma DNA from infected mouse cell cultures. *J. Mol. Biol. 26*, 365-369.

45. Coggins LW (1987). Electron microscopy in molecular biology: a practical approach. Eds. Sommerville J and Scheer U. IRL Press at Oxford University Press.

46. Israels SJ and Gerrard JM (1996). *Platelets: A Practical Approach.* Eds. Watson SP and Authi KS. IRL Press and Oxford University Press.

47. Kuschak TI, Paul JT, Wright J., Mushinski JF, and Mai S. (1999). FISH on purified extrachromosomal DNA molecules. Technical Tips Online *(in press).*

48. Mushinski JF, Bauer SR, Potter M, and Reddy EP (1983). Increased expression of myc-related oncogene mRNA characterizes BALB/c plasmacytomas induced pristane or Abelson murine virus. *Proc. Natl. Acad. Sci. USA* **80**, 1073-1077.

49. Gaubatz JW (1990). Extrachromosomal circular DNAs and genomic sequence plasticity in eukaryotic cells. *Mutation Res.* **237**, 271-292.

50. Classon M, Henriksson M, Sumegi J, Klein G, and Hammaskjold ML (1987). Elevated c-myc expression facilitates the replication of SV40 DNA in lymphoma cells. *Nature* **330**, 272-274.

51. Flores SC, Sunnerhagen P, Moore TK, and Gaubatz JW (1988). Characterization of repetitive families in mouse heart polydisperse circular DNAs: age-studies. *Nucl. Acids Res.* **16**, 3889-3906.

52. Wahl GM (1989). The importance of circular DNA in mammalian gene amplification. *Cancer Res* **49**, 1333-1340.

53. Cohen S, Regev A, and Lavi S (1997). Small polydispersed circular DNA (spcDNA) in human cells: association with genomic instability. *Oncogene* **14** 977-985.

54. VanDevanter DR, Piaskowski VD, Casper JT, Douglass EC, and Von Hoff, DD (1990). Ability of circular extrachromosomal DNA molecules to carry amplified MYCN proto-oncogenes in human neuroblastomas in vivo. *J. Natl. Cancer Institute* **82**, 1815-1821.

55. Hahn PJ (1993). Molecular biology of double-minute chromosomes. *Bioessays* **15**, 477-484.

56. Kaufman, RJ, Brown PC, and Schimke RT (1979). Amplified dihydrofolate reductase genes in unstably methotrexate-resistant cells are associated with double minute chromosomes. *Proc. Natl. Acad. Sci USA* **76**, 5669-5673.

57. Mai S, Fluri M, Siwarski D, and Huppi K (1996). Genomic instability in Myc-ER-activated Rat1a Myc-ER cells. *Chromosome Research* **4**, 365-371.

58. Coleman AE, Schröck E, Weaver Z, du Manoir S, Yang F, Ferguson-Smith MA, Ried T, and Janz S (1997). Previously hidden chromosome aberrations in BALB/c plasmacytomas uncovered by multicolor spectral karyotyping (SKY). *Cancer Res.* **57**, 4585-4592.

59. Felsher, DW and Bishop, JM (1999). Transient excess of MYC activity can elicit genomic instability and tumorigenesis. *Proc. Natl. Acad. Sci USA* **96**, 3940-3944.

60. Jiang W, Kahn SM, Zhou P, Zhang YJ, Cacace AM, Infante SD, Santella RM, and Weinstein IB (1993). Overexpression of cyclin D1 in rat fibroblasts causes abnormalities in growth control, cell cycle progression and gene expression. *Oncogene* **8**, 3447-3457.

61. Motokura T and Arnold A. Cyclin D and oncogenesis. *Curr. Opin. Genet. Dev.* **3**, 5-10.

62. Wang TC, Cardiff RD, Zuckerberg L, Lees E, Arnold A, and Schmidt EV (1994). Mammary hyperplasia and carcinoma in MMTV-cyclin D1 transgenic mice. *Nature* **369**, 669-671.

63. Zhou P, Jiang W, Zhang Y, Kahn SM, Schieren I, Santella RM, and Weinstein IB (1995). Antisense to cyclin D1 inhibits growth and reverses the transformed phenotype of human esophageal cancer cells. *Oncogene* **11**, 571-580.

64. Zhang S-Y, Liu S-C, Goodrow T, Morris R, and Klein-Szanto AJP (1997). Increased expression of G1 cyclins and cyclin-dependent kinases during tumor progression of chemically induced mouse skin neoplasms. *Mol. Carcinogenesis* **18**, 142-152.

65. Leach FS, Elledge SJ, Sherr CJ, Willson JKV, Markowitz S, Kinzler KW, and Vogelstein B (1993). Amplification of cyclin genes colorectal carcinomas. *Cancer Res.* **53**, 1986-1989.

66. Hanna Z, Jankowski M, Tremblay P, Jiang X, Milatovich A, Francke U and Jolicoeur P (1993). The *Vin-1* gene, identified by provirus inertional mutagenesis, is the cyclin D2. *Oncogene* **8**, 1661-1666.

67. Lücke-Huhle C (1994). Permissivity for methotrexate-induced DHFR gene amplification correlates with the metastatic potential of rat adenocarcinoma cells. *Carcinogenesis* **15**, 695-700.

Figures

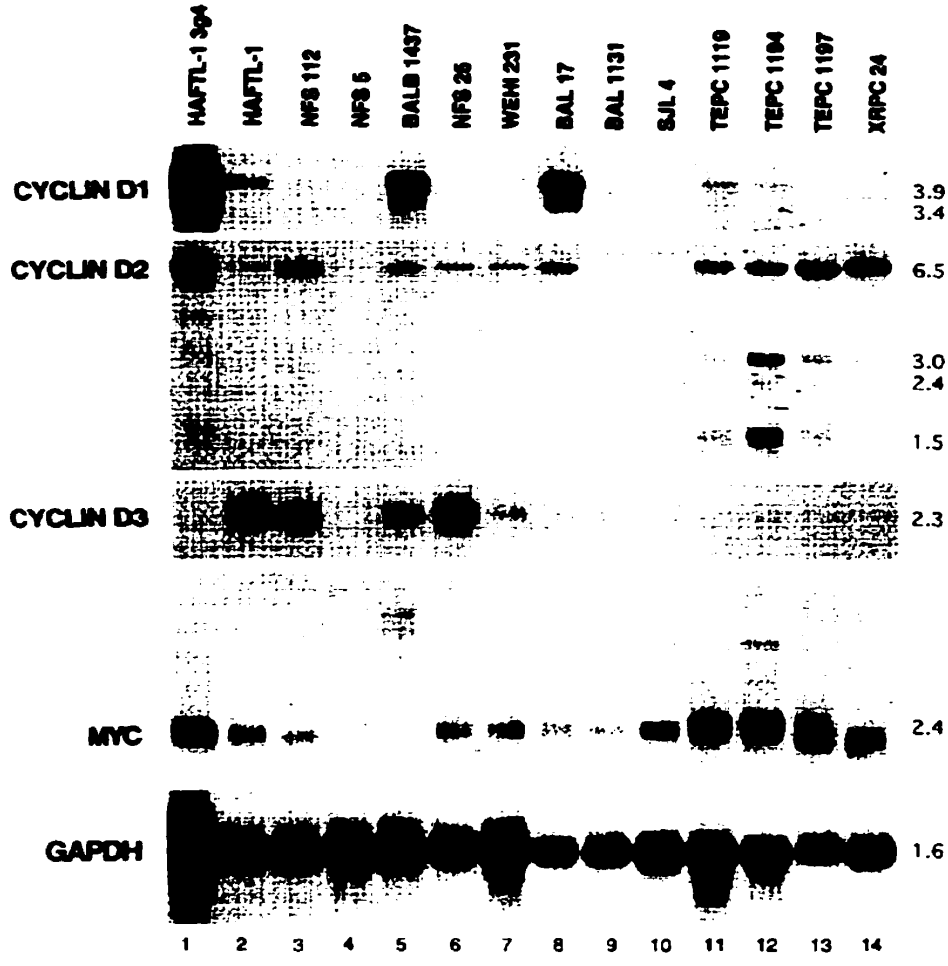

Figure. App.A.1. Cyclin expression in mouse B-lymphocytic tumors. Poly(A)$^+$ RNAs (5 μg) from a series of mouse B-lymphocytic cell lines (28) are arranged from left-to-right in increasing degree of maturation. HAFTL-1 3g4 and HAFTL-1 are two related clones of pro-B lymphocytes, the former having more myeloid characteristics than B-cell characteristics; NFS 112, NFS 5 and BALB 1437 are pre-B cell lines; NFS 25, WEHI 231, BAL 17 and BAL 1131 are mature B-cell lines, SJL 4 is a plasmablastic line; and TEPC 1119, TEPC 1194, TEPC 1197 and XRPC 24 are plasmacytoma lines. The blot was hybridized first with *cyclin D2* cDNA and then sequentially with the other hybridization probes indicated along the left margin, following stripping. Sizes of major hybridizing bands are indicated on the right.

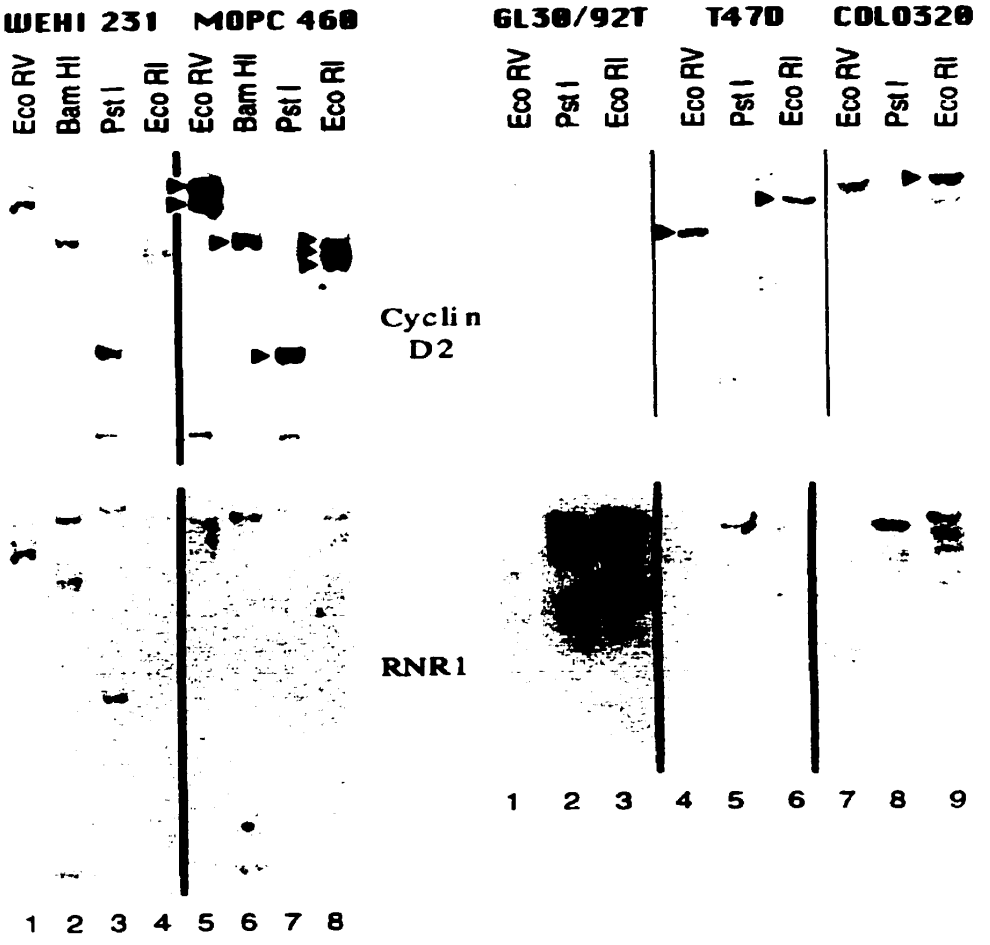

Figure App.A.2. Southern blot analyses of mouse and human cell lines hybridized with murine and human cyclin D2 cDNA probes, as indicated (upper panels). Mouse lines: WEHI 231 B-cell lymphoma (low Myc) and MOPC 460D plasmacytoma (high Myc); Human lines: GL30/92T primary fibroblasts (low Myc), T47D breast carcinoma cells (high Myc), and COLO320HSR colorectal carcinoma cells (very high Myc). Digests were carried out with the enzymes indicated. 10 μg of DNA were loaded per lane. The filters were rehybridized with the cDNA of mouse *R1* (lower panels) to control for amount of DNA loaded. More DNA from GL30/92T was loaded in the control wells to illustrate the restriction endonuclease products of the unamplified *cyclin D2* gene. Filled arrowheads point to amplified *cyclin D2* bands; empty arrowheads indicate lost bands that suggest another form of genomic instability in this tumor.

Figure App.A.3. Fluorescent in situ hybridization (FISH) studies with cyclin D2 probes and detection with FITC-labeled anti-digoxigenin antibody. A. COLO320HSR metaphase chromosomes stained with propidium iodide (human *cyclin D2* cDNA hybridization is seen as green fluorescing spots or dark green dots when found on chromosomes). B. MOPC 460 metaphase chromosomes stained with PI (mouse cyclin D2 genomic DNA hybridization is seen as green fluorescing spots or dark green dots when found on chromosomes). The arrows point to paired dark green dots that indicate the positions of the endogenous cyclin D2 loci. The imaging software generates the dark colors when an FITC signal is superimposed on a PI-stained chromatid. Single light green dots seen elsewhere in the spreads are interpreted as EEs that are loosely associated with these chromosomes. C and D. Metaphase chromosomes from mouse pre-B lymphoma cells that bear the 4HT-activatable pBabePuroMyc-ERTM expression vector were hybridized with *cyclin D2* on a DAPI background. Cells in C were not stimulated with 4HT; those in D were grown in 100 nM 4HT for 3 days. Arrows point to single-copy *cyclin D2* in C and to extrachromosomal elements in D. E-H. Metaphase chromosomes from ψ2 fibroblasts hybridized with *cyclin D2*. DAPI was used to counterstain DNA. The image in E shows a negative control of FISH analysis of 4HT-treated (3 days) ψ2 chromosomes from cells that have not received the Myc expression vector. F, G and H show metaphase and interphase chromosomes from cells bearing stable integration of pBabePuroMyc-ER^{TM}. Cells in F were not stimulated with 4HT; those in G and H were grown in 100 nM 4HT for 3 days.

Figure App.A.3. (A-D)

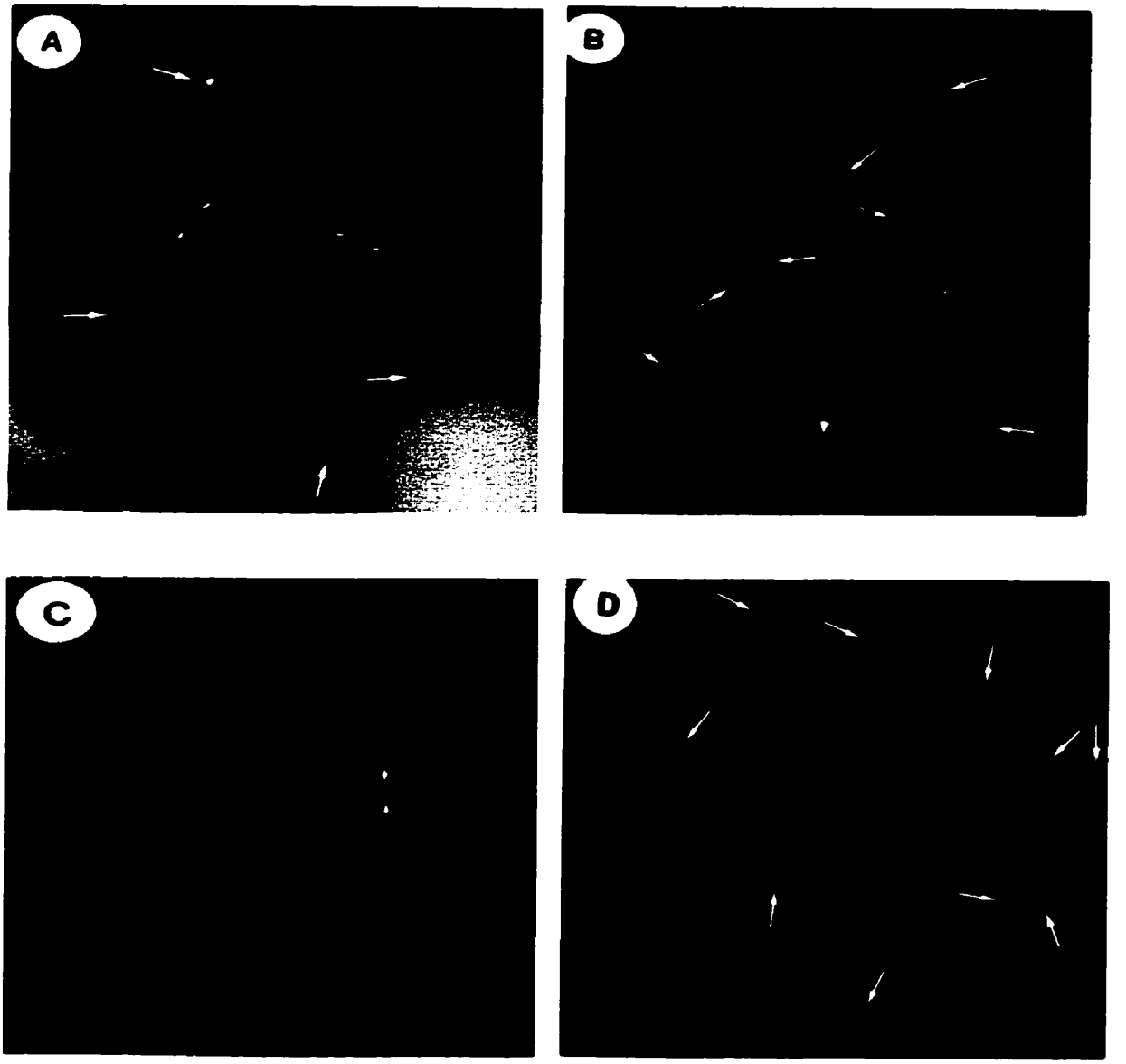

Figure App.A.3. (E-H)

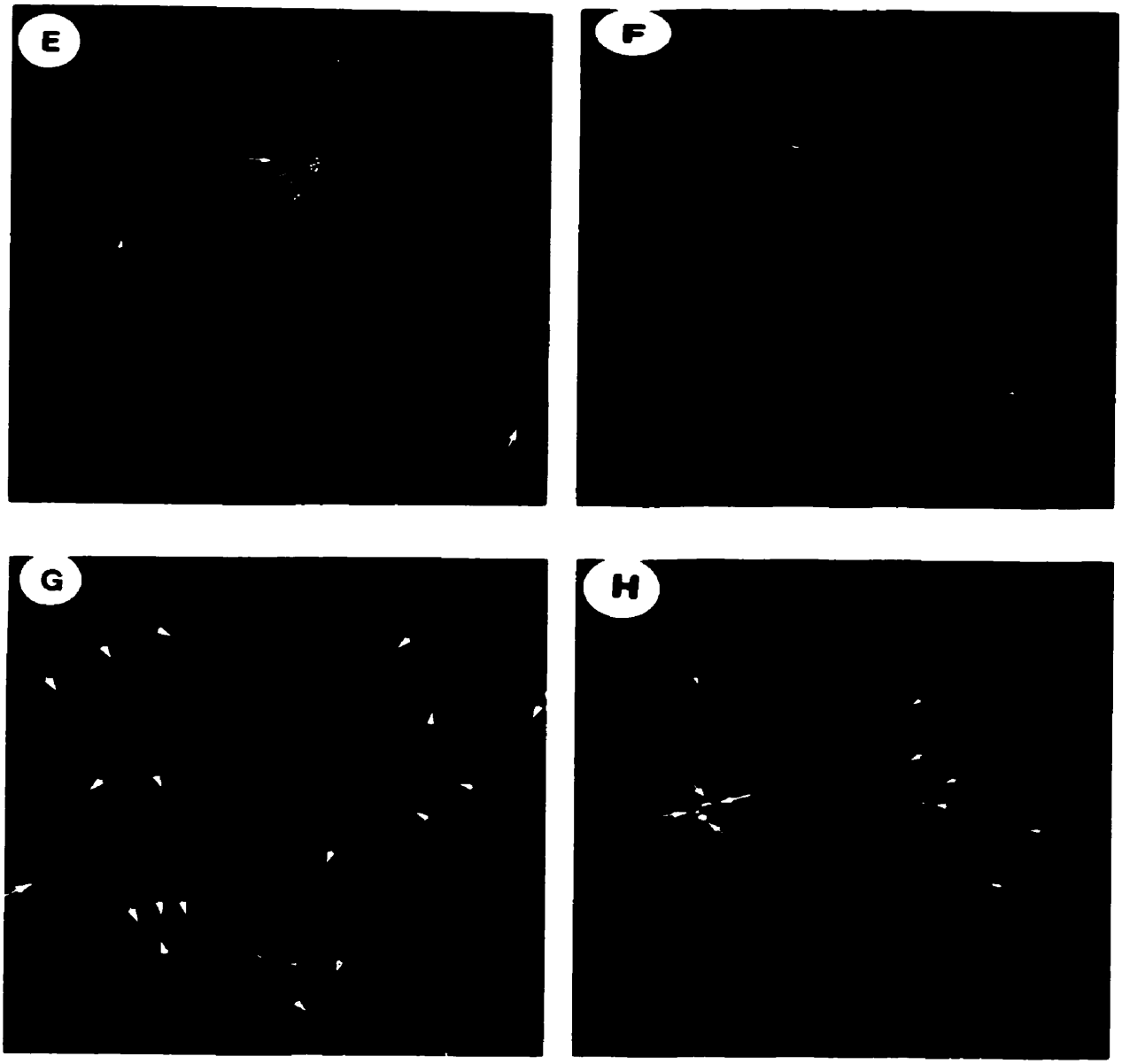

Figure App.A.4. Cyclin D2 expression after Myc activation. A. Northern blots of total RNA (15 μg) from cultures of mouse pre-B cells stably transduced with v-Abl (A-MuLV) or with v-Abl plus murine Bcl-2 plus pBabePuroMycER^{TM}. Both cell lines were treated with 4HT for 0, 1, 4 and 6 days, as indicated. Each blot was hybridized, first with cyclin D2 cDNA, and then sequentially with the other hybridization probes indicated along the right margin following stripping. Sizes of major hybridizing bands are indicated between panels. Ethidium-bromide-stained 28S ribosomal RNA bands are shown as loading controls. B. Western blots of 10 μg of protein per lane, isolated from pre-B cells, with and without pBabePuroMycER^{TM}, after different periods of stimulation with 4HT. Antibody specificity and size of detected protein bands are indicated between panels. Actin probing of duplicate blots is shown as loading control. C. Northern analysis of total RNA (conditions as in A) from mouse fibroblasts (ψ2 cells) with and without stable integration of pBabePuroMyc-ERTM, after different numbers of days of stimulation with 4-HT. GAPDH hybridization is included as a loading control.

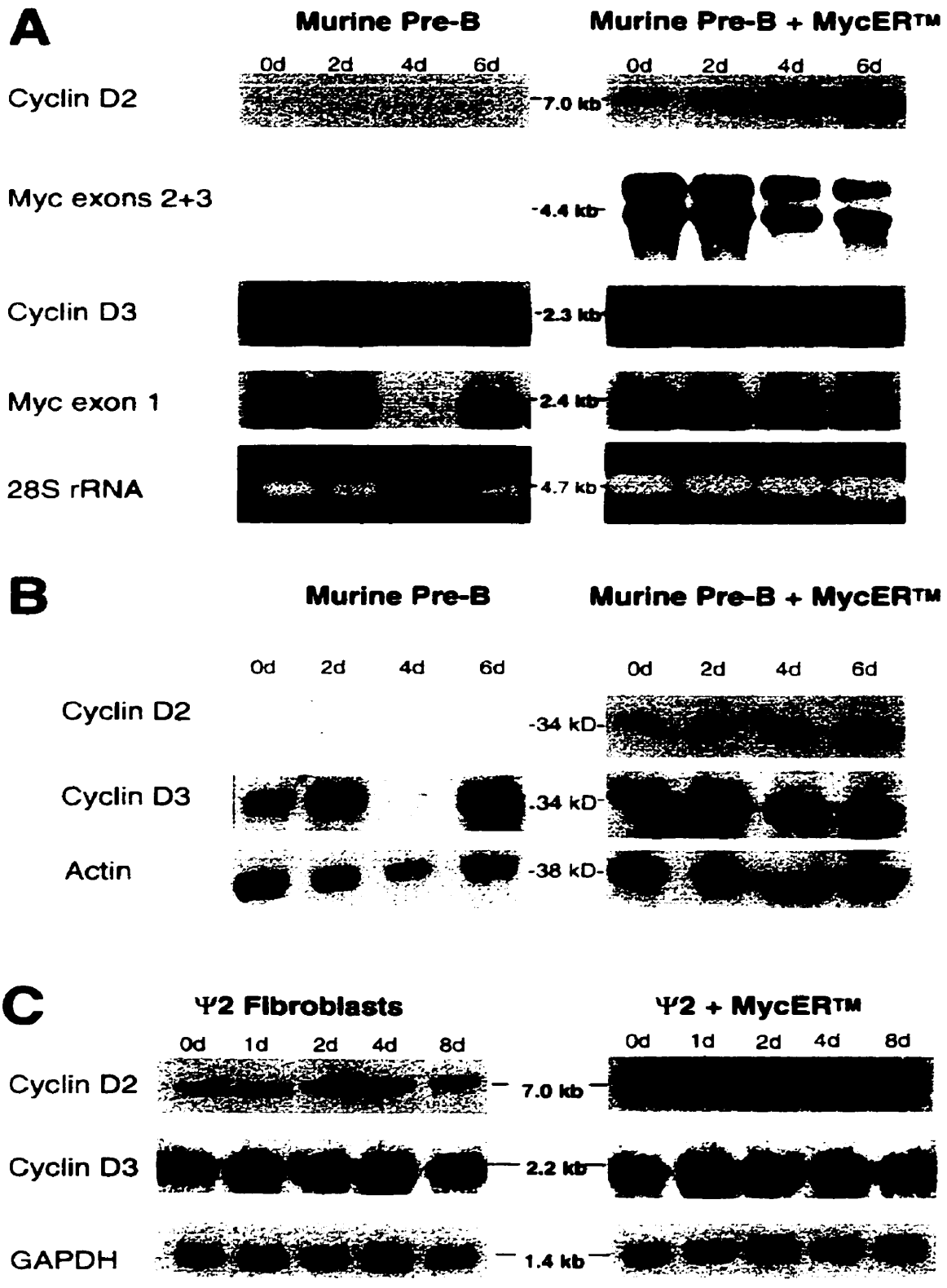

Figure App.A. 4.

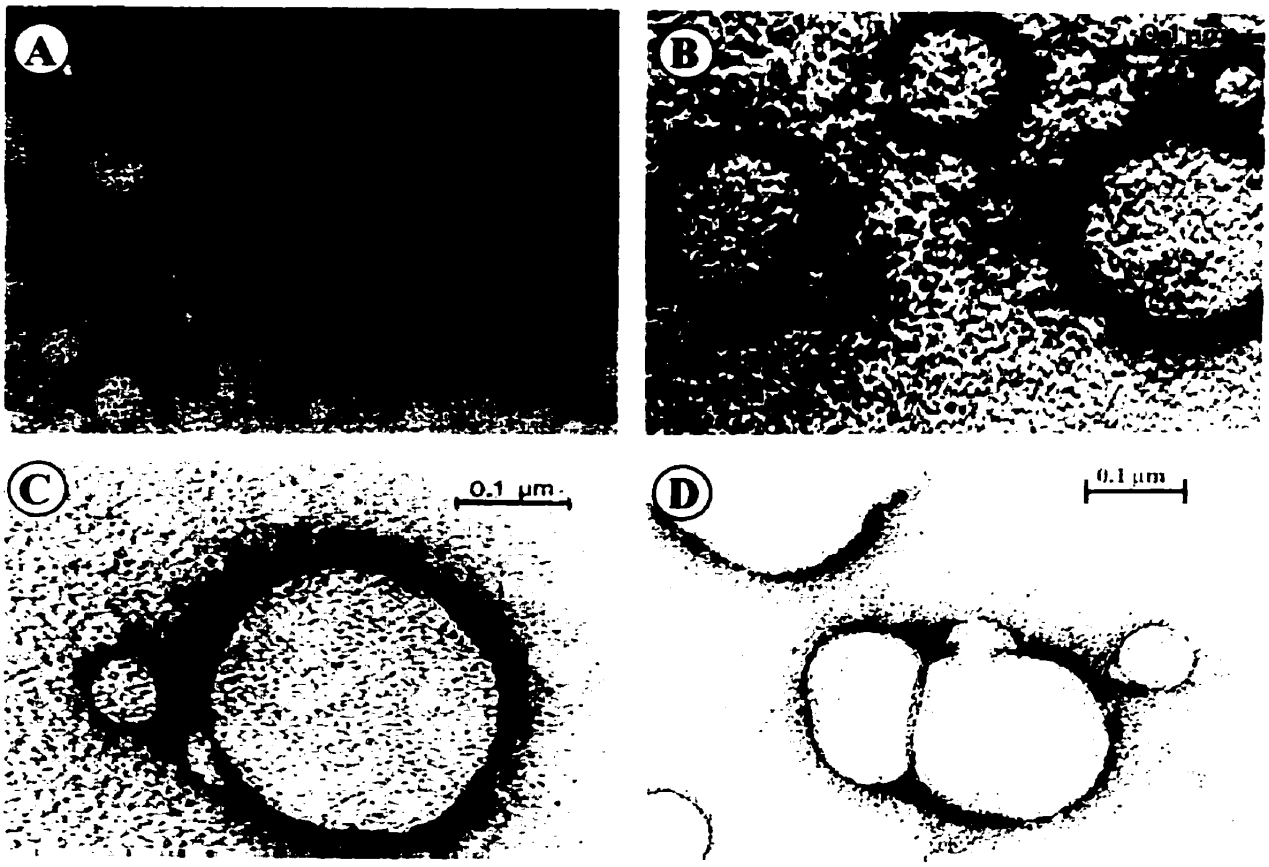

Figure App.A.5. Electron microscopy of extrachromosomal elements. EEs from pBabePuroMycER^{TM}-transduced pre-B cells before (A) and after 3 days of Myc activation by 4HT (B-D) were prepared according to Hirt (1967). These extracts were placed on formvar-covered grids, stained with uranyl acetate, tungsten shadowed and examined by transmission electron microscopy. Magnification was 41,000 x.

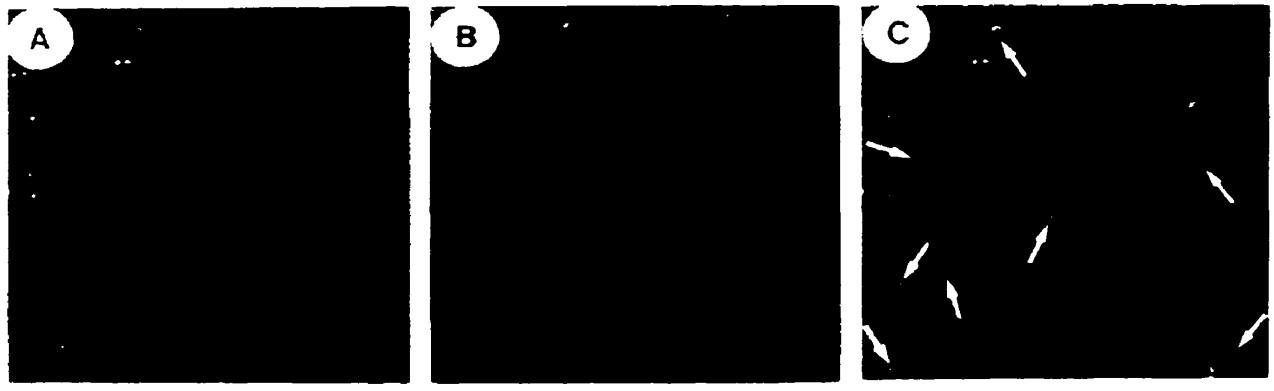

Figure App.A.6. FISH on extrachromosomal elements. Hirt extracts from pBabePuroMycER™-transduced pre-B cells were affixed to glass slides, stained with DAPI to identify EEs by their DNA content (ca. 90 blue dots shown in a). The slide was then hybridized to the ten cyclin D2 genomic probe to locate EEs bearing these sequences (shown as green fluorescent dots in b). In c, a composite image was created by overlaying the blue DAPI signals onto those of the green fluorescein-labeled anti-digoxygenin antibody that detects the cyclin D2 hybridization signals. The large white arrows in c point out the nine authentic cyclin D2-bearing EEs that are both DAPI- and fluorescein-positive. Generally only the larger DAPI-stained dots hybridized with the cyclin D2 probe. The small white arrow points out one of the rare fluorescein-positive spots that do not appear to colocalize with a DAPI-positive spot.

Appendix B

Preface

Appendix B is the full paper format of a manuscript published in the journal *Proceedings of the National Academy of Science, USA.* Francis Wiener[1], Theodore I. Kuschak[2], Shinsuke Ohno[3], Sabine Mai[2,4] (1999). Deregulated expression of c-Myc in a translocation negative plasmacytoma on extrachromosomal elements that carry *IgH* and *myc* genes. *Proc. Natl. Acad. Sci., USA* **24**: 13967-13972.

This paper was the first to demonstrate that DCPC21 mouse plasmacytoma harbors c-*myc* and *IgH* genes on extrachromosomal elements (EEs) and that *c-myc* is transcribed. The authors describe that in this plasmacytoma, c-Myc expression of the c-Myc oncoprotein is initiated outside the chromosomal locations of the c-*myc* gene, namely from extrachromosomal elements (EEs), which can be considered functional genetic units. These data also imply that other "translocation-negative" experimental and human tumors with fusion transcripts or oncogenic activation may indeed carry translocation(s), however in an extrachromosomal form.

Deregulated expression of c-Myc in a translocation negative plasmacytoma on extrachromosomal elements that carry *IgH* and *myc* genes.

Francis Wiener[1], Theodore I. Kuschak[2], Shinsuke Ohno[3], Sabine Mai[2,4]

Classification: Biological Sciences (Medical Sciences)

[1] Microbiology and Tumorbiology Center, Karolinska Institute, Box 280, S-171 77 Stockholm, Sweden

[2] The Genomic Centre for Cancer Research and Diagnosis, Manitoba Institute of Cell Biology, Manitoba Cancer Treatment and Research Foundation and the University of Manitoba, 100 Olivia Street, Winnipeg, MB R3E 0V9, Canada

[3] Department of Molecular Immunology, Cancer Research Institute Kanazawa University, 13-1, Takara-machi, Kanazawa 920, Japan

[4] corresponding author: The Genomic Centre for Cancer Research and Diagnosis, Manitoba Institute of Cell Biology and the University of Manitoba, 100 Olivia Street, Winnipeg, MB R3E 0V9; phone: 204-787-2135, FAX: 204-787-2190; e-mail: smai@cc.umanitoba.ca

ABSTRACT

The induced expression of c-Myc in plasmacytomas in BALB/c mice is regularly associated with non-random chromosomal translocations that juxtapose the *c-myc* gene to one of the immunoglobulin (*Ig*) loci on chromosome 12 (*IgH*), 6(*IgK*) or 16(*IgL*). The DCPC21 plasmacytoma belongs to a small group of plasmacytomas that are unusual in that they appear to be translocation-negative. In this paper, we show the absence of any *c-myc*-activating chromosomal translocation for the DCPC21, using fluorescent *in situ* hybridization, chromosome painting and spectral karyotyping. We find that DCPC21 harbors c-*myc* and *IgH* genes on extrachromosomal elements (EEs) from which *c-myc* is transcribed, as shown by *c-myc* mRNA tracks and extrachromosomal gene transfer experiments. The transcriptional activity of these EEs is further supported by the presence of the transcription-associated phosphorylation of histone H3 (H3P) on the EEs. Thus, our data suggest that in this plasmacytoma, c-Myc expression is achieved by an alternative mechanism. The expression of the c-Myc oncoprotein is initiated outside the chromosomal locations of the c-*myc* gene, *i.e.* from EEs, which can be considered functional genetic units. Our data also imply that other "translocation-negative" experimental and human tumors with fusion transcripts or oncogenic activation may indeed carry translocation(s), however in an extrachromosomal form.

INTRODUCTION

The activation of the *c-myc* gene is key to the development of all murine plasmacytomas (PCTs), resulting in deregulated levels of endogenous c-Myc protein expression (1-3). In the majority of pristane-induced mouse PCTs, the deregulation of *c-myc* transcription is achieved by chromosomal translocation that juxtaposes the c-*myc*/*pvt*-1 locus on chromosome 15 to one of the immunoglobulin (*Ig*) loci: on chromosome 12 (*IgH*), 6(*IgK*) or 16(*IgL*) (2,3).

In a few PCTs, classical G-banding analysis could not identify any of the plasmacytoma-associated typical or variant translocations (3). Molecular and cytogenetic analysis of the translocation-negative PCTs revealed that the overexpression of the *c-myc* gene was achieved by different means. c-Myc deregulation resulted from either promoter/enhancer insertion brought about by retroviral insertion into the 5' flanking region of *c-myc* (4), insertion of the *Ig* heavy chain enhancer (5) or complex genomic rearrangements (6,7). Although less than 1% of the PCTs analyzed to date belong to the group of translocation-negative plasmacytomas, they are of interest because they may reveal a new mechanism of plasmacytomagenesis. Consequently, the lack of cytogenetically identifiable translocations suggests alternate pathways by which c-Myc overexpression is achieved in this group of tumors.

To examine the mechanism(s) of c-Myc deregulation in translocation-negative PCTs, we focused our investigation on DCPC21, a plasmacytoma that had been induced by intraperitoneal implantation of a plastic diffusion chamber into a BALB/c female mouse (6). Previous work by these authors had suggested that DCPC21 exhibited complex molecular rearrangements leading to the *IgH-myc* gene juxtaposition by the

insertion of the *myc* and *pvt*-1 loci-containing chromosome 15 segment into the *IgH* locus on Chr 12 (7). The realization of such a complex rearrangements requires the occurrence of a paracentric inversion, a deletion/insertion, and multiple translocations both on chromosome and gene levels during the process of the *IgH-myc* illegitimate recombination (7).

Here we report that the results of classical and molecular cytogenetic analyses show that the DCPC21 plasmacytoma lacks any type of interchromosomal recombination that could cause the constitutive activation of the c-*myc* gene. However, chromosomal segments containing *c-myc* and *IgH* sequences are present - either alone or jointly - on extrachromosomal elements (EEs) in the DCPC21 plasmacytoma. We demonstrate that the deregulated expression of *c-myc* occurs on EEs, and this appears to be sufficient to sustain the malignant phenotype of the DCPC21 tumor.

MATERIALS AND METHODS

Tumor cells. DCPC21 was induced in a female BALB/c mouse by i.p. implantation of a Millipore diffusion chamber (8).

Trypsin-Giemsa Banding. Metaphase spreads were prepared without colcemid treatment. Trypsin-Giemsa banding was performed as described previously (9) and adapted to mouse chromosomes. Chromosome identification followed the recommendations of the Committee on Standardized Genetic Nomenclature for Mice (10).

Molecular cytogenetics. Chromosomes were analyzed by FISH (fluorescent *in situ* hybridization) as previously published (11,12). Analysis of slides was performed using a Zeiss Axiophot microscope, a PowerMacintosh 8100 computer, and a CCD camera (Photometrics); the analytical software used was IPLabSpectrum Version 3.1 (Signal Analytics, USA).

FISH probes and detection of hybridization. The following probes were used, *c-myc* (13), *IgH* (*pJ11*; 14) and *pvt-1* (15). The probes were labeled by random priming with either digoxigenin- or biotin-dUTP (Roche Diagnostics, Laval, Quebec, Canada). The detection of hybridization signals with digoxigenin-labeled probes was carried out using a fluorescein conjugated polyclonal sheep anti-digoxigenin- antibody (Roche Diagnostics). For the detection of hybridization signals obtained with biotinylated probes, we used a monoclonal anti-biotin antibody (Roche Diagnostics) followed by a Texas Red-conjugated goat anti-mouse-IgG secondary antibody (Southern Biotechnology Assoc., Inc., Birmingham, USA).

FISH-EEs (FISH on purified extrachromsomal DNA molecules). The total population of extrachromosomal elements (EEs) was purified and examined by FISH as described in (16). EEs were hybridized with *c-myc*, *IgH* and *pvt-1*. The specificity of these hybridizations was confirmed by the absence of hybridization signals with a negative control, *cyclin C* (11,16) and hybridization signals obtained with a positive control, *cot-1* DNA (not shown).

Chromosome painting. The chromosome paints used (CedarLane, Laboratories Limited, Hornby, Ontario, Canada) were a FITC-conjugated mouse chromosome 15 and a biotinylated mouse chromosome 12-specific paint. Hybridization of chromosome paints, alone or in combination with FISH probes, was carried out as described in the general FISH protocol. Chromosome 12 hybridization signals were detected with a monoclonal anti-biotin antibody (Roche Diagnostics) at 0.5 ng/slide followed by a Texas Red conjugated goat anti-mouse-IgG secondary antibody (Southern Biotechnology Assoc., Inc., Birmingham, USA) at 2.5 ng/slide. The hybridization signals of the FITC-labeled chromosome 15 paint were amplified using a rabbit anti-FITC antibody (CedarLane), followed by a FITC-labeled goat anti-rabbit IgG secondary antibody (Sigma). Both antibodies were used at 1:40 dilution.

SKY. Spectral karyotyping was performed using the ASI (Applied Spectral Imaging, CA, USA; Migdal Ha'Emek, Israel) kit for mouse spectral karyotying and the suppliers' hybridization protocols. Analyses were carried out using the Spectra Cube™ on a Zeiss Axiophot 2 microscope and the SkyView 1.2 software on a PC (PII-350).

mRNA track studies. mRNA tracks studies were carried out as described in (17) on freshly isolated ascitic DCPC21 tumor cells. The cells were cytospun onto microscopic slides (10^5 cells/slide) and fixed in formaldehyde (1% in 1xPBS/50mM $MgCl_2$). The slides were washed in 2xSSC, dehydrated sequentially in 70%, 90% and 100% ethanol. A denatured mouse *c-myc* probe, pMycEx2, a 460 bp PstI-fragment of *myc* exon 2 (gift from Dr. K. Huppi, NIH), was added in 50% formamide/2xSSC/50mM phosphate buffer,

10% dextran sulfate for overnight hybridization at 37°C in a humidified incubator. As expected, subsequent RNAse treatment removed any hybridization signals, and hybridization to chromosomes or extrachromosomal material was only achieved after the slides had been treated with RNAse and pepsin and denatured prior to the addition of FISH probes (see also 18).

Fluorescent immunohistochemistry. Immunohistochemistry was performed as described (12). The following antibodies were used, a monclonal anti-c-myc antibody, 3C7 (19) at 20 ng/slide. Visualization of this antibody was achieved with a Texas Red – conjugated secondary goat anti-mouse IgG antibody (Southern Biotechnology Assoc., Inc., Birmingham, USA) at 2.5 ng/slide. A sheep anti- CORE histone antibody (US Biological) was used at 5 ng/ slide and visualized with a FITC-conjugated donkey anti-sheep IgG antibody (Sigma) at 2.75 ng/slide. The anti-histone H3P antibody used is a histone H3-phophoserine monoclonal antibody from Dr. Z. Darzynkiewicz (20). It was used at 4.0 ng/slide and visualized with a Texas Red-conjugated goat anti-mouse IgG antibody (Southern Biotechnology Assoc., Inc., Birmingham, USA) at 2.5 ng/slide.

Southern analysis. For Southern analyses, 10 µg DNA from primary BALB/cRb6.15 spleen or DCPC21 tumor DNA was digested overnight with 40 units of either *Hin*dIII or *Sac*I restriction endonucleases (Roche Diagnostics) and electrophoretically separated on a 0.8% agarose gel, blotted onto Hybond XL membrane (Amersham Pharmacia Biotech), and baked at 80°C for 2 hours. Hybridizations and washes were carried out according to

standard procedures (21). The probes used were, *c-myc* (13), *pJ11* (14) *pvt-1* (15; 22), *JQ2* (7).

Electroporations. Spleen cells of BALB/cRb6.15 mice were harvested for extrachromosomal gene transfer studies as follows. Green fluorescent protein (GFP, pEGFP-N1, Clontech, Mississauga, Ontario, Canada) was used as a tracer molecule for determination of gene transfer efficiencies. Lymphocytes isolated from one spleen were divided into three groups: electroporation of GFP plus *c-myc/IgH*-carrying EEs (2.5 μg), electroporation of GFP (2.5 μg), and "mock" electroporation. Electroporations were carried out in OPTI-MEM solution (Canadian Life Technologies, Burlington, Ontario, Canada) using 1 ml Gene Pulser^R cuvettes, 0.4 cm (Bio-Rad, Hercules, CA, USA) using a Bio-Rad electroporator, model #1652076, and a Bio-Rad Capacitance Extender, model #1652087. The settings used were: 960K, 240V, cap. 25 units. Subsequent to electroporation, the cells were washed in complete medium (RPMI1640 with 10% fetal calf serum (Canadian Life Technolgies, Burlington, Ontario, Canada), 2 mM L-glutamine, 5 IU/ml of penicillin and 5 μg/ml streptomycin and 50 μM/ml β-mercaptoethanol and allowed to grow in complete medium in a humidified incubator at 37°C and in the presence of 5%CO_2. 24 hours after gene transfer, cells were cytospun onto microscope slides (10^5 cells/slide), and c-Myc protein expression was determined in splenic B cells that also expressed GFP. A FITC-conjugated anti-B220 antibody (Pharmingen, Mississauga, Ontario, Canada) was used to visualize splenic B cells on cytospin preparations. Fluorescent immunohistochemistry of the electroporated cells was carried out as previously described (12).

RESULTS

DCPC21 is a translocation-negative plasmacytoma harboring extrachromosomal elements

Karyotyping of DCPC21 metaphase spreads by standard G-banding revealed that chromosomes 15, 12, 6, and 16, regularly involved in mouse PCT-specific translocations, were not part of reciprocal translocation events (Figure App.B.1a). To confirm the results provided by G-banding, DCPC21 metaphases were further examined by chromosome painting, fluorescent *in situ* hybridization (FISH), and spectral karyotyping (SKY) (Figs. App.B.1b-e). Since the most frequent translocation (>90%) in pristane-induced mouse PCT transposes the c-*myc* containing segment of chromosome 15 into the neighborhood of the *IgH* gene loci on chromosome 12 (3), chromosome painting was performed to ascertain whether chromosomes 12 and 15 are carriers of cryptic rearrangements. The painting with chromosome 15- and 12-specific probes revealed the presence of four copies of chromosome 15 (green) and chromosome 12 (red) in the majority of the DCPC21 plates analyzed. More importantly, neither chromosome 15- nor chromosome 12-derived genetic material was found to be translocated or inserted into any other chromosome of DCPC21 metaphases (Figures. AppB. 1b and c).

When either chromosome 12 paint was combined with FISH using a c-*myc* probe or chromosome 15 paint used in combination with an *IgH* probe (*pJ11*), it was also evident that chromosomes 12 and 15 were not involved in reciprocal translocations (Figure App.B.1d and data not shown). However, extrachromosomal elements (EEs) carrying either c-*myc* or *IgH* genes alone or c-*myc* and *IgH* genes jointly became apparent (Figure App.B.1d arrow).

The possible involvement of the *IgK*- and *IgL*-carrying chromosomes 6 and 16 in *Ig/myc* translocation was analyzed by SKY (Figure App.B.1e). SKY corroborated the data obtained by standard cytogenetics, painting and FISH, namely, that DCPC21 does not carry any plasmacytoma-associated *c-myc*-activating translocation.

In addition, SKY revealed the nature and structure of the chromosomal aberrations detected by G-banding. Noteworthy, SKY showed that the duplicated D2 band on one of the chromosomes 15 (Figure App.B.1a, arrow) contained only chromosome 15-derived genetic material (Figure App.B.1e), excluding the likelihood of an interchromosomal rearrangement involving chromosome 15. The additional band on chromosome 9 was identified as derived from chromosome 16, while one copy of chromosome 16 was centromerically fused with one chromosome 19. A "hidden" chromosomal aberration, undetected by classical G-banding, was the insertion of chromosome 3-derived material into one chromosome 2. Since the aberrations involving chromosomes 9 and 2, as well as the fusion of chromosomes 16 and 19, were not consistently seen in all metaphases, they are likely chromosomal aberrations acquired during tumor progression, rather than during tumor initiation.

Classical cytogenetics, chromosome painting, FISH and SKY establish that the DCPC21 plasmacytoma lacks any chromosomal aberration that could reasonably be involved in the constitutive activation of the c-*myc* gene. However, the presence of *IgH* and *c-myc* sequences on extrachromosomal elements (EEs) suggests that these genetic entities may be responsible for the deregulation of c-Myc in this tumor.

Southern blot analysis shows rearrangements within the *IgH* locus and in the 5' flanking region of c-*myc*.

Southern blot analysis was performed with normal mouse spleen DNA and DCPC21 tumor DNA. The c-*myc* gene, visualized by using a mouse exon 2 -specific probe, showed no rearrangement(s) and exhibited identical hybridization patterns in HindIII- and SacI-digests of normal spleen and DCPC21 DNA (Figure App.B.2a). Similarly, *pvt*-1 showed no evidence of rearrangements (Figure App.B.2c). The stronger hybridization signals of *c-myc* and *pvt-1* in DCPC21 DNA reflect both the duplication of the *myc/pvt-1*-containing 15D2 band of one of the chromosome 15 (Figure App.B.1a, arrow) and the additional copies of chromosome 15 (Figure App.B.1). In contrast to the germ line bands observed with *c-myc* and *pvt-1*, rearrangements within the *IgH* sequences and in the 5' flanking region of *c-myc* became apparent when using the *IgH* probe (*pJ11*) as well as a 5' flanking probe of the *c-myc* gene (*JQ2*) (Figures. App.B.2 b and d respectively).

Since none of the bands that hybridized with *pJ11* co-hybridized with *JQ2*, it can be excluded that any of the additional bands represent a cryptic transposition of sequences detected by *pJ11* and *JQ2*. Furthermore, a transposition of *pvt*-1 and *c-myc* within the chromosomal DNA of DCPC21 is unlikely, since, as shown in Figure App.B.2, these two genes were not involved in translocation and or rearrangement events detectable in genomic DNA. These results suggest that the rearranged genomic bands represent intrachromosomal rearrangements, possibly due to the excison of c-*myc* and *IgH* sequences from the relevant chromosomes rather than interchromosomal recombination.

c-*myc* and *IgH* co-localize on extrachromosomal elements (EEs) and are functional genetic units

We consistently observed extrachromosomal *c-myc* and *IgH* hybridization signals in DCPC21 metaphases (Figure App.B.1). To analyze these EEs further, we performed FISH on the total population of EEs. Figure App.B.3 illustrates the findings for FISH-EEs hybridized with *c-myc* and *IgH* probes. In the majority of the cases, *c-myc* and *IgH* were found together on the large EEs (0.1-0.2 μm in diametre, as determined by electron microsopy (EM) measurements) (Figure App.B.3d). Noteably, c-*myc* and *IgH* were also found alone on EEs of smaller sizes (0.01μm in diametre) (Figures App.B. 3b-d). *pvt*-1 could be detected on some of the EEs, together with *c-myc* and *IgH* (not shown).

The co-localization of *c-myc/IgH* on some of the EEs raised the question whether these EEs are biologically active structures. To investigate this hypothesis, we analyzed whether these EEs were associated with active chromatin, could transcribe *c-myc* mRNA and confer c-Myc overexpression to resting primary B cells in extrachromosomal gene transfer studies.

To determine whether the EEs contained active genes, we first examined i) the presence of histones and of the transcription-associated phosphorylated form of histone H3 (H3P) (20,23) on the EEs and ii) carried out mRNA track studies (Figures App.B. 4a and b). Using a pan-histone antibody that detects all histones irrespective of chromatin activation, we found histones on the large, but not on the small EEs. To determine whether the former were also transcriptionally active, we examined the presence of H3P using a monoclonal anti-histone H3P antibody (Materials and Methods). We found that over 90% of the pan-histone-containing EEs also stained with the monoclonal anti-

histone H3P antibody, indicating that these EEs contained active chromatin (Figure App.B. 4a).

To examine whether *c-myc* mRNA was produced from these EEs, we carried out mRNA track studies. As shown in Figure App.B. 4b, we observed that multiple short *c-myc* RNA tracks, typical of episomal (extrachromosomal) gene transcription (17), were generated from DCPC21-EEs. To unequivocally demonstrate that the mRNA was derived from the EEs, we processed the identical slides for FISH after RNAse and pepsin treatment and following slide denaturation. Co-localizing c-*myc* mRNA (red signals) and *c-myc*-EEs DNA signals (green) are shown by arrows in Figure App.B. 4c. We consistently observed that all *c-myc* mRNA tracks colocalized with EEs that showed *c-myc* DNA by FISH. However, the number of *c-myc*-carrying EEs in a DCPC21 cell was higher than the amount of EEs that were transcribing *c-myc* mRNA.

To further examine the functional activity of DCPC21 EEs, we electroporated purified EEs into normal BALB/cRb6.15 spleen cells together with a vector expressing green fluorescent protein (GFP). The latter served as tracer molecule for gene transfer efficiency. The B lineage-specific marker B220 was used to determine the lineage origin of the electroporated cells. When purified DCPC21 EEs were introduced into normal BALB/cRb6.15 spleen cells, they conferred *c-myc* expression to GFP-expressing B220-positive B cells (Figure App.B. 5, panel A). However, within 24 hours, the DCPC-21 EEs induced cell death in the majority of the GFP-expressing B cells (>90%), while cells electroporated with GFP only survived. Cell death was associated with c-Myc overexpression and visible by the appearance of apoptotic bodies (Figure App.B. 5, panel B).

DISCUSSION

c-*myc*/*IgH*-carrying EEs represent an alternative mechanism of c-Myc overexpression in DCPC21 plasmacytoma.

In the present study, we have shown that the DCPC21 plasmacytoma lacks any of the usual chromosomal translocations associated with *c-myc* gene deregulation in plamacytomas. Instead we see the presence of *c-myc* and *IgH* together on EEs in this tumor. This raised the question whether c-Myc deregulation in this plasmacytoma was linked to the presence of these EEs. Several experiments have confirmed that the *c-myc*/*IgH*-carrying EEs express c-Myc. We have directly shown *c-myc* mRNA tracks and active chromatin associated histone H3 phosphorylation on these EEs. This was further confirmed by gene transfer experiments of the EEs. Transfer of EEs from DCPC21 cells into primary mouse B cells resulted in increased c-Myc expression followed by apoptotic cell death. We therefore conclude that the deregulated c-Myc expression in this plasmacytoma occurred by a mechanism not involving chromosomal translocation or viral insertion. This novel pathway of *c-myc* activation involves the formation of extrachromosomal elements that result in c-Myc expression levels similar to that seen in *Ig/myc* chromosomal translocations positive plasmacytomas.

Extrachromosomal DNA elements have been found in all organisms analyzed to date (for review see, 24). EEs may be generated transiently during normal lymphocyte development (25,26) but the size and numbers can vary depending on genotoxic treatments (27-29). Tumor cells often harbour EEs (30,31) and these EEs can contain oncogenes and drug resistance genes (32-38). In a previous study, the MOPC265 plasmacytoma cell line was shown to have a T(12;15) translocation that also contained *c-*

myc and *pvt-1* genes duplicated on chromosome 15 and on extrachromosomal elements (22). However, DCPC21 represents the first reported translocation-negative plasmacytoma carrying functional *c-myc*-transcribing extrachromosomal elements (EEs).

Model for the generation of DCPC21-EEs containing both *myc/pvt-1* and *IgH* sequences.

The presence of c-*myc/IgH*-containing EEs raises the question about the mechanism(s) for their formation in the DCPC21 plasmacytoma. One possible model that is consistent with the experimental data is as follows. This model assumes independent generation of *myc/pvt-1* and *IgH*-carrying EEs followed by recombination to generate *myc/Ig*- carrying EEs. Consistent with this model we find EEs of various sizes, some of which carry both *c-myc* and *IgH* or either gene alone. A possible source for generation of these extrachromosomal elements could be *Ig* switch recombination, since circular elements containing *Ig* sequences have been described in normal B cell development (25). EEs that confer a growth/survival advantage, such as deregulated c-Myc expression, to the cell would be selected and maintained. Since we showed increased apoptotic cell death after gene transfer of EEs into normal B cells other genetic events would also have to occur to prevent apoptosis during plasmacytomagenesis.

Are EEs causally involved in other of translocation negative tumors?

EEs are present in a variety of human tumors but their role in tumor initiation or progression is still poorly understood (39-41). The importance of amplified *c-myc* or *N-myc* genes, located on double minute chromosomes (DMs), for maintenance of tumorigenicity has been shown. Elimination of the DMs results in reduced tumorigenicity (42-44).

Other human neoplasia that normally show specific translocations also have translocation negative subsets. Recent analysis of a series of chronic myelogenous leukemia (CML) cells revealed an incongruity between the overexpression of the oncogenic *BCR-ABL* fusion protein, and the absence of cytogenetically detectable T(9;22)(q34;q11) Philadelphia (Ph) chromosome (45-50). In a recent investigation of the T(11;14) translocation and the overexpression of the *MLL-AF4* fusion gene in acute lymphoblastic leukemia (ALL), revealed that in 7 out of 18 patients the generation of *the MLL-AF4* protein occured without detectable T(11;14) translocations (51). Burkitt lymphomas (BLs) usually contain *Ig/myc*-juxtaposed chromosomal translocations (for review see, 52-54). We have recently found in a translocation-negative BL, c-Myc over expression from EEs containing *c-myc* and *IgH* sequences, without rearrangement of the chromosomal *c-myc* gene (unpublished data).

In conclusion, our results provide evidence that the EEs represent functional genetic units that may play an essential role transformation of the translocation-negative DCPC21 plasmacytoma. Our findings also suggest that other neoplasms with fusion transcripts or oncogene activation and amplification with no visible chromosomal translocations may indeed carry specific translocation(s) in an extrachromosomal form.

Acknowledgements. This research was supported by a University of Manitoba Research Development Fund, the Medical Research Council, the Manitoba Cancer Treatment and Research Foundation, and CFI (Canada Foundation for Innovation). We thank Drs. M. Mowat and G. Hicks for critical reading of this manuscript, and Margaret Skokan (ASI) for her help with SKY.

REFERENCES

1. Cory, S. (1986) *Adv. Cancer Res.* **47**, 189-234.
2. Ohno, S., Babonits, M., Wiener, F., Spira, J., Klein, G. and Potter, M. (1979) *Cell* **18**, 1001-1007.
3. Potter, M. and Wiener, F. (1992) *Carcinogenesis* **13**, 1681-1697.
4. Shaughnessy, J.D.,Jr, Owens, J.D., Wiener, F., Hilbert, D.M., Huppi, K., Potter, M. and Mushinski, J.F. (1993) *Oncogene* **8**, 3111-3121.
5. Fahrlander, P.D., Sumegi, J., Yang,J., Wiener,F., Marcu,K.B., Klein,G. (1984) *Proc.Natl. Acad. Sci. (USA)* **81**, 7046-7050.
6. Ohno,S., Migita,S., Murakami,S. (1989) *Oncogene* **4**, 1513-1517.
7. Ohno,S., Migita,S., Murakami,S. (1991) *Int J. Cancer* **40**, 102-108.
8. Merwin, R.M. and Redmon, I.W. (1963) *J. Natl. Cancer. Inst.* **31**, 998-1007.
9. Wang, H.C. and Fedoroff, S. (1971) *Nature* **235**, 52-54.
10. Committee on Standardized Genetic Nomenclature for Mice. New rules for nomenclatures of genes, chromosome anomalies and inbred strains. (1969) *Mouse News Letter* **17**, 481-187.
11. Mai, S., Hanley-Hyde, J., Fluri, M. (1996) *Oncogene* **12**, 277-288.
12. Fukasawa, K., Wiener, F., VandeWoude, G.F., Mai, S. (1997) *Oncogene* **15**, 1295-1302.
13. Mai, S. (1994) *Gene* **148**, 253-260.
14. Greenberg, R., Lang, R.B., Diamond, M.S., Marcu, K.B. (1982) *Nucleic Acids Res.* **10**, 7751-7761.

15. Huppi, K., Siwarski D., Skurla R., Klinman D., Mushinski J.F. (1990) *Proc Natl Acad Sci (USA)* **87**, 6964-6968.

16. Kuschak, T.I., Paul, J.T., Wright, J.A., Mushinski, J.F., Mai, S. (1999) TTOL http://www.biomednet.com/db/tto. T01669.

17. Szeles, A., Falk, K.I., Imreh, S., Klein, G. (1999) *J. Virol.* **73**, 5064-5069.

18. Lawrence, JB, Singer, RH and Marselle, LM. (1989) *Cell* **57**, 493-502.

19. Evan, G.I., Lewis, G.K., Ramsay, G., Bishop. J.M. (1985) *Mol. Cell. Biol.* **5**, 3610-3616.

20. Juan, G., Traganos, F., James, W.M., Ray. J.M., Roberge, M., Sauve, D.M., Anderson, H., Darzynkiewicz, Z. (1998) *Cytometry* **32**, 71-77.

21. Sambrook, J., Fritsch, E.F., Maniatis, T. Molecular Cloning. (1989) CSH Laboratory Press.

22. Mai, S., Hanley-Hyde, J., Coleman, A., Siwarski, D, Huppi, K. (1995) *Genome* **38**, 780-785.

23. Juan, G., Traganos, F., Darzynkiewicz, Z. (1999) *Exp Cell Res.* **246**, 212-220.

24. Gaubatz, J.W. (1990) *Mutat. Res.* **237**, 271-292.

25. Iwasato,T., Shimizu,A., Honjo,T., Yamagishi,H. (1990) *Cell* **62**, 143-149.

26. Matsuoka, M., Yoshida, K., Maeda, T., Usuda, S., Sakano, H. (1990) *Cell* **62**, 35-142.

27. Cohen, S., Lavi, S. (1996) *Mol. Cell. Biol.* **16**, 2002-2014.

28. Cohen, S., Regev, A., Lavi, S. (1997) *Oncogene* **14**, 977-985.

29. Regev, A., Cohen, S., Cohen, E., Bar-Am, I., Lavi, S. (1998) *Oncogene* **17**, 3455-3461.

30. Wahl, G.M. (1989) The importance of circular DNA in mammalian gene amplification. *Cancer Res.* **49**, 1333-1340.

31. Cox, D., Yuncken, C., Spriggs, A.I. (1965) *The Lancet* **58**, 55.

32. Fegan, C.D., White, D. and Sweeney, M. (1995) *Br. J. Haematol.* **90**, 486-488.

33. Wullich, B., Muller, H.W., Fischer, U., Zhang, K.D., and Meese, E. (1993) *Eur J Cancer* **29A**, 1991-1995.

34. Chen, T.L. and Manuelidis, L. (1989) *Genomics* **4**, 430-433.

35. Delinassios, J.G. and Talieri, M.J. (1983) *Experientia* **39**, 1394-1395.

36. Rowland, P 3d, Pfeilsticker, J. and Hoffee, P.A. (1985) *Arch Biochem Biophys.* **239**, 396-403.

37. Wettergren, Y., Kullberg, A. and Levan, G. (1995) *Hereditas* **122**, 125-134.

38. Stahl, F., Wettergren, Y. and Levan, G. (1992) *Mol. Cell. Biol.* **12**, 1179-1187.

39. Trent, J., Meltzer, P., Rosenblum, M., Harsh, G., Kinzler, K., Marshal, R., Feinberg, A., Vogelstein, B. (1986) *Proc. Natl. Acad. Sci. (USA)* **83**, 470-473.

40. Martinsson,T., Stahl,F., Pollwein,P., Wenzel,A., Levan,A., Schwab,M., Levan,A. (1988) Oncogene **4**, 437-441.

41. Von Hoff, D.D., Needham-Van Devanter,D.R., Yucel,Y., Windle, B.E., Wahl,G.M. (1988) *Proc. Natl. Acad. Sci. (USA)* **85**, 4804-4908.

42. Von Hoff, D.D., McGill,J.R., Forseth,B.J., Davidson,K.K., Bradley,T.P., Van Devanter, D.R., wahl, G.M. (1992) *Proc. Natl. Acad. Sci. (USA)* **89**, 8165-8169.

43. Eckhardt,S.G., Dai A., Davidson, K.K., Forseth, B.J., Wahl, G.M., Von Hoff,D.D. (1994) *Proc. Natl. Acad. Sci. (USA)* **91**, 6674-6678.

44. Shimizu, N., Nakamura, H., Kadota, T., Oda, T, Hirano, T. and Utiyama, H. (1994) *Cancer Res* **54**, 3561-3567.

45. van der Plas, D.C., Hermans, A.B., Soekarman, D., Smit, E.M., de Klein, A., Smadja, N., Alimena, G., Goudsmit, R., Grosveld, R., Hagemejer, A. (1989) *Blood* **73**, 1038-1044.

46. Kurzrock,R., Kantarjian,H.M., Shtalrid,M., Gutterman, J.U., Talpaz,M. (1990) *Blood* **75**, 445-452.

47. Costello,R., Lafage,M., Toiron,Y., Brunel,V., Sainty,D., Arnoulet,C., Mozziconacci, M.J., Bouabdallah,R., Gastau,J.A., Maranichi,D. (1995) *Br.J.Hematol* **90**, 346-352.

48. Selleri,L., Milia,G., Luppo,M., Temperani,P., Zucchini,P., Tagliafico,E., Astusi,T., Sari,M., Donelli,A., Castoldi,G.L. (1990) *Hematol.Pathol.* **4**, 67-77.

49. Janssen,J.W., Fonatsch,C., Ludwig,W.D., Bieder,H., Maurer,J., Bartram, C.R. (1992) *Leukemia* **6**, 463-464, 1992.

50. Estop,A.M., Sherer,C., Cieply,K., Groft, D., Burcoglu,A., Jhanwar,S., Thomas,J.(1997) *Cancer Genet.Cytogenet.* **96**, 174-176.

51. Uckun, F.M., Herman-Hatten,K., Crotty,M.L., Sensel,M.G., Sather,H.N., Tuel-Ajlgren,L., Sarquis,M.B., Bostrom,B., Nachman,J.B., Steinherz, P.G., Gaynon,P.S., Heerema, N. (1998) *Blood* **92**, 810-821.

52. Klein, G. (1989) *Genes Chromosomes Cancer* **1**, 3-8.

53. Klein, G. (1993) *Gene* **135**, 189-196.

54. Klein, G. (1995) *Int. J. Dev. Biol.* **39**, 715-718.

FIGURE LEGENDS

Figure App.B. 1. G-banding, chromosome painting, FISH and SKY prove that DCPC21 is a translocation-negative plasmacytoma.

(a) G-banded karyotype of DCPC21 lacking any plasmacytoma-associated chromosomal translocations involving Chrs 12(*IgH*), 6(*IgK*), 16(*IgL*) and 15 (*c-myc*). The duplicated band on one of the Chr 15 (arrow) was mapped to band 15D2 where *c-myc* is located. Additional chromosomal aberrations (see triangles), such as the elongated chromosome 9 and the marker chromosome M1 as well as the centromerically fused Rb16;19 and the Rb19 isochromosome are probably acquired during neoplastic progression (see text).

(b, c) Chromosome painting of DCPC21 metaphases with chromosome 12 (red) (b) and with chromosome 15 paint (green) (c). No translocation between chromosomes 12 and 15 is visible. In addition, no chromosome 12 or 15-derived material is found as part of any other chromosome.

(d) Painting of a DCPC21 metaphase with chromosome 12 (red) and FISH with *c-myc* (green). The arrow points a large extrachromosomal element (EE) that hybridizes with red and green indicating the presence of Chr 12-derived sequences and *c-myc* on the EE.

(e) SKY analysis of a DCPC21 metaphase. The data are presented as follows: The image in the top left corner of the composite shows a representative metaphase obtained with the Spectra Cube™ prior to the classification of the spectral colors.

The middle top image shows the inverted DAPI-banding of the same metaphase plate, the image in the right top corner displays the spectral colors as classifed by SkyView 1.2 (ASI). The bottom image shows identical chromosome pairs of non-classified (left) and classified DCPC21 chromosomes (right). SKY corroborates the results of the G-banding and chromosome painting: DCPC21 plasmacytoma cells do not exhibit any *c-myc*-activating translocation. SKY revealed the translocation of chromosome 16-derived material onto the telomeric part of chromosome 9 (see arrows) and the insertion of a chromosome 3-derived band into chromosome 2 (arrow). A centromeric fusion occurred between chromosomes 16 and 19 (Rb 16; 19). The M1 marker contains both Chrs X- and 5-derived chromosomal segments (arrow).

Figure App.B. 1 (a)

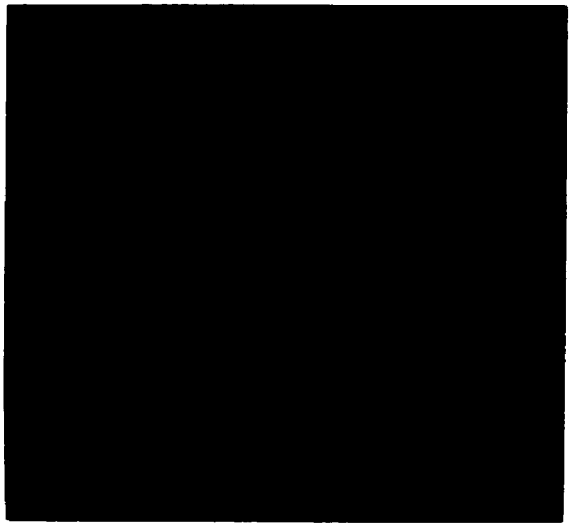

Figure App.B. 1 (b)

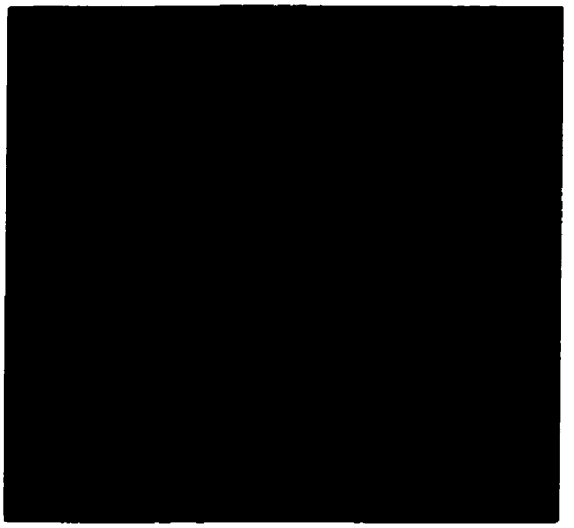

Figure App.B. 1 (c)

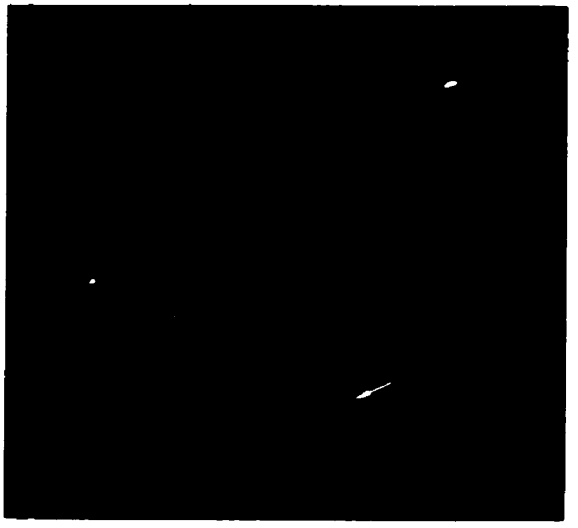

Figure App.B. 1 (d)

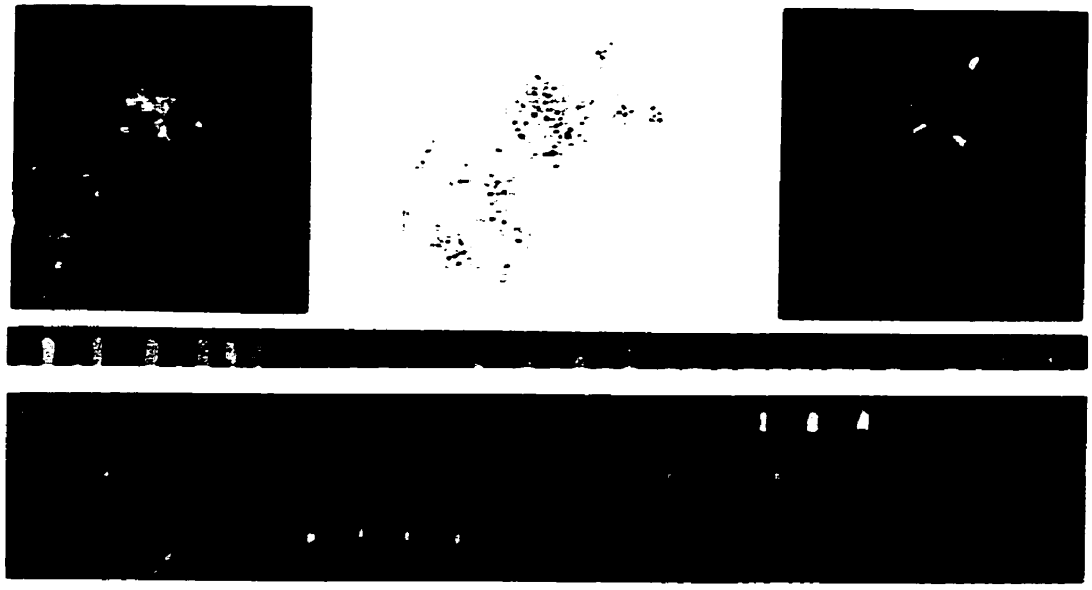

Figure App.B. 1(e)

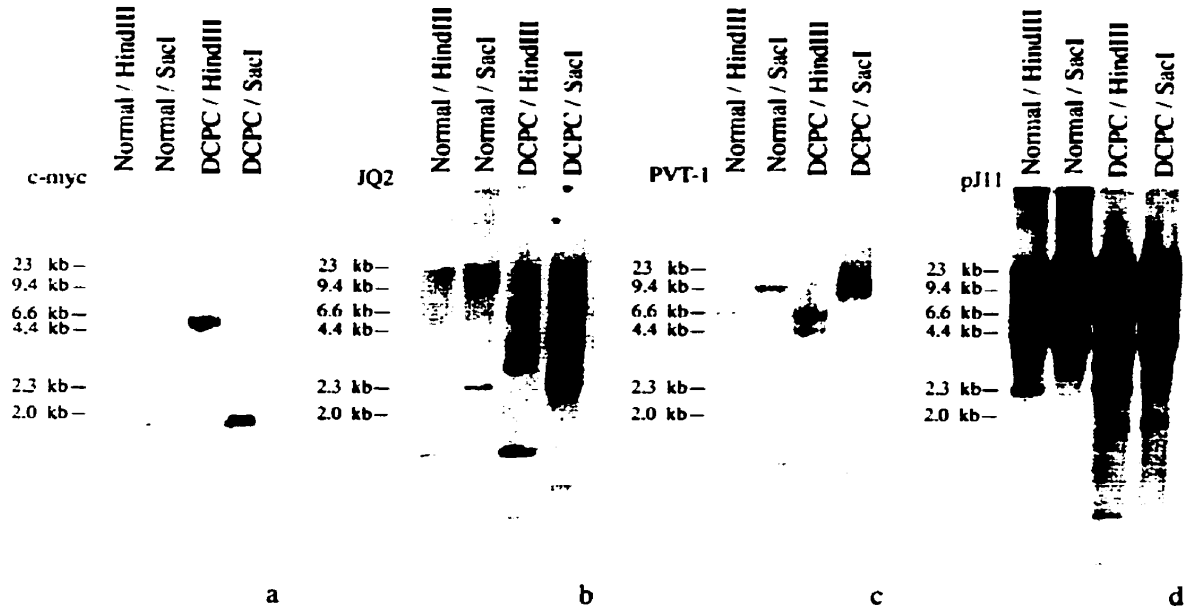

Figure App.B. 2 Southern analysis of normal and DCPC 21 genomic DNA.

Analysis of 10 μg of genomic DNA of DCPC21 plasmacytoma cells ("DCPC") and normal spleen cells ("normal"). The same blot was hybridized with *c-myc* (a), the 5' flanking region of *c-myc* (JQ2) (b), *pvt-1* (c) and *IgH* (pJ11) (d). Note that *c-myc* and *pvt-1* show germ line hybridization signals (lanes 1-4, respectively), while JQ2 and pJ11 (lanes 3 and 4, respectively) indicate rearrangements (for details see text). The stronger hybridization intensity of the *c-myc* and *pvt-1* signals (lanes 3 and 4, Figs. App.B. 2 a and c respectively) is consistent with the duplicated D2 band in chromosome 15 and the additional *c-myc* copies of the other 15 chromosomes (Figure App.B. 1a).

Figure App.B. 3. FISH-EEs.

Purified EEs were hybridized with *c-myc* (green) and *IgH* (*pJ11*, red).

(a) DAPI-counterstain of EEs. Only the large EEs are clearly visible (see arrows).

(b) and (c) The same large EEs shown in a) hybridized with *c-myc* (green) and *IgH* (red).

(d) Overlay of image b) and c) shows the large EEs in orange (see arrows). This indicates the co-localization of the *c-myc* and *IgH* signals on the large EEs. Small EEs carry one or the other hybridization signal and only occasionally both. Preliminary analysis of these EEs by electron microscopy indicates that the large EEs are 0.1-0.2μm in diametre, whereas the little ones are 0.01μm in diametre (data not shown).

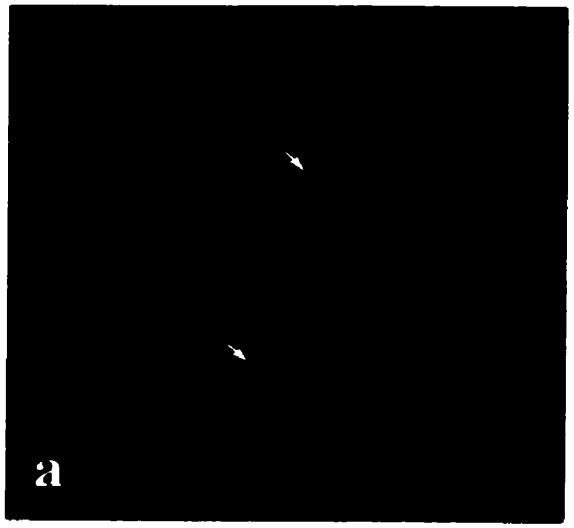

Figure App.B. 3 (a).

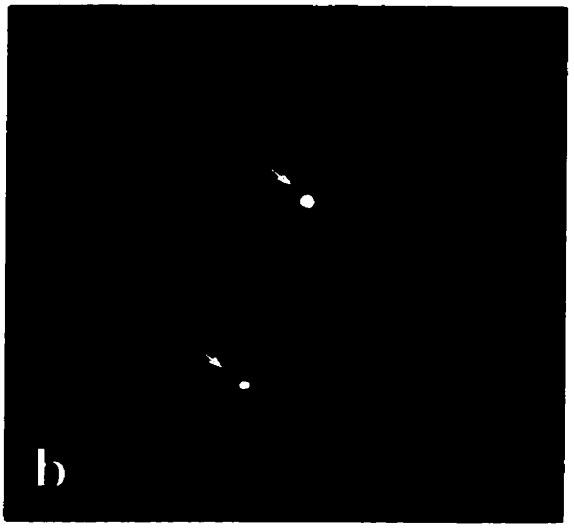

Figure App.B.3 (b).

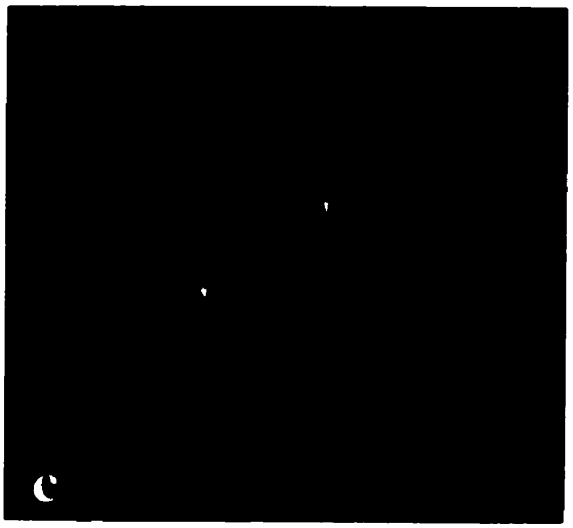

Figure App.B. 3 (c).

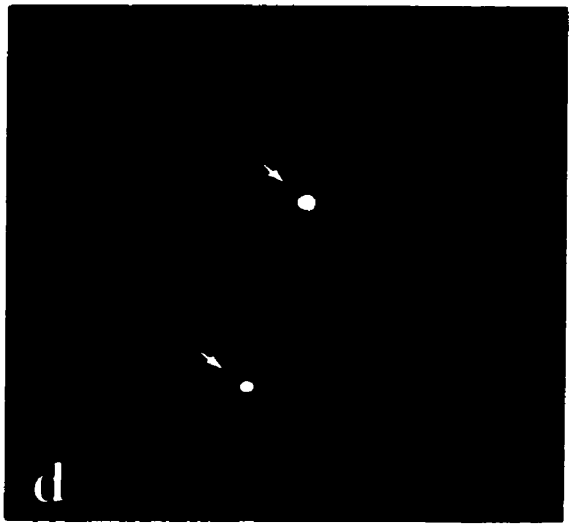

Figure App.B.3 (d).

Figure App.B. 4. The EEs are functional genetic units.

(a) Purified extrachromosomal DNA molecules were immunostained with anti-histone antibodies. EEs are counterstained with DAPI and therefore appear blue. Immunostaining with the pan-histone antibody appears green, while the anti-histone-H3P-stained targets appear red. Thus, EEs immunostained with pan-histone antibody plus DAPI appear greenish-whitish, whereas those stained with histone H3P plus DAPI appear redish. When histone H3P and pan-histone co-localize on the same EE, the color overlay is yellowish.

The image shows four large EEs (arrows) that are surrounded by a group of small EEs. The small EEs stain with DAPI only. The following EEs are pointed out by arrows: a pan-histone-immunostained EE is shown by a closed arrow. Three EEs pointed at with open arrows show co-localization of anti-pan-histone (green) - and anti-histone H3P (red) -antibodies.

(b) mRNA track study of *c-myc* in DCPC21 plasmacytoma cells. Red signals represent mRNA tracks produced in the cells. The tracks are short as expected from extrachromosomal DNA or episomes.

(c) FISH analysis of the sample shown in b). The *c-myc* gene was labeled with digoxigenin and visualized with an anti-digoxigenin-FITC antibody (Materials and Methods). Arrows point to those *c-myc*-carrying EEs (green) that also transcribe c-*myc* (compare b and c). Note that not all *c-myc*-bearing EEs are transcribing *c-myc*.

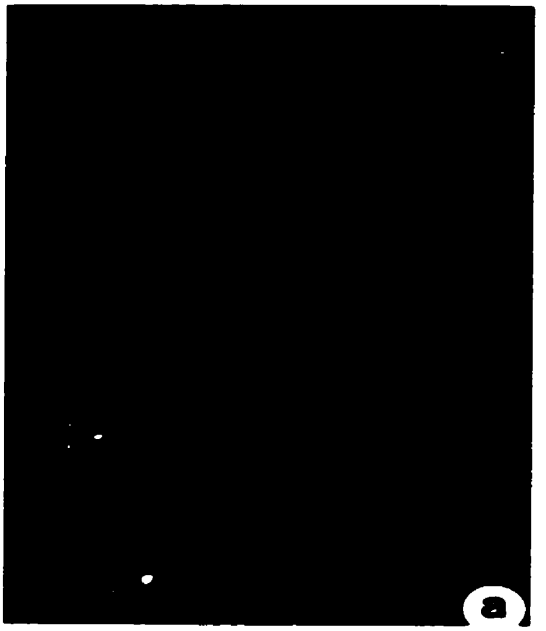

Figure App.B.4 (a)

Figure App.B.4 (b)

Figure App.B.4 (c)

Figure App.B. 5. Extrachromosomal gene transfer studies. Purified EEs were electroporated into primary spleen cells along a green fluorescent protein expressing vector that served as tracer molecule for gene transfer efficiency. B220 was used as cell surface marker for splenic B lymphocytes.

Panel A: GFP and c-Myc expression in primary B cells 24 hours following electroporation:

(a) B220–positive primary B cells as revealed by the FITC-conjugated (green) antibody on the membrane. The arrow points to a B cell expressing GFP. The greenish-whitish color is due to the overlay of the nuclear staining with DAPI (blue) and GFP (green).

(b) The B220-positive B cell that shows GFP expression also overexpresses c-Myc protein (red) (see arrow).

(c) Overlay of image a) and b): The orange nucleus shown expresses GFP and c-Myc (see arrow).

Panel B: Ninety percent of the electroporated primary B cells die 24 hours following transfer of EEs:

(a) GFP-expression in B220-positive B cells

(b) C-Myc-expression in B220-positive B cells

(c) Overlay of a) and b): The GFP-positive and B220-positive primary B cells that overexpress electroporated c-Myc die. Arrows point to some of the apoptotic bodies that form in these cells.

Figure App.B. 5 Panel A (a)

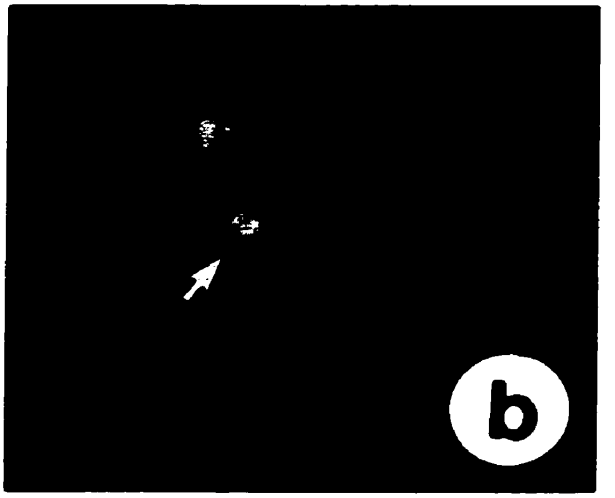

Figure App.B. 5 Panel A (b)

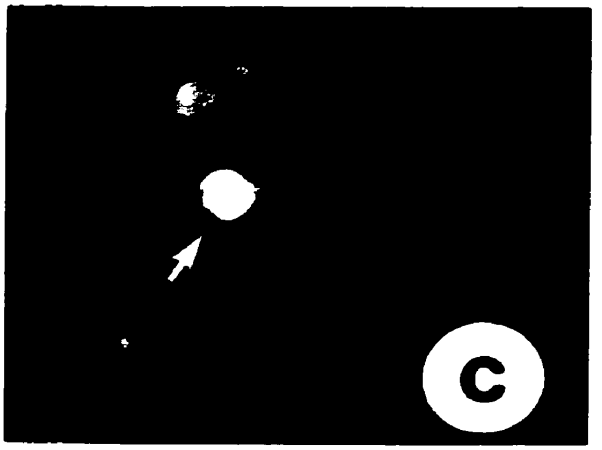

Figure App.B. 5 Panel A (c)

Figure App.B. 5 Panel B (a)

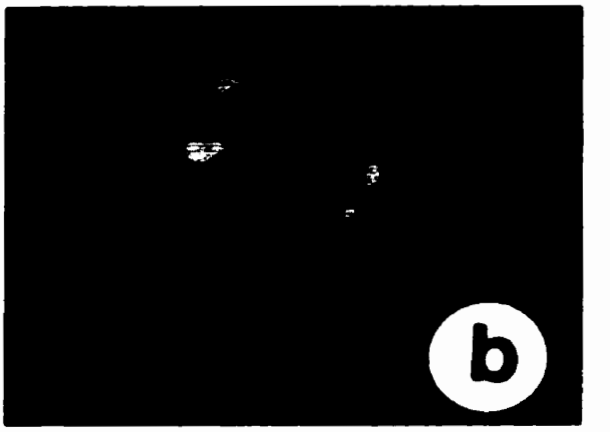

Figure App.B. 5 Panel B (b)

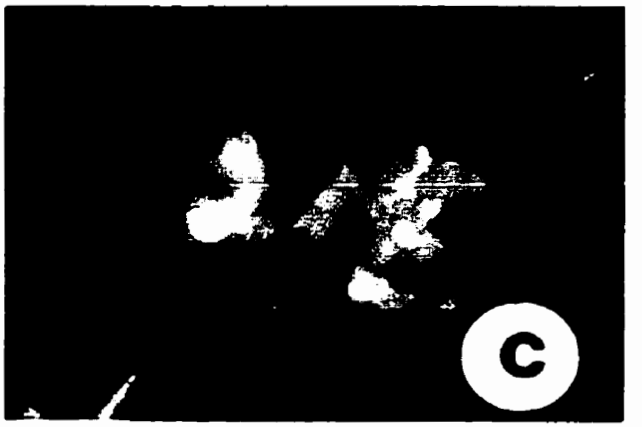

Figure App.B. 5 Panel B (c)